STUDIES ON VISCOELASTICITY IN ION-CONTAINING POLYMERS

STUDIES ON RUBBER ELASTICITY AND VISCOELASTICITY IN ION-CONTAINING POLYMERS

Abstract

This thesis investigates the effect of ions on rubber elasticity and viscoelasticity in polymers. The ratio of the moduli of an ionizable rubber in its acidic and ionic forms is predicted from simple considerations of entropy and chain dimensions. The experimentally determined ratio for a crosslinked poly(vinyl alcohol)-poly(acrylic acid) gel is found to agree semi-quantitatively with the predicted value.

A theoretical study of the dilute solution viscoelasticity of ion-containing polymers, employing a modification of the well-known bead-spring model, is presented. The study predicts an increase in intrinsic viscosity and a broadening in the distribution of relaxation times with increasing ion repulsion.

The effect of ions on the structure and viscoelasticity of poly(acrylic acid) is investigated as a function of the degree of ionization and the plasticizer content. The stress relaxation behaviour is analyzed in terms of a two-mechanism response and correlated with X-ray diffraction and dynamic mechanical studies.

Malcolm King

Ph.D., Chemistry

STUDIES ON RUBBER ELASTICITY AND VISCOELASTICITY

IN ION-CONTAINING POLYMERS

by

Malcolm King

A thesis sumbitted to the Faculty of Graduate Studies
and Research in partial fulfilment of the requirements
for the degree of Doctor of Philosophy

Department of Chemistry
McGill University
Montreal, Quebec
Canada

October 1972

TABLE OF CONTENTS

Page

Page

ACKNOWLEDGEMENTS

This program of research was carried out under the direction of Professor Adi Eisenberg. His guidance and attention, which have helped make this thesis possible, are gratefully acknowledged.

Thanks are also due to Professor B. C. Eu for his valuable suggestions in the formulation of the charged bead-spring theory; to Dr. R. St. John Manley for the use of his X-ray equipment and for a helpful discussion; to Dr. T. Yokoyama and Mr. Karl Taylor for the preparation of polymer samples; and to Messrs. Kluck, Klein, and Striegler for their technical contributions.

The generous support of the National Research Council of Canada through a 1967 Science Scholarship is acknowledged.

Finally, a special thank you to my wife Natalie not only for being a loving wife but also for service above and beyond the call of duty in typing this thesis.

INDEX OF TABLES INCLUDED IN TEXT

INDEX OF ILLUSTRATIONS AND SUPPORTING DATA

GLOSSARY OF SYMBOLS

A	$2\rho/kT$ for bead-spring models
A_0	cross-sectional area of a swollen rubber
$[A]$	concentration of carboxyl groups
$[A]_0$	initial concentration of carboxyl groups
A_n	amplitude of $n^{\underline{th}}$ vibration
a	thickness of polymer film; internuclear distance
a_T	shift factor (reduced time variable)
B	$4H/kT$ for dumbbell model; dimensionless constant ~1 in W.L.F. equation
B'	$2H'/kT$ for 3B2S model
$(B')_0$	$2H/kT$ for nonionic 3B2S model
b	shape factor
b_T	shift factor for secondary master curves
C	$\cos \theta$
C_1, C_2	$\cos \theta_1$, $\cos \theta_2$
C_n	carbon number of linear hydrocarbon derivative
c	$\cos \phi$
c_1, c_2	$\cos \phi_1$, $\cos \phi_2$
c_1^g, c_2^g	W.L.F. constants, referred to T_g
c_f	instrumental compliance (cm/g)
D	diffusion constant
$D(t)$	elongational compliance
$D'(\omega)$	real part of complex compliance
$D''(\omega)$	imaginary part of complex compliance

DSC	differential scanning calorimetry
d_0	sample thickness
d_B	Bragg spacing
d_g	amorphous spacing
E	$-q^2/2\varepsilon kT$ for bead-spring models; Young's modulus of swollen rubber
E(t)	time-dependent Young's modulus
E_0	Young's modulus of unswollen rubber
$E_r(t)$	reduced Young's modulus
EG	ethylene glycol
e.p.r.	election paramagnetic resonance
$\mathbb{F}$	relative vectorial sum of Hookean and Coulombic forces in dumbbell model
F_R	radial component of $\mathbb{F}$ in dumbbell model
F*(R)	complex distribution function of R
F_0*(R)	F*(R) for nonionic case
$\mathbb{F}_i$	vectorial sum of Hookean and Coulombic forces acting on bead i
FA	formamide
f	force of deformation
f_C	Coulombic force between chain ends in dumbbell
f_H	Hookean force between chain ends in dumbbell
f_g	free volume at T_g
f_{xi}	x-component of hydrodynamic drag on bead i
$G(\theta,\phi)$	function of θ and ϕ
G', G"	shear storage and loss moduli
G*(R)	complex distribution function of R

GL	glycerine
$g(\theta)$	function of θ
H	Hookean constant
H'	pseudo-Hookean constant
ΔH_a	apparent enthalpy of activation
Δh	deformation
$h(\phi)$	function of ϕ
h_o	sample length (between clamps)
h_1	distance between point of deformation and nearest clamp edge
I	moment of inertia; integral
i	$\sqrt{-1}$
J	normalization factor of distribution function
K	dimensionless constant ~1
k	Boltzmann constant
k_1, k_2	dimensionless constants
k_a	first order rate constant
L	length of swollen rubber
L_1	unstrained length of swollen rubber
M	molecular weight
M_c	molecular weight between crosslinks
M_n	number average molecular weight
M_v	viscosity average molecular weight
m	monomeric mole fraction of PAA in rubber
N	total number of chains
N_p	number of chains of component p

n_o	polymer concentration (cm^{-3})
P	degree of polymerization
P_p	P between crosslinks of p^{th} component
PAA	poly(acrylic acid)
PNaA	poly(sodium acrylate)
PVA	poly(vinyl alcohol)
PVA'	PVA in basic medium
$\mathbf{Q}$	transformation matrix
q	Coulombic charge
R	gas constant
$\mathbf{R}_i$	vectorial representation of the relative Cartesian coordinates X_i, Y_i, Z_i, or the spherical coordinates R_i, θ_i, ϕ_i
$\overline{R^2}_o$	expectation value of R^2 for unionized acid
$\overline{R^2}_\theta$	$\overline{R^2}_o$ in θ solvent
$\overline{R^2}_{f.r.}$	$\overline{R^2}_o$ in freely rotating configuration
Re{ }	real part of complex quantity
r	end-to-end distance of chains in rubber
$\mathbf{r}_o$	(vectorial) coordinates of center of mass
$\mathbf{r}_i$	vectorial representation of the laboratory-fixed Cartesian coordinates x_i, y_i, z_i
$\overline{r^2}$	mean square end-to-end distance of chains
$\overline{r^2}_o$	$\overline{r^2}$ in unstrained, unswollen network
$\overline{r^2}_f$	$\overline{r^2}$ in unconstrained state
$\overline{r^2}_{f.r.}$	$\overline{r^2}$ in freely rotating configuration
$\overline{r^2}_\theta$	$\overline{r^2}$ in θ solvent
$\overline{r_p{}^2}_o$	$\overline{r^2}_o$ for component p

$\overline{r_p^2}_f$	$\overline{r^2}_f$ for component p
S	sin θ
S_1, S_2	sin θ_1, sin θ_2
ΔS	entropy of deformation of the swollen network due to external strain
ΔS_o	entropy of deformation due to swelling
$\Delta S_o'$	$(\Delta S + \Delta S_o)$
$\Delta S_p'$	$\Delta S_o'$ for component p
S.R.	stress relaxation
s	sin θ
s_1, s_2	sin ϕ_1, sin ϕ_2
T	temperature
T_o	reference temperature
T_g	glass transition temperature
t	time
t_r	reduced time
tan δ	loss tangent, G"/G'
u(R)	real part of distribution function F*(R)
u_i	$i^{\underline{th}}$ trial value of $u'(R_1)$
V	volume of swollen rubber
V_o	unstrained, unswollen volume
V_1	unstrained, swollen volume
V_r	volume fraction of polymer
v(R)	imaginary part of distribution function F*(R)
v_i	$i^{\underline{th}}$ trial value of $v'(R_1)$
$\mathbb{v}_i$	relative solvent velocity at bead i

W.L.F.	Williams, Landel, and Ferry (equation of)
w_o	sample width
α	polymer coil expansion
α_f	free volume expansion coefficient
α_g	linear expansion coefficient below T_g
α_ℓ	linear expansion coefficient above T_g
β	eccentricity factor
γ_i	extension ratio of $i^{\underline{th}}$ coordinate due to both swelling and external strain
	logarithmic decrement
∇^2	$\frac{1}{R^2}\frac{\partial}{\partial R}\left(R^2\frac{\partial}{\partial R}\right)+\frac{1}{R^2 S}\frac{\partial}{\partial\theta}\left(S\frac{\partial}{\partial\theta}\right)+\frac{1}{R^2S^2}\frac{\partial^2}{\partial\phi^2}$
ε	dielectric constant of solvent
η^*	complex viscosity
$[\eta]$	intrinsic viscosity
$[\eta^*]$	complex intrinsic viscosity
$[\eta']$	real part of $[\eta^*]$
$[\eta"]$	imaginary part of $[\eta^*]$
$[\eta]_o$	$[\eta]$ of unionized material
η_s	solvent viscosity
$\kappa(t)$	shear rate for simple shear
$\boldsymbol{\kappa}(t)$	shear tensor
κ_o	amplitude of oscillatory shear
Λ_n	$n^{\underline{th}}$ member of infinite series representation of ψ
λ	wavelength; relaxation time of ionic dumbbell; separation constant
λ_o	relaxation time of nonionic dumbbell

λ_1	separation constant
λ_i	extension ratio of $i^{\underline{th}}$ coordinate due to external strain only; relaxation time of $i^{\underline{th}}$ mode of bead-spring model
$(\lambda_i)_o$	λ_i for nonionic case
$\mu\left(\frac{w_o}{d_o}\right)$	numerical factor in b
ν	frequency ($2\pi\omega$)
ν_o	frequency of supporting wire
ρ	frictional coefficient; density
ρ_o	density at reference temperature
τ	diffusion time
τ_p	contribution of polymer to shear stress
Ψ	distribution function of all laboratory-fixed space and time coordinates in bead-spring model
ψ	distribution function of relative space and time coordinates
ψ_o	time-independent, shear-independent ψ
ω	angular velocity
3B2S	three-bead/two-spring model

CHAPTER I

A REVIEW OF BACKGROUND LITERATURE AND A GENERAL DESCRIPTION OF THE STUDY

The incorporation of ions into a polymeric material can produce structural changes of considerable magnitude, the effect of which can generally be observed in the form of greatly modified viscoelastic behaviour. In the past decade, the pace of research into the structure and viscoelasticity of ion-containing polymers has increased sharply. Since this thesis draws from the growing store of knowledge in this area of research, it will be important to begin with a review of the most relevant background studies.

Three major areas of interest in the study of ion-containing polymers are dealt with in this thesis: rubber elasticity, dilute solution viscoelasticity, and bulk viscoelasticity. In each area, investigations have been made on nonionic polymers and, in each case, the approach to the study of the ion-containing polymer has been essentially to modify existing methods, so that changes in the parameters, other than those directly associated with the inclusion of ions, are restricted as much as possible in order to facilitate direct comparisons between the properties of corresponding ionic and nonionic systems.

A model for the viscoelastic behaviour of polymers must contain the basic elements of energy storage and energy dissipa-

tion. The most successful theories of polymer viscoelasticity have been those where the polymer is considered to behave like a flexible chain which assumes the average configuration in solution which minimizes its free energy. In the absence of severe restrictions to bond rotation or unusual solvent effects, the polymer configuration is governed largely by entropic considerations and is that of a more or less random coil.[1] Deviations from randomness, as may be induced by an externally applied stress, result in decreased entropy which, in the absence of dissipative factors and in an isothermal process, is equivalent to energy storage. This is the origin of elasticity in randomly coiled macromolecules; its importance will become apparent in Chapter II on rubber elasticity and in Chapter III on dilute solution viscoelasticity. This mode of energy storage is less important in the polymer solid state, where intermolecular restrictions to bond rotation are often quite severe. Some of the considerations in this case will be discussed later.

The inherent effect of ionic interaction on entropic energy storage in polymers can be isolated from considerations of energy dissipation by considering the elasticity of an ionizable rubber. The theory of ideal rubber elasticity[2] considers a rubber to be a network of non-interacting polymeric chains. One of the quantitative factors which determines the modulus of elasticity of an ideal network is the average dimension that the polymeric chains would assume were they not constrained by the crosslinks. In Chapter II, the theory of ideal rubber elasticity is applied

to a swollen, ionizable network. The ratio of the moduli of elasticity in the ionized and unionized states is predicted from the determination of polymer dimensions in model solvents. Experimental observations of the modulus of elasticity of a simple ionizable network — a rubber formed from poly(acrylic acid) and poly(vinyl alcohol) — show semi-quantitative agreement with the predictions from theory.

In the study of rubber elasticity, it is essential that the time span in which the effects of energy dissipation occur be less than the time of observation. However, in the case of rubbers, as in all real systems, energy dissipation occurs when the system is perturbed by applied stresses. Whether it is observable or not depends on the correct choice of frequency or time. In polymer solutions, the form of energy dissipation is of two general types; both of these can be classified as friction. One form of frictional dissipation results from the interaction between the polymer and the solvent. The form of this interaction in polymer solutions has been postulated by Kirkwood and Riseman,[3] using the principles of classical mechanics, and their formalism has been employed in most of the subsequent theoretical treatments of polymer viscoelasticity.

The other important type of friction is the "internal friction" which results from hindered rotation of bonds which lie along the polymer-chain backbone. This form of energy dissipation is highly dependent on polymer microstructure and is, in general,

very short-range in nature. Because of the complex and specific nature of this type of friction, theories which describe the time-dependent behaviour associated with it have been only moderately successful.[4] Fortunately, the usual frequency range associated with bond rotation is much greater than that associated with the motions in which polymer-solvent friction is important. Thus, if the region of interest is restricted to lower frequencies, only the time-averaged effects of bond rotation need be considered, and these are much better explored.[5,6] Hence, the development of viscoelastic theory for ion-containing polymers will be restricted to polymers in which the ionizable groups are sufficiently well separated to produce a negligible effect on short-range motions.

The viscoelastic theory which will be presented in detail in Chapter III is built upon the model described by Rouse[7] and Bueche[8] and subsequently modified by Zimm,[9] Tschoegl,[10] and others. This model depends on the statistical nature of the polymer configuration, which leads to entropic energy storage. Because of the Gaussian distribution of the separation of chain ends in an ideal polymer solution, there is a net restoring force on the ends of the coiled polymer which is proportional to their separation;[2] thus, the polymer tends to act like a Hookean spring of zero rest length. Furthermore, the polymer may be subdivided into arbitrary units each of which have this spring-like property, provided that the segments are of sufficient length to be statistically distributed. Thus, energy storage in the model is

that which would result from a series of coupled Hookean springs of zero rest length.

Energy dissipation in the model is considered to be of the same nature as that which results from the motion of beads in a viscous medium; that is, the retarding force on each bead is proportional to its velocity relative to that of the medium. For macromolecules, each monomer unit is considered to be equivalent to a bead moving in a viscous medium (the solvent); the proportionality constant between retarding force and velocity is termed the monomeric friction coefficient. For mathematical convenience, the frictional effect of all the monomer units in each submolecule is considered to be centered in the connector. The viscoelastic model for the macromolecule is thus considered to be a collection of beads joined together by Hookean springs. The one additional element necessary for stability in the model is Brownian motion, which is the effect of thermal energy, and which tends to hold the beads apart by randomization and prevent their collapse under the Hookean forces.

Despite its simplicity, the model has been used with considerable success in predicting the viscoelastic behaviour of polymers in dilute solution. Comparisons of the theory with experimental findings have appeared in a number of reviews and books.[11-13] Since none of the theory developed to this point has applied specifically to ion-containing polymers, further review will not be presented here.

In Chapter III, the basic model as presented by Rouse is modified to include the effects of ionic forces. With all the other parameters remaining the same, the beads are considered to contain electrostatic point charges. Because of the mathematical complexity involved, viscoelastic functions are derived for only the two simplest cases of the model — those with two beads and three beads respectively. Equations are written to describe the motion of the beads in a shearing flow. By combining the equations of motion with the equation of continuity for the beads, a second order differential equation known as the diffusion equation is obtained. The solution of the diffusion equation gives the distribution function of bead separation, from which the viscoelastic functions of interest can be calculated. Computation of the dynamic viscosity as a function of frequency for this simple model indicates that ionization produces an increase in relaxation times as well as a broadening in the distribution of relaxation times.

One of the inherent flaws in the dilute solution theory is that no account of the effect of intermolecular interactions on viscoelasticity is taken. Since all of the viscoelastic measurements that have been made on solutions of ionic polymers have been in the concentration range where intermolecular interactions are a major factor,[14-16] the application of dilute solution viscoelastic theory to ionic polymers anticipates experimental evidence which may be possible in the near future with recent developments in experimental technique, whereby viscoelastic

behaviour in very dilute solutions can be examined.[17]

In Chapter IV, the properties of ionic polymers in highly concentrated solutions are examined. In this region of polymer concentration, both ionic and nonionic intermolecular interactions play a significant role, while considerations of elastic energy storage and frictional loss still apply. The properties of polymers in solutions of very high concentration are similar to those of undiluted polymers. Most of the studies of relevance to this part of the thesis have been made on undiluted polymers; a detailed review of some of them is presented here.

Ion-containing polymers may be divided into several main classes. A number of studies of the mechanical properties of each class of polymers have been made. The first of these classes includes ion-containing inorganic polymers such as the phosphate[18] and the silicate[19-21] systems. The second group, which has been the subject of a recent review,[22] comprises the organic copolymers in which the ionizable fraction is small; systems of this type which have been the subject of recent studies include the ethylene ionomers,[23-26] the styrene ionomers,[27,28] and the carboxylic rubbers.[29] The third major class, on which the main focus of Chapter IV is placed, comprises ionizable organic homopolymers and copolymers containing a high percentage of ionizable material. These polymers, which are generally termed polyelectrolytes when they are in aqueous solution, have received considerable attention with respect to their

synthesis[30] and their solution properties.[31-33] The solid-state properties of polyelectrolytes have received much less attention; those studies that have been reported are discussed here. The work done on the first two classes of ion-containing polymers will not be reviewed in detail in this thesis, except for those studies which afford results or conclusions of relevance to the viscoelasticity and structure of polyelectrolytes.

The first reported study on the solid-state mechanical properties of polyelectrolytes is that of Fitzgerald and Nielsen.[27,34] They obtained viscoelastic data for several ion-containing polymers, including salts of poly(methacrylic acid), poly(acrylic acid), and a copolymer of acrylic acid containing 6% 2-ethylhexyl acrylate (in this thesis referred to as PMA, PAA and PAA-PEHA respectively). The studies showed that ionization produced drastic changes in the mechanical properties of these materials. Glassy Young's moduli of greater than 1×10^{11} dyn/cm^2 were reported for the sodium salts of PMA and PAA, while glassy shear moduli of various divalent salts (Zn, Pb, Ca) of PAA-PEHA were found to range between 5.5×10^{10} and 6.5×10^{10} dyn/cm^2. These values represent increases by a factor of about 1.5 for the sodium salts and about 2 for the divalent salts when compared with the corresponding moduli of the unionized polyacids. The moduli of the polyacids themselves are greater by a factor of 2 than those of typical nonionic, non-hydrogen-bonded polymers like polystyrene. The modulus values of the divalent salts cannot be taken too literally, because the method of preparation — simultaneous

molding and neutralization with metallic oxide — would likely produce an inhomogeneous product. As Nielsen points out,[34] the real moduli of the ionized materials are probably higher still.

In addition to the moduli, the glass transition temperatures of these ionized polyacids are greatly increased; they were not measured specifically, but no significant softening was observed up to 275°C. In fact, other tests indicated that they neither soften nor lose shape before their decomposition temperatures. Another notable change in the physical properties of polyelectrolytes is in the (glassy) linear expansion coefficient, α_g. The salts of the polyacids were found to have values of α_g as low as 1/4 of those of the unionized polymers. Indeed, in this property, as well as in others, polyelectrolyte salts are more like inorganic glasses than organic polymers.

The remarkable changes in the physical properties of these materials can be attributed to the crosslinking effect of ionic bonding which serves to greatly increase the strength of the intermolecular forces and thereby affect such properties as T_g, α_g, and modulus. The magnitude of the changes in these properties indicates that the strength of ionic bonding is much greater than that of hydrogen bonding.

In Chapter IV, an extensive study of the viscoelastic properties of plasticized poly(sodium acrylate) is described. The results of this study indicate that dramatic changes in the mechanical properties of polyelectrolytes occur even in the

presence of plasticizers. Both the glassy modulus and the breadth of the glass transition are observed to increase with increasing degrees of neutralization. Significant variations in the mechanical properties of the fully neutralized polymers are found to occur with different types and amounts of plasticizer.

Although stress relaxation measurements on solid polyelectrolytes were not reported in the studies by Fitzgerald and Nielsen, their investigations did show that, in a copolymer of styrene and sodium methacrylate (7.5%), the rate of stress relaxation was greatly retarded by ionic bonding. Their studies also pointed out that the effect of hydrogen bonding on stress relaxation is very minor when compared with the effect of ionic bonding. This indicates that the lifetimes of hydrogen bonds are much shorter than those of ionic bonds; at ca. 130°C, they exhibit a negligible effect on a stress relaxation experiment, while the effect of ionic bonding at that temperature is highly significant in retarding the relaxation rate.

The investigations by Fitzgerald and Nielsen indicate that polyelectrolytes show promise as structural materials because of their mechanical and thermal properties. However, the difficulties involved in their preparation and the inherent uncertainties in their composition and structure have stalled further development. More recently, a study[35] of the glass transition temperature, T_g, in plasticized salts of poly(acrylic acid) has elucidated the effect of ionic bonding on this aspect of polyelectrolytes. In this case, the composition of the mate-

rial was controlled by neutralizing the polyacid in solution and casting the plasticized material from solvent. T_g's for poly(sodium acrylate) were measured for two plasticizer systems — water and formamide. Extrapolation of the values of T_g to zero plasticizer content in each case gave T_g for the undiluted salt (250°C). The T_g's for other salts of PAA — potassium, cesium, and a sodium-calcium mixture — were established in a similar fashion. The results of this study indicate that T_g is a linear function of q/a, the ratio of the cation charge and the internuclear distance between anion and cation at closest approach. Similar relationships were established earlier for the phosphates and silicates.[36] From the relationship established for the acrylate series, it is possible to predict values of T_g for the undiluted divalent salts, which cannot be prepared in this manner.

Studies have been made to determine the effect of ions on the supermolecular structure of polymers. Changes in supermolecular structure brought about by ionization are likely to be crucial in their effect on viscoelastic properties. Only one structural investigation specifically in the area of glassy polyelectrolytes has been reported. As part of a study made by Wilson, Longworth, and Vaughn,[37] X-ray diffraction analysis of fully neutralized poly(acrylic acid) and poly(methacrylic acid) showed the appearance of Bragg spacings of 12 Å in both of these non-crystalline polymers. This phenomenon can be attributed to the effect of ion aggregation which could result in a two-phase

structure in which regions of high and low ionic content (and thus high and low electron density) would occur. The observed maxima in the diffracted X-ray intensity may thus be associated with the average separation of ion aggregates within domains which are of necessity at least several times larger than 12 Å in size. The latter conclusion is based on the fact that any structured material in which the domains do not contain at least several repeat units could not give rise to a maximum in scattered intensity which would correspond to that repeat unit. The actual dimensions of ionic domains (which could, in fact, be macroscopic) have not been determined, and no further evidence on the solid-state structure of polyelectrolytes has been published. In Chapter IV of this thesis, the results of further X-ray analysis of neutralized poly(acrylic acid) will be presented. It will be shown that, although phase separation occurs with every plasticizer used, the variation in structure with the type and amount of plasticizer is small.

Although the extent of investigations into the structure of glassy polyelectrolytes has been minimal, a number of studies have been made on various copolymers with low ionic contents. These studies have shown that most of these materials exist in a two-phase structure in which the ionic material is concentrated in one of the phases. X-ray diffraction analysis of the sodium salts of various ethylene-methacrylic acid copolymers[37] have shown maxima in the scattered intensity which correspond to spacings of 19 to 27 Å in samples of varying acid content and degree

of neutralization. These dimensions are identified with the average separation of ion aggregates within ion-containing domains. In a subsequent study,[38] an additional maximum in scattered intensity corresponding to a spacing of 83 Å was observed in both the cesium and the sodium salts of an ethylene ionomer. This peak did not occur in the unneutralized material, nor did it vary with annealing; it was therefore associated with the ionic phase. It can be interpreted as corresponding to the average spacing between clusters of ionic material, which may be thought of as aggregates of ion multiplets separated by nonionic material and held together by electrostatic forces. This two-phase structure in ethylene ionomers has recently been confirmed in a study of polyethylene modified by the addition of phosphonic acid side groups.[39] Electron microscopy of the cesium salt of this copolymer showed domains of 50 to 80 Å in diameter which did not exist in the unneutralized material.

Similar structural effects have been observed in ionomers of styrene and of butadiene and in carboxy-terminated butadiene polymers. In a study of the divalent salts of carboxy-terminated butadienes,[40] low-angle X-ray scattering measurements indicate a periodicity of 70 Å in a Mn^{++} salt; an e.p.r. spectral analysis of the Cu^{++} salt of the same material shows the structure of the ionic phase to be essentially that of copper acetate, an aggregate containing two Cu^{++} ions and four carboxyl anions. Ionomers of butadiene and methacrylic acid were studied by electron microscopy;[41] both the ionized and unionized forms of the polymer

appear to exist in a domain structure — regions of high acid or ion content dispersed in a matrix of butadiene. The size of the domains is found to vary within each sample; dimensions varying from 13 to 26 Å were recorded. This study indicates that even in unionized copolymers, a two-phase structure is likely if the components differ significantly in polarity. Recent investigations into the structure of styrene-methacrylic acid ionomers[42] have shown the existence of clusters of ionic material with average separations of 70 to 75 Å for salt contents of greater than 6 mol%. For lower concentrations of ionic material, no evidence of phase separation is observed. It is proposed that above a critical ion concentration, phase separation occurs; this conclusion is reinforced by rheological and other evidence.

Theoretical justification for the existence of clusters of ions in organic polymers has been presented by Eisenberg,[43] based on thermodynamic arguments. The model employed is a hypothetical polymeric material of the ethylene ionomer type, with ionizable groups widely spaced along non-crystallizable chains. The driving force for ion aggregation is the energy gained by the formation of dipoles and multipoles. It is assumed that ions aggregate in tightly packed multiplets whose size is severely restricted by steric considerations to groups of no more than eight ion pairs. The energy gained in this aggregation process is considerable, and such multiplets are assumed to be quite stable. It is postulated that these multiplets may be further associated into clusters. The energy for cluster formation is also electrostatic; the size

of the clusters can be predicted by balancing the gain in electrostatic free energy against the loss in entropic free energy which results from the non-random distributions of chain segments in the nonionic material separating the clusters. The calculation of cluster sizes is based on a number of determinable parameters, including ion concentration. Significantly, the theory predicts that, for any given material, there is a certain minimum concentration of ions required for the formation of clusters.

The accuracy of the calculations of cluster sizes is limited by the lack of account taken for polymer microstructure which influences not only the size and geometry of the multiplets that can be formed, but also the variation in entropic free energy in the nonionic phase. The latter limitation could be expected to be quite severe in the case of polyelectrolytes in which the separation of the ionic groups is small. However, the formation of clusters still seems reasonable on the basis of electrostatic considerations. It must be remembered that the clustering theory is an equilibrium theory. Since it does not consider the transient nature of the clusters, it cannot be used to predict time-dependent properties such as viscoelasticity. One of the aims of Chapter IV is to investigate the effect of ion aggregation on viscoelasticity in solid polyelectrolytes and thereby to elucidate the transient nature of the polymer superstructure. It will be shown that the viscoelastic data can be analyzed in terms of two concurrent relaxation mechanisms, using

methods of analysis that have been previously applied only to non-phase-separated polymers. The contribution of each mechanism to the total viscoelastic response can be associated with the yielding of each phase.

REFERENCES

[1] P. J. Flory, "Principles of Polymer Chemistry," Cornell U. P., Ithaca, N.Y. (1953), Chap. X.

[2] L. R. G. Treloar, "The Physics of Rubber Elasticity," Oxford U. P., London (1958), Chap. IV.

[3] J. G. Kirkwood and J. Riseman, J. Chem. Phys., 16, 565 (1948).

[4] H. Janeschitz-Kriegl, Fortschr. Hochpolym.-Forsch., 6, 170 (1969).

[5] M. V. Volkenstein, "Configurational Statistics of Polymer Chains," Wiley, New York (1963).

[6] T. M. Birshtein and O. B. Ptitsyn, "Conformations of Macromolecules," Wiley, New York (1966).

[7] P. E. Rouse, Jr., J. Chem. Phys., 21, 1272 (1953).

[8] F. Bueche, J. Chem. Phys., 22, 603 (1954).

[9] B. H. Zimm, J. Chem. Phys., 24, 269 (1956).

[10] N. W. Tschoegl, J. Chem. Phys., 39, 149 (1963).

[11] R. E. DeWames, W. F. Hall, and M. C. Shen, J. Chem. Phys., 46, 2782 (1967).

[12] W. L. Peticolas, Rubber Chem. Technol., 36, 1422 (1963).

[13] J. D. Ferry, "Viscoelastic Properties of Polymers," 2nd ed., Wiley, New York (1969), Chap. IX.

[14] A. Silberberg and P. F. Mijnlieff, J. Polym. Sci., A-2, 8, 1089 (1970).

[15] A. Konno and M. Kaneko, Makromol. Chem., 138, 189 (1970).

[16] M. Sakai, I. Noda, and M. Nagasawa, J. Polym. Sci., A-2, 10, 1047 (1972).

[17] J. L. Schrag and R. M. Johnson, Rev. Sci. Instrum., 42, 224 (1971).

[18] A. Eisenberg, Fortschr. Hochpolym.-Forsch., 5, 59 (1967).

[19] "Non-crystalline Solids," ed. V. O. Frechette, Wiley, New York (1960).

[20] "Physics of Non-crystalline Solids," ed. J. A. Prins, North-Holland, Amsterdam (1965).

[21] A. Eisenberg and K. Takahashi, J. Non-Cryst. Solids, 3, 279 (1970).

[22] E. P. Otocka, J. Macromol. Sci., C5, 275 (1971).

[23] T. C. Ward and A. V. Tobolsky, J. Appl. Polym. Sci., 11, 2403 (1967).

[24] W. J. MacKnight, L. W. McKenna, and B. E. Read, J. Appl. Phys., 38, 4208 (1967).

[25] E. P. Otocka and T. K. Kwei, Macromolecules, 1, 401 (1968).

[26] K. Sakamoto, W. J. MacKnight, and R. S. Porter, J. Polym. Sci., A-2, 8, 277 (1970).

[27] W. E. Fitzgerald and L. E. Nielsen, Proc. Roy. Soc. (London), A282, 137 (1964).

[28] A. Eisenberg and M. Navratil, J. Polym. Sci., B, 10, 537 (1972).

[29] A. V. Tobolsky, P. F. Lyons, and N. Hata, Macromolecules, 1. 515 (1968).

[30] M. F. Hoover, J. Macromol. Sci., A4, 1327 (1970).

[31] "Ion Exchange: A Series of Advances," Vol. I, ed. J. A. Marinsky, Dekker, New York (1966).

[32] S. A. Rice and M. Nagasawa, "Polyelectrolyte Solutions," Academic, New York (1961).

[33] F. Oosawa, "Polyelectrolytes," Dekker, New York (1971).

[34] L. E. Nielsen, Polym. Eng. Sci., 9, 356 (1969).

[35] A. Eisenberg, H. Matsuura, and T. Yokoyama, J. Polym. Sci., A-2, 9, 2131 (1971).

[36] A. Eisenberg, Macromolecules, 4, 125 (1971).

[37] F. C. Wilson, R. Longworth, and D. J. Vaughn, A.C.S. Polymer Preprints, 9, 505 (1968).

[38] B. W. Delf and W. J. MacKnight, Macromolecules, 2, 309 (1969).

[39] P. J. Phillips, J. Polym. Sci., B, 10, 443 (1972).

[40] M. Pineri, M. Lambert, C. Meyer, and A. M. Levelut, paper presented to VI International Congress of Rheology, Lyon, 1972.

[41] C. L. Marx, J. A. Koutsky, and S. L. Cooper, J. Polym. Sci., B, 9, 167 (1971).

[42] M. Navratil, Ph.D. thesis, McGill Univ., 1972.

[43] A. Eisenberg, Macromolecules, 3, 147 (1970).

CHAPTER II

THE MODULUS OF PLASTICIZED IONIC RUBBERS

A. Introduction

In this chapter, the time-independent effects of ions on mechanical properties are examined. It has been found in a number of ion-containing systems, as pointed out in Chapter I, that ionic polymers in the glassy state have much higher moduli than corresponding nonionic polymers. It is pertinent to ask whether this effect extends beyond the glass transition point and specifically into the rubbery region. Because of the tendency of ions to aggregate and thus act as additional crosslinks,[1] one would expect that the modulus of elasticity of an ionized rubber would be greater than that of the corresponding unionized material. However, it should be remembered that ionic aggregates do not form crosslinks in the conventional sense, since they often have a significant time dependence, as will be shown in Chapter IV. It is of interest, therefore, to determine if there is an intrinsic effect of ions, other than increased crosslinking, which would cause a higher modulus to persist into the rubbery region.

Since a rubber is ideally a network of non-interacting polymer chains,[2] and since rubber elasticity is inherently an intramolecular phenomenon, it is imperative to eliminate the

effects of ion aggregation in order to determine the effect of ions on rubber elasticity in terms of intramolecular parameters. This can be accomplished by plasticizing the rubber with a liquid of high dielectric constant. It will be shown that under these circumstances the ions have only a small effect on the modulus and that from the change in polymer dimensions alone a semi-quantitative prediction of the variation in modulus on ionization can be obtained.

A rubber system in which the effects of ion aggregation can be eliminated and which, in addition, has been well studied[3] is the crosslinked poly(acrylic acid)-poly(vinyl alcohol) system (PAA-PVA). Ion aggregation effects can be eliminated by allowing the polymers to swell in aqueous media. Accordingly, a series of PAA-PVA films were prepared after the method of Kuhn, et al.[3] The films were crosslinked by heating, swollen in aqueous media, and subsequently studied in both acidic and ionic forms. The rubbery modulus was measured at a single temperature as a function of the volume fraction of polymer. When the results were compared at a common volume fraction, it was found that the modulus of the ionic form was lower than that of the acidic form, in contrast to what one might anticipate intuitively.

In one attempt to rationalize this result, free-chain dimensions in solvent systems similar to the swollen polymer environment were determined by viscometry and used to predict the ratio of the moduli in acidic and ionic forms from simple rubber

elasticity theory. In another attempt to predict this ratio, θ dimensions, as published in the literature, were employed. Both attempts lead to correct qualitative agreement, but both underestimate the effect somewhat.

The first part of the subsequent discussion will be devoted to the derivation of a theory for a two-component rubber, one component of which is ionizable. Subsequently, the experimental aspects will be discussed, and the theoretical predictions compared with experimental results. Finally, several reasons will be suggested which might explain the discrepancy between theory and experiment.

B. Theory

Consider a unit cube of a rubber which consists of a mutually interpenetrating network of two types of chains. In the present case, the two types of chains are PAA and PVA. The nature of the crosslink in the PAA-PVA rubber system is taken to be a simple esterification.[4] It is assumed, for the purposes of this calculation, that each crosslink is tetrafunctional and that from each crosslink emanate two chains of PAA and two of PVA.

Suppose that a unit cube of such a polymer undergoes isotropic swelling in the ratio $1/V_r$, where V_r is the total volume fraction of polymer in the mixture. The length of each edge of the cube in the swollen, unstrained state is given by $1/V_r^{1/3}$.

If the network is subsequently deformed by an external force to the dimensions γ_1, γ_2, γ_3, the total difference in network entropy between the unstrained, unswollen state and the strained, swollen state for each type of chain, p, is given by[2,5]

$$\Delta S_p' = -\frac{1}{2} N_p k \left(\overline{r_p^2}_o / \overline{r_p^2}_f\right) \left(\gamma_1^2 + \gamma_2^2 + \gamma_3^2 - 3\right) \qquad (1)$$

The expressions $\overline{r_p^2}_o$ and $\overline{r_p^2}_f$ represent the mean square end-to-end distances of the chains in the unstrained, unswollen network and in the free state, respectively. It is assumed that $\overline{r_p^2}_o$ and $\overline{r_p^2}_f$ are not equal.

For a network consisting of two types of chains, the total entropy of deformation of the network, $\Delta S_o'$, including both swelling and deformation resulting from the externally applied force, is simply the sum of the entropies of the components

$$\Delta S_o' = \Delta S_1' + \Delta S_2' = -\frac{1}{2} k \left[\left(\overline{r_1^2}_o / \overline{r_1^2}_f\right) N_1 + \left(\overline{r_2^2}_o / \overline{r_2^2}_f\right) N_2\right] \times$$

$$\left(\gamma_1^2 + \gamma_2^2 + \gamma_3^2 - 3\right) \qquad (2)$$

where the subscripts 1 and 2 on S, r and N refer to the two components. The change in entropy due to the isotropic swelling in the ratio $1/V_r^{1/3}$ in the absence of stress is

$$\Delta S_o = -\frac{1}{2} k \left[\left(\overline{r_1^2}_o / \overline{r_1^2}_f\right) N_1 + \left(\overline{r_2^2}_o / \overline{r_2^2}_f\right) N_2\right] \times$$

$$\left(3V_r^{-2/3} - 3\right) \qquad (3)$$

Therefore, the entropy of deformation of the swollen network, ΔS, is simply the difference of $\Delta S_o'$ and ΔS_o

$$\Delta S = \Delta S_o' - \Delta S_o = -\frac{1}{2} k \left[\left(\overline{r_1^2}_o / \overline{r_1^2}_f \right) N_1 + \left(\overline{r_2^2}_o / \overline{r_2^2}_f \right) N_2 \right] \times \left(\gamma_1^2 + \gamma_2^2 + \gamma_3^2 - 3V_r^{-2/3} \right) \quad (4)$$

It is more convenient to express ΔS in terms of the extensions λ_1, λ_2, λ_3, referred to the swollen, unstrained network, where $\lambda_1 = \gamma_1 V_r^{1/3}$, etc. Thus

$$\Delta S = -\frac{1}{2} k \left[\left(\overline{r_1^2}_o / \overline{r_1^2}_f \right) N_1 + \left(\overline{r_2^2}_o / \overline{r_2^2}_f \right) N_2 \right] \times \left(\lambda_1^2 + \lambda_2^2 + \lambda_3^2 - 3 \right) V_r^{-2/3} \quad (5)$$

If changes in the internal energy of the system on deformation of the swollen network are neglected, the force of extension, f, of a swollen rubber of length L and volume V is given by

$$f = -T \left(\partial \Delta S / \partial L \right)_{T,V} \quad (6)$$

For simple extension of a rubber, $\lambda_1 = L/L_1$, where L_1 is the value of L in the unstrained, swollen state. Therefore,

$$f = -\left(T/L_1 \right) \left(\partial \Delta S / \partial \lambda_1 \right)_{T,V} \quad (7)$$

If the rubber is considered to be incompressible, then $V = V_1$, the unstrained, swollen volume, and

$$\lambda_2 = \lambda_3 = (\lambda_1)^{-1/2} \quad (8)$$

Hence, the relationship

$$\lambda_1^2 + \lambda_2^2 + \lambda_3^2 - 3 = \lambda_1^2 + 2/\lambda_1 - 3 \quad (9)$$

is obtained. By substituting Eq. 9 in Eq. 5 and differentiating the result in Eq. 7, the expression for the force is obtained

$$f = (kT/L_1)\ [(\overline{r_1^2}_o/\overline{r_1^2}_f)\ N_1 + (\overline{r_2^2}_o/\overline{r_2^2}_f)\ N_2\ ] \times (\lambda_1 - 1/\lambda_1^2)\ V_r^{-2/3} \qquad (10)$$

The Young's modulus, E, is then given by the ratio of stress to strain

$$E = (f/A_o)/(L/L_1 - 1)$$
$$= (kT/V_1)\ [(\overline{r_1^2}_o/\overline{r_1^2}_f)\ N_1 + (\overline{r_2^2}_o/\overline{r_2^2}_f)\ N_2\ ] \times [(\lambda_1 - 1/\lambda_1^2)/(\lambda_1 - 1)]\ V_r^{-2/3} \qquad (11)$$

In the limit of small strains, this becomes

$$E = (3kT/V_1)\ [(\overline{r_1^2}_o/\overline{r_1^2}_f)\ N_1 + (\overline{r_2^2}_o/\overline{r_2^2}_f)\ N_2]\ V_r^{-2/3} \qquad (12)$$

If V_o is the unswollen, unstrained volume, then $V_1 = V_o/V_r$, and the Young's modulus becomes

$$E = (3kT/V_o)\ [(\overline{r_1^2}_o/\overline{r_1^2}_f)\ N_1 + (\overline{r_2^2}_o/\overline{r_2^2}_f)\ N_2]\ V_r^{1/3} \qquad (13)$$

It is clear that, in the simplest approximation where $\overline{r^2}_o/\overline{r^2}_f$ is considered to be unity[2] and $(N_1 + N_2)$ becomes the total number of chains, the equation for the Young's modulus assumes the familiar form

$$E = E_o\ V_r^{1/3} \qquad (14)$$

where E_o is the modulus of the unswollen network.

Now consider the specific case of a rubber formed from a mixture of PAA (monomeric mole fraction m) and PVA (monomeric mole fraction [1 - m]). The mixture is cast as a film from aqueous solution, crosslinked by heating, and subsequently

swollen in water. Since it was assumed that each crosslink is the junction of two chains of PAA and two chains of PVA, it must hold that

$$N_{PAA} = N_{PVA} = N/2 \tag{15}$$

Therefore, the degrees of polymerization between crosslinks, P_p, are in the ratio of the monomeric mole fractions; that is

$$P_{PVA}/P_{PAA} = (1 - m)/m \tag{16}$$

The relative values of $\overline{r_{PVA}^2}_o$ and $\overline{r_{PAA}^2}_o$ can be deduced by balancing the force on each crosslink, keeping in mind that each crosslink must be the junction of two PAA chains and two PVA chains. The retractive force exerted by each chain is proportional to the end-to-end distance, r, as given by[6]

$$f = 3kT\ r/\overline{r^2}_f \tag{17}$$

Since the average tension exerted on the PAA chains must be equal and opposite to the average tension exerted on the PVA chains in any one direction, and considering that the sample is isotropic, the relationship

$$(\overline{r_{PAA}^2}_o)^{1/2}/\overline{r_{PAA}^2}_f = (\overline{r_{PVA}^2}_o)^{1/2}/\overline{r_{PVA}^2}_f \tag{18}$$

may be written. A similar relationship holds for the ionic form

$$(\overline{r_{PNaA}^2}_o)^{1/2}/\overline{r_{PNaA}^2}_f = (\overline{r_{PVA}^2}_o)^{1/2}/\overline{r_{PVA'}^2}_f \tag{19}$$

where the symbol PVA' refers to the basic medium, and PNaA is poly(sodium acrylate). It should be recalled, however, that it is not the mean square end-to-end distances of the two types of

chains that are equal, but only the average tension under which the chains find themselves.

It is more convenient to rewrite Eq. 12 using Eq. 15, with PAA representing component 1 and PVA component 2

$$E = (3NkT/2V_o)\ [(\overline{r_{PAA}^2}_o/\overline{r_{PAA}^2}_f) + (\overline{r_{PVA}^2}_o/\overline{r_{PVA}^2}_f)]\ V_r^{1/3} \qquad (20)$$

Substitution of Eq. 18 in Eq. 20, for the polymer in the acidic form, gives

$$E_{acidic} = (3NkT/2V_o)\ [(\overline{r_{PAA}^2}_o/\overline{r_{PAA}^2}_f) + (\overline{r_{PVA}^2}_f/\overline{r_{PAA}^2}_f)^2\ (\overline{r_{PAA}^2}_o/\overline{r_{PVA}^2}_f)]\ V_r^{1/3} \qquad (21)$$

or

$$E_{acidic} = (3NkT/2V_o)\ (\overline{r_{PAA}^2}_o/\overline{r_{PAA}^2}_f) \times (1 + \overline{r_{PVA}^2}_f/\overline{r_{PAA}^2}_f)\ V_r^{1/3} \qquad (22)$$

Similarly, for the polymer in the ionic form

$$E_{ionic} = (3NkT/2V_o)\ (\overline{r_{PNaA}^2}_o/\overline{r_{PNaA}^2}_f) \times (1 + \overline{r_{PVA'}^2}_f/\overline{r_{PNaA}^2}_f)\ V_r^{1/3} \qquad (23)$$

The ratio $\overline{r_{PNaA}^2}_o/\overline{r_{PAA}^2}_o$ may be obtained by equating the total root mean square distances between crosslinks for both components in acidic and basic forms, at constant volume fraction of polymer

$$(\overline{r_{PAA}^2}_o)^{1/2} + (\overline{r_{PVA}^2}_o)^{1/2} = (\overline{r_{PNaA}^2}_o)^{1/2} + (\overline{r_{PVA'}^2}_o)^{1/2} \qquad (24)$$

Combining Eq. 24 with Eqs. 18 and 19 yields

$$\overline{r_{PAA}^2}_o \left(1 + \overline{r_{PVA}^2}_f / \overline{r_{PAA}^2}_f\right)^2 = \overline{r_{PNaA}^2}_o \left(1 + \overline{r_{PVA'}^2}_f / \overline{r_{PNaA}^2}_f\right) \tag{25}$$

From Eqs. 22 and 23, the ratio of the Young's moduli at constant V_r is obtained

$$\frac{E_{acidic}}{E_{ionic}} = \frac{\left(\overline{r_{PAA}^2}_o / \overline{r_{PAA}^2}_f\right)\left(\overline{r_{PVA}^2}_f / \overline{r_{PAA}^2}_f + 1\right)}{\left(\overline{r_{PNaA}^2}_o / \overline{r_{PNaA}^2}_f\right)\left(\overline{r_{PVA'}^2}_f / \overline{r_{PNaA}^2}_f + 1\right)} \tag{26}$$

With Eq. 25 the ratio simplifies to

$$\frac{E_{acidic}}{E_{ionic}} = \frac{\overline{r_{PNaA}^2}_f + \overline{r_{PVA'}^2}_f}{\overline{r_{PAA}^2}_f + \overline{r_{PVA}^2}_f} \tag{27}$$

Since the present system deals with equal numbers of chains of each component, this ratio is simply the ratio of the average mean square end-to-end distances of the free chains

$$E_{acidic}/E_{ionic} = (\overline{r^2}_f)_{basic}/(\overline{r^2}_f)_{acidic} \tag{28}$$

It is evident that Eq. 28 is formally the same as that obtained for an ionizable rubber consisting of a single component. The determination of the mean square end-to-end distances of the free chains and hence the prediction of the ratio of the moduli will be discussed in the subsequent sections.

C. Experimental Procedures

Films suitable for the measurement of the rubbery modulus were prepared from a 50:50 mixture (by weight) of PVA and PAA.

The PVA (99% hydrolyzed, P = 1700-1800) was obtained from Matheson Coleman & Bell and used without further preparation. The PAA used in the preparation of the films was of medium molecular weight ($M_v = 1.4 \times 10^5$) and was assumed to be atactic. A description of its preparation and molecular weight characterization is given in Appendix A of Chapter IV.

A mixture of PAA and PVA of equal parts by weight was dissolved in water and cast in a flat-bottomed polystyrene container. The water was evaporated at 50°C until a clear flexible film was obtained. This film was then divided into two portions which were heated at 110°C for periods of 0.5 hr and 1.5 hr, respectively, in order to produce two different crosslink densities. Both of the films obtained were found to swell but not dissolve in water. It was found that the film of higher crosslink density was not suitable for mechanical measurements because it was easily ruptured when swollen; thus, only the more lightly crosslinked film, which was quite elastic in nature, was used in subsequent measurements. While no specific tests were performed, no evidence of incompatibility was observed in visual examinations of the films. Kuhn's investigations,[3] carried out in similar concentration regions, also revealed no such problem, presumably due to the high swelling ratios used.

The film studied was first allowed to swell in distilled water overnight. The modulus was measured at a single temperature (25°C ± 1°C) as a function of the weight fraction of polymer. The measurements were made in a sealed stress

relaxometer (described in detail elsewhere[8]). For each weight fraction, the force of extension was observed as a function of time; after initial rapid relaxation, the force was generally constant. For lower swelling ratios where the force did not remain constant within experimental error, the data were discarded. The extensions were always from 5% to 10%, in which range the elastic response was found to be linear.

The weight fractions were obtained from the polymer weights taken immediately after each force measurement, so that weight loss due to saturation of the sample chamber with water vapor during temperature equilibration was not a factor. The density of the sample as a function of the weight fraction of polymer was measured pycnometrically at 25°C, with paraffin oil as the confining fluid. This procedure allowed the calculation of volume and, hence, volume fraction of polymer in each case.

After the study of the modulus of the acidic form, the film was immersed in 1N NaOH solution for several hours. The time required for diffusion, τ, was calculated from the data of Kuhn, et al.,[3] taking $D \simeq 10^{-5}$ cm^2 sec^{-1} as the value of the diffusion constant of the base in the embedded fluid. For a film thickness $a \simeq 0.2$ cm, $\tau = a^2/2D \simeq 0.5$ hr. Hence, the time allowed for diffusion was more than adequate.

As before, the modulus was measured as a function of the weight fraction of polymer. With the aid of density measurements as a function of weight fraction, the modulus as a function of

volume fraction was obtained. As a check on reversibility, the films were re-soaked overnight in HCl, and then in water. The modulus was found to return to its initial value within the limits of experimental error.

Mixed solvents, representing the low molecular weight analogs of the acidic and ionic forms of the polymer mixtures, were prepared. For the acidic form, the solvent was a mixture (by volume) of propionic acid (15%), ethyl alcohol (15%) and water (70%); for the ionic form, a mixture of sodium propionate (15%), ethyl alcohol (15%) and water (70%) was chosen. The volume percentages were selected to give the same volume percent of water as the point of comparison of the swollen polymers and also the same ratio of alcohol to acid as in the polymer mixture.

Intrinsic viscosity determinations (at 25°C) in the above two solvent mixtures were made for a series of PAA samples of various molecular weights, as described in Appendix A of Chapter IV. These were used to determine relationships between $[\eta]$ and M_v in acidic and basic media. The relationships obtained were

$$[\eta]_{PAA} = 8.9 \times 10^{-4} M_v^{0.54} \tag{30}$$

$$[\eta]_{PNaA} = 16 \times 10^{-4} M_v^{0.50} \tag{31}$$

Intrinsic viscosity determinations in the above two media were also made for a series of commercially obtained PVA samples. In addition to the material described earlier, the PVA samples were three grades of Elvanol (from Dupont) with reported values

of P = 500-600, 1700-1800, and 2400-2500, respectively. The molecular weights of these samples were determined by membrane osmometry in aqueous solution at 25°C, using a Hewlett Packard 502 High Speed Membrane Osmometer. Values of M_n in the range 1.9×10^4 to 6.7×10^4 were obtained, in line with but somewhat lower than those expected from reported degrees of polymerization. For the PVA used in the preparation of films, $M_n = 5.7 \times 10^4$ was obtained.

D. Experimental Results

Since the theory predicts Young's modulus of a swollen rubber to vary as $V_r^{1/3}$, E versus $V_r^{1/3}$ was plotted for both the acidic form and the ionic form of the rubber. These results are shown graphically in Fig. 1. Typical error limits are shown for two points of each line; a more complete error analysis is presented in Appendix A. The data represent values for three different films, crosslinked for the same length of time, indicating the good reproducibility of the modulus measurements.

The best straight line was obtained for each of the two forms by a least squares method, and the moduli obtained were compared at a common volume fraction of polymer. For the volume fraction $V_r = 0.3$, the values of modulus obtained were

$$E_{acidic} = 8.75 \times 10^6 \text{ dyn/cm}^2 \tag{32}$$

$$E_{ionic} = 6.1 \times 10^6 \text{ dyn/cm}^2 \tag{33}$$

FIGURE 1

Young's modulus versus $V_r^{1/3}$ for rubber in acidic and ionic forms. Data points indicated: sample 1 (○), sample 2 (□), sample 3 (◎). ——— :best fit to $E = A + B V_r^{1/3}$; — — : best fit to $E = C V_r^{1/3}$; ····· : comparison at $V_r = 0.3$.

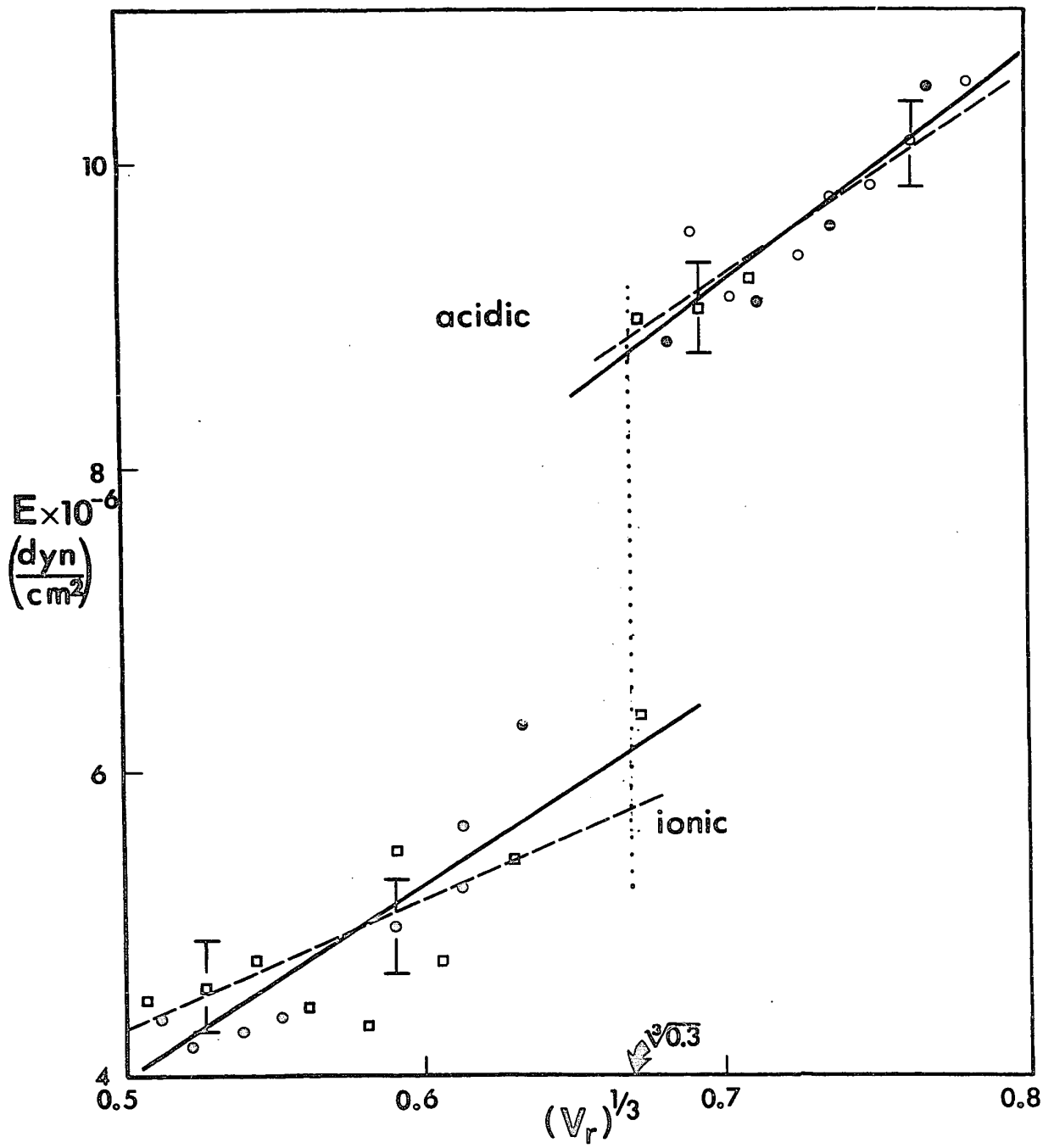
10
8
6
4
$E \times 10^{-6}$
$\left(\frac{dyn}{cm^2}\right)$
acidic
ionic
$\sqrt[3]{0.3}$
0.5
0.6
0.7
0.8
$(V_r)^{1/3}$

From these, the ratio of the moduli was calculated

$$E_{acidic}/E_{ionic} = 1.43 \tag{34}$$

It will be shown that the value of this ratio, as predicted by theory, is in the same direction (i.e., greater than 1) but smaller than that obtained by experiment.

The two best linear relationships (solid lines in Fig. 1) are given by

$$E_{acidic} \times 10^{-6} = -1.37 + 15.1\ (V_r)^{1/3} \tag{35}$$

$$E_{ionic} \times 10^{-6} = -2.33 + 12.6\ (V_r)^{1/3} \tag{36}$$

The standard deviations of E_{acidic} and E_{ionic} are 0.20 and 0.36, respectively. It should be pointed out, however, that with only slight increases in the deviations, the lines can be made to pass through the origin. These lines are the dashed lines in Fig. 1, represented by the relationships

$$E_{acidic} \times 10^{-6} = 13.2\ (V_r)^{1/3} \tag{37}$$

$$E_{ionic} \times 10^{-6} = 8.6\ (V_r)^{1/3} \tag{38}$$

the standard deviations being 0.21 and 0.40, respectively. Thus, within the limits of experimental error, the modulus as a function of volume fraction can be adequately reproduced by the elementary theory.

E. Comparison of Experiment with Theory

The values of $\overline{r_{PAA}^2}_f$ and $\overline{r_{PVA}^2}_f$ with respect to the actual polymer network are unknown. However, they may be estimated in

two different ways. At one extreme, it may be said that the polymers find themselves in a medium which approximates θ solvent conditions. The polymer dimensions in this case would be the unperturbed dimensions. At the other extreme, the values of $\overline{r^2}_f$ may be determined from the measurement of polymer dimensions in solvent conditions which approximate those in the real polymer, assuming that the polymer is far from θ conditions.

In the former case, the dimensions may be expressed in terms of a characteristic ratio, $\sigma = (\overline{r^2}_\theta / \overline{r^2}_{f.r.})^{1/2}$. σ has been measured for PAA[7] and for PNaA[9] in actual θ solvents, and it has been estimated for PVA[10] although no θ solvent was obtained. These results are summarized in Table I.

TABLE I

POLYMER	σ	REFERENCE
PAA	1.85 ± .05	7, 11
PNaA	2.38	9
PVA	2.04 ± .10	10, 11

The value of $(\overline{r^2}_{f.r.}/P)$ is a constant (9.49×10^{-16} cm^2) for vinyl polymers. Hence,

$$\overline{r^2}_\theta \propto \sigma^2 P \tag{39}$$

Combining Eq. 39 with Eqs. 28 and 16, the ratio

$$\frac{E_{acidic}}{E_{ionic}} = \frac{\sigma_{PVA}^2 \times (1 - m) + \sigma_{PNaA}^2 \times m}{\sigma_{PVA}^2 \times (1 - m) + \sigma_{PAA}^2 \times m} \qquad (40)$$

is obtained. For a 50:50 mixture of PVA and PAA by weight ($m = 0.38$), this ratio has the value 1.22.

In the latter case, where model solvents are used to approximate the solvent environment in the real system, polymer chain dimensions can be estimated from intrinsic viscosity data.[11] Because $\overline{r^2}_f/P$ is a function of the degree of polymerization in non-θ solvents, the overall average molecular weight between crosslinks, M_c, was estimated from the rubbery modulus data, using the simple approximation[2]

$$E/V_r^{1/3} \simeq 3\rho RT/M_c \qquad (41)$$

Since $E/V_r^{1/3} \simeq 1.3 \times 10^7$ dyn/cm^2, then $M_c \simeq 7500$. At this value of M

$$\overline{r_{PNaA}^2}_f/\overline{r_{PAA}^2}_f = ([\eta]_{PNaA}/[\eta]_{PAA})^{2/3} = 1.16 \qquad (42)$$

This ratio is quite insensitive to the value of M_c. (At M = 3000, for example, it is 1.18.)

The intrinsic viscosity measurements of PVA in the two solvent systems indicated that the variation in polymer dimensions between acidic and basic media is small, and at M = 7500, the value of $\overline{r_{PVA'}^2}_f/\overline{r_{PVA}^2}_f$ was taken to be unity. Application of these values of $\overline{r^2}_f$ in Eq. 27 for m = 0.38 leads to a prediction of $E_{acidic}/E_{ionic} = 1.06$, considerably lower than the estimate from unperturbed dimensions, although the ratio is still greater than 1.

F. Discussion

Several possible reasons can be offered for the lack of quantitative agreement between experiment and theory. First of all, as mentioned above, one of the assumptions used in the development of the theory was that the nature of the crosslink in the PAA-PVA rubber system was taken to be simple esterification. While this is relatively well established,[4] it is quite possible that crosslinking of a different nature could occur. As a matter of fact, one could conceive of a network formed, say, by anhydride crosslinks, where the active chains are mostly PAA and PVA acts mainly as a filler. In this case, the ratio of the moduli in acidic and ionic forms would be the same as that for a rubber network formed from a single ionizable component. Using the approximation that the polymer dimensions are the unperturbed dimensions, the predicted value of E_{acidic}/E_{ionic} for PAA, as obtained from the characteristic ratios and Eq. 28, is 1.65.

If such defects as PAA-PAA crosslinks do occur, it is probable that they would be only a fraction of the total number of crosslinks in the network. A study of the kinetics of anhydride formation in PAA has shown that this reaction is mainly intramolecular;[12] furthermore, as is shown in Appendix B, its rate is low under the conditions employed in this study. However, even a small amount of intermolecular anhydride formation could change the relative numbers of chains of each component. If the number of active PAA chains were significantly greater

than the number of PVA chains, then the value of E_{acidic}/E_{ionic} would be expected to lie somewhere between the values of 1.22 for a two-component rubber (PAA-PVA) and 1.65 for a single-component rubber (PAA). If the original molecular weights of PVA and PAA were different, then the numbers of active chains of each component would be unequal, because there would be unequal numbers of chain ends. However, in the present case, the original molecular weights of PAA and PVA were chosen to be similar. Hence, this should not affect the results appreciably.

Another possibility of error is introduced in the neglect of changes in internal energy with extension; that is, in assuming a purely entropic force. If the variation in internal energy with extension, $(\partial E/\partial L)_{T,V}$, were roughly the same in both cases, then most of this error could be expected to be cancelled in determining the ratio of moduli. However, the variation in internal energy could very well be significantly different for ionic and nonionic chains. In part, $(\partial E/\partial L)_{T,V}$ for an isolated ionic chain would be expected to be lower than the same quantity for the corresponding nonionic chain, because extension would relieve some of the long-range effect of electrostatic repulsion. However, in an ionic gel whose volume does not change on extension, the change in electrostatic energy with extension should be zero, and this effect should not be expected to contribute in the present case. Since the embedding medium for the ionized form of the rubber is of considerable ionic strength, the long-range interactions of the fixed ions will be effectively screened by

the mobile electrolyte. Thus, one would expect only essentially short-range interactions of fixed ions, which are considerable, but which modify only the unperturbed dimensions. It is possible, however, that there may be more subtle electrostatic or internal energy effects for which this argument does not account.

The above reasoning might explain why 1.22, the value of E_{acidic}/E_{ionic} for the case where unperturbed dimensions are assumed, is an underestimate. The following arguments show that the attempt to use low molecular weight analogs as model solvents yields a drastic underestimate of E_{acidic}/E_{ionic}.

One reason for the difficulty in comparing dimensions measured in low molecular weight analog solvents with those in the polymer network environment was suggested by Flory,[13] who proposed the following relationship for polymer coil expansion, α, for dilute solutions of polymers in their oligomers

$$\alpha^5 - \alpha^3 = KP^{1/2}/P_s \qquad (43)$$

where $K \simeq 1$ and P and P_s are the degrees of polymerization of the polymer and the solvent, respectively. This formulation suggests that the values of α in low molecular weight analogs greatly overestimate the values of α in the polymer network, where the solvent is the polymer itself. In effect, this would suggest that the polymers are much closer to a θ environment in the swollen network than they are in the model solvents. This would then provide some justification for using the unperturbed dimensions as the better estimate of the free polymer dimensions.

A second reason for the inaccuracy of the comparison between low molecular weight analog solvents and the solvent environment presented in the polymer network lies in the fact that the contribution of excluded volume to the entropy of polymer networks is different than that of polymer solutions by virtue of the constraints presented by the crosslinks. Mijnlieff and Jaspers[14] point out that, at significant swelling ratios, the number of conformations that the chains can assume becomes more limited, and the overlap regions of nearby chains are considerably reduced. In more extreme cases, intersection of a chain with other chains is considerably less probable than in the solution of equivalent polymer concentration. Since the rubbery modulus is compared at constant volume fraction of diluent, this entropic effect, which is a function of volume fraction, should be cancelled out in determining the ratio of moduli.

However, this entropic effect does influence the choice of the model polymer environment from which the values of $\overline{r^2}_f$ must be obtained. Since a network chain has less contact with other chains than it would have if there were no crosslinks to constrain it, it follows that it must have more contact with the diluent. This means that the environment of the network chains is more like that of the diluent alone than that of the diluent — low-molecular-weight-analog system taken as a model. The extent of this deviation is not easily determined. However, it can be assumed that increasing the amount of diluent (in the

present case, water) in the model solvent will affect an ionic polymer (PNaA) differently than a nonionic polymer (PAA). In fact, the likely result would be an increase in the ratio $\overline{r_{PNaA}^2}_f/\overline{r_{PAA}^2}_f$ as the water content of the solvent increased, and would help to account for the discrepancy between prediction and experiment.

It should be pointed out that the Young's moduli pertinent to the present case could not have been calculated from the data of Kuhn, et al.,[3] for the reason that their measurements of extension versus applied stress were taken in a system completely immersed in solvent, in which case the volume fraction of polymer varied upon neutralization and acidification. The changes in extension that they measured were due to Donnan osmotic force, which is not relevant in measuring the rubbery modulus of a network in which the amount of diluent is kept constant.

Finally, it should be made clear that the observed effect of a ratio of $E_{acidic}/E_{ionic} > 1$ should be generally observable for all ionizable rubbers where effects of aggregation can be removed. The reason for this is the same reason that ionization of a polymer generally produces an increase in the unperturbed dimensions of a polymer chain. If ionization caused a decrease in polymer dimensions, then one would expect to see an increase in modulus on ionization.

G. Conclusions

The rubbery modulus of a crosslinked ionizable rubber has been explored in a system where the additional crosslinking effect of ion aggregation has been eliminated by plasticizing the rubber with a liquid of high dielectric constant. Experimentally, a rubber was prepared by thermally crosslinking a mixture of poly(acrylic acid) and poly(vinyl alcohol). The moduli of the swollen rubber in its acidic and ionic forms were measured and compared at a common volume fraction. In addition, a theory for the modulus of such a two-component rubber was derived and the predictions from the theory were compared with the experimental results. It was found that the predicted ratio of the moduli in the acidic and ionic forms was in the same direction as determined experimentally, but that the calculation underestimated the magnitude of the effect.

REFERENCES

[1] A. Eisenberg, Macromolecules, 3, 147 (1970).

[2] L. R. G. Treloar, "The Physics of Rubber Elasticity," Oxford U. P., London (1958), Chap. IV.

[3] W. Kuhn, A. Ramel, O. Walters, and H. Kuhn, Fortschr. Hochpolym.-Forsch., 1, 540 (1960).

[4] H. Noguchi, Busseiron Kenkyu, 69, 78 (1953).

[5] M. S. Green and A. V. Tobolsky, J. Chem. Phys., 14, 80 (1946).

[6] Treloar, op. cit., Chap. III.

[7] S. Newman, W. R. Krigbaum, C. Laugier, and P. J. Flory, J. Polym. Sci., 14, 451 (1954).

[8] M. Navratil, Ph.D. thesis, McGill Univ., 1972.

[9] A. Takahashi and M. Nagasawa, J. Amer. Chem. Soc., 86, 543 (1964).

[10] H. A. Dieu, J. Polym. Sci., 12, 417 (1954).

[11] M. Kurata and W. H. Stockmayer, Fortschr. Hochpolym.-Forsch., 3, 196 (1963).

[12] A. Eisenberg, T. Yokoyama, and E. Sambalido, J. Polym. Sci., A-1, 7, 1717 (1969).

[13] P. J. Flory, J. Chem. Phys., 17, 303 (1949).

[14] P. F. Mijnlieff and W. J. M. Jaspers, J. Polym. Sci., A-2, 7, 357 (1969).

APPENDIX A

EXPERIMENTAL ERROR

The modulus is given experimentally by the relationship presented in Eq. 11

$$E = (f/A_o)/(L/L_1 - 1) \tag{A1}$$

Each of the quantities inherent in the above equation is subject to experimental error:

force	- ±0.5 g when no observable relaxation occurs, ±1.0 g when observable relaxation occurs, generally 2 or 3%.
area	- ∿5% if measured directly. However, since the area is calculated from the length, weight and density, only the errors in these quantities need be considered.
length	- ±0.01 cm, generally ∿0.5%.
weight	- ±2 mg with high vapor loss in ionic form, ±1 mg with low vapor loss in acidic form, generally ∿0.5%.
density	- ∿0.5% throughout.
extension	- ±0.0002 cm, generally <0.1%.

Thus, a typical error calculation for each form is as follows:

$$\text{acidic form - error} = \frac{1}{55}\,(\text{force}) + \frac{.01}{1.52} \times 2\,(\text{length, twice}) + \frac{.001}{.261}\,(\text{weight}) + 0.5\%\,(\text{density}) \simeq 4\%$$

$$\text{ionic form - error} = \frac{1}{50}\,(\text{force}) + \frac{.01}{2.05} \times 2\,(\text{length}) + \frac{.002}{.434}\,(\text{weight}) + 0.5\%\,(\text{density}) \simeq 4\%$$

APPENDIX B

EXTENT OF ANHYDRIDE FORMATION IN PAA

As discussed in Section C of this chapter, the PAA-PVA mixture was crosslinked by heating at 110°C, in one case for 0.5 hr and in the other for 1.5 hr. The study of the kinetics of anhydride formation in PAA by Eisenberg, et al.,[11] showed that anhydride formation was a first order reaction whose rate constant (in sec^{-1}) can be expressed as

$$k_a = 2.5 \times 10^9 \exp(-2.6 \times 10^4/RT) \qquad (B1)$$

Hence, at 110°C, the value of k_a is 3.6×10^{-6} sec^{-1}, and the rate of anhydride formation may be expressed as

$$-d[A]/dt = 3.6 \times 10^{-6} [A] \qquad (B2)$$

where [A] is the concentration of carboxyl groups. Solution of this differential equation gives the degree of anhydride formation

$$1 - [A]/[A]_o = 1 - \exp(-k_a t) \qquad (B3)$$

Thus, the degree of anhydride formation is 0.65% after 0.5 hr and 1.9% after 1.5 hr.

Although the polymer used in this study was not pure PAA, the degrees of anhydride formation could be expected to be similar to those calculated above, since the reaction is mainly intramolecular. The fraction of intermolecular reactions is unknown, but it would be expected to be smaller than in pure PAA, because of the decreased concentration of PAA in the polymer mixture.

CHAPTER III

THE DILUTE SOLUTION VISCOELASTICITY OF SIMPLE IONIC POLYMERS

A. Introduction

In Chapter I, the theoretical approach to the dilute solution viscoelasticity of polymers was introduced. The model employed with the greatest success is the well-known bead-spring model. This model represents the polymer as a collection of beads on which all of the frictional interaction with the solvent occurs; the beads are joined together by Hookean springs of zero rest length and held apart by Brownian motion forces. The effect of ionization in this model is obtained by considering that the beads contain point charges of equal magnitude. The resulting electrostatic forces between the beads provide an additional parameter in the expression of the equations of motion of the beads.

A realistic model, which would incorporate a large number of charges per chain, presents considerable difficulties. Thus, as a first step in the development of a theory for the dilute solution viscoelasticity of ionic polymers, the elastic dumbbell model (two beads, one spring) was used. This model can serve two purposes in this development — it forms the basis for the description of more complex bead-spring models, and it serves as a

model, itself, for simple ionic polymers which can be readily synthesized, such as carboxy-terminated polymers[1] and polymeric zwitterions.[2] Experimental techniques for the measurement of very dilute solution viscoelastic properties, although still very difficult, are becoming increasingly available,[3] and it is to be expected that experimental data on dilute solutions of ionic polymers may soon appear. Thus, materials such as those mentioned above might be used to test the validity of the model.

In Section B of this chapter, equations of motion will be developed for the two simplest charged bead-spring models — the elastic dumbbell and the three-bead/two-spring assembly. From these equations, the diffusion equation for the distribution function of bead separation in shearing flow will be formulated. The solution of this second order differential equation yields the viscoelastic functions of interest. Because the solution of the diffusion equation for the ionic dumbbell necessitates the use of approximate methods, the approximate solution for the non-ionic dumbbell, whose viscoelastic functions are known in closed form, will be derived in order to evaluate the correctness of the procedure. A more rigorous mathematical proof of the validity of the method will also be offered. Then the same methods will be applied to the ionic dumbbell in order to calculate the intrinsic viscosity and the real and imaginary parts of the complex viscosity in steady and dynamic shear as a function of frequency and for a range of values of the charge and spring parameters. The values are chosen to correspond to real polymers for which the

charged bead-spring model would be appropriate, such as linear dicarboxylic acids and polymeric zwitterions for the dumbbell, and linear triacids for the three-bead model.

It is found that, in the case of the ionic dumbbell, a single relaxation time is retained; that is, the shapes of the curves of dynamic viscosity versus reduced frequency are unchanged, except for a simple shift in the relaxation time. For like charged dumbbells, it is found that both the intrinsic viscosity and the relaxation time increase with increasing charge, while for oppositely charged dumbbells, the intrinsic viscosity and relaxation time decrease.

For the three-bead/two-spring model, whose solution depends in part on the solution of the elastic dumbbell, two single relaxation times are obtained, as in the corresponding nonionic case. As expected from the dumbbell calculations, the intrinsic viscosity increases with increasing charge, as do both relaxation times. In addition, the longer relaxation time increases by a proportionally larger amount than the shorter relaxation time. This leads to the conclusion that in systems of a large number of charges per chain, the distribution of relaxation times would broaden.

B. Theory

The recent review by Bird, et al.[4] gives the derivation of viscoelastic properties of dumbbell suspensions in various types

of flows. Equations are derived in terms of a generalized type of dumbbell in which the connector may be elastic or rigid. The model chosen here is a dumbbell which consists of two beads joined by a connector which is taken to be a Hookean spring of zero rest length. The beads are considered to contain equal electrostatic point charges which yield an additional term for the force which acts on the beads. The suspension of dumbbells is assumed to be at infinite dilution.

If the beads are assigned the space and time coordinates $(x_1,y_1,z_1,t) = (\mathbf{r}_1,t)$ and $(x_2,y_2,z_2,t) = (\mathbf{r}_2,t)$, respectively, then the distribution function, which is a function of all these coordinates, may be taken as $\Psi(\mathbf{r}_1,\mathbf{r}_2,t)$. Ψ may be determined from the diffusion equation which is obtained by combining the equations of motion of the beads with the equation of continuity for the distribution function.

The equations of motion are obtained by equating the inertial force (mass × acceleration) to the sum of the hydrodynamic drag force, the Brownian motion force, and the forces acting along the line of the connector (which are due to the Hookean spring and the electrostatic charges on the beads). The equations obtained are thus

$$m\ddot{\mathbf{r}}_i = -\rho\,(\dot{\mathbf{r}}_i - \mathbf{v}_i) - kT\,(\partial/\partial\mathbf{r}_i)\,\ln\Psi + \mathbf{F}_i\,, \qquad i=1,2 \qquad (1)$$

The expressions $\dot{\mathbf{r}}_i$ and $\ddot{\mathbf{r}}_i$ are the first and second derivatives of $\mathbf{r}_i$ with respect to time. ρ is the friction coefficient of a bead moving through the solvent. $\mathbf{v}_i$ is the relative solvent

velocity at bead i. Hydrodynamic interaction is neglected in this treatment; that is, the motion of bead 2 is not considered to affect the fluid velocity at bead 1, and vice versa. $\mathbf{F}_i$ is the force along the line of the connector acting on bead i and contains Coulombic and Hookean terms. The expression $-kT\,(\partial/\partial \mathbf{r}_i)\,\ln\Psi$ is that used for the "time-averaged" Brownian motion force acting on bead i.[4,5]

The term $\mathbf{v}_i$ can be equated to $[\kappa\cdot\mathbf{r}_i]$, the dot product of κ, a second order tensor which, for homogeneous flows, is independent of position but dependent on time, and $\mathbf{r}_i$, the position vector. κ is specific to the pattern of flow selected. For shearing flows, the components of $[\kappa\cdot\mathbf{r}]$ become greatly simplified to $v_x = \kappa_{xy}y = \kappa y$, and $v_y = v_z = 0$, where κ is the shear rate for simple shear.

Subtraction of Eq. 1 for i = 1 and i = 2, and the substitution of the relative coordinate

$$\mathbf{R} = (\mathbf{r}_1 - \mathbf{r}_2)/2 = (X,Y,Z)$$

gives

$$\dot{\mathbf{R}} = [\kappa\cdot\mathbf{R}] - (kT/2\rho)\,(\partial/\partial\mathbf{R})\,\ln\psi + \mathbf{F}/\rho \qquad (2)$$

Here

$$\mathbf{F}_1 - \mathbf{F}_2 = 2\mathbf{F}_1 = 2\mathbf{F}$$

since $\mathbf{F}_1 = -\mathbf{F}_2$ for a dumbbell. In forming Eq. 2, the inertial terms, $m\ddot{\mathbf{r}}_i$, are neglected since they are assumed to be small. Also, the relevant distribution function is now $\psi = \psi(\mathbf{R},t)$, the distribution of the relative position vector $\mathbf{R}$.[5]

The continuity equation, which may be derived simply from the law of conservation of mass, is given in terms of the distribution function and the relative position vector by[6]

$$\partial\psi/\partial t = - \{\partial/\partial \mathbf{R} \cdot (\dot{\mathbf{R}}\psi)\} \tag{3}$$

The law of conservation of mass applies to the present case, since the total value of ψ over all space is fixed; therefore, Eqs. 2 and 3 may be combined to give the diffusion equation

$$\frac{\partial \psi}{\partial t} = - \frac{\partial}{\partial \mathbf{R}} \cdot \left([\kappa \cdot \mathbf{R}] - \frac{kT}{2\rho} \frac{\partial}{\partial \mathbf{R}} + \frac{\mathbf{F}}{\rho} \right) \psi \tag{4}$$

Following the notation of Bird,[4] it will be convenient to express this equation in the spherical coordinates, R, θ, ϕ, where $X = RSc$, $Y = RSs$ and $Z = RC$, and where $S = \sin\theta$, $C = \cos\theta$, $s = \sin\phi$, $c = \cos\phi$. This gives, in spherical coordinates

$$\begin{aligned} \frac{2\rho}{kT} \frac{\partial \psi}{\partial t} = {} & \frac{1}{R^2} \frac{\partial}{\partial R} \left\{ R^2 \left(\frac{\partial \psi}{\partial R} - \frac{2\rho}{kT} [\kappa \cdot R]_R \psi - \frac{2}{kT} F_R \psi \right) \right\} \\ & + \frac{1}{RS} \frac{\partial}{\partial \theta} \left\{ S \left(\frac{1}{R} \frac{\partial \psi}{\partial \theta} - \frac{2\rho}{kT} [\kappa \cdot R]_\theta \psi \right) \right\} \\ & + \frac{1}{RS} \frac{\partial}{\partial \phi} \left(\frac{1}{RS} \frac{\partial \psi}{\partial \phi} - \frac{2}{kT} [\kappa \cdot R]_\phi \psi \right) \end{aligned} \tag{5}$$

For shearing flows, the components of $[\kappa \cdot \mathbf{R}]$ are

$$[\kappa \cdot R]_R = S^2 sc R\kappa$$

$$[\kappa \cdot R]_\theta = SCsc R\kappa$$

$$[\kappa \cdot R]_\phi = - Ss^2 R\kappa$$

The term F_R in Eq. 5 is the sum of a Hookean term and a Coulombic term, and as such is a function of R only. $\mathbf{F}$ is given by

$$\mathbf{F} = \mathbf{F}_1 = H(\mathbf{r}_2 - \mathbf{r}_1) - (q^2/\varepsilon)\ (\mathbf{r}_2 - \mathbf{r}_1)/|\mathbf{r}_2 - \mathbf{r}_1|^3$$

$$= -\ 2H\mathbf{R} + (q^2/4\varepsilon)\,\mathbf{R}/R^3 \qquad (6)$$

where H is the Hookean spring constant, q is the charge on each bead, and ε is the dielectric constant of the solvent. Hence, the radial component is given by

$$F_R = -\ 2HR + q^2/4\varepsilon R^2$$

By making the further substitutions

$$A = 2\rho/kT$$

$$B = 4H/kT$$

$$E = -\ q^2/2\varepsilon kT$$

Eq. 5 simplifies to

$$A\,\frac{\partial\psi}{\partial t} = \left[\frac{\partial^2}{\partial R^2} + \left(BR + \frac{2}{R} + \frac{E}{R^2}\right)\frac{\partial}{\partial R} + 3B + \frac{C}{R^2S}\,\frac{\partial}{\partial\theta} + \frac{1}{R^2}\,\frac{\partial^2}{\partial\theta^2} + \frac{1}{R^2S^2}\,\frac{\partial^2}{\partial\phi^2}\right]\psi$$

$$- A\kappa sc\left[S^2R\,\frac{\partial}{\partial R} + SC\,\frac{\partial}{\partial\theta} - \frac{s}{c}\,\frac{\partial}{\partial\phi}\right]\psi \qquad (7)$$

If κ is a periodic function of time, it may be written in the form

$$\kappa(t) = \kappa_o\, e^{i\omega t}$$

An approximate solution of Eq. 7 can be obtained by replacing ψ by an infinite series in powers of κ

$$\psi = \psi_o \sum_{n=0}^{\infty} (A\kappa)^n\, \Lambda_n\ , \qquad \Lambda_o \equiv 1$$

When coefficients of $(A\kappa)^n$ are equated, a recursion relationship for Λ_n results.

Bird, et al.[4] point out that κ is more correctly described by the function

$$\kappa(t) = \mathrm{Re}\ \{\kappa_0^*\ \exp(i\omega t)\}$$

where κ_0^* is a complex quantity. However, since the calculation of viscosity will require only the first two terms of the power series for ψ, the simple exponential notation is sufficient to give the correct result.

The exact solution of ψ_0 is obtained by solving Eq. 7 for $\kappa = 0$

$$\psi_0 = \text{const.} \times \exp(E/R - BR^2/2) \tag{8}$$

The arbitrary constant is unimportant, since it may be removed by normalizing the distribution function. This solution is consistent with the boundary condition of $\psi_0(0) = \psi_0(\infty) = 0$. [$\psi_0(0)$ must equal zero since the Coulombic force at R = 0 becomes infinite.]

If the series approximation is substituted for ψ in Eq. 7, and coefficients of $(A\kappa)^n$ are equated, one obtains for $n \geq 1$

$$\left[\frac{\partial^2}{\partial R^2} + \left(\frac{2}{R} + BR + \frac{E}{R^2}\right)\frac{\partial}{\partial R} + 3B + \frac{C}{R^2 S}\frac{\partial}{\partial \theta} + \frac{1}{R^2}\frac{\partial^2}{\partial \theta^2} + \frac{1}{R^2 S^2}\frac{\partial^2}{\partial \phi^2} - in\omega A\right]\Lambda_n\psi_0$$

$$= \left(scS^2R\frac{\partial}{\partial R} + scSC\frac{\partial}{\partial \theta} - s^2\frac{\partial}{\partial \phi}\right)\Lambda_{n-1}\psi_0 \tag{9}$$

In particular for n = 1, inserting ψ_0 as given in Eq. 8 and recalling that $\Lambda_0 \equiv 1$, Eq. 9 becomes

$$\left[\frac{\partial^2}{\partial R^2} + \left(\frac{2}{R} - BR - \frac{E}{R^2}\right)\frac{\partial}{\partial R} + \frac{C}{R^2 S}\frac{\partial}{\partial \theta} + \frac{1}{R^2}\frac{\partial}{\partial \theta^2} + \frac{1}{R^2 S^2}\frac{\partial^2}{\partial \phi^2} - i\omega A\right]\Lambda_1 = -S^2 sc\left(\frac{E}{R} + BR^2\right) \qquad (10)$$

The solution of this equation will be the solution of physical interest for low shear rates (small κ) and may be expressed in the form

$$\psi = \psi_0 (1 + A\kappa\Lambda_1) \qquad (11)$$

Experimentally, this is justified because values of κ for dynamic shear are generally low, and higher members of the series can be neglected.

For the three-bead/two-spring system (3B2S), if one considers only the case of identically charged beads joined by springs of equal Hookean force constants, then one can express three equations of motion for the three beads; these can be combined into two equations in internal coordinates. If the same coordinate transformation that is used for the nonionic case is employed, two distinct relaxation times for the ionic case will be obtained which can be compared with those of the nonionic model.

The distribution function is given by

$$\Psi = \Psi(\mathbf{r}_1, \mathbf{r}_2, \mathbf{r}_3, t)$$

The equations of motion of the beads may thus be written

$$m\ddot{\mathbf{r}}_i = -\rho(\dot{\mathbf{r}}_i - \mathbf{v}_i) - kT(\partial/\partial \mathbf{r}_i) \ln \Psi + \mathbf{F}_i, \quad i=1,2,3 \qquad (12)$$

The symbols in Eq. 12 have the same significance as in Eq. 1. The expressions for the F_i may be written as

$$\mathbf{F}_1 = H(\mathbf{r}_2 - \mathbf{r}_1) - \frac{q^2(\mathbf{r}_2 - \mathbf{r}_1)}{\varepsilon |\mathbf{r}_2 - \mathbf{r}_1|^3} - \frac{q^2(\mathbf{r}_3 - \mathbf{r}_1)}{\varepsilon |\mathbf{r}_3 - \mathbf{r}_1|^3}$$

$$\mathbf{F}_2 = H(\mathbf{r}_1 + \mathbf{r}_3 - 2\mathbf{r}_2) - \frac{q^2(\mathbf{r}_1 - \mathbf{r}_2)}{\varepsilon |\mathbf{r}_1 - \mathbf{r}_2|^3} - \frac{q^2(\mathbf{r}_3 - \mathbf{r}_2)}{\varepsilon |\mathbf{r}_3 - \mathbf{r}_2|^3}$$

$$\mathbf{F}_3 = H(\mathbf{r}_2 - \mathbf{r}_3) - \frac{q^2(\mathbf{r}_2 - \mathbf{r}_3)}{\varepsilon |\mathbf{r}_2 - \mathbf{r}_3|^3} - \frac{q^2(\mathbf{r}_1 - \mathbf{r}_3)}{\varepsilon |\mathbf{r}_1 - \mathbf{r}_3|^3} \qquad (13)$$

H, q, and ε have the same meaning as in Eq. 6.

It will be shown in Section D that the ionic dumbbell has a relaxation time which is given by a simple multiplicative shift of that of the nonionic dumbbell. This is equivalent to the result which would have been obtained if the 1–2 (or 2–3) Coulombic force were combined with the 1–2 (or 2–3) Hookean force and the sum expressed as a "pseudo-Hookean" force with a new constant, H'. This is done with the 1–2 and 2–3 Coulombic forces in Eq. 13; if this step were not taken, then subsequent coordinate separation would be impossible. Since the 1–3 Coulombic force has no Hookean counterpart, it remains unchanged in Eq. 13. Hence, one can write

$$\mathbf{F}_1 = H'(\mathbf{r}_2 - \mathbf{r}_1) - \frac{q^2(\mathbf{r}_3 - \mathbf{r}_1)}{\varepsilon |\mathbf{r}_3 - \mathbf{r}_1|^3}$$

$$\mathbf{F}_2 = H'(\mathbf{r}_1 + \mathbf{r}_3 - 2\mathbf{r}_2)$$

$$\mathbf{F}_3 = H'(\mathbf{r}_2 - \mathbf{r}_3) - \frac{q^2(\mathbf{r}_1 - \mathbf{r}_3)}{\varepsilon |\mathbf{r}_1 - \mathbf{r}_3|^3} \qquad (14)$$

The calculation of the values of H' will be left for Section D.

The relative coordinates $\mathbf{r}_0$, $\mathbb{R}_1$, and $\mathbb{R}_2$ are obtained by the same coordinate transformation used by Zimm[5] for the nonionic case

$$\mathbb{R} = \mathbf{Q}^{-1} \cdot \mathbf{r}$$

$$\partial/\partial\mathbb{R} = \mathbf{Q}^{T} \cdot \partial/\partial\mathbf{r}$$

If the matrix $\mathbf{Q}$ is taken to be

$$\mathbf{Q} = \begin{bmatrix} 1 & 1 & 1 \\ 1 & 0 & -2 \\ 1 & -1 & 1 \end{bmatrix} \tag{15}$$

then the relative coordinates are given by

$$\mathbf{r}_0 = (\mathbf{r}_1 + \mathbf{r}_2 + \mathbf{r}_3) \qquad \text{(center of mass)}$$

$$\mathbb{R}_1 = (\mathbf{r}_1 - \mathbf{r}_3)/2$$

$$\mathbb{R}_2 = (\mathbf{r}_1 + \mathbf{r}_3 - 2\mathbf{r}_2)/6$$

As in the dumbbell case, the relevant distribution function is now $\psi(\mathbb{R}_1, \mathbb{R}_2, t)$, which is constant with respect to $\mathbf{r}_0$.

The relative equations of motion for $\mathbb{R}_1$ and $\mathbb{R}_2$ are then obtained by combining Eq. 12 for i = 1, 2, 3 in the same ratios as the coordinates given above and inserting the values of $\mathbb{F}_i$ from Eq. 14. This yields

$$\dot{\mathbb{R}}_1 = [\kappa \cdot \mathbb{R}_1] - \frac{kT}{2\rho} \frac{\partial}{\partial \mathbb{R}_1} \ln \psi - \frac{H'}{\rho} \mathbb{R}_1 + \frac{q^2}{4\varepsilon\rho} \frac{\mathbb{R}_1}{|\mathbb{R}_1|^3}$$

$$\dot{\mathbb{R}}_2 = [\kappa \cdot \mathbb{R}_2] - \frac{kT}{6\rho} \frac{\partial}{\partial \mathbb{R}_2} \ln \psi - \frac{3H'}{\rho} \mathbb{R}_2 \tag{16}$$

The continuity equation, in relative coordinates, is given by

$$\partial\psi/\partial t = - \{\partial/\partial \mathbf{R}_1 \cdot (\dot{\mathbf{R}}_1 \psi) + \partial/\partial \mathbf{R}_2 \cdot (\dot{\mathbf{R}}_2 \psi)\} \tag{17}$$

Hence, the diffusion equation obtained by combining Eqs. 16 and 17 is

$$\frac{\partial \psi}{\partial t} = \frac{\partial}{\partial \mathbf{R}_1} \cdot \left([\kappa \cdot \mathbf{R}_1] - \frac{kT}{2\rho} \frac{\partial}{\partial \mathbf{R}_1} - \frac{H'}{\rho} \mathbf{R}_1 + \frac{q^2}{4\varepsilon\rho} \frac{\mathbf{R}_1}{|\mathbf{R}_1|^3} \right) \psi$$

$$- \frac{\partial}{\partial \mathbf{R}_2} \cdot \left([\kappa \cdot \mathbf{R}_2] - \frac{kT}{6\rho} \frac{\partial}{\partial \mathbf{R}_2} - \frac{3H'}{\rho} \mathbf{R}_2 \right) \psi \tag{18}$$

With the usual conversion to spherical coordinates, and with the substitutions

$$A = 2\rho/kT$$

$$B' = 2H'/kT$$

$$E = - q^2/2\varepsilon kT$$

one obtains

$$\begin{aligned} A \frac{\partial \psi}{\partial t} = & \left[\frac{\partial^2}{\partial R_1^2} + \left(\frac{2}{R_1} + B' R_1 + \frac{E}{R_1^2} \right) \frac{\partial}{\partial R_1} + 3B' \right. \\ & \left. + \frac{1}{R_1^2} \frac{\partial^2}{\partial \theta_1^2} + \frac{C_1}{R_1^2 S_1} \frac{\partial}{\partial \theta_1} + \frac{1}{R_1^2 S_1^2} \frac{\partial^2}{\partial \theta_1^2} \right] \psi \\ & - A\kappa S_1 C_1 \left[(S_1^2 R_1) \frac{\partial}{\partial R_1} + (S_1 C_1) \frac{\partial}{\partial \theta_1} - \frac{S_1}{C_1} \frac{\partial}{\partial \phi_1} \right] \psi \\ & + \frac{1}{3} \left[\frac{\partial^2}{\partial R_2^2} + \left(\frac{2}{R_2} + 9B' R_2 \right) \frac{\partial}{\partial R_2} + 27B' \right. \\ & \left. + \frac{1}{R_2^2} \frac{\partial^2}{\partial \theta_2^2} + \frac{C_2}{R_2^2 S_2} \frac{\partial}{\partial \theta_2} + \frac{1}{R_2^2 S_2^2} \frac{\partial^2}{\partial \phi_2^2} \right] \psi \\ & - A\kappa S_2 C_2 \left[(S_2^2 R_2) \frac{\partial}{\partial R_2} + (S_2 C_2) \frac{\partial}{\partial \theta_2} - \frac{S_2}{C_2} \frac{\partial}{\partial \phi_2} \right] \psi \end{aligned} \tag{19}$$

As in the dumbbell case, an infinite series solution for ψ is assumed. For n = 0, the exact solution is obtained

$$\psi_0 = \text{const.} \times \exp(E/R_1 - B'R_1^2/2 - 9B'R_2^2/2) \tag{20}$$

As before, this solution is the one which is consistent with the boundary conditions, $\psi(0) = \psi(\infty) = 0$. For E = 0, it is identical with that obtained for the nonionic case.

By substituting the series expansion for ψ in Eq. 19, the recursion relation for Λ_n is obtained

$$\left[\nabla_1^2 + \left(B'R_1 + \frac{E}{R_1^2}\right)\frac{\partial}{\partial R_1} + 3B\right]\Lambda_n\psi_0$$

$$+ \frac{1}{3}\left[\nabla_2^2 + 9B'R_2\frac{\partial}{\partial R_2} + 27B'\right]\Lambda_n\psi_0 - in\omega A\Lambda_n\psi_0$$

$$= \sum_{i=1}^{2}\left(s_i c_i S_i^2 R_i \frac{\partial}{\partial R_i} + s_i c_i S_i C_i \frac{\partial}{\partial \theta_i}\right.$$

$$\left. - s_i^2 \frac{\partial}{\partial \phi_1}\right)\Lambda_{n-1}\psi_0 \tag{21}$$

For simplicity, the operators ∇_1^2 and ∇_2^2 are not expanded. In particular for n = 1, one obtains, by substituting for ψ_0

$$\left[\nabla_1^2 - \left(B'R_1 + \frac{E}{R_1^2}\right)\frac{\partial}{\partial R_1}\right]\Lambda_1$$

$$+ \frac{1}{3}\left[\nabla_2^2 - 9B'R_2\frac{\partial}{\partial R_2}\right]\Lambda_1 - i\omega A\Lambda_1$$

$$= -S_1^2 s_1 c_1\left(\frac{E}{R_1} + B'R_1^2\right) - 9S_2^2 s_2 c_2 B'R_2^2 \tag{22}$$

As in the case of the dumbbell, the solution of this equation will be the solution of physical interest for low shear rates.

C. Application of Theory to Shearing Flow

For the dumbbells, the shear stress per unit volume, τ_p, is given by the expression[7]

$$\tau_p = n_o \sum_{j=1}^{2} \langle (y_j - y_o)\ f_{xj} \rangle \tag{23}$$

The triangular brackets in Eq. 23 indicate the calculation of the expectation value of the quantity they contain. In Eq. 23, n_o is the concentration of dumbbells and f_{xj} is the hydrodynamic drag on bead j. y_j and y_o are the y-coordinates of the $j^{\underline{th}}$ bead and the center of mass respectively. The expressions for f_{xj} are obtained from Eq. 1

$$f_{x_1} = H\ (x_2 - x_1) - \frac{q^2\ (x_2 - x_1)}{\varepsilon\ |r_2 - r_1|^3} - kT\ \frac{\partial}{\partial x_1} \ln \Psi$$

$$f_{x_2} = H\ (x_1 - x_2) - \frac{q^2\ (x_1 - x_2)}{\varepsilon\ |r_2 - r_1|^3} - kT\ \frac{\partial}{\partial x_2} \ln \Psi \tag{24}$$

The expectation values of terms containing $(\partial/\partial x_j)\ \ln \Psi$ are zero since $\psi(\infty) = 0$. Upon conversion to relative spherical coordinates, the remaining terms yield the expression

$$\tau_p = - n_o \{4H \langle R^2 S^2 sc \rangle - (q^2/2\varepsilon) \langle S^2 sc/R \rangle\} \tag{25}$$

Hence the relative complex viscosity is given by

$$\eta^* - \eta_s = - \tau_p/\kappa$$

$$= (n_o/\kappa) \{4H \langle R^2 S^2 sc \rangle - (q^2/2\varepsilon) \langle S^2 sc/R \rangle\} \qquad (26)$$

It is to be noted that the expectation values may be time dependent.

For steady shear ($\omega = 0$), a particular solution of Eq. 10 in closed form is available

$$\Lambda_1 = R^2 S^2 sc/2 \qquad (27)$$

Λ_1 is identical with that obtained for the nonionic dumbbell in the case of steady shear; for low shear rates, it is the solution of physical interest. Evaluation of the expectation values will immediately give the relative viscosity from which the intrinsic viscosity can be obtained. The results of such calculations will be discussed in the next section.

For dynamic shear, Λ_1 has the form

$$\Lambda_1 = F^*(R)\ S^2 sc \qquad (28)$$

where $F^*(R)$ is a complex function of R only. (See Appendix A.) Substitution of Eq. 28 in Eq. 10 results in the equation

$$\left[\frac{\partial^2}{\partial R^2} + \left(\frac{2}{R} - \frac{E}{R^2} - BR\right)\frac{\partial}{\partial R} - \frac{6}{R^2} - i\omega A\right] F^* = - \left(\frac{E}{R} + BR^2\right) \qquad (29)$$

For the nonionic case ($E = 0$), the relevant particular solution of Eq. 29 is

$$F_o^*(R) = R^2/(2 + i\omega A/B) \qquad (30)$$

For the ionic case, it is assumed that $F^*(R)$ approaches $F_o^*(R)$ asymptotically at large values of R, where the effects of the electrostatic charges will be small. At low values of R, it is assumed that $F^*(R)$ deviates from $F_o^*(R)$, but retains the same sign, since it is a distribution function, and has the value 0 at some (very) small value of R, consistent with the condition that the Coulombic force varies as $1/R^2$ and would be very large at small values of R. Anticipating the need for numerical calculation, it is worthwhile to point out that, since the force would become infinite at R = 0, it is necessary to choose the lower boundary to be a small value of R. Specifically, for calculational purposes, the lower boundary is chosen to equal 1 Å; it will be shown that this value is not critical, as long as it is sufficiently small. An estimate of the error involved in this approximation is presented in Appendix B.

By replacing the expectation values with their integral forms, one obtains, from Eqs. 11 and 26

$$\eta^* - \eta_s = \frac{n_o}{\kappa J}\left\{4H\int_0^{2\pi}\int_0^{\pi}\int_0^{\infty}\psi_o\ (1 + A\kappa\Lambda_1)\ R^4dR\ S^3d\theta\ scd\phi\right.$$

$$\left. - \frac{q^2}{2\varepsilon}\int_0^{2\pi}\int_0^{\pi}\int_0^{\infty}\psi_o\ (1 + A\kappa\Lambda_1)\ RdR\ S^3d\theta\ scd\phi\right\} \qquad (31)$$

The normalization factor of the distribution function, J, is defined as

$$J = \int_0^{2\pi}\int_0^{\pi}\int_0^{\infty}\psi_o\ R^2dR\ Sd\theta\ d\phi$$

Upon substitution of the expressions for ψ_0 and Λ_1, as given in Eqs. 8 and 28, into Eq. 31, and integration of all but the radial terms, the expression simplifies to

$$\eta^* - \eta_s = \frac{n_0 A}{15} \left\{ \frac{\int F^*(R)\ \exp(E/R - BR^2/2)\ (4HR^4 - q^2R/2\varepsilon)\ dR}{\int R^2\ \exp(E/R - BR^2/2)\ dR} \right\} \quad (32)$$

In Eq. 32 and in subsequent equations, the limits of integration are understood to be 0 and ∞.

To be consistent with the notation of Bird[4] and Zimm,[5] $A/B = \rho/2H$ is replaced by $2\lambda_0$, where λ_0 is the relaxation time of the nonionic dumbbell. Also, by substituting for H and q^2/ε, Eq. 32 becomes

$$\eta^* - \eta_s = \frac{2n_0 kT\lambda_0 B}{15} \left\{ \frac{\int F^*(R)\ \exp(E/R - BR^2/2)\ (BR^4 + ER)\ dR}{\int R^2\ \exp(E/R - BR^2/2)\ dR} \right\} \quad (33)$$

For the nonionic dumbbell (E = 0), Eqs. 30 and 33 yield

$$(\eta^* - \eta_s)_0 = \frac{n_0 kT\lambda_0}{1 + i\omega\lambda_0} \left\{ \frac{B^2}{15} \frac{\int R^6\ \exp(-BR^2/2)\ dR}{\int R^2\ \exp(-BR^2/2)\ dR} \right\} \quad (34)$$

Evaluation of the above definite integrals gives the final result

$$(\eta^* - \eta_s)_0 = n_0 kT\lambda_0/(1 + i\omega\lambda_0) \quad (35)$$

This expression is the same as that obtained by Zimm[5] without the necessity of specifically determining ψ.

For the ionic dumbbell, Eq. 29 is solved for different values of the constants B, E and ωA. F*(R) is obtained by a

boundary value method which is as follows: In Eq. 29, the substitution

$$F^*(R) = u(R) + iv(R)$$

is made. Then by equating real and imaginary parts, one obtains the simultaneous equations

$$u'' = \left(\frac{E}{R^2} + BR - \frac{2}{R}\right) u' + \frac{6}{R^2} u - \omega A v - \frac{E}{R} - BR^2$$

$$v'' = \left(\frac{E}{R^2} + BR - \frac{2}{R}\right) v' + \frac{6}{R^2} v + \omega A u \qquad (36)$$

The boundary conditions for the upper boundary are

$$u(R \text{ large}) = u_0(R \text{ large}) = 2(R \text{ large})^2/(4 + \omega^2 A^2/B^2)$$

$$v(R \text{ large}) = v_0(R \text{ large}) = -(\omega A/B)(R \text{ large})^2/(4 + \omega^2 A^2/B^2)$$

and for the lower boundary

$$u(R \text{ small}) = v(R \text{ small}) = 0$$

The choice of upper boundary, R large, is somewhat arbitrary, but the solution is rather insensitive to it provided that R is chosen to be sufficiently large. The boundary was chosen so that the ratio of Coulombic to Hookean force, $(E/R^2)/(BR)$, was smaller than 0.01% for each value of B and E used. (This value provides an estimate of the error at the upper boundary.) Eq. 36 was solved for various sets of the constants B, E and ωA. For each set, initial values of u' and v' at the upper boundary were chosen. Then, by employing a Runge-Kutta initial value method,[8] u(R) and v(R) were obtained by stepwise approximation to the lower boundary. The values of u' and v' at the upper boundary were then

varied by successive refinements until the lower boundary condition ($u = v = 0$) was approximately satisfied. (The computer program for this method of solution is presented in Appendix C, along with a sample calculation.) Finally, insertion of the function

$$u(R) + iv(R) = F^*(R)$$

in Eq. 33 and numerical evaluation of the resulting integrals gave the relative complex viscosity as a function of ωA, B, and E.

For the 3B2S system, the analysis of the stress due to the polymer follows the same pattern as for the dumbbell system. The stress per unit volume due to the polymer is given by

$$\tau_p = n_o \sum_{j=1}^{3} \left\langle (y_j - y_o)\ f_{xj} \right\rangle \tag{37}$$

where the symbols have the same meaning as in Eq. 23. The expressions for f_{xj} are obtained from the equation of motion (Eq. 12) as in the dumbbell case. With the transformation to relative spherical coordinates, and the elimination of terms containing $(\partial/\partial x_i)$ ln Ψ, which vanish upon integration, the stress becomes

$$\tau_p = - n_o \{2H' \left\langle R_1^2 S_1^2 s_1 c_1 \right\rangle + 18H' \left\langle R_2^2 S_2^2 s_2 c_2 \right\rangle - (q^2/4\varepsilon) \left\langle S_1^2 s_1 c_1 / R_1 \right\rangle\} \tag{38}$$

Finally, the complex viscosity is given by

$$\eta^* - \eta_s = - \tau_p/\kappa$$

$$= (n_o/\kappa) \{2H' \langle R_1^2 S_1^2 s_1 c_1 \rangle + 18H' \langle R_2^2 S_2^2 s_2 c_2 \rangle$$

$$- (q^2/4\varepsilon) \langle S_1^2 s_1 c_1 / R_1 \rangle\} \qquad (39)$$

For steady shear ($\omega = 0$), the particular solution of interest (for low shear rates) is obtained as

$$\Lambda_1 = R_1^2 S_1^2 s_1 c_1/2 + 3R_2^2 S_2^2 s_2 c_2/2 \qquad (40)$$

This is identical to Zimm's solution[5] for the nonionic 3B2S system.

For dynamic shear, Λ_1 has the form

$$\Lambda_1 = F^*(R_1)\ S_1^2 s_1 c_1 + G^*(R_2)\ S_2^2 s_2 c_2 \qquad (41)$$

for the same arguments as given in Appendix A for the dumbbell. $G^*(R_2)$, which contains no explicit ionic terms, is formally the same as that obtained for the nonionic case

$$G^*(R_2) = 9R_2^2/(6 + i\omega A/B') \qquad (42)$$

$F^*(R_1)$ is formally the same as that obtained for the dumbbell case, except that the constant B' is defined differently. Hence, the same numerical solutions as those obtained for the dumbbell may be used.

Replacement of expectation values by the appropriate integrals in Eq. 39, and evaluation of all but the radial terms results in

$$\eta^* - \eta_s = \frac{n_0 A}{15} \times$$

$$\left\{ \frac{\int F^*(R_1)\, \exp(E/R_1 - B'R_1^2/2)\, (2H'R_1^4 - q^2R_1/2\varepsilon)\, dR_1}{\int R_1^2\, \exp(E/R_1 - B'R_1^2/2)\, dR_1} + \frac{\int G^*(R_2)\, \exp(-9B'R_2^2/2)\, (18H'R_2^4)\, dR_2}{\int R_2^2\, \exp(-9B'R_2^2/2)\, dR_2} \right\} \tag{43}$$

Replacement of $A/B' = \rho/H'$ by $2\lambda_1$, where λ_1 is the longest relaxation time of the assembly, and substitution for H' and q^2/ε gives

$$\eta^* - \eta_s = \frac{2n_0 kT\lambda_1 B'}{15} \times$$

$$\left\{ \frac{\int F^*(R_1)\, \exp(E/R_1 - B'R_1^2/2)\, (B'R_1^4 + ER_1)\, dR_1}{\int R_1^2\, \exp(E/R_1 - B'R_1^2/2)\, dR_1} + \frac{\int G^*(R_2)\, \exp(-9B'R_2^2/2)\, (9B'R_2^4)\, dR_2}{\int R_2^2\, \exp(-9B'R_2^2/2)\, dR_2} \right\} \tag{44}$$

For the nonionic case (where $E = 0$), $F^*(R_1)$ becomes

$$F_0^*(R_1) = R_1^2/(2 + i\omega A/B') \tag{45}$$

Hence, insertion of the expressions for $F^*(R_1)$ and $G^*(R_2)$ in Eq. 44 results in the expression for the viscosity as obtained by Zimm[5]

$$(\eta^* - \eta_s)_0 = \frac{n_0 kT\lambda_1 (B')^2}{15} \left\{ \frac{1}{1 + i\omega\lambda_1} \frac{\int R_1^6\, \exp(-B'R_1^2/2)\, dR_1}{\int R_1^2\, \exp(-B'R_1^2/2)\, dR_1} + \frac{81}{3 + i\omega\lambda_1} \frac{\int R_2^6\, \exp(-9B'R_2^2/2)\, dR_2}{\int R_2^2\, \exp(-9B'R_2^2/2)\, dR_2} \right\}$$

$$= n_0 kT\lambda_1 \left[1/(1 + i\omega\lambda_1) + 1/(3 + i\omega\lambda_1)\right]$$

or

$$(\eta^* - \eta_s)_o = n_o kT \sum_{j=1}^{2} \frac{\lambda j}{1 + i\omega\lambda_j} \tag{46}$$

since $\lambda_2 = \lambda_1/3$ for the nonionic case.

For the ionic case in dynamic shear, the exact solution for $G^*(R_2)$ is given in Eq. 42. This gives the shorter relaxation time, λ_2. For the longer relaxation time, λ_1, one need only reinterpret the constant B and employ the same solution as obtained for the dumbbell. An example of this will be given in the next section.

D. Calculations and Results

The constants A, B and E, which appear in Eq. 7 and in subsequent equations, were estimated by comparison with the physical parameters of real polymers. A real system which could be approximated by the ionic dumbbell model is the series of linear dicarboxylic salts. For sufficiently long diacid chains, the distribution of end-to-end distances can be described as Gaussian, in which case the attractive force, f_H, between the ends of the chain is given by[9]

$$f_H = (3kT/\overline{R^2}_o)\ R$$

where R is the end-to-end distance. $\overline{R^2}_o$ is the mean square value of R in the unionized acid. The constant $3kT/\overline{R^2}_o$ is thus associated with H as given in Eq. 6, and hence with B in Eq. 7. It

must not be forgotten that this is only an approximation which has its limitations for short-chain polymers. For the doubly ionized acid, the Coulombic force, f_c, between the chain ends is given by the same expression as for the dumbbell model

$$f_c = - q^2/\varepsilon R^2$$

where the symbols have the same meaning as in Eq. 6; hence, E is given by $- q^2/2\varepsilon kT$. The value of ε is taken to be that of the pure solvent, although it is recognized that it would be decreased somewhat by presence of the polymer itself.

The constant $A = \rho/2kT$ contains the indeterminate quantity ρ, which is related to the relaxation time, λ_o, of the nonionic dumbbell by $\lambda_o = \rho/4H = A/2B$. Since we are only interested in the fractional change in the relaxation time upon ionization, λ_o is included in the expression for reduced frequency, $\omega\lambda_o$.

A different class of materials for which the ionic dumbbell model may apply is the series of macromolecular zwitterions. In this case, the Coulombic force would be attractive, and as a result, the dumbbell model would have to be applied with some caution, since the attractive force increases without limit as R becomes small. Obviously, the dumbbell model does not account for the chain nature of real polymers. However, for small values of E, the distribution function of end-to-end distances may be cut off at a small value of R in order to evaluate the viscoelastic functions.

The values of B can be estimated from intrinsic viscosity data on the unionized material in the appropriate solvent. In the absence of such data, estimates can be made from the dimensions of known polymers of equivalent flexibility.

To determine how variations in the relevant physical parameters affect the relaxation time, several numerical values of both E and B were used in Eq. 29 for a range of values of ωA (or equivalently $\omega\lambda_0$); for the dicarboxylic acids, $E = -q^2/\varepsilon kT$, as defined earlier, and $B = 3/\overline{R^2}_\theta$. Some typical examples are described below:

(i) for an ionized C_{10} dicarboxylic acid in water at 25°C ($\varepsilon = 78.5$), $E = -3.55$ Å and $B = 0.096$ Å^{-2}, taking the mean square end-to-end distance to be the same as that of polyethylene in a θ solvent;[10] i.e., $\sigma = 1.63$.

(ii) for an ionized C_{30} dicarboxylic acid in water at 25°C, $B = 0.032$ Å^{-2} and $E = -3.55$ Å as in (i). A comparison of (i) and (ii) shows the effect of changing chain length, while keeping charges constant.

(iii) for an ionized C_{30} dicarboxylic acid in ethanol at 25°C ($\varepsilon = 24.3$), $E = -11.5$ Å and $B = 0.032$ Å^{-2}. A comparison of (ii) and (iii) shows the effect of decreasing the dielectric constant (which is equivalent to increasing the charge). The value of B will also change with the change in solvent, but no account is taken here of variations in the dimensions of the unionized polymer

which result from excluded volume considerations.

(iv) for a C_{30} zwitterion in water at 25°C, which may or may not exist as such under these circumstances, E = +3.55 Å and B = 0.032 $Å^{-2}$. The distribution function, ψ, was cut off at 2 Å for the calculation. A comparison of (ii) and (iv) shows the effect of changing the sign of E.

It should be realized that these examples are taken for illustrative purposes only, and not as a prediction of what will actually be encountered in experiments. It is obvious that a variety of factors which affect these parameters have been neglected, but further refinements in such a simple model would be unwarranted.

For each set of values of E and B, $[\eta]/[\eta]_0$, the intrinsic viscosity relative to that of the unionized material, was calculated from Eq. 33. In preliminary graphs, it was found that $[\eta]/[\eta]_0$ varied approximately linearly with both E and $B^{1/2}$; therefore, the viscosities, which are shown in Fig. 1 (solid line), are plotted as a function of the dimensionless parameter, $-EB^{1/2}$, which reflects the ratio of charge to end-to-end distance.

Then, for each set of values of E and B, the functions $[\eta']/[\eta]$ and $[\eta'']/[\eta]$ were calculated for a range of values of $\omega\lambda_0$. For each system, they form a curve, which within calculational error, is of the same shape as that for the unionized polymer. As an example of this, $[\eta'']/[\eta]$ is plotted in Fig. 2 as

FIGURE 1

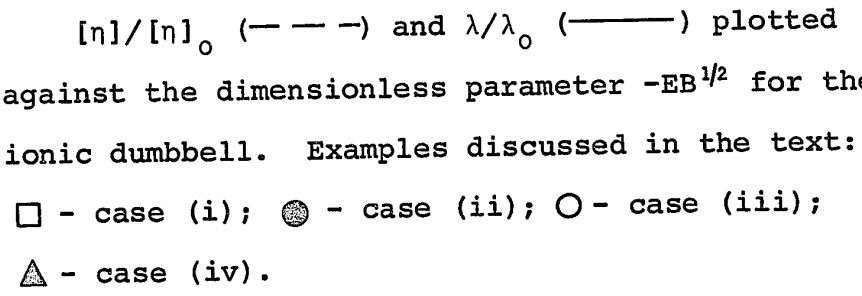
$[\eta]/[\eta]_o$ (— — —) and λ/λ_o (———) plotted
against the dimensionless parameter $-EB^{1/2}$ for the
ionic dumbbell. Examples discussed in the text:
□ - case (i); ◍ - case (ii); ○ - case (iii);
△ - case (iv).

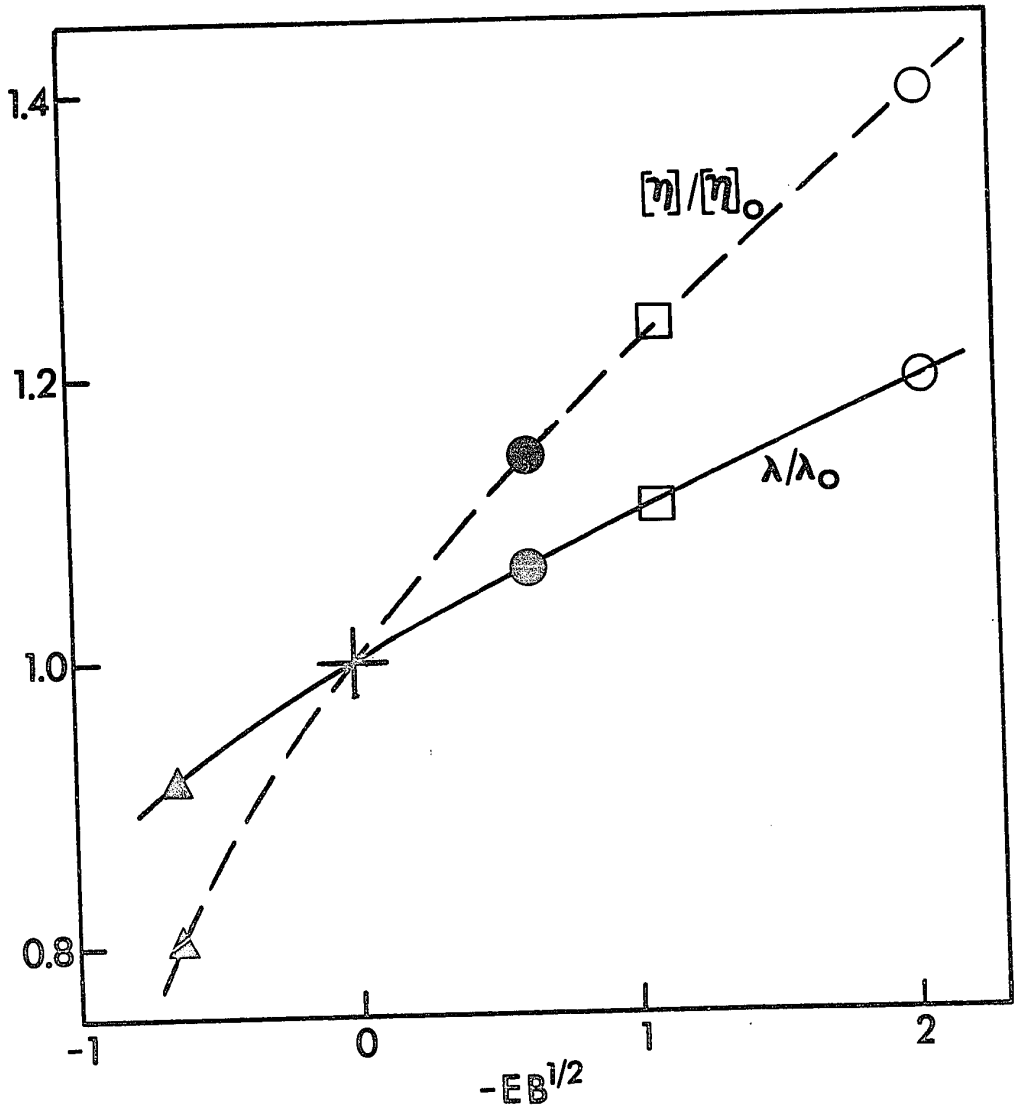
1.4
1.2
1.0
0.8
-1
0
1
2
$-EB^{1/2}$
$[\eta]/[\eta]_o$
λ/λ_o

FIGURE 2

$[\eta'']/[\eta]$ versus $\omega\lambda_o$ for C_{10} diacid in water in nonionic (————) and ionic (— — —) forms.

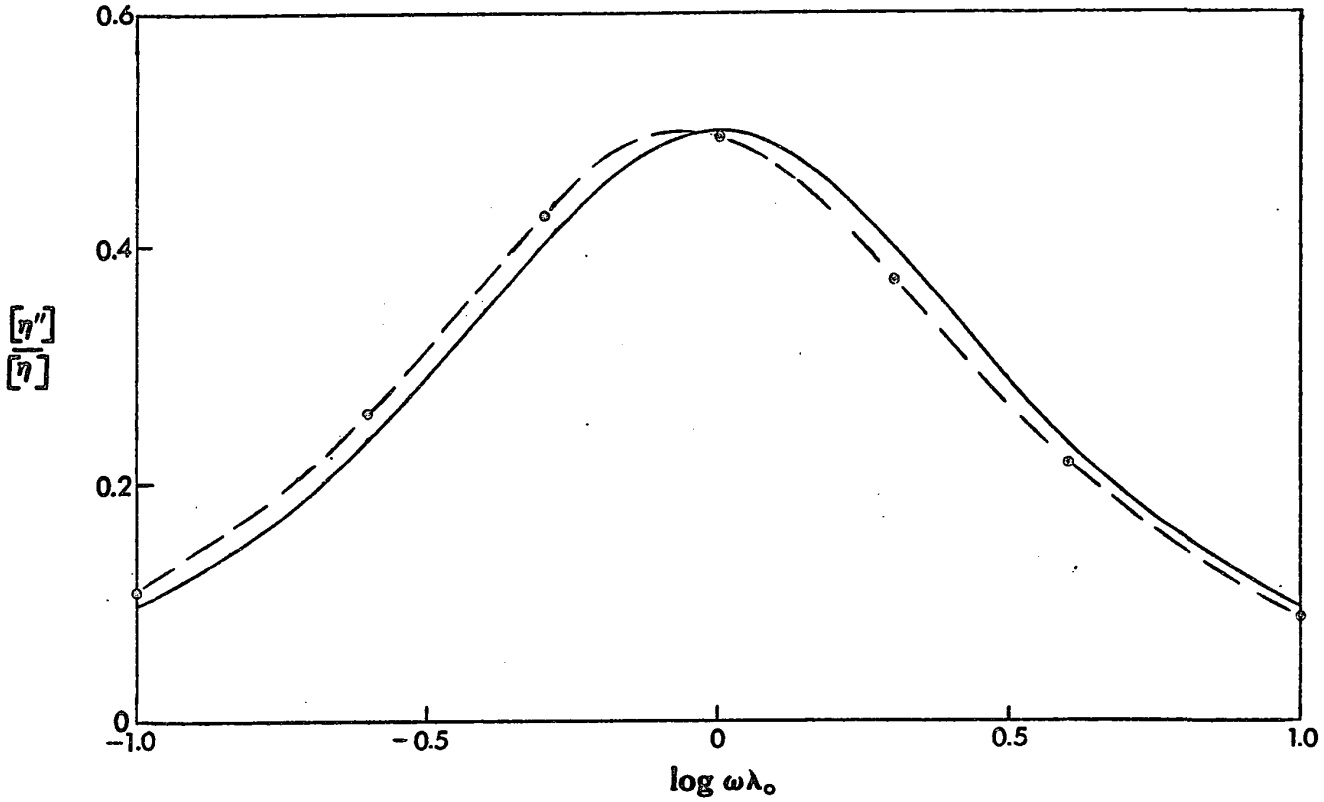
0.6
0.4
0.2
0
[η'']
[η]
−1.0
−0.5
0
0.5
1.0
log ωλ₀

a function of $\omega\lambda_o$ for the C_{10} diacid described in case (ii) in both its unionized and ionized forms. These curves can all be normalized to the nonionic curves by a simple multiplicative factor in relaxation time. For the case of the C_{10} diacid, the value of λ/λ_o, based on nine points (not all shown), is 1.106 with a standard deviation of 0.006. The values of λ/λ_o are plotted in Fig. 1 (dashed line) as a function of $EB^{1/2}$. The function λ/λ_o forms a single curve versus $EB^{1/2}$ as did the function $[\eta]/[\eta]_o$. The points representing the four cases described above are indicated in Fig. 1.

A simple shift in the relaxation time might be obtained from the theory if it is considered that the presence of ions merely results in a new, "pseudo-Hookean" force constant, H', which will be a function of the parameter $EB^{1/2}$. Since $\lambda/\lambda_o = H/H'$, the value of H' can be obtained for any value of $EB^{1/2}$ from the plot of λ/λ_o (Fig. 1).

For the 3B2S system, consider a linear C_{20} triacid whose two Hookean springs have the same constant, H, as that of the corresponding diacid in case (i) above. Since B' is defined differently than B, one obtains $(B')_o = 2H/kT = 0.048\ \text{Å}^{-2}$ for the unionized triacid. E remains the same (-3.55 Å). For the ionized acid, the pseudo-Hookean constant, H', is obtained from the plot of λ/λ_o versus $EB^{1/2}$ for the dumbbell (Fig. 1). Thus, in this case, H'/H = 1/1.106, and therefore B' = 0.048/1.106.

Then using the solution of Eq. 29 for $\omega\lambda = 1$, (although

any value of $\omega\lambda$ would give the same result since a single relaxation time is obtained), the additional fractional increase in λ_1 is found to be 1.075. Hence, the overall increase in λ_1 is given by

$$\lambda_1/(\lambda_1)_0 = 1.075 \times 1.106 = 1.19$$

while the increase in λ_2 is given by

$$\lambda_2/(\lambda_2)_0 = 1.106$$

Recalling that $(\lambda_1)_0/(\lambda_2)_0 = 3$ for the nonionic 3B2S system, then the ratio of relaxation times in the ionic 3B2S system for C_{20} triacid is given by

$$\lambda_1/\lambda_2 = 3.23$$

The ratio of the intrinsic viscosities of the ionized and the unionized C_{20} triacids is obtained by substitution of Eq. 40 in Eq. 39 and evaluation of the resulting integrals. For this example

$$[\eta]/[\eta]_0 = 1.244$$

Similar calculations were performed on the triacids corresponding to cases (ii) and (iii) of the dumbbell model; that is, for a C_{60} triacid in water and in ethanol, respectively. In each case the ratios λ_1/λ_2 and $[\eta]/[\eta]_0$ were obtained. These ratios are plotted in Fig. 3 as a function of the parameter $E(B')_0^{1/2}$.

It can be seen that a broadening of the distribution of relaxation times is predicted for the ionic 3B2S system. This

FIGURE 3

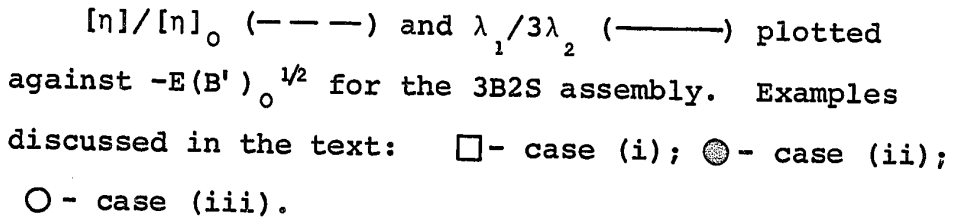
$[\eta]/[\eta]_o$ (— — —) and $\lambda_1/3\lambda_2$ (———) plotted against $-E(B')_o^{1/2}$ for the 3B2S assembly. Examples discussed in the text: □- case (i); ◍- case (ii); ○- case (iii).

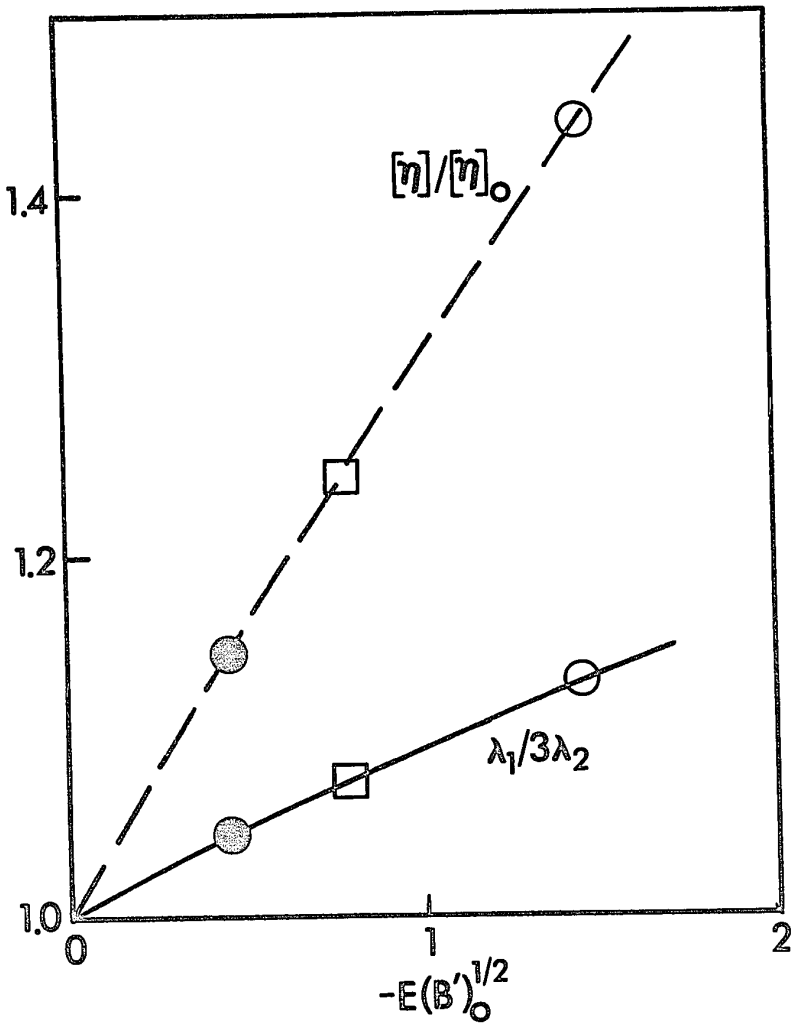
1.4
1.2
1.0
0
1
2
$[\eta]/[\eta]_o$
$\lambda_1/3\lambda_2$
$-E(B')_o^{1/2}$

broadening increases approximately linearly with $-E(B')_0^{1/2}$, the parameter which reflects the ratio of charge to end-to-end distance. The intrinsic viscosities also increase approximately linearly with this parameter. The values obtained are slightly higher than the corresponding cases in the dumbbell system because of the increased contribution of the longest relaxation time.

E. Discussion

In this treatment, no account was taken for the concentration of the polymer, since the effect of the ions would be expected to be greatest at infinite dilution. The effect of either an increase in the concentration of polymer or the addition of a simple electrolyte would be to screen out some of the Coulombic interaction. However, either of these possibilities could be taken into account by a modified expression for the Coulombic force, such as that provided by the Debye-Hückel approximation.[11]

Also, at finite polymer concentration, a complication in the viscoelastic effect could conceivably arise because of the finite time required for the rearrangement of the counterion atmosphere around a polymer ion. However, recent investigations on counterion relaxation times[12] indicate that they are much higher than those likely to be encountered in polymer relaxations.

F. Conclusions

A theoretical investigation of the dilute solution viscoelasticity of simple ionic polymers was undertaken. The bead-spring model of Rouse was modified to include electrostatic charges in the beads. For the two simplest cases of this model (the elastic dumbbell and the three-bead/two-spring assembly), the diffusion equation for the distribution function of bead separation in shearing flow was formulated. Numerical solutions were obtained for a range of values of the charge and spring parameters. The values were chosen to correspond to real polymers for which the charged bead-spring model would be appropriate, such as linear dicarboxylic acids and polymeric zwitterions for the dumbbell, and linear triacids for the three-bead model. It was found that the effect of ions can be described by simple multiplicative shifts in the relaxation times of the uncharged material. For like charged dumbbells, both the relaxation time and the intrinsic viscosity increase; for oppositely charged dumbbells, both of these functions decrease in value. For the three-bead model, the intrinsic viscosity and both of the relaxation times increase. In addition, the ratio of the two relaxation times increases, indicating a broadening in the distribution of relaxation times.

REFERENCES

[1] E. P. Otocka, M. Y. Hellman, and L. L. Blyler, J. Appl. Phys., 40, 4221 (1969).

[2] V. Jaacks and N. Mathes, Makromol. Chem., 131, 295 (1970).

[3] J. L. Schrag and R. M. Johnson, Rev. Sci. Instrum., 42, 224 (1971).

[4] R. B. Bird, H. R. Warner, Jr., and D. C. Evans, Fortschr. Hochpolym.-Forsch., 8, 1 (1971).

[5] B. H. Zimm, J. Chem. Phys., 24, 269 (1956).

[6] L. E. Malvern, "Introduction to the Mechanics of a Continuous Medium," Prentice-Hall, Englewood Cliffs, N.J. (1969), pp. 205-207.

[7] J. G. Kirkwood and J. Riseman, J. Chem. Phys., 16, 565 (1948).

[8] L. Collatz, "The Numerical Treatment of Differential Equations," 3rd ed., Springer, Berlin (1966).

[9] L. R. G. Treloar, "The Physics of Rubber Elasticity," Oxford U. P., London (1958), Chap. III.

[10] "Polymer Handbook," ed. J. Brandrup and E. H. Immergut, Interscience, New York (1966).

[11] R. W. Gurney, "Ions in Solution," Dover, New York (1962).

[12] D. J. Allen, S. M. Neale, and P. J. T. Tait, J. Polym. Sci., A-2, 10, 433 (1972).

APPENDIX A

Angular Dependence of $\Lambda_1(R,\theta,\phi)$

The solution of Eq. 10 for Λ_1, for E = 0, is

$$(\Lambda_1)_{E=0} = S^2sc\,\frac{R^2}{2 + i\omega A/B}$$

This suggests that the angular dependence of Λ_1 for $E \neq 0$ is the same. To test this, try $\Lambda_1 = S^2scF^*(R)$. Then Eq. 10 becomes

$$S^2scR^2\left[\frac{\partial^2}{\partial R^2} + \left(\frac{2}{R} - \frac{E}{R^2} - BR\right)\frac{\partial}{\partial R}\right]F^*(R)$$

$$- 6S^2scF^*(R) + S^2sc\left[\frac{C}{S}\frac{\partial}{\partial\theta} + \frac{\partial^2}{\partial\theta^2} + \frac{1}{S^2}\frac{\partial^2}{\partial\phi^2}\right]F^*(R)$$

$$= - S^2sc\,(ER + BR^4) + i\omega AR^2S^2scF^*(R) \qquad \text{(A1)}$$

On elimination of S^2sc, Eq. A1 becomes

$$\left[\frac{\partial^2}{\partial R^2} + \left(\frac{2}{R} - \frac{E}{R^2} - BR\right)\frac{\partial}{\partial R} - \frac{6}{R^2} - i\omega A\right]F^*(R) = -\left(\frac{E}{R} + BR^2\right) \qquad \text{(A2)}$$

where $F^*(R)$ has the form $F^*(R) = u(R) + iv(R)$.

If the solution of Λ_1 is actually of the form

$$\Lambda_1 = S^2scF^*(R)\cdot G(\theta,\phi)$$

then the solution of Λ_1 must be obtained from

$$\frac{1}{F^*(R)}R^2\left[\frac{\partial^2}{\partial R^2} + \left(\frac{2}{R} - \frac{E}{R^2} - BR\right)\frac{\partial}{\partial R} - \frac{6}{R^2} - i\omega A\right]F^*(R)$$

$$+ \frac{1}{G(\theta,\phi)}\left(\frac{C}{S}\frac{\partial}{\partial\theta} + \frac{\partial^2}{\partial\theta^2} + \frac{1}{S^2}\frac{\partial^2}{\partial\phi^2}\right)G(\theta,\phi)$$

$$= - \frac{ER + BR^4}{F^*(R)\;G(\theta,\phi)} \qquad \text{(A3)}$$

Eq. A3 is of the non-homogeneous type. If the term on the right side of Eq. A3 is set equal to zero, and each part of the resulting homogeneous equation is set equal to λ, then, by the usual method for solving partial differential equations

$$\left(\frac{\partial^2}{\partial\theta^2} + \frac{C}{S}\frac{\partial}{\partial\theta} + \frac{1}{S^2}\frac{\partial^2}{\partial\phi^2} + \lambda\right) G(\theta,\phi) = 0 \qquad \text{(A4)}$$

If $G(\theta,\phi)$ is replaced by $g(\theta)h(\phi)$, and λ_1 is introduced, one obtains

$$\frac{1}{g(\theta)}\left(\frac{\partial^2}{\partial\theta^2} + SC\frac{\partial}{\partial\theta} + \lambda S^2\right) g(\theta) = \frac{1}{h(\phi)}\frac{\partial^2}{\partial\phi^2} h(\phi) = +\lambda_1^2 \qquad \text{(A5)}$$

Hence, for $h(\phi)$

$$h'' + \lambda_1^2 h = 0 \qquad \text{(A6)}$$

If λ_1^2 is positive,

$$h = k_1 (\cos \lambda_1\phi + i \sin \lambda_1\phi) + k_2 (\cos \lambda_1\phi - i \sin \lambda_1\phi) \qquad \text{(A7)}$$

The boundary condition for x–y plane symmetry is $h(\phi) = h(\phi + \pi)$, since one must be able to interchange ends of the dumbbell. This requires that

$$(k_1 + k_2) \cos \lambda_1\phi = (k_1 + k_2) \cos \lambda_1(\phi + \pi)$$

$$(k_1 - k_2) \sin \lambda_1\phi = (k_1 - k_2) \sin \lambda_1(\phi + \pi)$$

Since there is no real, non-zero value of λ_1 for which this is true, the only solution for $\lambda_1^2 > 0$ is the trivial one, $h \equiv 0$. If λ_1^2 is negative,

$$h = k_1 e^{\lambda_1\phi} + k_2 e^{-\lambda_1\phi}$$

and, according to the boundary condition, $k_1 = k_2 = 0$. Hence, the only non-trivial solution of Eq. A6 is that for which $\lambda_1^2 = 0$, namely

$$h = k_1 + k_2\phi$$

The boundary condition requires that $k_2 = 0$, and thus

$$h = k_1 = \text{const.}$$

Since the constant is arbitrary, h may be set equal to 1, and the constant included in $F^*(R)$.

For $g(\theta)$, then, Eq. A5 becomes

$$\left(\frac{\partial^2}{\partial\theta^2} + SC\,\frac{\partial}{\partial\theta} + \lambda S^2\right) g(\theta) = 0$$

or

$$g'' + \frac{\sin 2\theta}{2}\, g' + \lambda \sin^2\theta\, g = 0 \qquad \text{(A7)}$$

For $\lambda \neq 0$, symmetry of the distribution demands that $g(\theta) = g(\pi - \theta)$, since the flow and shearing force are both in the x–y plane. By inspection of Eq. A7, the only conceivable function which is consistent with this symmetry condition [that θ may be replaced by $(\pi - \theta)$] is $g \equiv 0$. Hence, in order to obtain a non-trivial solution of $g(\theta)$, λ must equal zero. In this case, either g = const. or

$$g = \frac{\sin 2\theta}{8} + k_1\theta + k_2$$

Again, the symmetry conditions imply that $k_1 = 0$, and, since $\sin 2\theta \neq \sin 2(\pi - \theta)$, it is concluded that g = const. As before, g can be set equal to 1. Thus

$$\Lambda_1 = F^*(R)S^2sc$$

as assumed.

APPENDIX B

Calculational Error at Low Values of R

It is possible to estimate the error which results from replacing the integrals in Eq. 33 by expressions of the type

$$\int_0^\infty \psi_o \, F^*(R) \, R^4 \, dR = \int_0^\epsilon \psi_o \, F^*(R) \, R^4 \, dR + \int_\epsilon^\infty \psi_o \, F^*(R) \, R^4 \, dR$$

where ε is small, and setting

$$\int_0^\epsilon \psi_o \, F^*(R) \, R^4 \, dR = 0$$

At low values of R, terms in R^2 and R and constant terms may be disregarded in Eq. 29, since they are very much smaller than terms in $1/R$ and $1/R^2$. Eq. 29 then becomes

$$\frac{\partial^2}{\partial R^2} F^* + \left(\frac{2}{R} - \frac{E}{R^2}\right) \frac{\partial}{\partial R} F^* - \frac{6}{R^2} F^* = - \frac{E}{R} \qquad \text{(B1)}$$

By substitution, it is found that the solution at low values of R is the same as that for steady shear

$$\underset{R \to 0}{F^*(R)} = \frac{R^2}{2} \qquad \text{(B2)}$$

Also, at low values of R

$$\underset{R \to 0}{\psi_o(R)} = \exp(E/R) \qquad \text{(B3)}$$

Therefore

$$\int_0^\epsilon \psi_o \, F^*(R) \, R^4 \, dR = \frac{1}{2} \int_0^\epsilon \exp(E/R) \, R^6 \, dR$$

$$= - \frac{E^7}{2} \int_{-E/\epsilon}^\infty (e^{-X}/X^8) \, dX \qquad \text{(B4)}$$

The integral in Eq. B4 is finite and may be readily evaluated by approximation. As a typical example, for E = -3.55 Å and ε = 1 Å, as in case (i)

$$\int_0^{\varepsilon} \psi_o \, F^*(R) \, R^4 \, dR = 0.2 \text{ Å}^7$$

Since (for $\omega\lambda = 1$)

$$\int_{\varepsilon}^{\infty} \psi_o \, F^*(R) \, R^4 \, dR = (1.3 - 1.4i) \times 10^6 \text{ Å}^7$$

for the same example, the error involved is negligible. This is clearly the case for all reasonable values of E and ε.

APPENDIX C

Program for the Approximate Solution of a Second Order Differential Equation in a Complex Plane

Eq. 29 is a second order differential equation of the type

$$F'' = (P_1 + iP_2)\, F' + (Q_1 + iQ_2)\, F + (G_1 + iG_2) \qquad (C1)$$

where P_1, P_2, Q_1, Q_2, G_1, and G_2 are all non-complex functions of R and continuous in the interval R_1, R_2. F(R), the unknown distribution function, is assumed to be a complex function of R and continuous in the interval R_1, R_2; also, it is assumed to be continuously positive, because it is a distribution function. F(R) may be written

$$F(R) = u(R) + iv(R) \qquad (C2)$$

where u and v are non-complex functions of R. Substitution of Eq. C2 in Eq. C1 and separation of the real and imaginary terms gives the simultaneous differential equations

$$\begin{aligned} u'' &= P_1 u' - P_2 v' + Q_1 u - Q_2 v + G_1 \\ v'' &= P_2 u' + P_1 v' + Q_2 u + Q_1 v + G_2 \end{aligned} \qquad (C3)$$

Eq. C3, which is the general form of Eq. 36, can be solved by a modification of the Runge-Kutta method.[8] This procedure is actually a means of solving an initial value boundary problem where the values of u, u', v, and v' are all known at some initial value R_0. However, it may be used to solve a problem where the values u and v are known at two boundary points R_1 and R_2. In this case, two pairs of trial values of $u'(R_1)$ and $v'(R_1)$ are chosen for one boundary point, and two trial solutions are ob-

tained. From the values of $u(R_2)$ and $v(R_2)$ obtained at the second boundary point, a new pair of trial values of $u'(R_1)$ and $v'(R_1)$ are chosen by linear interpolation to produce a better approximate solution. Because the function F(R) is complex, solutions must be obtained by consecutively varying u'(R) while holding v'(R) fixed, and vice versa. So, in fact, nine trial solutions in all must be obtained in order to obtain one approximate solution. The scheme by which values of $u'(R_1)$ and $v'(R_1)$ are chosen is given in Table I, below. If it is desired to improve on this first approximation, the same steps must be repeated, but with smaller variations in the trial values of $u'(R_1)$ and $v'(R_1)$.

TABLE I

Step	$u'(R_1)$	$v'(R_1)$
1	u_1 (chosen)	v_1 (chosen)
2	u_2 (chosen)	
3	u_3 (interpolated)	
4	u_1	v_2 (chosen)
5	u_2	
6	u_4 (interpolated)	
7	u_1	v_3 (interpolated)
8	u_2	
9	u_5 (interpolated)	

The ease with which a solution is obtained depends somewhat on the judicious choice of the trial values of $u'(R_1)$ and $v'(R_1)$. If approximate values of $u'(R_1)$ and $v'(R_2)$ are known or can be estimated, then u_1, u_2, v_1, and v_2 should be chosen to lie on either side of the expected real values; however, this is not an absolute requirement. In the present case, the solution was facilitated by choosing values of u_1, u_2, v_1, and v_2 in the vicinity of known values of $u'(R_1)$ and $v'(R_1)$ for the nonionic case.

The fortran language program used for this computational procedure is described below. The arrangement of data cards and the interpretation of the sample output are self-explanatory. In this program, double precision variables are used throughout the iterative procedure because the error is cumulative and, with the small intervals chosen here, the differences between successive values are often very small. The program is written with the specific functions $P_1(R)$, etc. obtained from Eq. 36, but other functions may be substituted, provided they meet the required condition of continuity. Finally, the program evaluates the function

$$\int_0^\infty F^*(R)\ \exp(E/R - BR^2/2)\ (BR^4 + ER)\ dR$$

as required in Eq. 33.

Program "RUNGE"

```
C     APPROX. DIST. FUNCTION BY RUNGE-KUTTA METHOD IN COMPLEX PLANE
C       DIST. FUNCTION OBTAINED FROM FOLLOWING EQUATION
C       PSI=PSI0(1+A*KAPPA*LAMBDA1)
C       PSI0=EXP(E/R-B*R**2/2)
C       LAMBDA1=F*(R)*S**2*S*C
C       PSI = PSI0*(1 + A*KAPPA*LAMBDA1)
C       PSI0 = EXP(E/R - B*R**2/2)
C       LAMBDA1 = F*(R)*S**2*S*C
C       F" = (P1 + I*P2)*F' + (Q1 + I*Q2)*F + (G1 + I*G2)
C       F*(R) = U(R) + I*V(R)
```

```
      DIMENSION WORD(20)
      REAL*8 P1,P2,Q1,Q2,G1,G2
      REAL*8 H,R,U,V,X,Y,R0,RF,U0,UF,V0,VF
      REAL*8 U1,U2,V1,V2,UF1,UF2,VF1,VF2,DU,DV
      REAL*8 C1,C2,C3,C4,D1,D2,D3,D4,X0,Y0
      REAL*8 E,B,A,PSI0,S1,S2,S3,S4
C     DEFINE FUNCTIONS P1(R),P2(R),Q1(R),Q2(R),G1(R),G2(R)
      P1(R)=2./R-E/R**2-B*R
      P2(R)=0.
      Q1(R)=-6./R**2
      Q2(R)=-A
      G1(R)=-E/R-B*R**2
      G2(R)=0.
      READ(5,88)WORD
C     1 CARD  ALPHAMERIC LABEL
      WRITE(6,89)WORD
      READ(5,90)E,B,A
C     1 CARD  CONSTANTS IN ABOVE FUNCTIONS
      READ(5,90)R0,RF,U0,UF,V0,VF
C     1 CARD  INIT. & FINAL BDY. & VALUES OF U & V AT BDY.
      READ(5,90)U1,U2,V1,V2
C     1 CARD  TRIAL VALUES OF U'(R0) & V'(R0)
      READ(5,91)ITER
C     1 CARD  NO. OF ITERATIONS IN EACH STEP
      H=(RF-R0)/DFLOAT(ITER)
C     H IS INTERVAL WIDTH
      DU=U2-U1
      DV=V2-V1
      I=0
      DO 3 J=1,3
      U1=U2-DU
      IF(J.EQ.2) V1=V2
      IF(J.EQ.3) V1=V1-(VF2-VF)/(VF2-VF1)*DV
      DO 2 K=1,3
      IF(K.EQ.2) U1=U2
      IF(K.EQ.3) U1=U1-(UF2-UF)/(UF2-UF1)*DU
      I=I+1
      WRITE(6,95)I,U1,V1
      R=R0
      U=U0
      V=V0
      X=U1*H
      Y=V1*H
      PSI0=DEXP(E/R-B*R**2/2)
      S1=PSI0*U*R**4
      S2=PSI0*V*R**4
      S3=PSI0*U*R
      S4=PSI0*V*R
      JK=J+K
      IF(JK.EQ.6) WRITE(6,94)
      IF(JK.EQ.6) WRITE(6,92)R,U,V,X,Y,PSI0
```

```
      DO 1 L=1,ITER
      X0=X
      Y0=Y
      C1=-(P1(R)*X-P2(R)*Y+(Q1(R)*U-Q2(R)*V-G1(R))*H)*H/2.
      D1=-(P1(R)*Y+P2(R)*X+(Q1(R)*V+Q2(R)*U-G2(R))*H)*H/2.
      R=R+H/2.
      U=U+X/2.+C1/4.
      V=V+Y/2.+D1/4.
      X=X+C1
      Y=Y+D1
      C2=-(P1(R)*X-P2(R)*Y+(Q1(R)*U-Q2(R)*V-G1(R))*H)*H/2.
      D2=-(P1(R)*Y+P2(R)*X+(Q1(R)*V+Q2(R)*U-G2(R))*H)*H/2.
      X=X0+C2
      Y=Y0+D2
      C3=-(P1(R)*X-P2(R)*Y+(Q1(R)*U-Q2(R)*V-G1(R))*H)*H/2.
      D3=-(P1(R)*Y+P2(R)*X+(Q1(R)*V+Q2(R)*U-G2(R))*H)*H/2.
      R=R+H/2.
      U=U+X0/2.+C3-C1/4.
      V=V+Y0/2.+D3-D1/4.
      X=X0+2.*C3
      Y=Y0+2.*D3
      C4=-(P1(R)*X-P2(R)*Y+(Q1(R)*U-Q2(R)*V-G1(R))*H)*H/2.
      D4=-(P1(R)*Y+P2(R)*X+(Q1(R)*V+Q2(R)*U-G2(R))*H)*H/2.
      U=U+(C1+C2-2.*C3)/3.
      V=V+(D1+D2-2.*D3)/3.
      X=X0+(C1+2.*C2+2.*C3+C4)/3.
      Y=Y0+(D1+2.*D2+2.*D3+D4)/3.
      PSI0=DEXP(E/R-B*R**2/2)
      S1=S1+PSI0*U*R**4
      S2=S2+PSI0*V*R**4
      S3=S3+PSI0*U*R
      S4=S4+PSI0*V*R
      IF(JK.EQ.6) WRITE(6,92)R,U,V,X,Y,PSI0
    1 CONTINUE
      S1=-H*(S1*B+S3*E)
      S2=H*(S2*B+S4*E)
      IF(JK.EQ.6) WRITE(6,93)S1,S2
      IF(JK.LT.6) WRITE(6,96)U,V
      IF(K.EQ.1) UF1=U
      UF2=U
    2 CONTINUE
      IF(J.EQ.1) VF1=V
      VF2=V
    3 CONTINUE
   88 FORMAT(20A4)
   89 FORMAT('1',20A4)
   90 FORMAT(7D11.3)
   91 FORMAT(I4)
   92 FORMAT(D10.3,5D12.4)
   93 FORMAT('0 I =',D11.4,' - I*',D10.4)
   94 FORMAT('0',3X,'R',11X,'U',11X,'V',10X,'U''*H',10X,'V''*H',
     110X,'PSI0')
   95 FORMAT('0STEP',I2,'  U''(R0) =',D18.10,'  V''(R0) =',D18.10)
   96 FORMAT('0',9X,'U(RF) =',D13.5,8X,'V(RF) =',D13.5)
      STOP
      END
```

Sample Output

```
      C10 DIACID SALT IN H2O, OMEGA*LAMBDA = 1

STEP 1  U'(R0) =  0.2500000000D 02  V'(R0) = -0.2500000000D 02
         U(RF) = -0.89311D 03        V(RF) =  0.33108D 03
STEP 2  U'(R0) =  0.2400000000D 02  V'(R0) = -0.2500000000D 02
         U(RF) = -0.80686D 03        V(RF) =  0.12096D 03
STEP 3  U'(R0) =  0.14644603710 02  V'(R0) = -0.2500000000D 02
         U(RF) =  0.29200D-08        V(RF) = -0.18447D 04
STEP 4  U'(R0) =  0.2500000000D 02  V'(R0) = -0.2600000000D 02
         U(RF) = -0.68299D 03        V(RF) =  0.41732D 03
STEP 5  U'(R0) =  0.2400000000D 02  V'(R0) = -0.2600000000D 02
         U(RF) = -0.59675D 03        V(RF) =  0.20721D 03
STEP 6  U'(R0) =  0.1708079806D 02  V'(R0) = -0.2600000000D 02
         U(RF) = -0.16348D-08        V(RF) = -0.12466D 04
STEP 7  U'(R0) =  0.2500000000D 02  V'(R0) = -0.2808419137D 02
         U(RF) = -0.24508D 03        V(RF) =  0.59707D 03
STEP 8  U'(R0) =  0.2400000000D 02  V'(R0) = -0.2808419137D 02
         U(RF) = -0.15884D 03        V(RF) =  0.38696D 03
STEP 9  U'(R0) =  0.2215829331D 02  V'(R0) = -0.2808419137D 02

     R          U          V          U'*H       V'*H       PSIO
0.500D 02  0.6250D 03 -0.6250D 03 -0.1108D 02  0.1404D 02  0.7142D-52
0.495D 02  0.6128D 03 -0.6123D 03 -0.1162D 02  0.1320D 02  0.7773D-51
0.490D 02  0.6007D 03 -0.5998D 03 -0.1186D 02  0.1268D 02  0.8260D-50
0.485D 02  0.5886D 03 -0.5875D 03 -0.1194D 02  0.1234D 02  0.8568D-49
0.480D 02  0.5765D 03 -0.5754D 03 -0.1191D 02  0.1211D 02  0.8677D-48
    :          :          :          :          :          :
0.250D 01  0.5296D 00 -0.1970D 01 -0.4963D 00  0.6208D 00  0.1791D 00
0.200D 01  0.1085D 00 -0.1394D 01 -0.3429D 00  0.5368D 00  0.1399D 00
0.150D 01 -0.1416D 00 -0.8694D 00 -0.1355D 00  0.5519D 00  0.8419D-01
0.100D 01  0.3175D-09 -0.2922D-07  0.8470D 00  0.1958D 01  0.2738D-01

  I = 0.8475D 03 - I*0.9297D 03
```

CHAPTER IV

THE VISCOELASTICITY OF HIGHLY CONCENTRATED SOLUTIONS OF POLYELECTROLYTES

A. Introduction

In Chapter I, the results of thermomechanical and structural studies on solid-state polyelectrolytes were discussed. These studies have shown that ionization produces vast changes in the thermomechanical behaviour of undiluted polyelectrolytes. The theoretical study presented in Chapter III showed that in dilute solution, where no intermolecular interaction occurs, the effect of ionization on viscoelasticity is small. Likewise, the study of rubber elasticity in Chapter II showed that the inherent effect of ions is small where ion aggregation is suppressed. In this chapter, it will be shown that the dramatic effects of ionization on the viscoelastic properties of polyelectrolytes can still be observed even with the addition of considerable amounts of plasticizer, as long as ion aggregation is not disrupted.

The polyelectrolytes used in this study were a series of plasticized sodium salts of poly(acrylic acid). Stress relaxation curves were prepared for this material as a function of the type and amount of plasticizer and of the degree of neutralization. It will be shown from stress relaxation measurements taken over 3.5 decades of time that time-temperature superposition of

viscoelastic data is not valid in these materials. Thus, for comparative purposes, modulus-temperature curves will be presented to illustrate the variation in viscoelastic behaviour in this system.

It will be shown that the X-ray diffraction measurements on the polyacrylate salts support a structure in which ion aggregation occurs. Then the rheological data will be analyzed according to the two-mechanism response expected of some micro-phase-separated materials. It will be shown by direct and indirect evidence that the mechanism which dominates the short-time behaviour above T_g is adequately described by the W.L.F. equation and thus can likely be attributed to a normal diffusional process. The mechanism which corresponds to the long-time deviations in the pseudo-master curves is of low activation energy (17-32 kcal) and is essentially a pure viscosity. The possible relationship of this mechanism to the ionic phase is discussed. Finally, a correlation between dynamic and static mechanical data suggests the existence of a third relaxation mechanism in this polymer system.

B. Experimental Procedures

1. Sample Preparation

Samples of plasticized poly(sodium acrylate) — PNaA — were prepared in the form of films suitable for the measurement of viscoelastic, thermal, and structural parameters. The synthesis

and the molecular weight determination of the poly(acrylic acid) — PAA — from which the films were made are described in Appendix A. The PAA samples used in this part of the study were obtained as unfractionated polymers with molecular weights in the range 2.9×10^5 to 9.9×10^5, as determined from intrinsic viscosity measurements.

The PAA samples were neutralized by titration with aqueous alkali hydroxide of approximately unit normality. The latter solutions had been previously standardized against potassium hydrogen phthalate. The PAA was first weighed and then dissolved in a small amount of water. No particular attempt was made to thoroughly dry the PAA because of its tendency to crosslink and decarboxylate under prolonged heating.[1] In the cases where complete neutralization was required, titrations were carried out to phenolphthalein end-point. Based on the known amount of alkali hydroxide added and assuming complete neutralization (see Appendix A), the dry weight of PAA was calculated and used in subsequent determinations of plasticizer content. The differences between the weights of PAA as determined by titration and those directly measured were attributed to the water content of the polymer. This was normally found to be about 5% by weight, in line with reported values.[2] Partially neutralized polymers were prepared by adding to a weighed amount of polymer of known water content (determined by simultaneous complete neutralization of another sample) the quantity of alkali hydroxide required to produce the desired degree of neutralization.

The aqueous solutions of polymer and alkali were then concentrated by evaporation to about 10% polymer by weight. For the preparation of samples with non-aqueous plasticizer, an excess weight of plasticizer was added to the solution, which was then degassed and poured into tared, flat-bottomed polystyrene containers (approximate dimensions 5 cm by 2 cm by 1 cm). Evaporation was continued until the desired level of plasticizer content was reached. In the case of formamide-plasticized polymers, the addition of excess plasticizer was repeated, because of the high volatility of formamide, in order to ensure the elimination of the water. It is possible that a small percentage of water still remained in these samples, but it was assumed to be inconsequential.

In the preparation of water-plasticized polymers, the same procedure was used, except of course for the addition of excess plasticizer. For polymers of low plasticizer content, where the material would be brittle at room temperature, strips of film were cut to the desired size before all the water had evaporated. For comparative purposes, the plasticizer contents were expressed as volume percentages, assuming a negligible volume of mixing. Density measurements on similar ion-containing polymers, the PAA-PVA mixtures discussed in Chapter II, indicated that the error involved in this conversion is small.

For each of the materials on which stress relaxation measurements were to be made, the glass transition temperature and the thermal expansion coefficient were measured. The apparatus

employed for the measurement of T_g by thermal expansion has been previously described by Eisenberg and Sasada.[3] For some of the samples, T_g measurements were also made by differential scanning calorimetry (DSC). The thermal expansion method was deemed more useful for T_g measurements, however, since coefficients of thermal expansion could be obtained at the same time; also, no additional sample preparation was required since the films used in stress relaxation measurements could be used directly in the thermal expansion apparatus.

2. Stress Relaxation

Stress relaxation measurements were carried out on the prepared films of polymer. Two stress relaxometers were used in making these measurements. The two devices differed essentially in only one aspect, namely the method of control of the sample environment. Measurements in the range -100°C to +60°C were carried out in a device described schematically in Fig. 1; measurements in the range 40°C to 250°C were made in apparatus described in detail elsewhere.[4] All measurements were performed under a positive pressure of nitrogen.

The stress relaxation experiments proceeded in the following manner. Measurements were normally made in an ascending sequence of temperatures, starting from below T_g and continuing until the loss of plasticizer became significant. Thus, the first measurements were normally made on glassy polymers ($E > 10^{10}$ dyn/cm^2). For this reason, the first measurements em-

FIGURE 1

Schematic cross-section of low-temperature stress relaxometer; h_0 and h_1 as described in text.

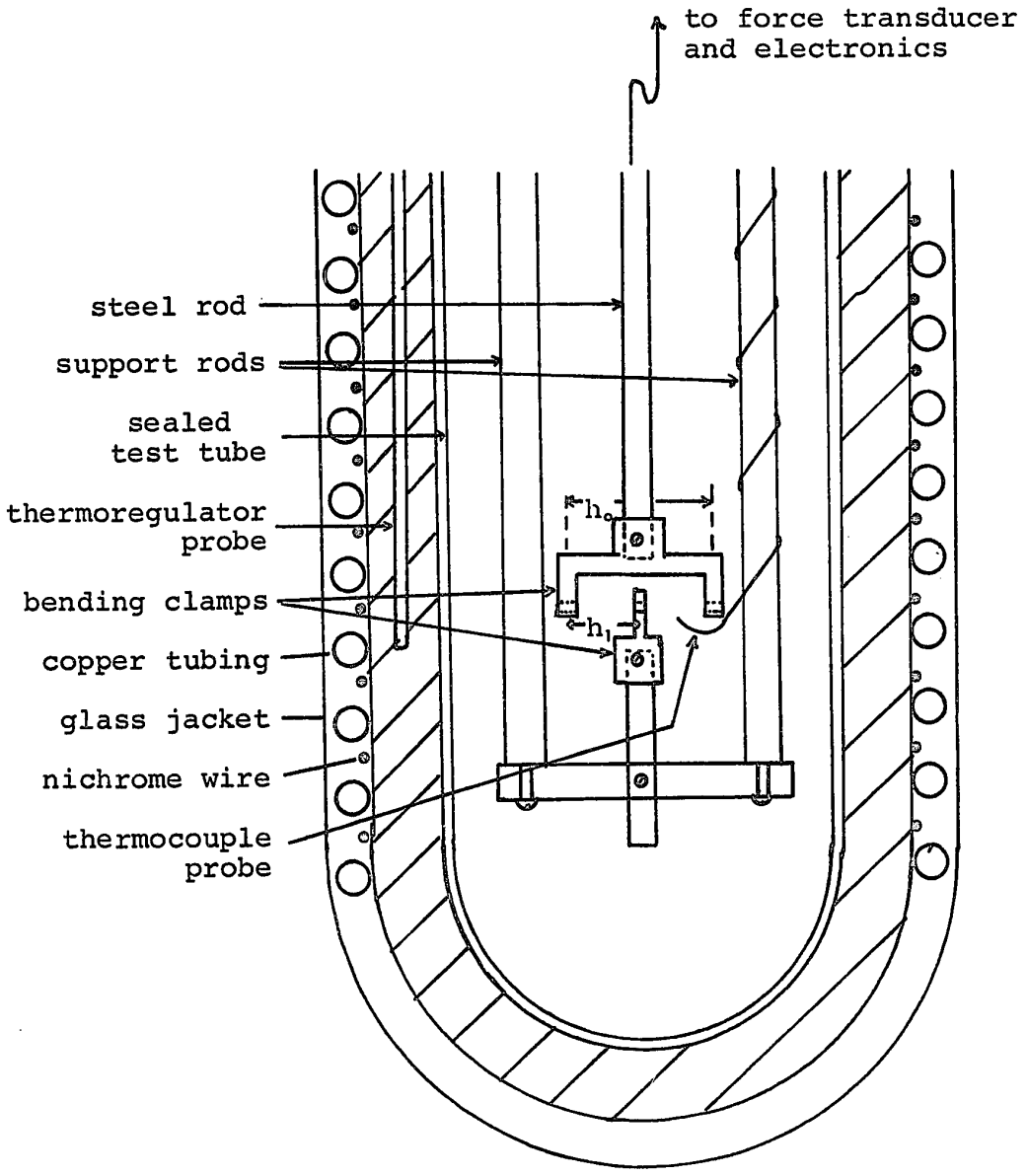
to force transducer
and electronics
steel rod
support rods
sealed
test tube
thermoregulator
probe
bending clamps
copper tubing
glass jacket
nichrome wire
thermocouple
probe
h_o
h_i

ployed a bending deformation. The sample was inserted in the bending clamps and kept under a positive pressure of nitrogen. Temperature control was maintained to a tolerance of ±0.1° during any one run. When the desired temperature was attained, with the temperature controller operating, the stress relaxation run was begun.

The deformation of the sample was accomplished in as short a time as possible, generally in about 0.2 sec; thus, for readings taken at times greater than 2 sec (factor of 10), the effect of a finite deformation time was considered to be negligible.[5] The magnitude of the deformation relative to the sample dimensions was maintained within a level in which linear viscoelastic effects could be observed. An extensive discussion of the sources of error in stress relaxation measurements of this type has been presented.[6] A brief summary of these is given in Appendix B.

In any one run, the sample was maintained at constant deformation and constant temperature for periods of time up to 2×10^4 sec. The force of deformation was continuously recorded on chart paper and was read at intervals of time which increased in approximately logarithmic fashion. The dimensions of the sample and of the clamps were measured and recorded. These values were used to calculate the shape factor, which relates the modulus to the stress-strain ratio. From the shape factor and the values of stress and strain, the modulus was calculated as a function of time for each temperature. This procedure and the

results of such calculations are described in detail in subsequent portions of this chapter.

As the temperature was increased and the modulus of the polymer decreased to the point that bending measurements could no longer be accurately made, deformations in the stretching mode were begun. The procedure involved in stretching measurements is generally the same as outlined above, except that the shape factor for the calculation of modulus is different. In some cases, where values of modulus less than 10^6 dyn/cm^2 were anticipated, measurements in compression were made. For compression, the same shape factor as for stretching applies. Generally, however, the modulus did not fall to such a low value before significant plasticizer loss occurred.

The formulae used in calculating Young's modulus, E(t), in the various modes of deformation are given as follows[7]

$$E(t) = 981\ bf/(\Delta h - c_f f) \qquad (1)$$

where b is the shape factor, Δh is the deformation, f is the force (in grams), and c_f is a correction for instrumental compliance. If all quantities are given in c.g.s. units, then E(t) has the dimensions dyn/cm^2. The shape factors are:

(i) for bending

$$b = 4h_o^3\beta^3(1 - \beta)/w_o d_o^3 \qquad (2)$$

h_o, w_o, and d_o represent the unstrained length, width, and thickness of the film, respectively; $\beta = h_1/h_o$ is an eccen-

tricity factor (≤ 0.5), where h_1 is the distance between the point of deformation and the nearest edge of the clamp (see Fig. 1). For $h_1 = h_o/2$

$$b = h_o^3/4w_o d_o^3 \tag{3}$$

(ii) for stretching

$$b = h_o/w_o d_o \tag{4}$$

Since volatile plasticizers were used, the variation in sample weight was monitored, and measurements were discontinued after a weight loss of 1% was observed. It is reasonable to assume that the weight loss of plasticizer was essentially diffusion controlled, since measurements could be taken at relatively high temperatures for the low plasticizer content materials before significant plasticizer loss occurred. Occasional measurements were taken in random order of temperatures to ensure that the loss of plasticizer to the extent of 1% did not produce a loss of reproducibility.

3. Dynamic Mechanical Measurements

A brief dynamic mechanical study of PNaA was undertaken using a torsion pendulum. The apparatus used and the general procedure for such measurements are described in detail elsewhere.[6] Measurements were made in the region from ca. -100°C to the temperature at which significant plasticizer loss was apparent. In the vicinity of T_g, account of the modulus of the

supporting wire was taken in order to calculate the values of modulus and tan δ.[4] The formulae employed are listed below:

(i) for storage modulus

$$G' = \frac{4\pi^2 I}{b} (\nu^2 - \nu_o^2 - \nu^2\Delta^2/4\pi^2) \tag{5}$$

ν is the measured frequency of vibration, ν_o is the natural frequency of the supporting wire, and I is the moment of inertia. b, the shape factor, and Δ, the logarithmic decrement, are defined below.

(ii) for loss modulus

$$G'' = \frac{4\pi I}{b} \nu^2\Delta \tag{6}$$

(iii) for loss tangent

$$\tan \delta = G''/G' \tag{7}$$

Δ is defined as

$$\Delta = \frac{1}{m} \ln \frac{A_n}{A_{(n+m)}} \tag{8}$$

where A_n and $A_{(n+m)}$ are the amplitudes of the $n^{\underline{th}}$ and $(n+m)^{\underline{th}}$ vibrations. The shape factor in torsion is given by

$$b = w_o d_o^3 \mu(w_o/d_o)/16h_o \tag{9}$$

$\mu(w_o/d_o)$ is a numerical factor dependent on the shape of the sample;[4] all other symbols in Eq. 9 are identical with those in Eq. 2.

4. X-Ray Diffraction

An X-ray diffraction study of some cesium and sodium salts of PAA was performed. Cesium salts of PAA were made in the same fashion as the sodium salts described previously. X-ray scattering patterns were obtained at room temperature using nickel-filtered copper radiation (λ = 1.54 Å) generated by a Rich Seifert X-ray source operating at 40 kV and 20 mA. The patterns were recorded photographically in a conventional wide-angle camera with a 0.05 cm pin hole and a 6.6 cm sample-to-film distance. The photographs were microdensitometered using a Joyce, Loebl double-beam recording microdensitometer. Exposure times varied with the type of material, but were generally 4-6 hr.

C. Experimental Results

1. Materials

A summary of the polymer samples for which mechanical properties data were obtained is presented below in Table I. The polymer samples were coded according to their compositions. The codes are of the form wX-yZ; where w represents the degree of neutralization in percent; X represents the counterion, either Na or Cs; y represents the volume percent plasticizer in the sample; and Z is the symbol representing each of the plasticizers used: ethylene glycol (EG), formamide (FA), glycerine (GL), and water (H_2O). In addition, T_g, α_g, and α_ℓ, as measured by thermal

expansion, and M_v, as discussed in Appendix A, are given in Table I for each polymer.

TABLE I

Composition	T_g (°C)	α_g ($\times 10^5$)	α_ℓ ($\times 10^5$)	M_v ($\times 10^{-5}$)
00Na-23FA	1	2.2	6.2	9.9
10Na-26FA	2	2.8	6.5	5.1
22Na-23FA	-1	—	—	4.7
39Na-25FA	23	—	—	4.7
67Na-27FA	41	2.7	7.0	4.7
100Na-22FA	97	2.8	7.5	4.7
100Na-29FA	71	2.5	6.7	9.9
100Na-37FA	45	2.6	6.8	7.9
100Na-43FA	15	3.0	9.0	7.9
100Na-48FA	0*	—	—	2.9
100Na-52FA	-15	3.5	10.9	2.9
100Na-67FA	-100*	—	—	2.9
100Na-72FA	-88*	—	21.0	5.1
100Na-54EG	-21	3.7	12.3	4.7
100Na-54GL	-9	2.4	6.9	5.1
100Na-55GL	-28	2.6	10.0	2.9
100Na-66GL	-34	2.5	9.6	2.9
100Na-50H_2O	-18	3.0	20.	4.7
100Na-54H_2O	-25	3.3	25.	5.1
100Na-58H_2O	-28	3.5	25.	4.7

*T_g by DSC

2. Pseudo-master Curves

For each of the materials listed in Table I, stress relaxation experiments were performed. Each experiment consisted of several constant temperature runs in which readings of the force at constant deformation were obtained over a period of time. These data were used to calculate the modulus as a function of time and temperature by the application of the appropriate formulae from Eqs. 1-4. Examples of the type of results obtained are shown in the following four figures; the curves of modulus versus time (depicted on a doubly logarithmic scale) for each constant temperature run appear in the central portion of each figure. In each figure, temperatures in °C are shown and every fourth reading is plotted. The significance of the solid lines in each figure will be made clear presently.

The S.R. results shown in Figs. 2-5 are for only a few selected materials to which specific reference is made in subsequent sections of the text. The remaining S.R. curves, described in the text as modulus-temperature curves, are presented more fully in Appendix B.

With materials for which the principle of time-temperature superposition of viscoelastic data is valid, master curves of reduced modulus versus reduced time can be prepared by shifting the curves of modulus versus time so that the overlap between successive curves is maximized.[8] The shifts are made both horizontally (in time) and vertically (in modulus), according to the

FIGURE 2

Stress relaxation curves for 100Na-48FA. Symbols: E_r versus t as a function of temperature (°C), every fourth point shown. Solid lines: pseudo-master curves.

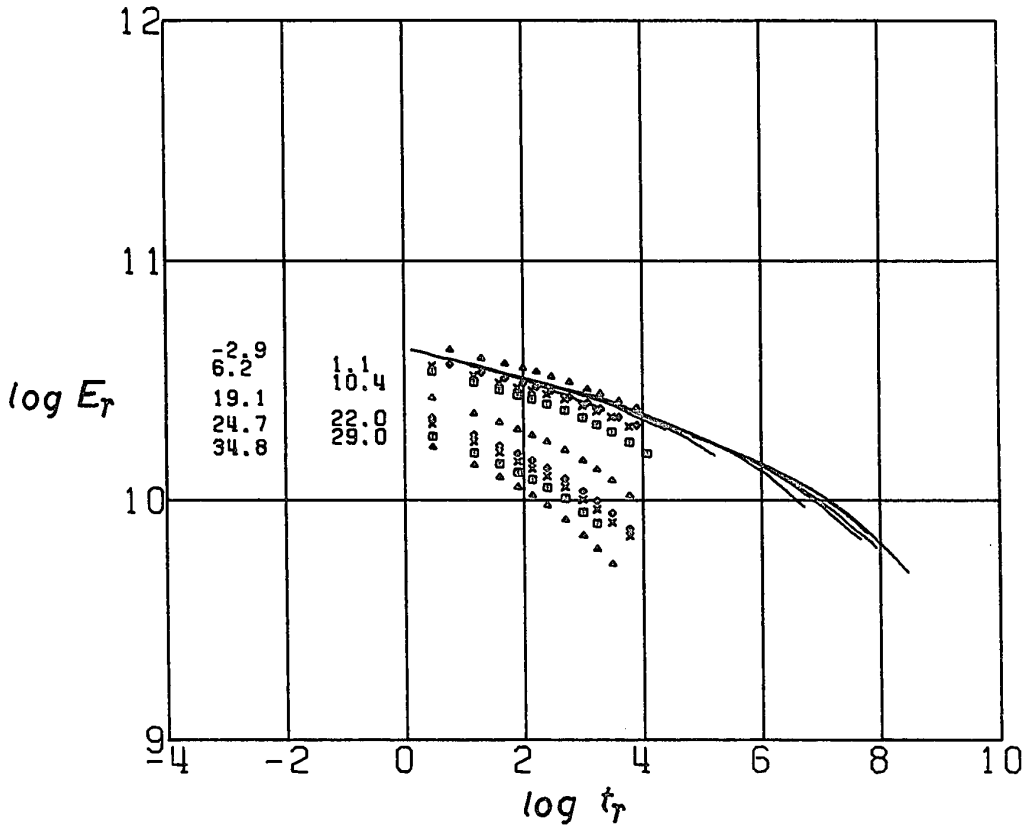
12
11
10
9
-4
-2
0
2
4
6
8
10
log E_r
log t_r
-2.9
6.2
19.1
24.7
34.8
1.1
10.4
22.0
29.0

FIGURE 3

Stress relaxation curves for 100Na-55GL. Symbols: E_r versus t as a function of temperature (°C), every fourth point shown. Solid lines: pseudo-master curves.

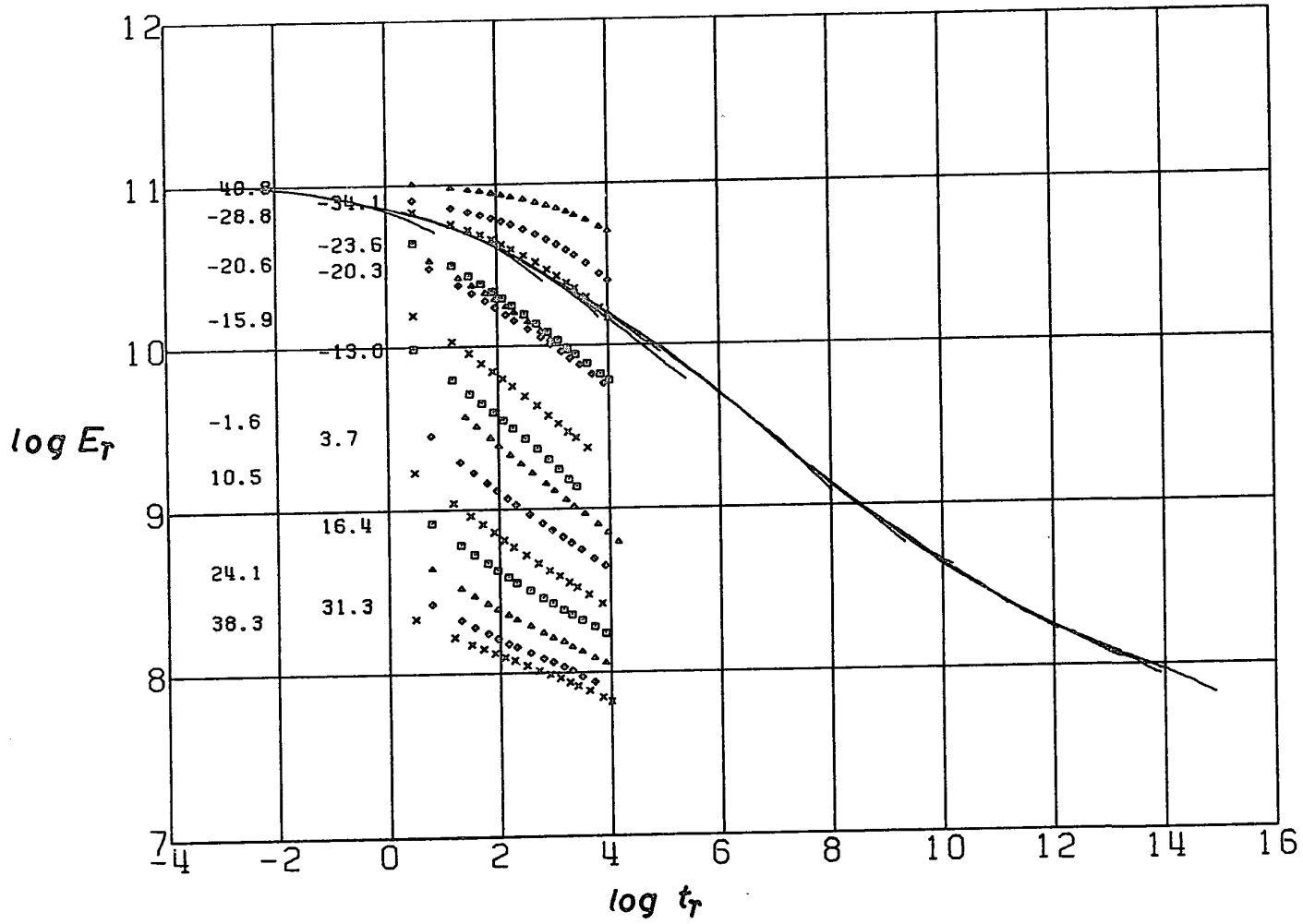
12
11
10
9
8
7
-4
-2
0
2
4
6
8
10
12
14
16
log E_r
log t_r
40.8
-34.1
-28.8
-23.6
-20.6
-20.3
-15.9
-13.0
-1.6
3.7
10.5
16.4
24.1
31.3
38.3

FIGURE 4

Stress relaxation curves for 100Na-66GL. Symbols: E_r versus t as a function of temperature (°C), every fourth point shown. Solid lines: pseudo-master curves.

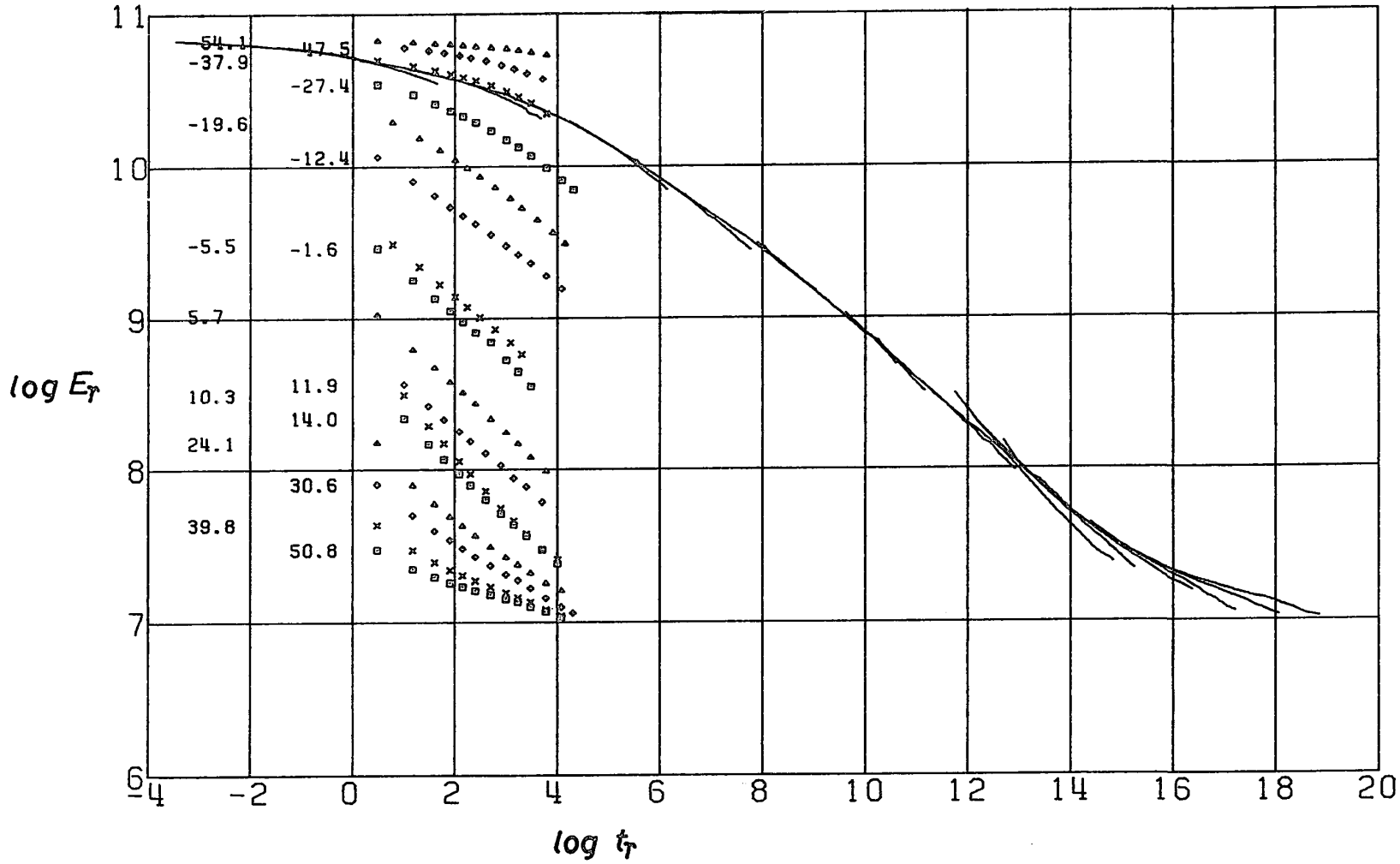
11
10
9
8
7
6
-4
-2
0
2
4
6
8
10
12
14
16
18
20
log E_r
log t_r
54.1
-37.9
-19.6
-5.5
5.7
10.3
24.1
39.8
47.5
-27.4
-12.4
-1.6
11.9
14.0
30.6
50.8

FIGURE 5

Stress relaxation curves for 100Na-50H_2O. Symbols: E_r versus t as a function of temperature (°C), every fourth point shown. Solid lines: pseudo-master curves.

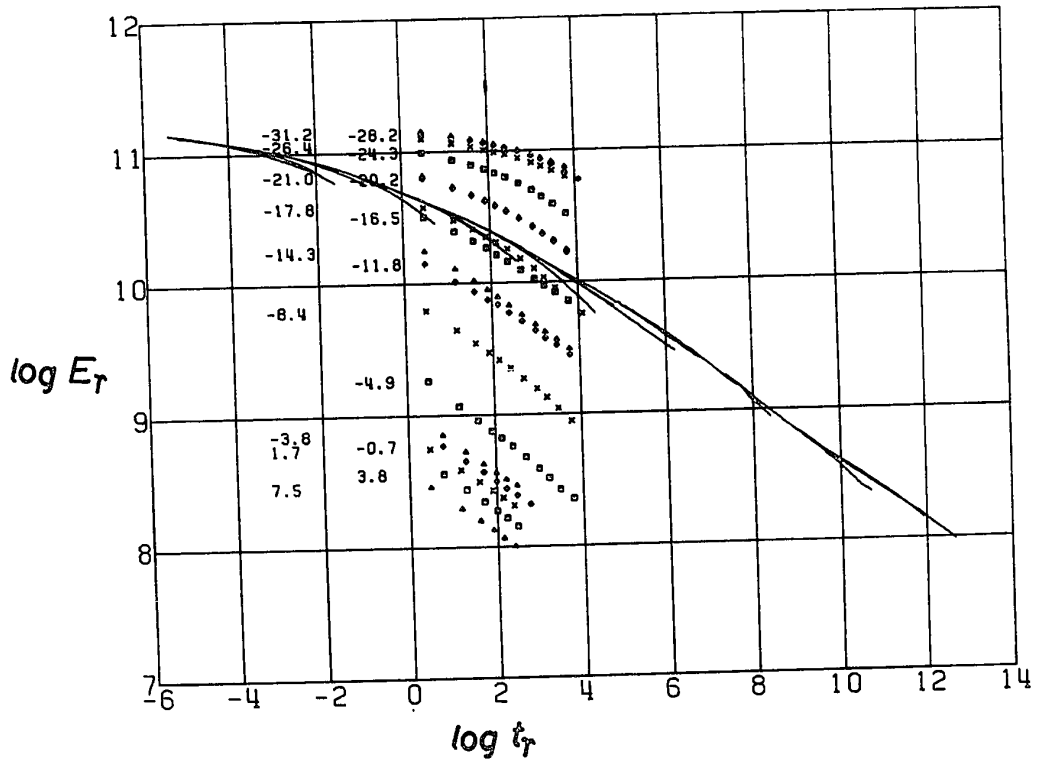
12
11
10
9
8
7
-6
-4
-2
0
2
4
6
8
10
12
14
log E_T
log t_T
-31.2
-26.4
-21.0
-17.8
-14.3
-8.4
-3.8
1.7
7.5
-28.2
-24.3
-20.2
-16.5
-11.8
-4.9
-0.7
3.8

reduction parameters

$$E_r(t) = \frac{T_o \rho_o}{T \rho} \; E(t) \tag{10}$$

$$t_r = t/a_T \tag{11}$$

The reference point for the measurement of T_o and ρ_o is normally taken as T_g. a_T, the shift factor, is obtained by determining the horizontal shift between two successive curves, after the vertical reduction parameters have been applied.

In the present system, initial attempts to prepare master curves in the above-described manner indicated that time-temperature superposition could not generally be achieved. As a result, the procedure was modified slightly so that overlap between successive curves was maximized in the short-time regions. The computer program used to calculate the shift factors for this form of overlap from original S.R. data is presented in Appendix C. The attempts at drawing master curves in this way are shown as the solid lines in Figs. 2-5. The contributions of the moduli which correspond to the longer times in any given constant temperature relaxation are seen to deviate downward from the upper envelope of E_r versus t_r. This is apparent for each of the materials presented in Figs. 2-5, where S.R. data were measured over about 3.5 decades of time. In the S.R. data presented in Appendix B, similar deviations are apparent in most of the curves (although the magnitude of the deviations varies considerably), but since the runs cover shorter periods of time (about 2.5 decades), the lack of superposition is not as dramatic.

It is apparent that the curves presented in Figs. 2-5 are not true master curves but what may be termed pseudo-master curves, which describe only the short-time relaxation behaviour at any given temperature. It is worth stressing that the same pattern is obtained whether measurements are made in order of increasing temperature or not. This was tested for 100Na-48FA (Fig. 2) and for 100Na-50H_2O (Fig. 5). Also, the lack of superposition cannot be attributed to the loss of plasticizer because this would result in deviations of the opposite direction, and would certainly not lead to reproducible results.

3. Modulus-Temperature Curves

Because the pseudo-master curves determine short-time behaviour only, it is not surprising that the variations in their shapes are closely paralleled by the variations in the shapes of curves of 10-sec modulus versus temperature. Because of their greater ease of presentation and simplicity in interpretation, modulus-temperature curves are used to illustrate the variation in mechanical behaviour of these polymers with the percentage and type of plasticizer and with the degree of neutralization. In Fig. 6, the 10-sec Young's modulus as a function of absolute temperature is shown for PAA samples with degrees of neutralization between 0% and 100% and with a common plasticizer content (ca. 27% formamide). The stars on each curve indicate the position of T_g as given in Table I. It is worthwhile to note the rise in glassy modulus — by about a factor of 3 — and the great

FIGURE 6

10-sec modulus of PAA versus temperature as a function of the degree of neutralization (formamide content ca. 27%). The stars on each curve indicate the position of T_g.

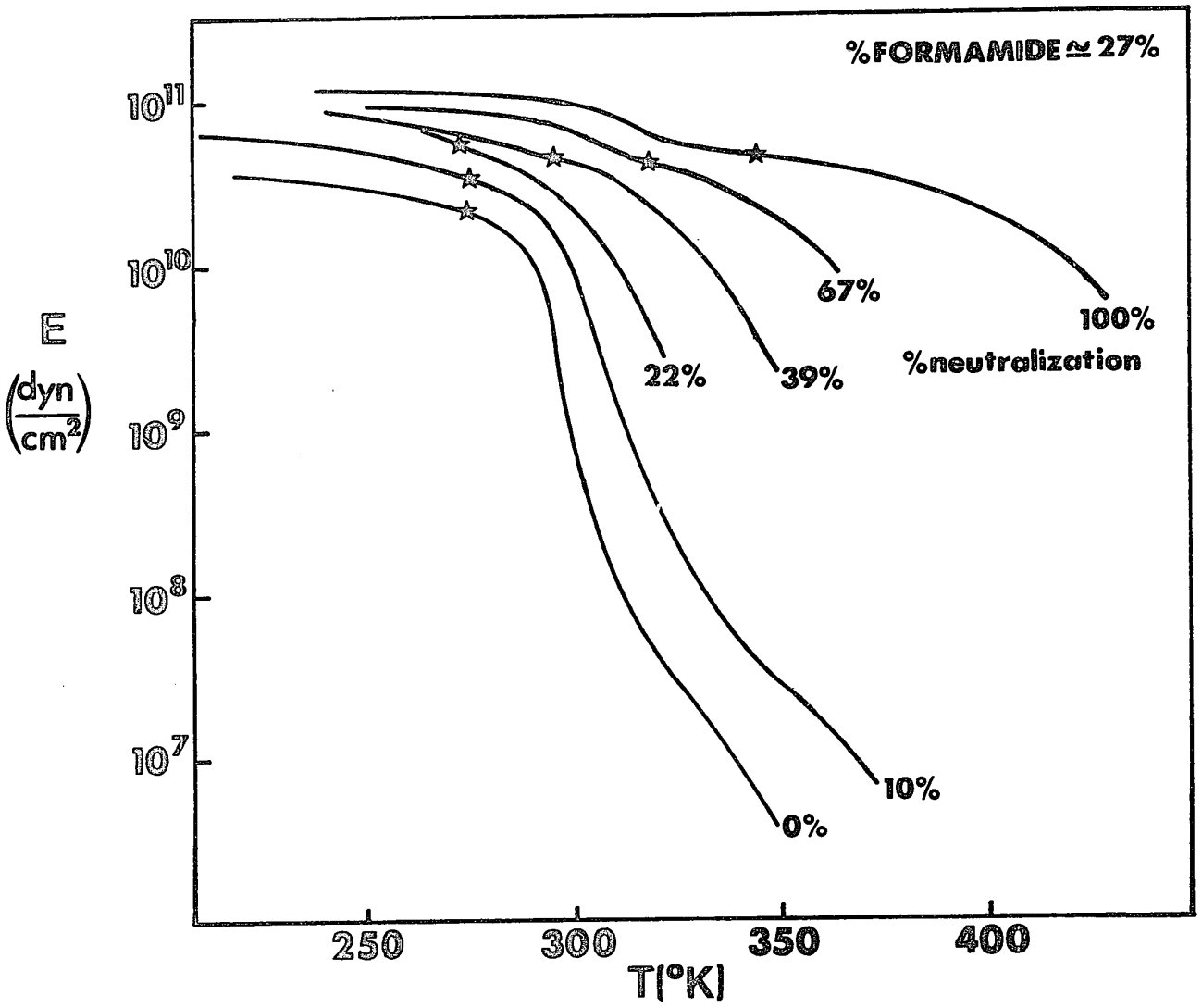
%FORMAMIDE ≃ 27%
10^{11}
10^{10}
10^{9}
10^{8}
10^{7}
E
$\left(\frac{dyn}{cm^2}\right)$
67%
100%
%neutralization
22%
39%
10%
0%
250
300
350
400
T[°K]

increase in the breadth of the transition as the ion content increases. It is clear that the high glassy moduli must be due to additional intermolecular bonding which results from the presence of ions.

Fig. 7 illustrates the variation in the modulus of the fully neutralized polymer as a function of the percentage of formamide. One can see that the broadness of the transition and the glassy modulus decrease with increasing plasticizer content, as one might expect. In Figs. 6 and 7, an inflection point below T_g appears in the modulus-temperature curves for low percentages of formamide and high degrees of neutralization. This inflection point seems to correlate with the occurrence of a broad shoulder in the loss tangent below T_g, as indicated by the dynamic mechanical measurements to be discussed in more detail below.

The shapes of some of the modulus-temperature curves presented in Figs. 6 and 7 are reminiscent of those obtained for partially crystalline polymers such as low density polyethylene.[9] However, the X-ray diffraction patterns obtained from a variety of PAA salts showed no evidence of any crystallinity.

Figs. 8 and 9 show the modulus-temperature behaviour of PNaA plasticized with glycerine and water, respectively. In these two cases, the range of plasticizer content is considerably less than for formamide, so the great variation in the shapes of the curves is not as apparent. However, it is readily seen that the rate of relaxation, which parallels the decrease in modulus

FIGURE 7

10-sec modulus of PNaA versus temperature as a function of formamide content. The stars on each curve indicate the position of T_g.

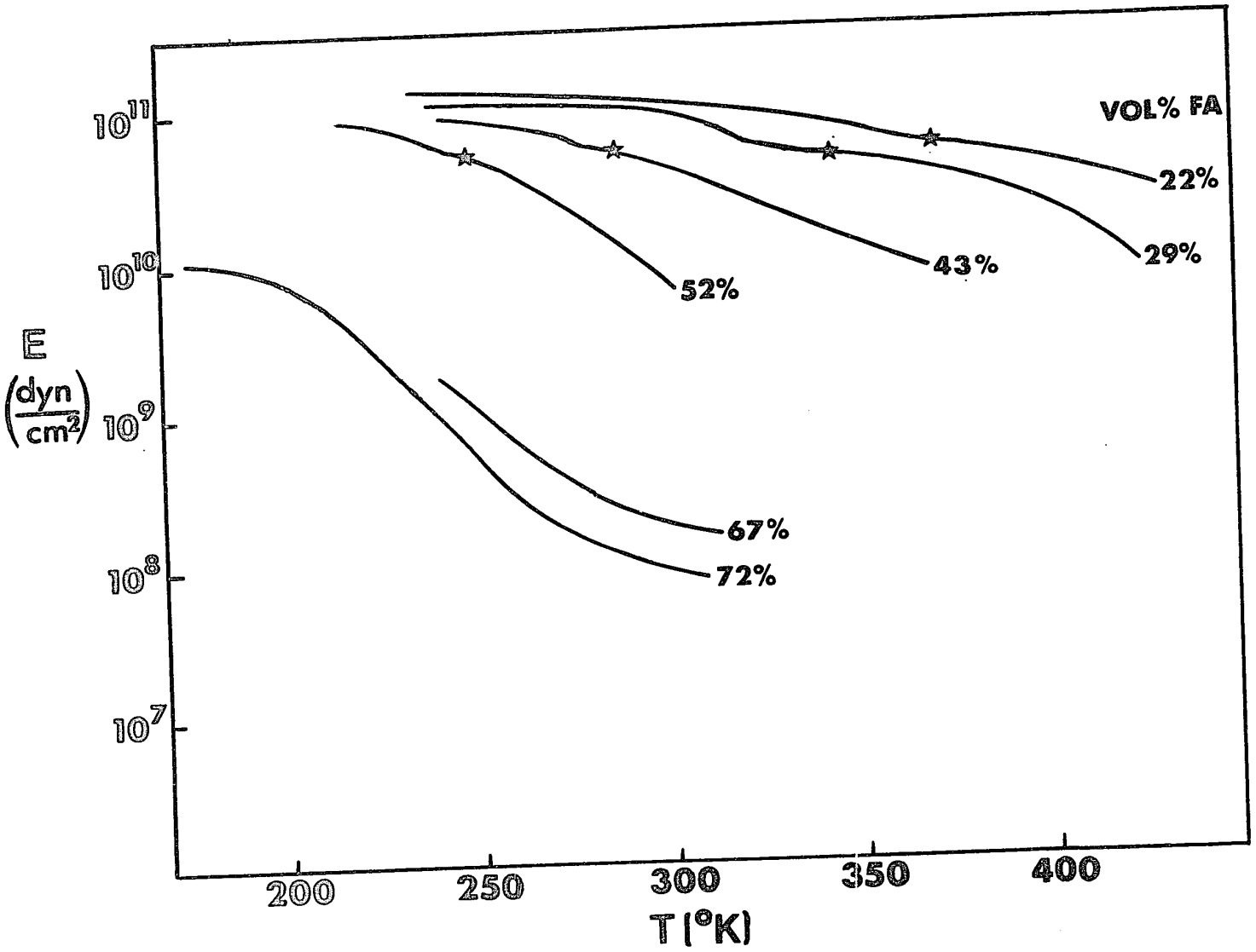
VOL% FA
22%
29%
43%
52%
67%
72%
E
(dyn/cm²)
10¹¹
10¹⁰
10⁹
10⁸
10⁷
200
250
300
350
400
T (°K)

FIGURE 8

10-sec modulus of PNaA versus temperature as a function of glycerine content. The stars on each curve indicate the position of T_g.

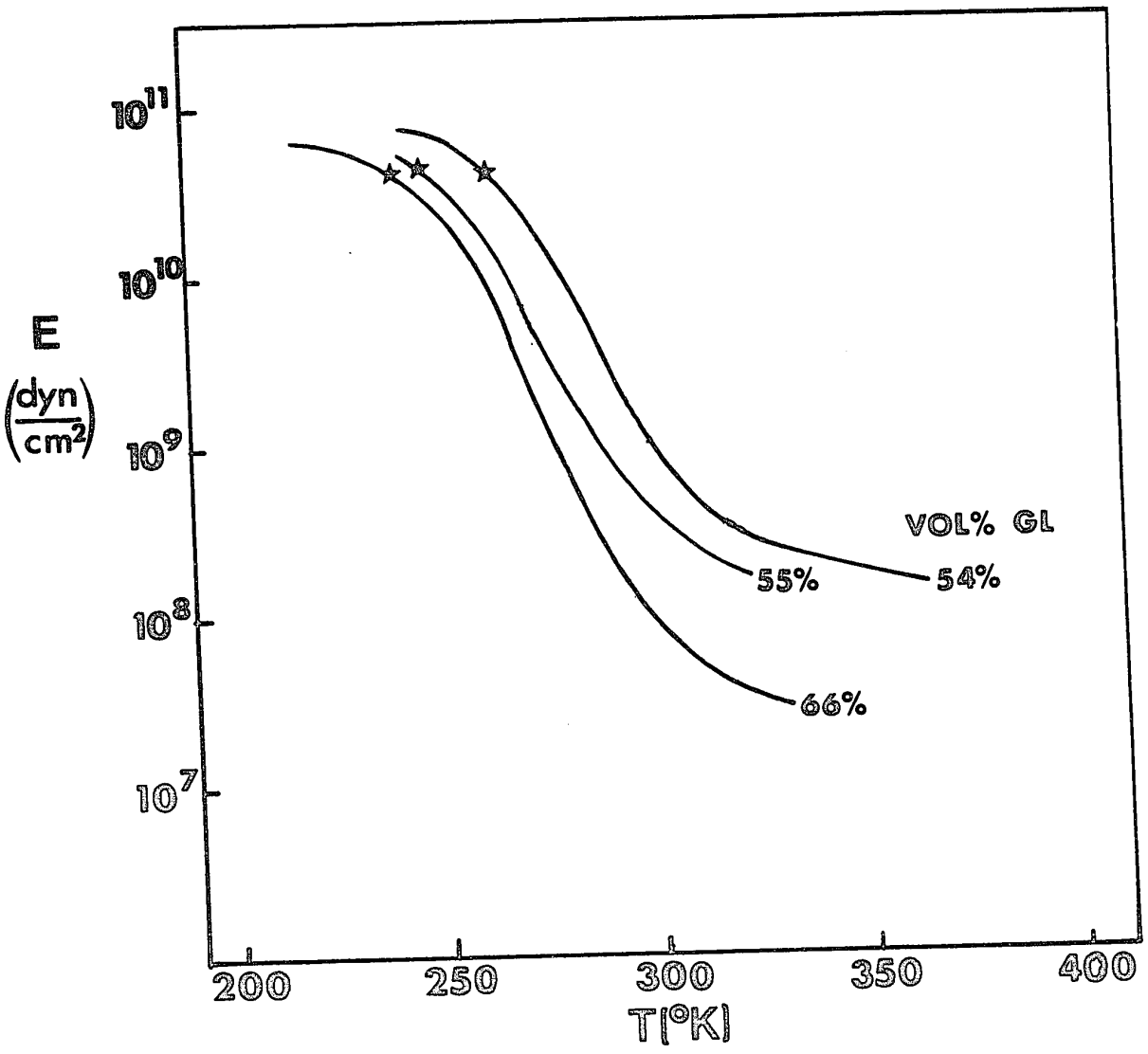
E
(dyn/cm²)
10¹¹
10¹⁰
10⁹
10⁸
10⁷
200
250
300
350
400
T(°K)
VOL% GL
54%
55%
66%

FIGURE 9

10-sec modulus of PNaA versus temperature as a function of water content. The stars on each curve indicate the position of T_g.

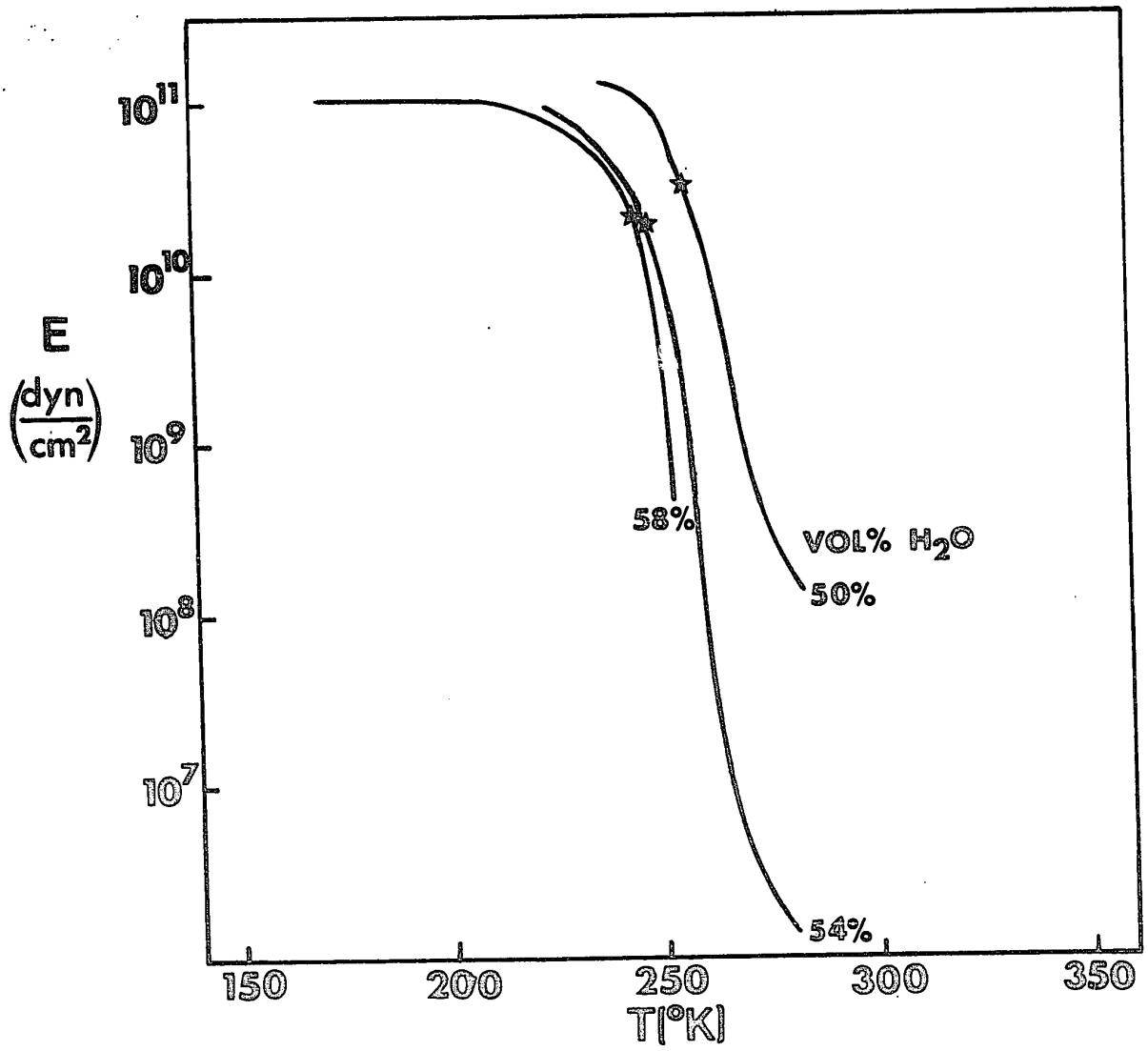
E
(dyn/cm²)
10¹¹
10¹⁰
10⁹
10⁸
10⁷
58%
VOL% H₂O
50%
54%
150
200
250
300
350
T(°K)

with temperature, is considerably greater than for formamide.

A direct comparison of the effect of plasticizer on the modulus-temperature behaviour of PNaA is shown in Fig. 10. The curves drawn in this figure were all obtained for approximately the same volume fraction of plasticizer. The glassy moduli and the glass transition temperatures of these polymers are all very similar. However, above T_g, the great variation in the efficiency of these plasticizers is apparent. This variation is a good indication that the plasticizer plays a very important role in determining the lifetimes of the ionic bonding.

4. Dynamic Mechanical Results

Measurements of the loss tangent, tan δ, at ca. 1 Hz as a function of temperature were made on three samples of PNaA: 100Na-50H_2O, 100Na-48FA and 100Na-55GL. The data are shown in Fig. 11, normalized with respect to the primary transition, for the sake of clarity. The dotted lines in Fig. 11 indicate the regions which were inaccessible to measurement of tan δ. Although the relative intensities are different, each curve shows a primary maximum and a broad shoulder just below it in temperature. It should be recalled that inflection points below T_g were observed in the modulus-temperature curves of PNaA at low formamide contents and high degrees of ionization. This shoulder in the loss tangent seems thus to correlate with the inflection points in the modulus-temperature curves of the PNaA-formamide series. The fact that no inflection point is seen in the PNaA-

FIGURE 10

10-sec modulus of PNaA versus temperature for four different plasticizers (ca. 54%). The stars on each curve indicate the position of T_g.

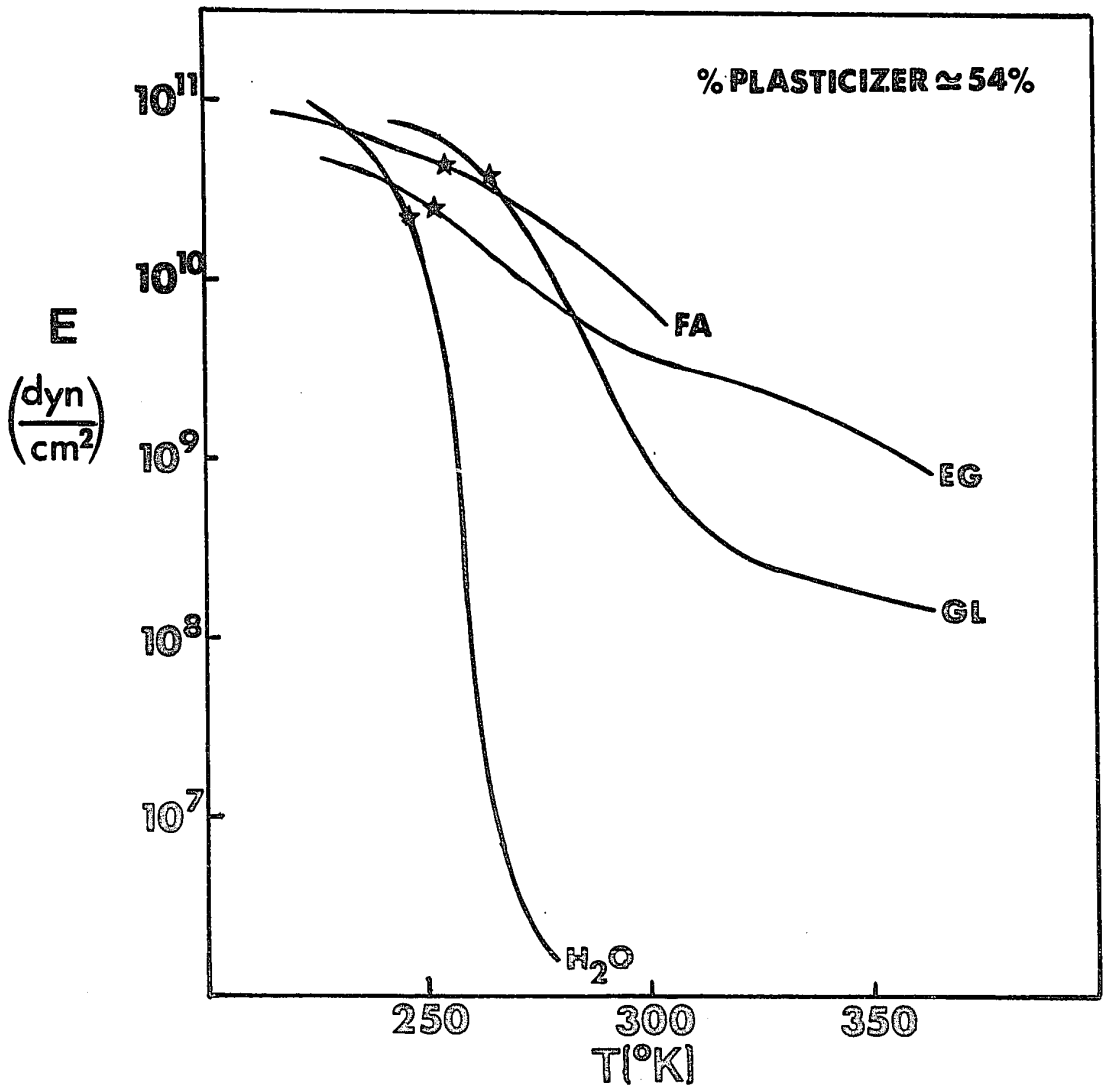
% PLASTICIZER ≃ 54%
E
(dyn/cm²)
10¹¹
10¹⁰
10⁹
10⁸
10⁷
FA
EG
GL
H₂O
250
300
350
T[°K]

FIGURE 11

tan δ versus $(T - T_g)$ for PNaA with three different plasticizers (□ — FA; Δ — GL; O — H_2O). The dotted lines represent regions inaccessible to measurement.

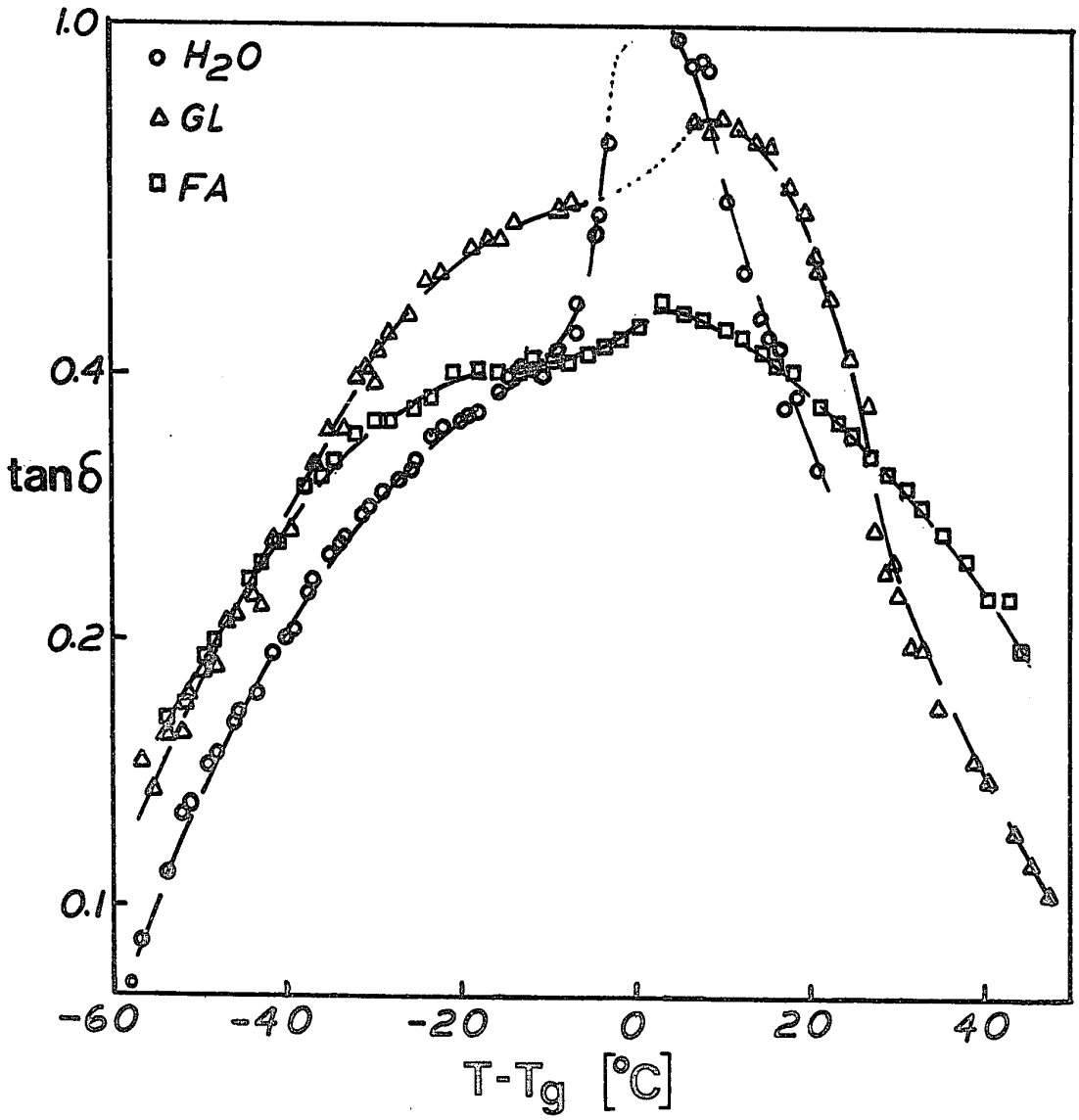
1.0
0.4
0.2
0.1
tanδ
H2O
GL
FA
-60
-40
-20
0
20
40
T-Tg [°C]

water or PNaA-glycerine series is likely due to the fact that the intensity of the shoulder is considerably less than that of the primary maximum in the latter two cases and the effect of the sub-T_g shoulder on the modulus would be relatively small.

5. X-Ray Diffraction

X-ray diffraction patterns were obtained for a number of plasticized salts of PAA. Since the X-ray study was not intended to be comprehensive in itself but was undertaken in support of the thermomechanical study, diffraction patterns were obtained

TABLE II

Plasticizer Content	% Ion Content	Counterion	d_g (Å) Inner Halo	Outer Halo
FA (23%)	0	—	12.1 ± 0.3	6.7 ± 0.2
H_2O (~5%)	0	—	12.1	6.7
H_2O (~5%)	1	Cs	12.3	6.7
H_2O (~5%)	5	Cs	13.4	6.2
H_2O (~10%)	25	Cs	14.3	—
H_2O (~20%)	100	Cs	15.0	—
FA (38%)	100	Cs	15.4	—
FA (29%)	100	Na	15.0	5.0
FA (48%)	100	Na	14.4	4.8
H_2O (low)	100	Na	15. *	

*Calculated from data presented in ref. 11

only for selected samples chosen mainly to correspond to materials on which mechanical measurements had been made. All of the X-ray patterns recorded showed either one or two diffuse halos in the range $4° < 2\theta < 40°$, where 2θ is the scattering angle. In each case, d_g, the dimension associated with the scattering, was obtained from[10]

$$d_g = 1.22\ d_B = 1.22\ \lambda/(2 \sin \theta) \qquad (12)$$

The results are presented in Table II, above, along with typical error limits, mainly due to the diffuseness of the halos.

D. Discussion

1. Structure

The X-ray diffraction patterns obtained in unionized PAA are similar to those observed in other amorphous polymers, such as polystyrene.[10] With increasing cesium content, the longer spacing increases, while the shorter spacing disappears. For the fully neutralized polymers, similar values of the longer spacing are seen in both cesium and sodium salts, and for both water and formamide as plasticizers; however, in the sodium salts, an outer halo is still observable. The scattering pattern obtained for the unionized material indicates that a type of amorphous order exists even here. This is not surprising, since the extent of hydrogen bonding in PAA should be considerable, and associations between the carboxyl groups could lead to a partially ordered structure.

It is assumed that cesium and sodium salts of PAA have es-

sentially the same structure. This was not tested specifically in this system, but rheological considerations have shown it to be true for styrene-methacrylic acid ionomers.[4] Non-crystalline X-ray maxima are associated with the average separation between recurrent centers of relatively high electron density. Because the electron density of cesium is much higher than that of the other atoms involved, the single halo observed in PCsA samples can likely be attributed to an average spacing between regions of high cesium content. The fact that a second halo is observed in PNaA is reasonable, since sodium, with an electron density not much greater than carbon, would not dominate the diffraction pattern like cesium. This evidence is therefore consistent with a microphase-separated structure (regions of high and low ionic content) for this polymer system. This conclusion is supported by a number of other factors which include the predictions based on thermodynamic arguments[12] and the evidence of phase separation in other organic ion-containing polymers, as discussed in Chapter I, as well as the rheological evidence in the present system, to be discussed shortly.

The longer spacings in the fully neutralized PAA samples provide a measure of the size of the ionic aggregates. Based on simple stoichiometry and assuming the complete incorporation of carboxyl groups, the number of ion pairs per aggregate is estimated to be about 25. The fact that the longer spacings do not vary much with the type of plasticizer indicates that the structure in glassy PNaA is not very dependent on the type of plasti-

cizer. However, X-ray diffraction is not sensitive to dynamic phenomena. The time dependence of the structure, on which the rheological properties depend, must be investigated by other means.

2. Separation of Relaxation Mechanisms

In Figs. 2-5, as well as in those presented in Appendix B, non-superposability of stress relaxation curves can be observed in varying degrees. In every case, the deviations at long times for any given constant temperature relaxation are toward lower values of modulus; this fact suggests the existence of two concurrent relaxation mechanisms with different activation energies. Similar viscoelastic responses have been observed in a variety of other non-crystalline polymers. In a number of cases, the lack of superposability has been attributed to a secondary relaxation mechanism: side-chain motion in the poly(alkyl methacrylates);[13,14] spontaneous bond interchange in polymeric sulfur;[15] and lanthanum-catalyzed bond interchange in the polyphosphates.[16]

In the present system, a two-mechanism viscoelastic response would be in line with the two-phase structure, since each phase could be expected to yield in response to the applied stress. In such a system, the contributions of the two mechanisms to the total compliance should be additive.[13] The method used in separating the contributions of the two mechanisms, as employed by Eisenberg and Teter,[15] is outlined below.

The upper envelope of modulus versus reduced time and the moduli of the original stress relaxation curves were converted to compliance values by the method of Hopkins and Hamming,[17] with the aid of a computer program written for this purpose. This program is outlined in Appendix D. It was found that, in regions of rapid stress relaxation, the values generated by this method differed significantly from those generated by the more approximate relationship[8]

$$J(t) = \sin m\pi/m\pi \; G(t) \qquad (13)$$

Shift factors for the individual curves of compliance versus time were recalculated by maximizing the overlap between their short-time regions. No significant differences were noted in the shift factors calculated from the original moduli. The conversion of stress relaxation data to compliances results in a pseudo-master curve of compliance versus reduced time. An example of such a curve is shown in Fig. 12, for $100Na\text{-}50H_2O$. The data in Fig. 12 correspond to those in Fig. 5; on the scale shown here, the curves are nearly mirror images.

It is assumed that, at any given temperature, the short-time compliance is mainly due to the primary relaxation mechanism; the upward deviations from the lower envelope of compliance versus reduced time are therefore due to the second mechanism, whose contribution is computed by means of point-by-point subtraction of compliance values from the lower envelope and the individual deviations in compliance corresponding to long-time relaxations at

FIGURE 12

Computed pseudo-master curve in compliance for $100Na\text{-}50H_2O$. Subtracted compliances and corresponding temperatures (°C) are shown.

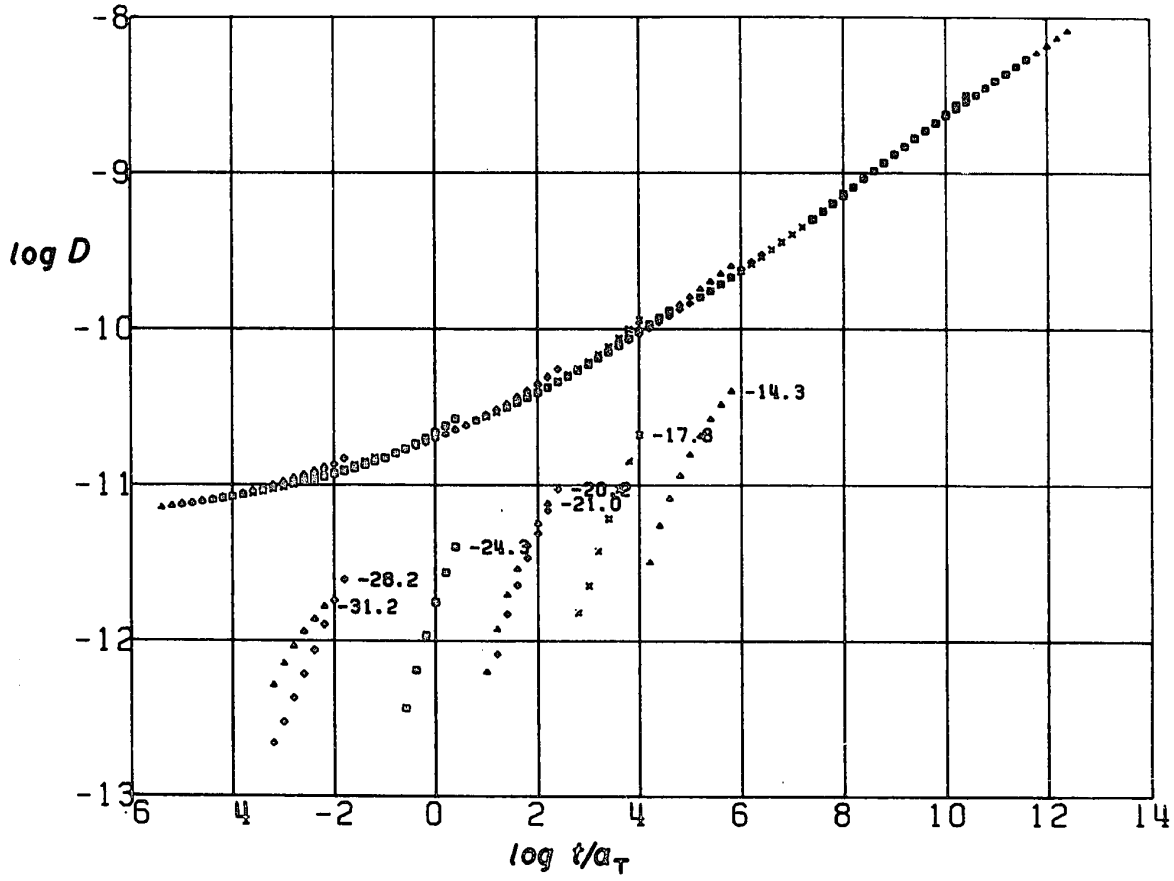
-8
-9
-10
-11
-12
-13
log D
-6
-4
-2
0
2
4
6
8
10
12
14
log t/a_T
-14.3
-17.8
-20
-21.0
-24.3
-28.2
-31.2

any given temperature. These subtracted curves of compliance versus reduced time for the system 100Na-50H_2O are also shown in Fig. 12.

The subtracted curves of compliance versus reduced time are converted back to real time by subtraction of the original shift factors, a_T. These curves are then reshifted into a secondary master curve of subtracted compliance versus reduced time by shifting horizontally with respect to one of the curves chosen as a reference. As a result, a new set of shift factors, b_T, is obtained. The result of this procedure for the curves in Fig. 12 is shown in Fig. 13. Similar curves were obtained for the two systems 100Na-66GL (S.R. data in Fig. 4) and 100Na-48FA (S.R. data in Fig. 2). These curves are presented in Figs. 14 and 15. The implications of the dashed lines in Figs. 13-15, representing a theoretical slope of unity, will be discussed later.

For each of the three materials discussed above, two master curves are obtained — the upper envelope, representing the short-time relaxation behaviour, and the secondary master curve, representing the long-time deviations from the envelope. The significance of the two master curves should be pointed out; just as one master curve allows the complete description of the viscoelastic response in a system with a single relaxation mechanism, then two master curves allow the complete description of the viscoelastic response in a system with two relaxation mechanisms.

FIGURE 13

Master curve of subtracted compliance for 100Na-50H_2O. Individual curves and corresponding temperatures (°C) are shown. Dashed line: theoretical slope of 1.

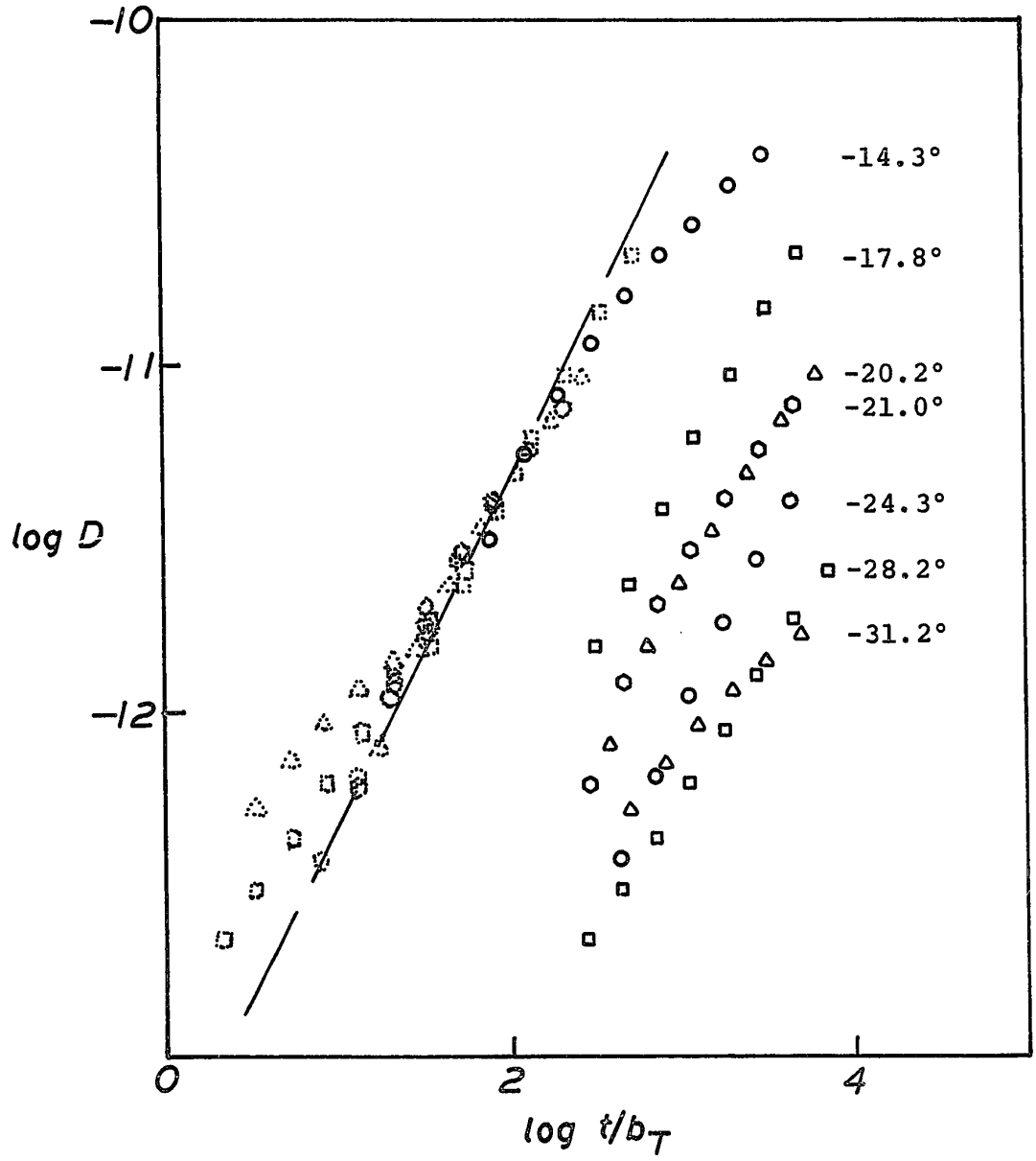
-10
-11
-12
log D
0
2
4
log t/b_T
-14.3°
-17.8°
-20.2°
-21.0°
-24.3°
-28.2°
-31.2°

FIGURE 14

Master curve of subtracted compliance for 100Na-66GL. Individual curves and corresponding temperatures (°C) are shown. Dashed line: theoretical slope of 1.

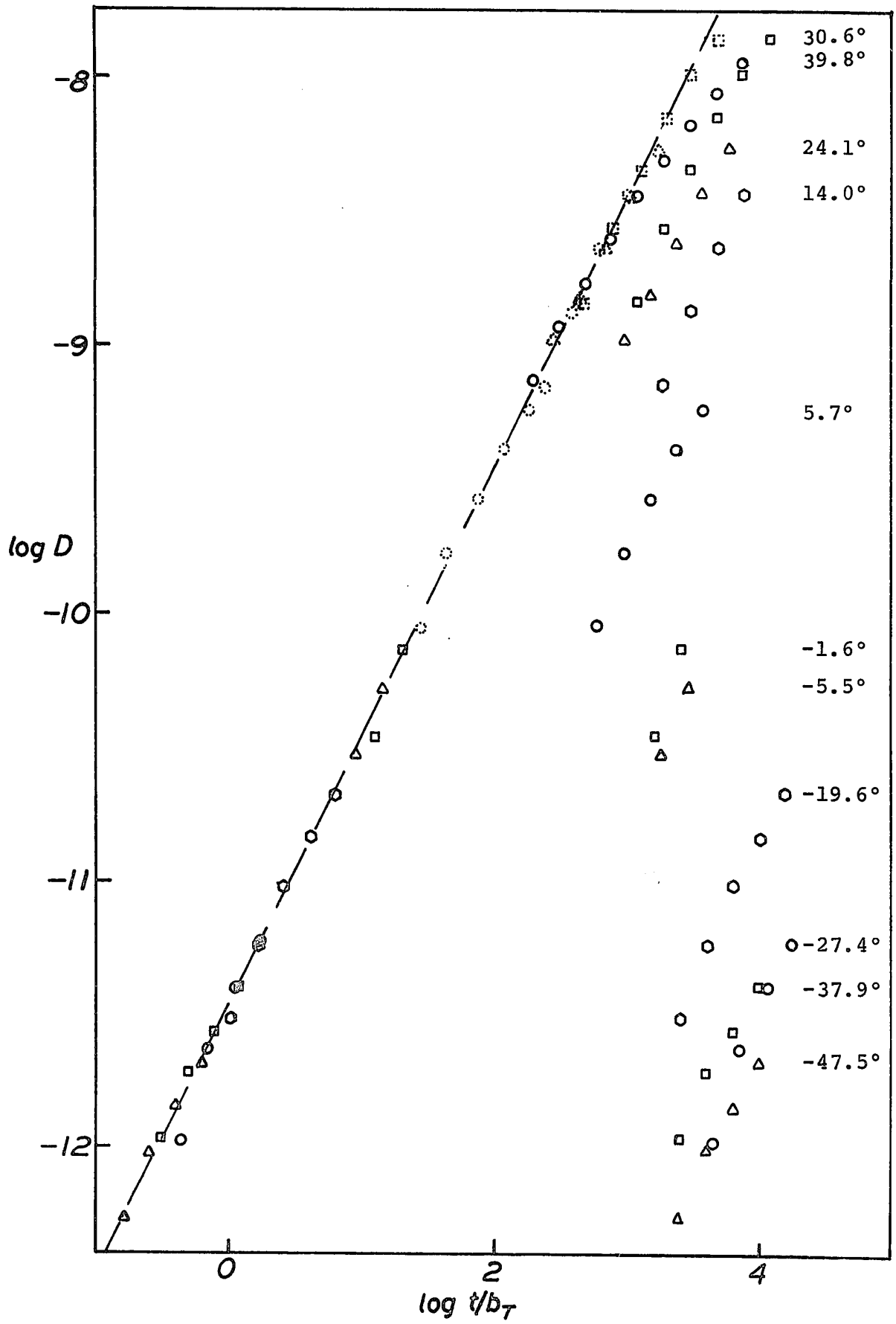
30.6°
39.8°
24.1°
14.0°
5.7°
-1.6°
-5.5°
-19.6°
-27.4°
-37.9°
-47.5°
-8
-9
-10
-11
-12
log D
0
2
4
log t/b_T

FIGURE 15

Master curve of subtracted compliance for 100Na-48FA. Individual curves and corresponding temperatures (°C) are shown. Dashed line: theoretical slope of 1.

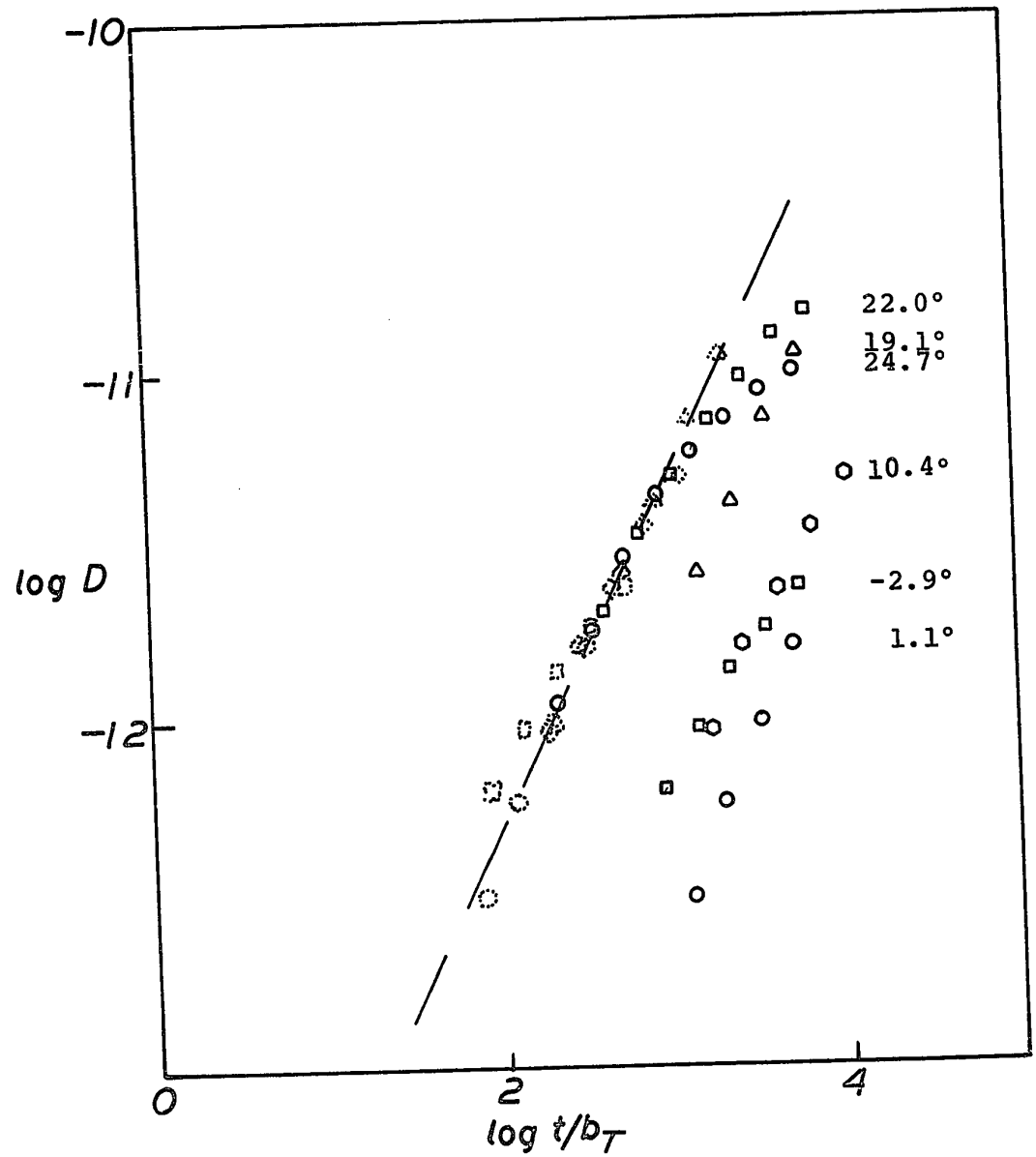
-10
-11
-12
log D
0
2
4
log t/b_T
22.0°
19.1°
24.7°
10.4°
-2.9°
1.1°

3. Nature of Primary Mechanism

The natures of the two relaxation processes and their relationships with the polymer structure are not perfectly clear; however, an analysis of their temperature dependences will be useful in relating them to physical processes. The mechanism whose contribution dominates the short-time behaviour above T_g can be investigated by an analysis of the primary shift factors, a_T, which contribute to the primary master curves.

It is of interest to determine whether the shift factors corresponding to the primary mechanism follow an Arrhenius-type temperature dependence, or whether they obey the W.L.F. equation[8]

$$\log a_T = - c_1^g (T - T_g)/(c_2^g + T - T_g) \qquad (14)$$

where the W.L.F. parameters c_1^g and c_2^g are referred to T_g. The W.L.F. equation can be rewritten in the following form

$$- \frac{1}{\log a_T} = \frac{c_2^g}{c_1^g} \frac{1}{T - T_g} + \frac{1}{c_1^g} \qquad (15)$$

Thus, from the slope and intercept of a plot of $- 1/\log a_T$ versus $1/(T - T_g)$, the constants c_1^g and c_2^g can be determined.

This procedure was followed for two samples from the series PNaA-glycerine, where a wide range of temperature above T_g is accessible for S.R. measurements. Values of $\log a_T$ from the temperature range $(T_g + 30°) < T < (T_g + 90°)$ were used to establish the linear relationships shown in Fig. 16. The W.L.F. parameters, obtained by a least-squares analysis, are also indicated in

FIGURE 16

- $1/\log a_T$ versus $1/(T - T_g)$ for PNaA-glycerine. W.L.F. parameters are indicated.

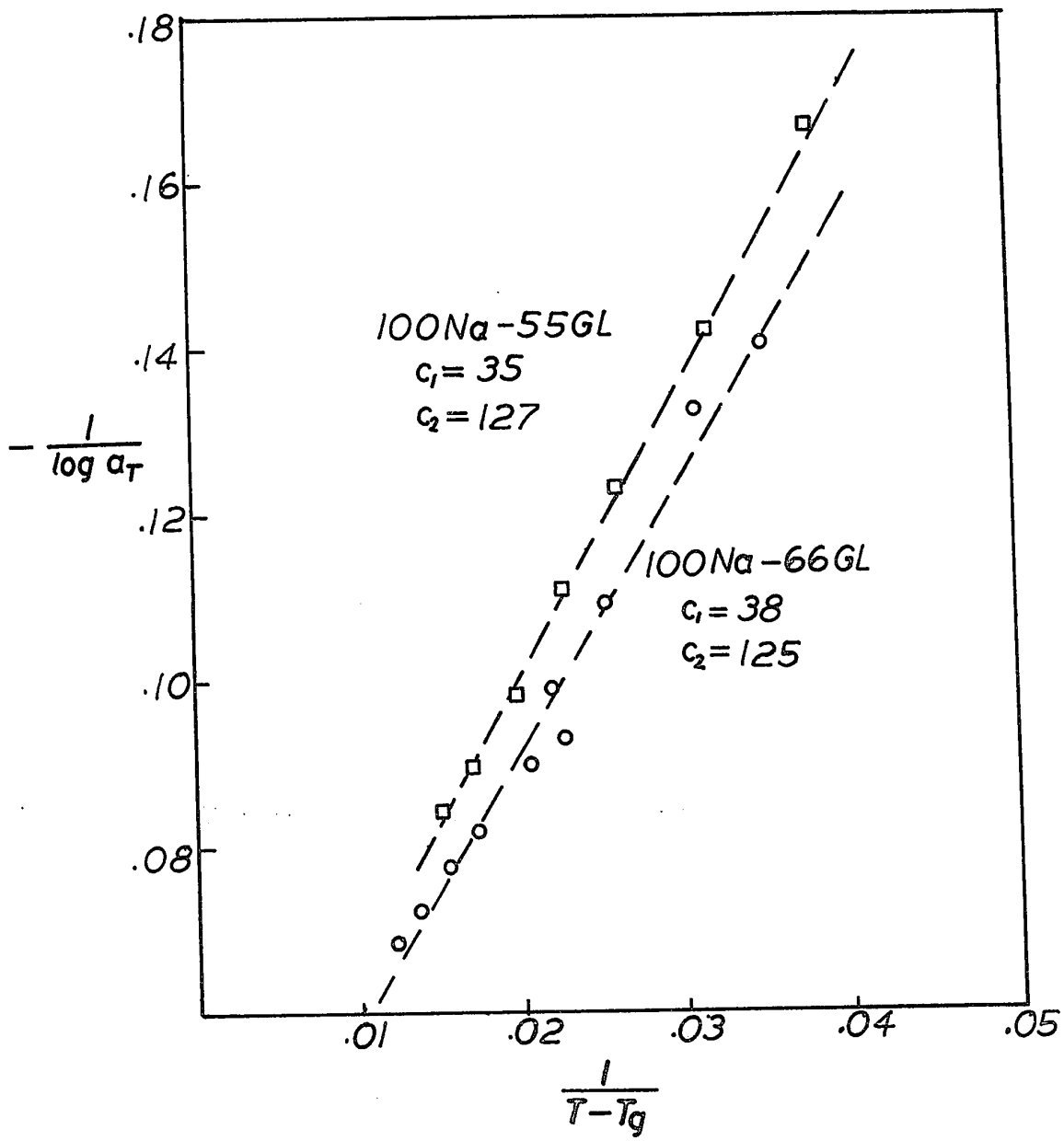
.18
.16
.14
.12
.10
.08
$-\frac{1}{\log a_T}$
100Na-55GL
$c_1 = 35$
$c_2 = 127$
100Na-66GL
$c_1 = 38$
$c_2 = 125$
.01
.02
.03
.04
.05
$\frac{1}{T - T_g}$

Fig. 16. The two sets of parameters do not differ significantly.

Plots of log a_T versus 1/T for the above two materials show definite curvature in the same temperature range. Since the latter curves should be linear for an Arrhenius temperature dependence, it can be concluded that the short-time shift factors in the system PNaA-glycerine are of W.L.F. type.

With volatile plasticizers, notably formamide and water, the accessible temperature range above T_g is small because of plasticizer loss. Thus, the establishment of W.L.F. parameters from stress relaxation measurements is impossible in these plasticized systems. However, there is other evidence, to be presented shortly, to support the applicability of the W.L.F. equation to the primary relaxation process even in these cases.

In all of the materials studied, the short-time shift factors, a_T, could be drawn to fit an Arrhenius-type temperature dependence in the immediate region of T_g. Examples of this can be seen in Fig. 17, in which log a_T versus 1/T is plotted for the series PNaA-formamide. The fact that the shift factors fit well with an Arrhenius-type temperature dependence in the vicinity of T_g cannot be considered significant in establishing the true temperature dependence, however, since the two forms of temperature dependence are generally indistinguishable in this range.

The W.L.F. equation can be used to predict the apparent activation energy at T_g, $(\Delta H_a)_{T_g}$; the relationship, which can be derived from Eq. 14, is given by[8]

FIGURE 17

Log a_T versus 1/T for PNaA-formamide.
Formamide percentages indicated.

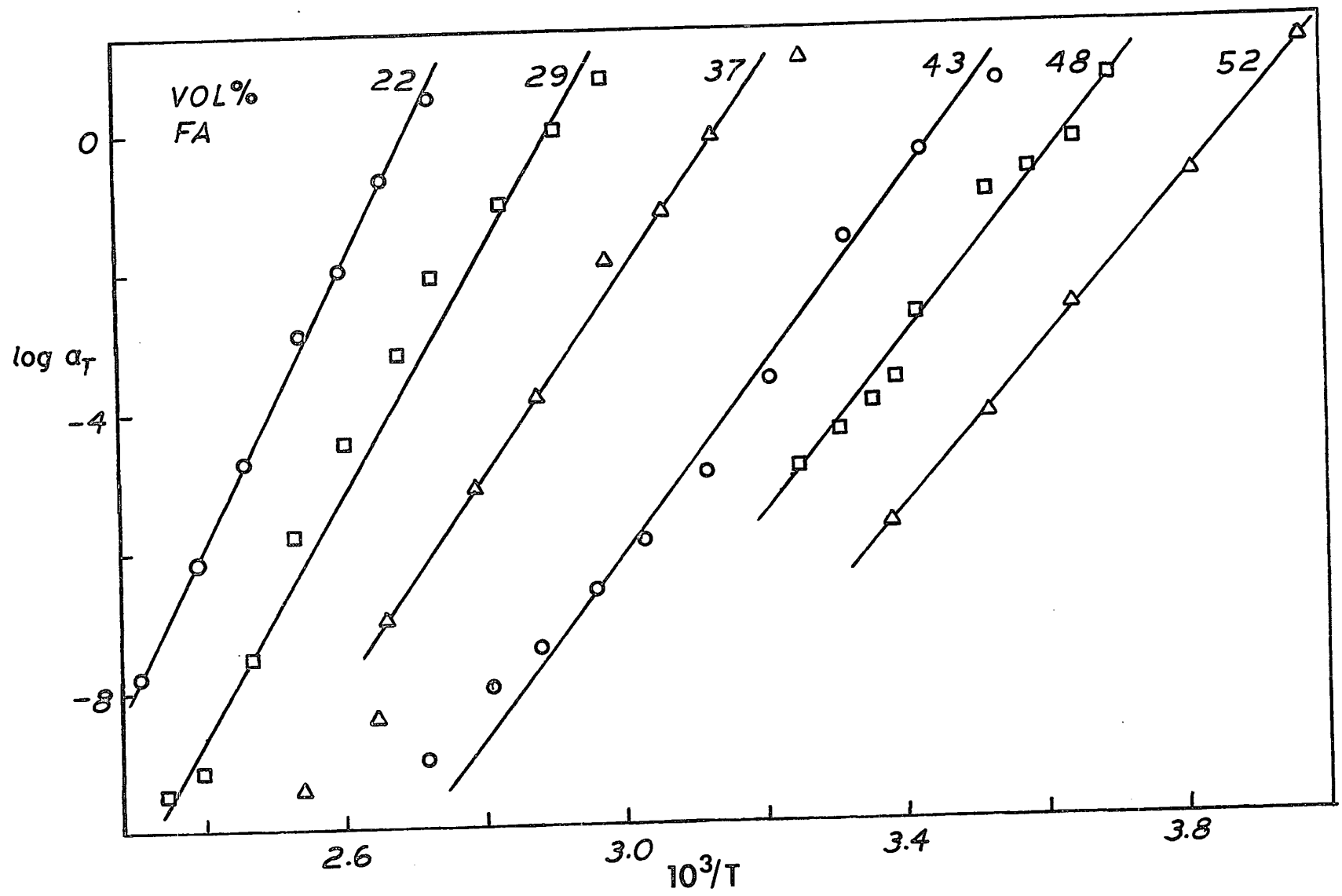
VOL%
FA
22
29
37
43
48
52
0
-4
-8
log a_T
2.6
3.0
3.4
3.8
$10^3/T$

$$(\Delta H_a)_{T_g} = 2.303\ R\ (c_1^g/c_2^g)\ T_g^2 \qquad (16)$$

Although the constants c_1^g and c_2^g would not be established for the formamide series, the proportionality between $(\Delta H_a)_{T_g}$ and T_g^2 can be demonstrated. From linear relationships of the type obtained in Fig. 17, values of $(\Delta H_a)_{T_g}$ were computed. For the PNaA-formamide series, these values were found to increase monotonically with decreasing plasticizer content (see Table III, page 135) and, as can be seen in Fig. 18, a linear relationship exists between $(\Delta H_a)_{T_g}$ and T_g^2.

This linear relationship can be predicted from Eq. 16 if it is assumed that the ratio c_1^g/c_2^g is constant in the range of composition studied. The W.L.F. parameters are given formally by[8]

$$c_1^g = B/2.303\ f_g$$
$$c_2^g = f_g/\alpha_f \qquad (17)$$

where f_g is the fractional free volume at T_g, α_f is the free volume expansion coefficient and $B \simeq 1$. Within a single plasticizer-polymer system, f_g is likely to be relatively constant and, as can be seen from Table I, the variation in α_f ($\simeq \alpha_\ell - \alpha_g$) is small. Thus, it is reasonable to assume that c_1^g/c_2^g is either constant or, at worst, a slowly varying function of the plasticizer content. Therefore, it can be concluded that the W.L.F. equation applies to the formamide series as well.

In view of the evidence to support the applicability of the W.L.F. equation to the primary relaxation process in PNaA, it

FIGURE 18

$(\Delta H_a)_{T_g}$ versus T_g^2 for PNaA-formamide. Formamide percentages indicated.

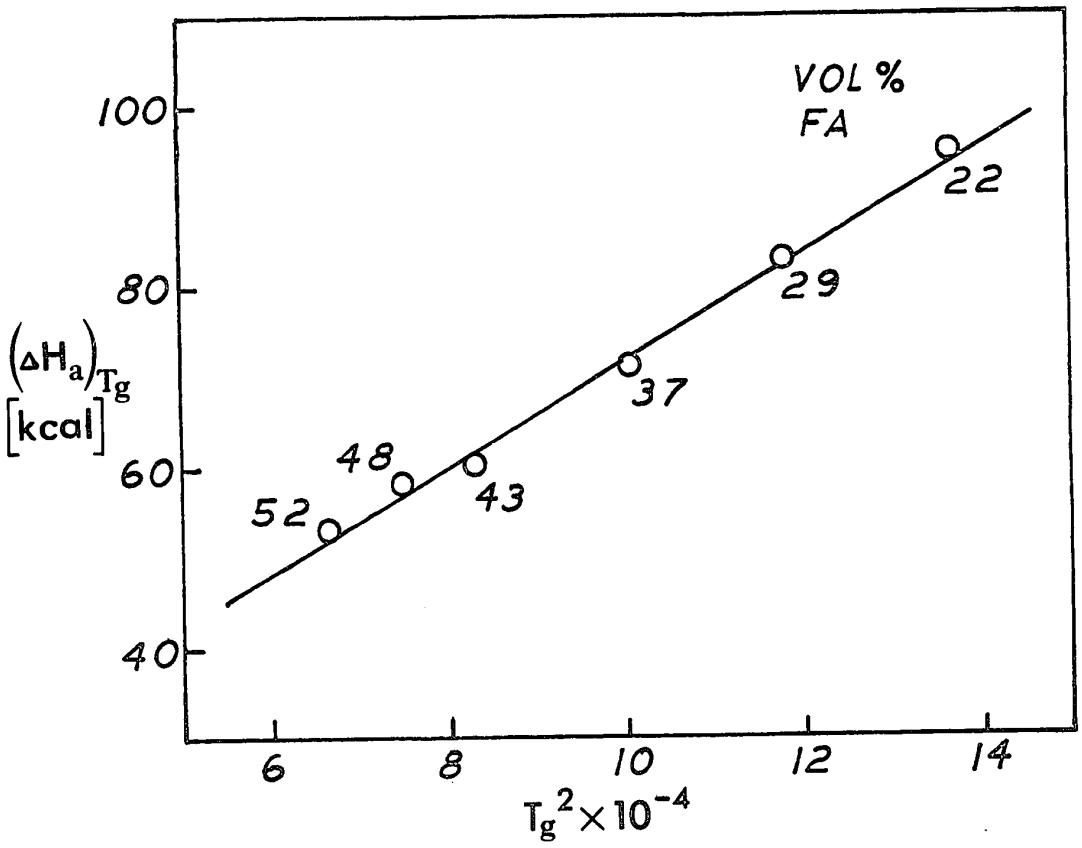
VOL %
FA
22
29
37
43
48
52
100
80
60
40
$(\Delta H_a)_{Tg}$
[kcal]
6
8
10
12
14
$T_g^2 \times 10^{-4}$

is reasonable to attribute its mechanism to the same type of diffusional process that characterizes the glass transition in most nonionic polymers. This assignment is also reasonable in view of the magnitude of the activation energy associated with the primary mechanism. By extrapolating the linear relationship obtained in Fig. 18 to the T_g of undiluted PNaA (T_g = 250°C, as reported by Eisenberg et al.[18]), $(\Delta H_a)_{T_g}$ = 175 kcal is obtained. This value is in general agreement with values which can be obtained for a wide variety of thermorheologically simple polymers by the application of Eq. 16.

The variation in $(\Delta H_a)_{T_g}$ with the percentage of plasticizer was studied only in the formamide system because of the narrow range of plasticizer contents employed in the other cases. Values of $(\Delta H_a)_{T_g}$ in the PNaA-glycerine series, calculated from Eq. 16 and the W.L.F. parameters in Fig. 16, were found to be somewhat higher than those at the corresponding value of T_g in the formamide series. $(\Delta H_a)_{T_g}$ for the primary mechanism in 100Na-50H_2O, obtained from the Arrhenius plot in Fig. 19, is higher still. These values, as well as those contributing to Fig. 18, are presented below in Table III.

It can be seen that the variation in apparent activation energy with the type of plasticizer (for similar values of % plasticizer) is in the order FA < GL < H_2O. This is the same order in which the rate of relaxation at constant % plasticizer increases (see Fig. 10). It is also the order in which the intensity of the primary peak in tan δ increases, as seen in Fig. 11.

FIGURE 19

Log a_T, log b_T versus 1/T for 100Na-50H_2O.

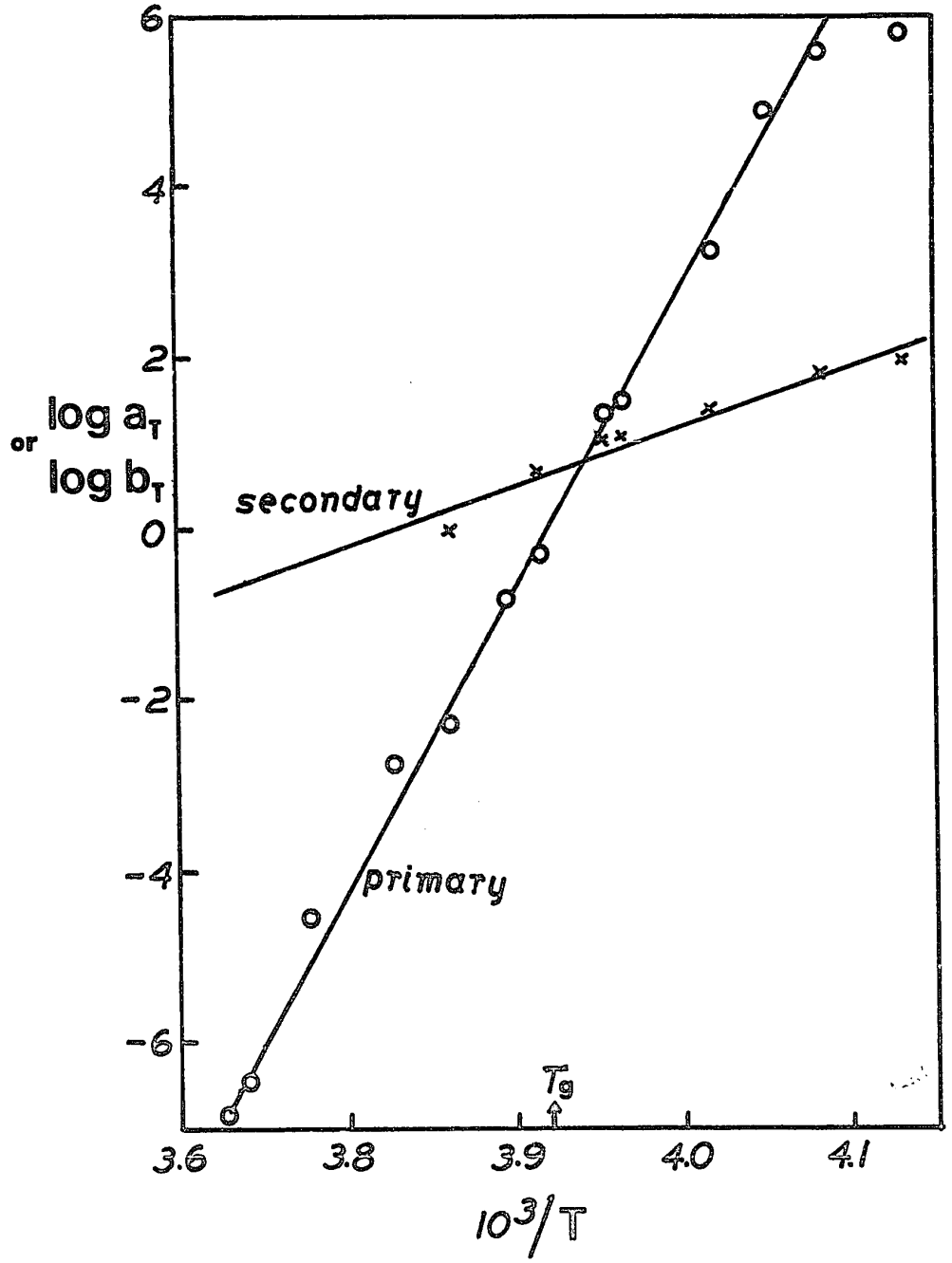
6
4
2
0
-2
-4
-6
or log a_T
log b_T
secondary
primary
T_g
3.6
3.8
3.9
4.0
4.1
$10^3/T$

TABLE III

Composition	T_g (°C)	$(\Delta H_a)_{T_g}$ (kcal)
100Na-22FA	97	95
100Na-29FA	71	83
100Na-37FA	45	71
100Na-43FA	15	61
100Na-48FA	0	58
100Na-52FA	-15	55
100Na-55GL	-28	76
100Na-66GL	-34	79
100Na-50H_2O	-18	160
00Na-23FA	1	96

Incidentally, the primary transition in PAA-formamide (see Fig. 21 in Appendix B) is also described by the W.L.F. equation, as might be expected. The constants $c_1^g = 35$ and $c_2^g = 127$ were obtained for 00Na-23FA from shift factors in the region $(T_g + 10°) < T < (T_g + 70°)$. The breadth of the transition in the unionized polymer is somewhat greater than that observed in non-hydrogen-bonded polymers such as polystyrene.[4] It is impossible to make a direct comparison with the transition in undiluted PAA, because of the dehydration and decarboxylation which occurs in PAA above its T_g;[1] however, the broadened transition may be merely a plasticizer

effect, due to induced local heterogeneities, as has even been observed in concentrated polystyrene solutions.[19]

Application of Eq. 16 to the above W.L.F. parameters yields the value $(\Delta H_a)_{T_g}$ = 96 kcal. Since this value is essentially the same as that obtained for the ionized material at the same plasticizer content (see Table III), it is a further indication that the primary mechanism in PNaA above T_g is essentially nonionic in nature.

4. Nature of Secondary Mechanism

The activation energy associated with the secondary process can be calculated from the shift factors used in obtaining master curves of the type shown in Figs. 13-15. The Arrhenius plot for the secondary mechanism in 100Na-50H_2O is shown in Fig. 19. The activation energies obtained varied from 32 kcal for 100Na-50H_2O to 17 kcal for both 100Na-66GL and 100Na-48FA. The variations in these values with the percent plasticizer were not tested because of the insufficient number of long-time runs and the tediousness of the method. It is difficult to specifically define the relaxation process involved in this polymer, but it is quite possible that it could correspond to the decomposition of an ion aggregate by the removal and subsequent migration of one ion pair. The amount of energy involved in this process would depend on the size and geometry of the aggregate and on a number of other factors, including the solvating effect of the plasticizer. The observed values of activation energy, which lie between 17

and 32 kcal, seem reasonable for such a mechanism.

Whatever its form, if the secondary relaxation process were due to the yielding of an ionic phase, its contribution to the compliance would correspond to a pure viscosity in the same fashion as bond interchange.[20] In this case, the approximate relationship

$$D(t) \simeq t/\eta \tag{18}$$

should hold. It can be seen in Figs. 13-15, by comparison with the doubly logarithmic slopes of unity, that this is a reasonable approximation. Thus, it can be concluded that the secondary mechanism is essentially viscous in nature.

5. Correlation with Dynamic Mechanical Data

The correlation of the sub-T_g shoulder observed in the dynamic mechanical study with one of the relaxation processes observed in the stress relaxation experiments should be possible through an analysis of the activation energies of the two dynamic mechanical peaks. This would involve dynamic mechanical measurements in a frequency range in which the peaks would be separated. Assuming that the sub-T_g transition is of lower activation energy than the primary transition, as might be expected, the separation of the peaks would require lower frequencies than those available on a torsion pendulum.

One method of investigating dynamic mechanical behaviour at low frequencies is by the conversion of stress relaxation data

to a dynamic mechanical function. This was done for some members of the PNaA-formamide series. The static creep compliance, D(t), which had been obtained from stress relaxation data in the manner described above (page 121), was converted to dynamic compliance by the method of Schwarzl and Struik,[21] assuming a semi-logarithmic approximation of third order for D(t). This computational procedure is included in the program described in Appendix D.

Although the conversion to dynamic compliance is highly sensitive to experimental errors and is inherently subject to large uncertainties because of truncation errors, it was nevertheless possible to qualitatively reproduce the pattern in tan δ that can be obtained from direct mechanical measurements using a torsion pendulum. This can be seen in Fig. 20, for 100Na-43FA, in which two peaks in tan δ in the vicinity of T_g are seen. Calculations of the activation energy for the sub-T_g in the PNaA-formamide series are tabulated below; the values obtained are quite scattered, and the variation in them is likely indicative of the magnitude of the error involved.

TABLE IV

Composition	$(\Delta H_a)_{T_g}$	$(\Delta H_a)_{\text{sub-}T_g}$
100Na-22FA	95	77
100Na-29FA	83	55
100Na-37FA	71	26
100Na-43FA	61	57

FIGURE 20

Computed tan δ versus T (°C) for 100Na-43FA at three frequencies: Δ - 0.1 Hz, $\square$ - 0.10 Hz, O - 0.001 Hz. T_g is indicated.

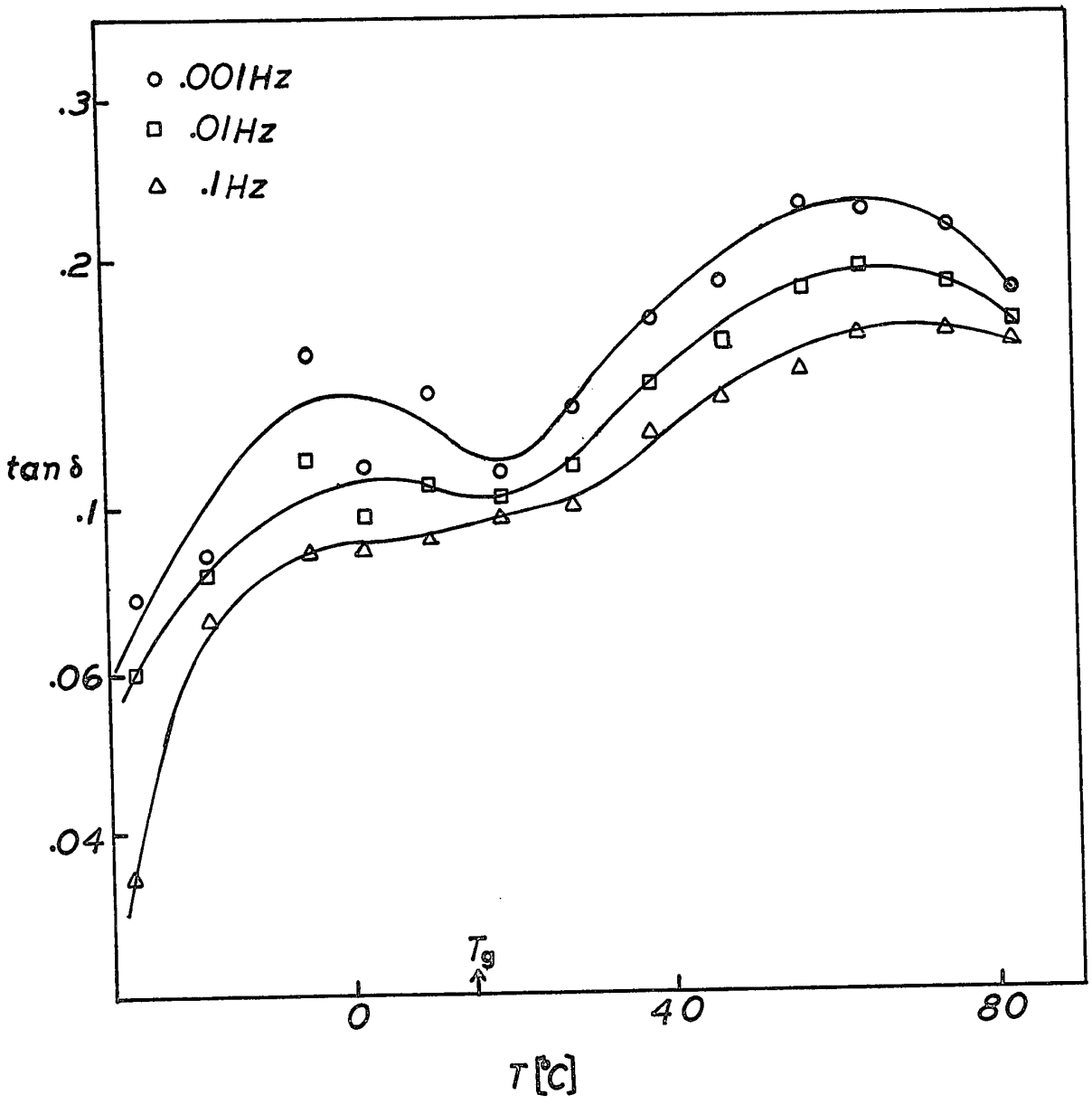
.001Hz
.01Hz
.1Hz
.3
.2
tan δ
.1
.06
.04
T_g
0
40
80
T [°C]

Since the range of values of $(\Delta H_a)_{sub\text{-}T_g}$ is close to values observed for the primary process in the same series, this mechanism could be expected to be competitive in stress relaxation. Thus, it is possible that the pseudo-Arrhenius region observed in the vicinity of T_g is in fact the result of two competitive relaxation mechanisms. This possibility would not necessarily negate the applicability of the W.L.F. equation to the primary process. It is even possible that both processes are describable in terms of the W.L.F. equation, as has been suggested in some phase-separated polymers.[22]

It was not possible, by the technique described above, to reproduce the pattern observed in PNaA-glycerine or PNaA-water. This may be due to the fact that the intensity of the sub-T_g peak in these two cases is too small in relation to the intensity of the primary transition.

E. Conclusions

This chapter has provided a survey of the viscoelastic properties of highly concentrated solutions of poly(sodium acrylate). Stress relaxation measurements taken as a function of the type and amount of plasticizer and the degree of neutralization have shown several major trends. First of all, there is a remarkable broadening in the glass transition as the ion content increases from 0 to 100%;in addition, there is a marked rise in the glassy modulus (by a factor of about 3) and in the glass

transition temperature, as observed by other workers. Secondly, the breadth of the transition in the fully neutralized polymer decreases as the plasticizer content increases. Finally, the breadth of the transition, but not the glassy modulus, varies considerably with the type of plasticizer.

Dynamic mechanical measurements indicate the existence of a broad shoulder in the loss tangent in the region below T_g. Structural investigations, by amorphous X-ray scattering, indicate a phase-separated structure consistent with the prediction that ions aggregate in organic polymers. The variation in the glassy structure of the fully neutralized polymer with the type and amount of plasticizer is small, as could be expected from the modulus-temperature behaviour.

The time dependence of the structure was investigated by analyzing the stress relaxation data in terms of a two-mechanism response. From this analysis, two master curves were obtained, one corresponding to the short-time relaxations and one corresponding to the deviations at long times. The latter mechanism was found to be essentially a pure viscosity, and was assumed to be ionic in nature. The former mechanism was found, by direct and indirect evidence, to be describable in terms of nonionic, free-volume theory (the W.L.F. equation) and was therefore assumed to be of the same diffusional nature as the primary mechanism in normal linear polymers.

A correlation between the stress relaxation behaviour and the dynamic mechanical results was provided by the conversion of static modulus to dynamic compliance. The pattern in the loss tangent curves obtained experimentally was qualitatively reproduced by the conversion procedure. From this analysis, it was suggested that a third, competitive mechanism is involved in the stress relaxation behaviour of poly(sodium acrylate) below T_g.

REFERENCES

[1] A. Eisenberg, T. Yokoyama, and E. Sambalido, J. Polym. Sci., A-1, 7, 1717 (1969).

[2] L. J. T. Hughes and D. B. Fordyce, J. Polym. Sci., 22, 509 (1956).

[3] A. Eisenberg and T. Sasada, in "Physics of Non-crystalline Solids," ed. J. A. Prins, North-Holland, Amsterdam (1965), p.99.

[4] M. Navratil, Ph.D. Thesis, McGill Univ., 1972.

[5] R. E. Kelchner and J. J. Aklonis, J. Polym. Sci., A-2, 9, 609 (1971).

[6] B. Cayrol, Ph.D. Thesis, McGill Univ., 1972.

[7] L. E. Nielsen, "Mechanical Properties of Polymers," Reinhold, New York (1967), Chap. I.

[8] J. D. Ferry, "Viscoelastic Properties of Polymers," 2nd ed., Wiley, New York (1970), Chap. XI.

[9] M. Takayanagi, Mem. Fac. Eng. Kyushu Univ., 23, 41 (1963).

[10] R. F. Boyer and H. Keskkula, in "Encyclopedia of Polymer Science and Technology," Vol. 13, Wiley, New York (1970), pp. 224-229.

[11] F. C. Wilson, R. Longworth, and D. J. Vaughn, A.C.S. Polymer Preprints, 9, 505 (1968).

[12] A. Eisenberg, Macromolecules, 3, 147 (1970).

[13] J. D. Ferry, W. C. Child, Jr., R. Zend, D. M. Stern, M. L. Williams, and R. F. Landel, J. Colloid Sci., 12, 53 (1957).

[14] W. C. Child, Jr. and J. D. Ferry, J. Colloid Sci., 12, 327, 389 (1957).

[15] A. Eisenberg and L. A. Teter, J. Phys. Chem., 71, 2332 (1967).

[16] A. Eisenberg and S. Saito, J. Macromol. Sci., A2, 799 (1968).

[17] I. L. Hopkins and R. W. Hamming, J. Appl. Phys., 28, 906 (1957).

[18] A. Eisenberg, H. Matsuura, and T. Yokoyama, J. Polym. Sci., A-2, 9, 2131 (1971).

[19] L. L. Chapoy, Ph.D. Thesis, Princeton Univ., 1969.

[20] A. V. Tobolsky, "Properties and Structure of Polymers," Wiley, New York (1960).

[21] F. R. Schwarzl and L. C. E. Struik, Advan. Mol. Relaxation Processes, 1, 201 (1968).

[22] D. G. Fesko and N. W. Tschoegl, J. Polym. Sci., C, 35, 51 (1971).

[23] S. Newman, W. R. Krigbaum, C. Laugier, and P. J. Flory, J. Polym. Sci., 14, 451 (1954).

[24] H. P. Gregor and M. Frederick, J. Polym. Sci., 23, 451 (1957).

APPENDIX A

Preparation of PAA

The PAA samples used in this study were prepared in part by Dr. T. Yokoyama (and reported in ref. 1 of this chapter) and in part by Mr. Karl Taylor, using a similar method. Since the latter work is unpublished, and is of relevance to this thesis, it is included here.

The PAA was prepared by the polymerization of acrylic acid in toluene with benzoyl peroxide (Bz_2O_2) initiator. The acrylic acid used in the preparation was obtained from Anachemia Chemicals and purified by vacuum distillation. The polymerizations were carried out in a well-stirred reaction kettle at ca. 50°C. A solution of Bz_2O_2 in 50 ml toluene was added dropwise to a solution of 140 ml acrylic acid and 1050 ml toluene. The weight of Bz_2O_2 added varied from 0.02 g to 0.85 g. All of the chemicals used in the preparation were of reagent grade.

The reactions were allowed to continue until about 70% complete. The polymer precipitate was then collected and dried to constant weight at 80°C, under vacuum. The molecular weights of the PAA samples were determined by viscometry in dioxane solution at 30°C, using the relationship[2,3]

$$[\eta] = 8.5 \times 10^{-4} M_v^{0.50} \qquad \text{(A1)}$$

The values of M_v obtained are reported in Table V , below, along with the initiator/monomer ratios used in the synthesis. It is apparent that all of the polymers are polydisperse.

Also tabulated below are the intrinsic viscosity determinations of PAA in the acidic and basic media described in Chapter II (page 31) and used to establish the relationships reported there. The accuracy of the relationships should not be taken

too seriously, since only a relative effect was desired.

TABLE V

initiator / monomer	$[\eta]_{dioxane}$	M_v ($\times 10^{-5}$)	$[\eta]_{acidic}$	$[\eta]_{basic}$
0.04%	0.60	5.1	1.14	1.10
0.06%	0.58	4.7	1.14	1.07
0.18%	0.46	2.9	—	—
0.15%	0.41	2.3	0.75	0.72
0.06%	0.32	1.4	0.62	0.61
1.2%	0.28	1.1	0.51	0.52

In the titration of PAA with aqueous NaOH, the phenolphthalein end-point was taken to indicate complete neutralization. A study of the potentiometric titration of PAA by various alkali metal and quaternary ammonium bases has been made.[24] This study showed that titration of PAA with alkali metal bases results in a fairly sharp end-point in the vicinity of pH = 9-10. The variation in pH with the degree of neutralization indicates that over the usual transition range for phenolphthalein (pH = 8-10), the inherent titration error is about 1-2%; this error, which is of a systematic nature, is reflected in the uncertainty in the sample composition.

APPENDIX B

Additional Pseudo-master Curves

Pseudo-master curves for the materials listed in Table I, but not specifically referred to in the text, are illustrated here. From the data contained in these figures, the modulus-temperature curves, shown in Figs. 6-10, were prepared. The shift factors were obtained by the method described in Appendix C. In a few cases, where no overlap was found, but where the lack of overlap was not too great, shift factors were computed by extrapolation. For two materials, 100Na-54H_2O and 100Na-58H_2O, the lack of overlap was too severe to permit the determination of shift factors even by extrapolation. For these materials, only modulus-temperature curves are reported. However, the original stress relaxation data are included in the Tables of Supporting Data.

Each of the following figures shows reduced modulus versus time (every fourth point indicated, temperatures in °C) and the pseudo-master curve of reduced modulus versus reduced time. All reductions are with reference to T_g, except in Figs. 31 and 32, where T_g was out of range. In the latter cases, the reference curve is the one at the lowest temperature. The order of presentation is summarized in Table VI, on the following page.

The major errors contributing to the modulus determinations from Eq. 1 can be summarized as follows:

(i) Systematic error in the determination of b — 10-20%. This error is constant throughout any one mode of deformation and is largely irrelevant, since it does not affect the shape of a S.R. curve.

(ii) Random error in the measurement of deformation — ±0.0002 cm, typically 1-2%. This error is reflected in the determination of the shift factor.

(iii) Random error in the measurement of force — ±1 g. This error is only significant at long times, when it can be as high as 10%. It does not affect the calculation of shift factors, which depend only on short-time readings, but it strongly influences the subtractive procedure used to determine the secondary master curves, where relative errors are as high as 20%.

TABLE VI

Composition	Fig.No.	Page Figure	Page Data
00Na-23FA	21	149	186
10Na-26FA	22	149	187
22Na-23FA	23	150	188
39Na-25FA	24	150	189
67Na-27FA	25	151	190
100Na-22FA	26	151	191
100Na-29FA	27	152	193
100Na-37FA	28	152	195
100Na-43FA	29	153	196
100Na-52FA	30	153	197
100Na-67FA	31	154	198
100Na-72FA	32	154	199
100Na-54EG	33	155	200
100Na-54GL	34	155	201
100Na-54H_2O	—	—	202
100Na-58H_2O	—	—	203

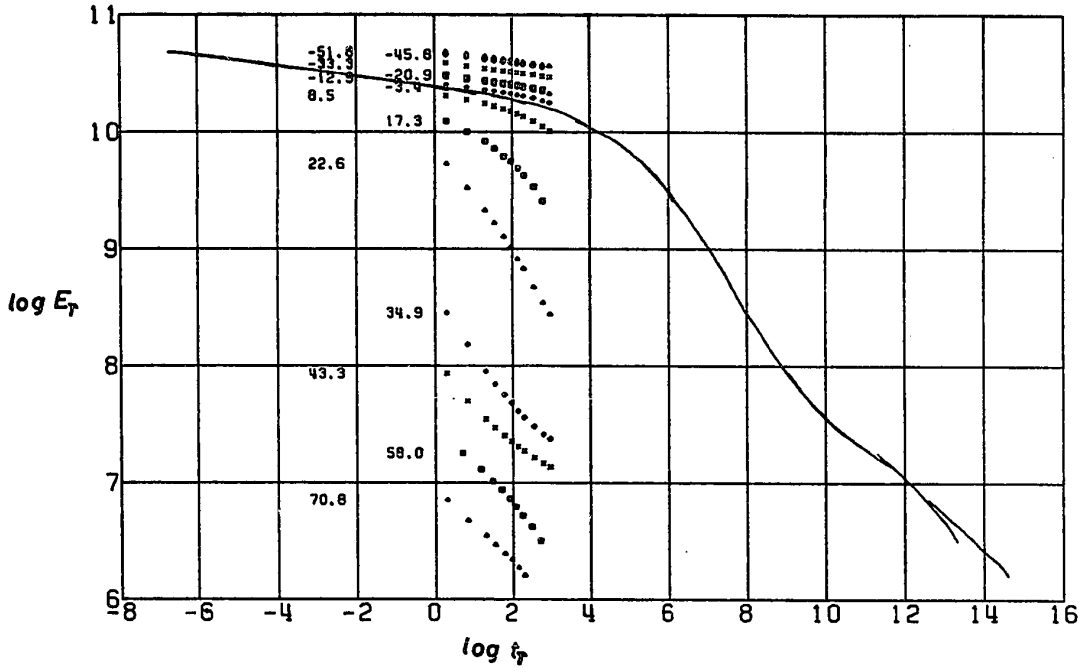

FIGURE 21 — 00Na-23FA

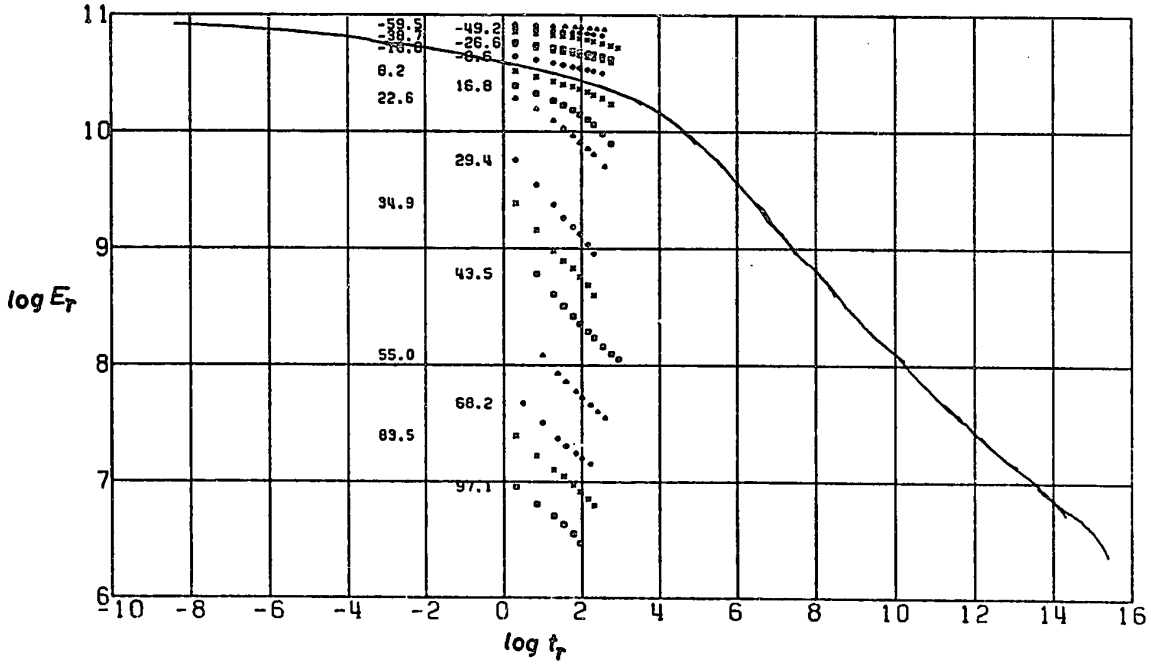

FIGURE 22 — 10Na-26FA

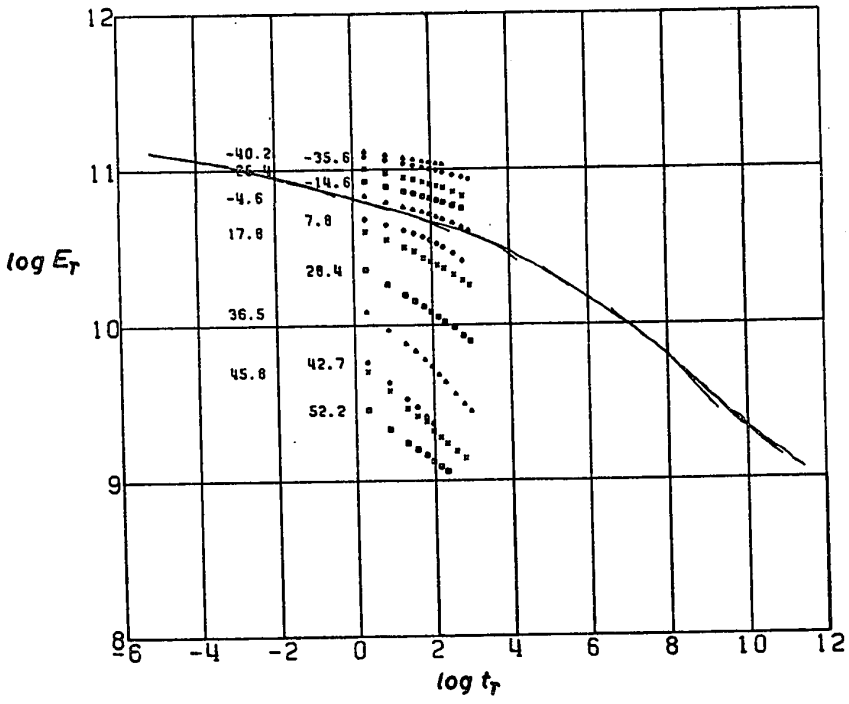

FIGURE 23 — 22Na-23FA

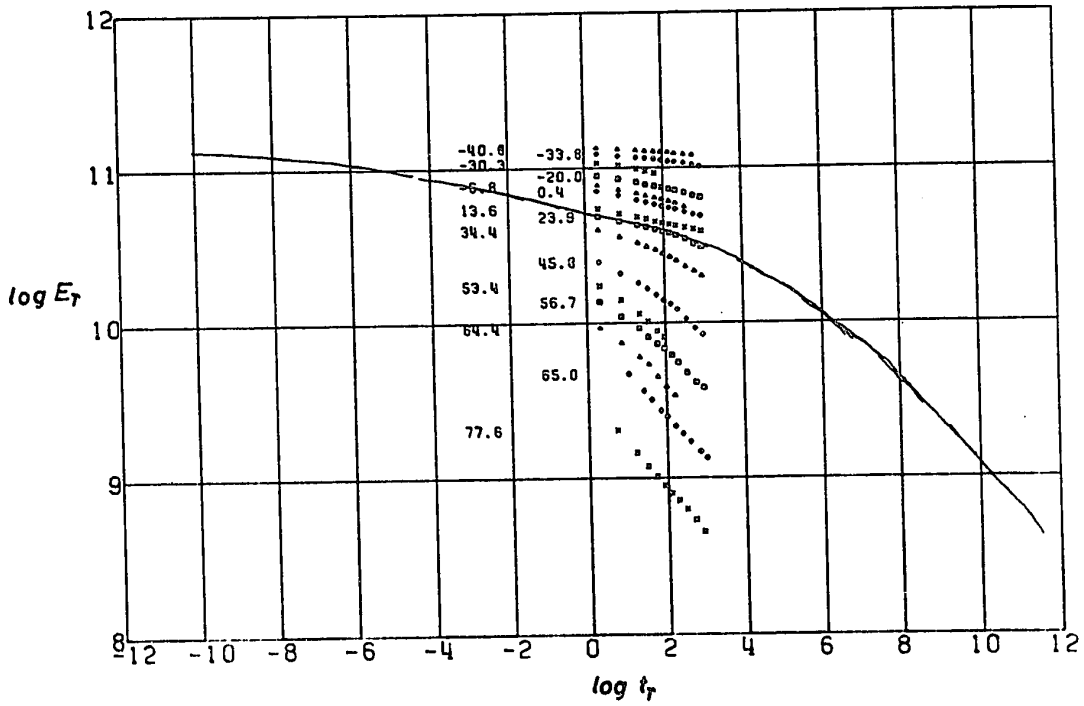

FIGURE 24 — 39Na-25FA

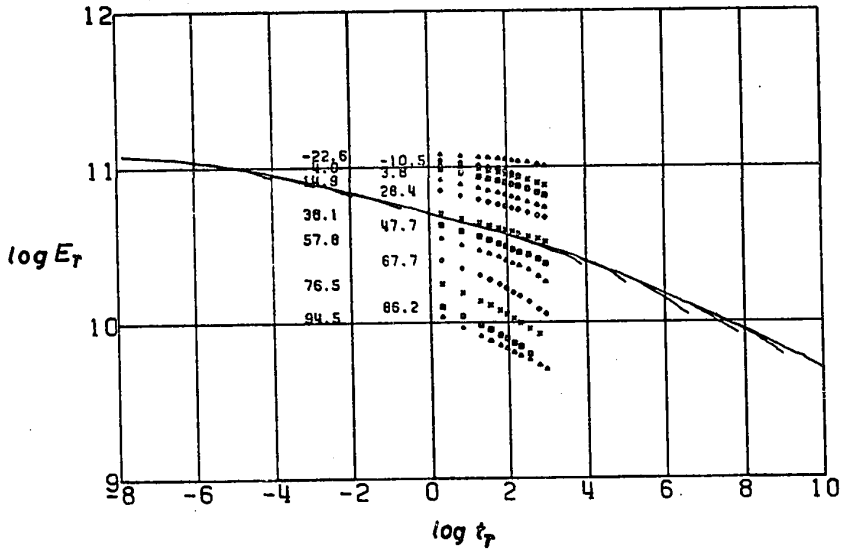

FIGURE 25 — 67Na-27FA

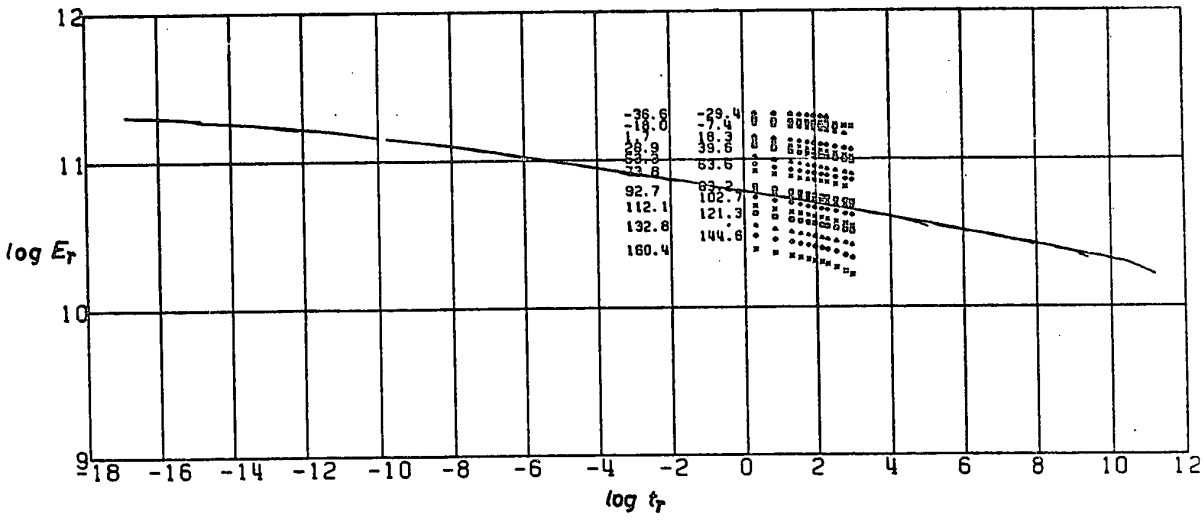

FIGURE 26 — 100Na-22FA

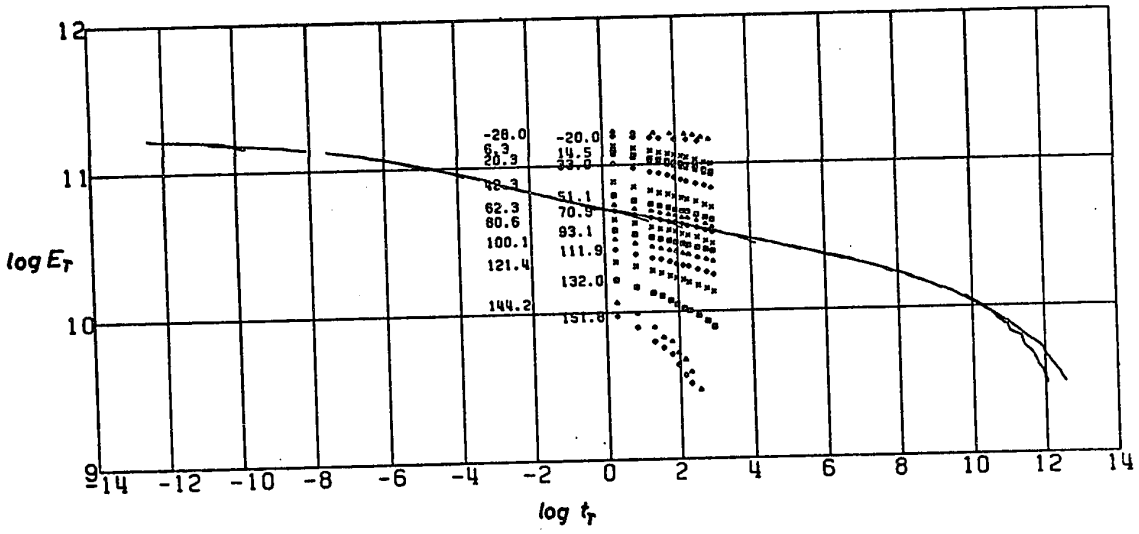

FIGURE 27 — 100Na-29FA

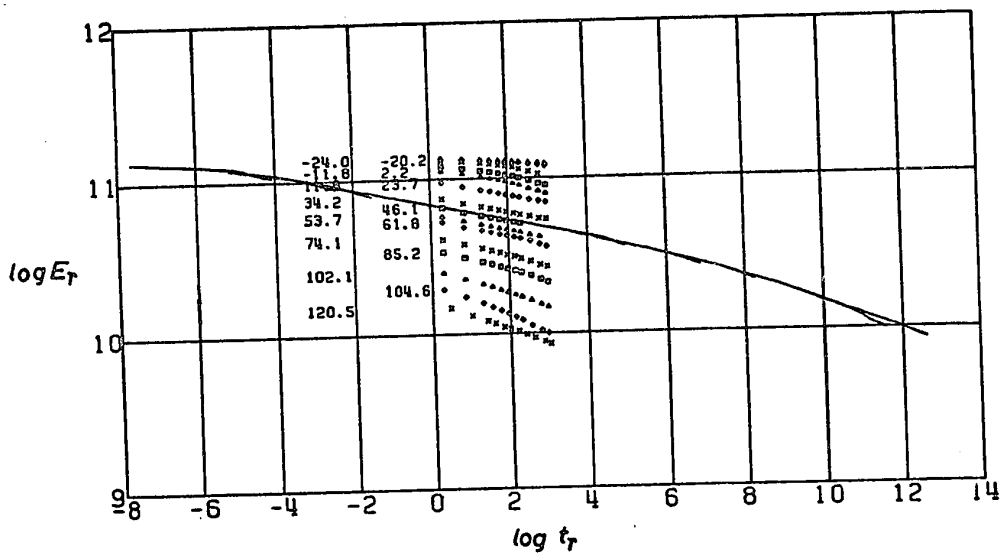

FIGURE 28 — 100Na-37FA

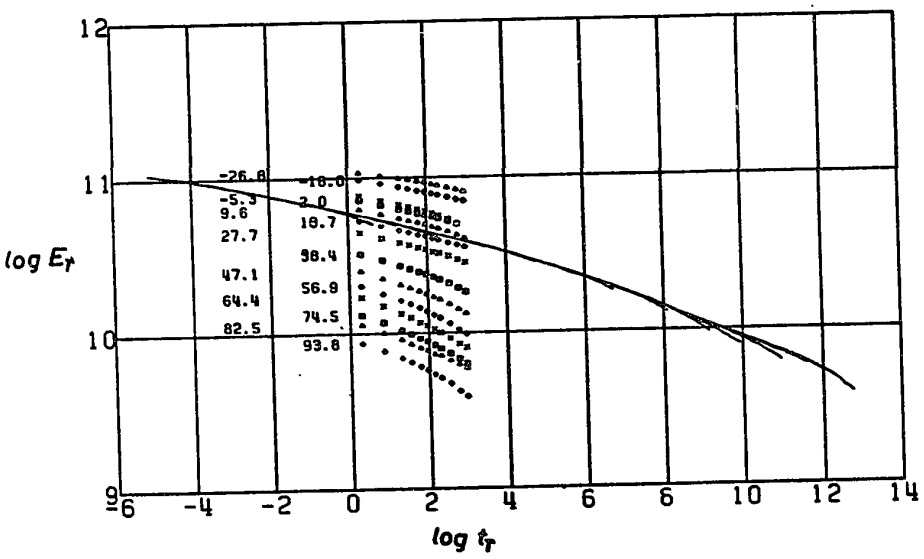

FIGURE 29 — 100Na-43FA

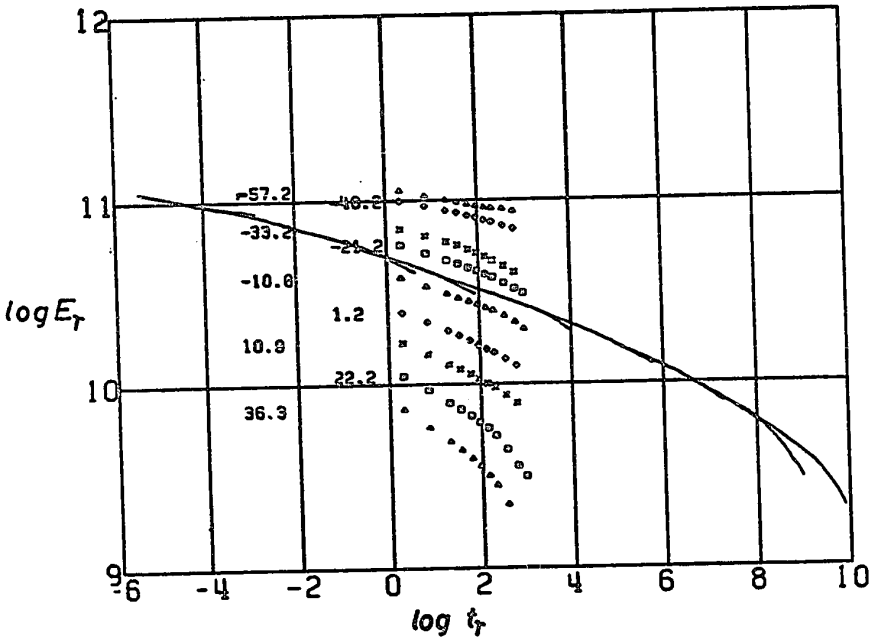

FIGURE 30 — 100Na-52FA

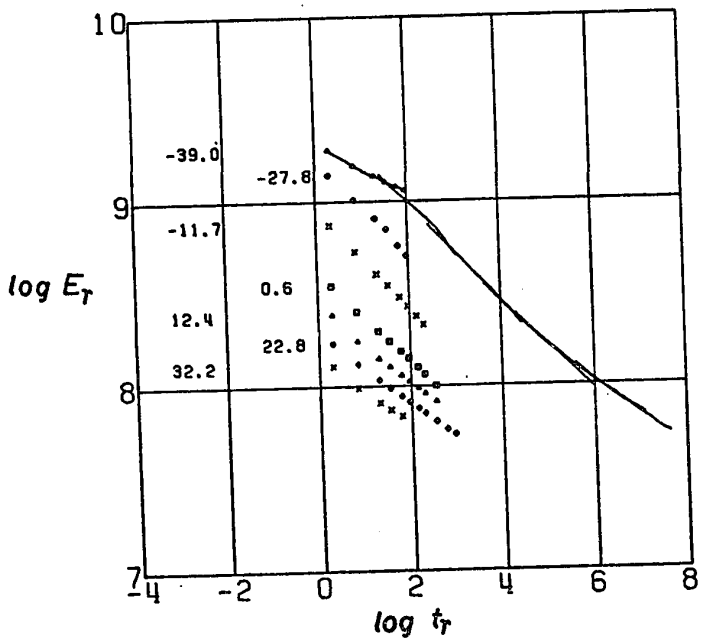

FIGURE 31 — 100Na-67FA

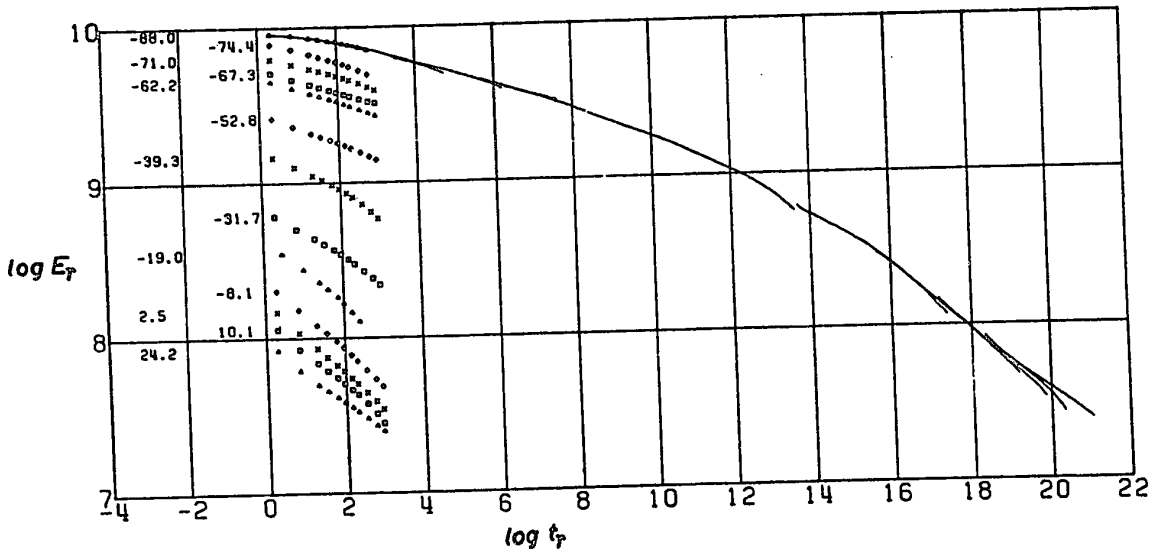

FIGURE 32 — 100Na-72FA

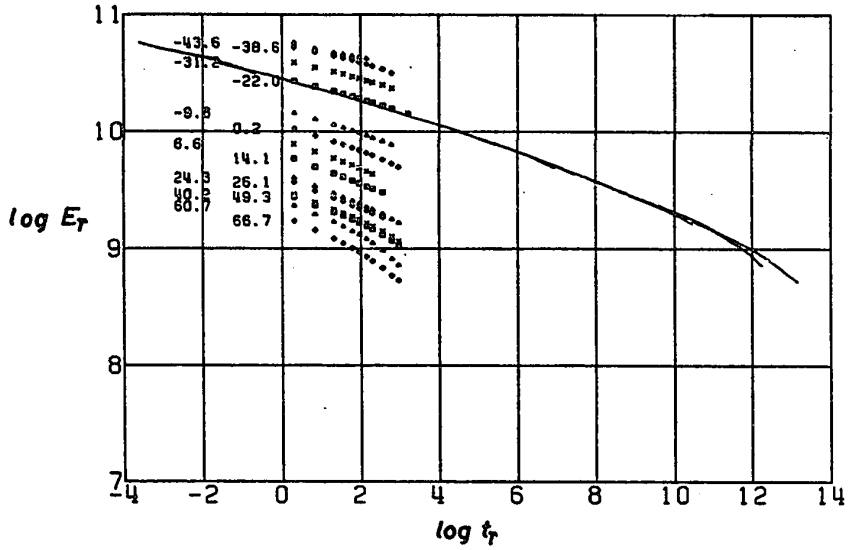

FIGURE 33 — 100Na-54EG

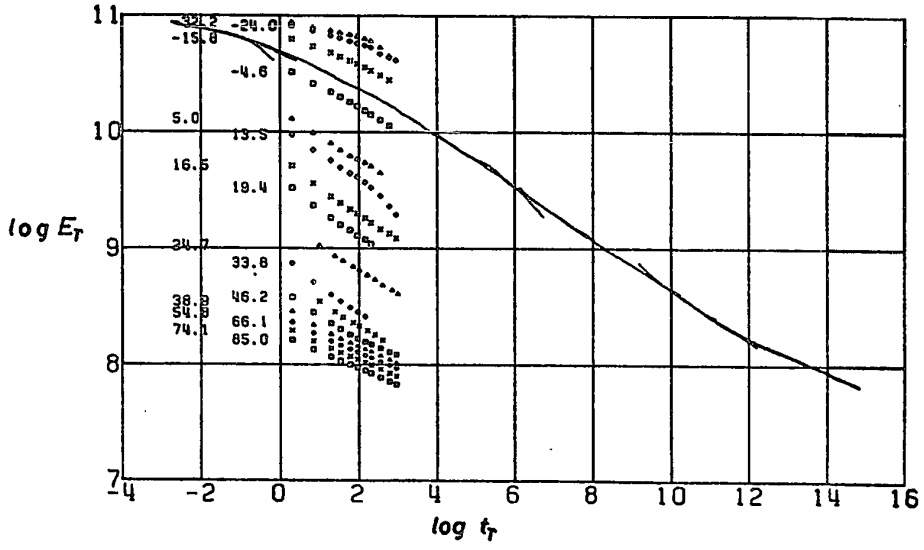

FIGURE 34 — 100Na-54GL

APPENDIX C

Program for the Calculation of Shift Factors

The following program is designed to compute the shift factors for a series of stress relaxation runs at successively increasing temperatures. It requires a discrete set of force versus time data at each temperature, plus a number of parameters including T_g (or any convenient reference temperature); α_g and α_ℓ (these need only be estimates); c_f, Δ_h, and b, as defined in Eqs. 1-4, pages 97-98. The arrangement of the data cards is self-explanatory. A sample output is included.

Program "MASCURVE"

```
C       SHIFT FACTORS FROM FORCE VS TIME VS TEMPERATURE
        DIMENSION F(60),E(60),EPR(60),T(60),WT(60),ELOG(60)
        DIMENSION CUMA(50),DEG(50),WORD(20)
C       DIMENSION(20) ALLOWS FOR ALPHAMERIC LABEL OF 80 CHARACTERS
C       DIMENSION(50) ALLOWS FOR MAXIMUM 50 RUNS
C       DIMENSION(60) ALLOWS FOR MAXIMUM 60 POINTS PER RUN
        READ(5,89)WT
C       3 CARDS: WEIGHTING FACTORS IN DETERMINING OVERLAP
C       IF COMPLETE OVERLAP EXPECTED, WT(I)=1.0
        READ(5,92)NTIME
C       1 CARD: NO. OF TIME SETS
        DO 1001 KLM=1,NTIME
        READ(5,90)T
C       4 CARDS: SET OF DISCRETE TIMES AT WHICH FORCE VALUES ARE READ
C       T IS NORMALLY CONSTANT FOR ONE SAMPLE
        READ(5,92)NCURV
C       1 CARD: NO. OF CURVES PER TIME SET
        DO 1001 JKL=1,NCURV
        READ(5,86)WORD
C       1 CARD: ALPHAMERIC LABEL, MAX. 80 CHARACTERS
        WRITE(6,87)WORD
        READ(5,92)L,CORR
C       1 CARD: L=0; CORR IS INSTRUMENTAL COMPLIANCE IN CM/G
        READ(5,91)NN,NSUM,ALPHAG,ALPHAL,TG
C       1 CARD: NN IS NO. OF SHAPE FACTORS; NSUM IS TOTAL NO. OF RUNS;
C       ALPHAG AND ALPHAL ARE EXP. COEFF. BELOW AND ABOVE TG;
C       EXP. COEFFS. NEED ONLY BE ESTIMATES
C       ALL TEMPERATURES IN DEG. K
        CUMA(1)=0.
        K=0
        MPR=1
        EPR(MPR)=10**14
C       A VALUE HIGHER THAN ALL POSSIBLE MODULI
```

```
      DO 1000 IJK=1,NN
      READ(5,92)N,CONST
C     1 CARD N IS NO. OF RUNS FOR GIVEN SHAPE FACTOR;
C     CONST IS SHAPE FACTOR IN C.G.S. UNITS
      DO 100 I=1,N
      K=K+1
      READ(5,92)M,DEL,TEMP
C     1 CARD: M IS NO. OF POINTS IN RUN, INCLUDING BLANKS;
C     DEL IS DEFORMATION IN CM; TEMP IS IN DEG. K
      READ(5,89)(F(L),L=1,M)
C     UP TO 3 CARDS: FORCE READINGS; IF NO READING TAKEN, LEAVE BLANK
      DEG(K)=TEMP
      ALG=0.
      WSUM=0.
      ALPHA=ALPHAG
      IF(TEMP-TG)61,61,62
   62 ALPHA=ALPHAL
   61 C=CONST*TG/TEMP*(1.+3.*ALPHA*(TEMP-TG))
      DO 101 J=1,M
      E(J)=C*F(J)/(DEL-CORR*F(J))
      IF(E(J).GT.1.0) ELOG(J)=ALOG10(E(J))
      IF(WT(J).EQ.0.) GO TO 101
      IF(E(J)-EPR(MPR))101,11,11
   11 IF(J.GT.MPR)GO TO 101
      DO 4 LL=J,MPR
      IF(EPR(LL).EQ.0.)GO TO 4
      GO TO 1
    4 CONTINUE
    1 IF(EPR(LL)-E(J))101,2,2
    2 DO 5 L=LL,MPR
      LLL=L-1
      IF(EPR(L).EQ.0.)GO TO 5
      IF(EPR(L)-E(J))12,12,5
   12 IF(EPR(LLL))101,13,3
   13 LLL=LLL-1
      GO TO 12
    3 ALG=ALG+WT(J)*(ALOG10(T(J))-ALOG10(T(LLL))-ALOG10(EPR(LLL)/E(J))/
     1ALOG10(EPR(LLL)/EPR(L))*ALOG10(T(L)/T(LLL)))
      WSUM=WSUM+WT(J)
      GO TO 101
    5 CONTINUE
  101 CONTINUE
      IF(K.EQ.1) GO TO 800
      IF(WSUM)8,8,9
    8 WSUM=1.
    9 ALG=ALG/WSUM
      CUMA(K)=ALG+CUMA(K-1)
  800 CONTINUE
      WRITE(6,93)K,TEMP,ALG,CUMA(K)
C     RUN NO.; TEMP.; LOG SHIFT; CUMULATIVE SHIFT
      WRITE(6,95)(ELOG(J),T(J),J=1,M)
C     PAIRS OF VALUES OF LOG E AND TIME
      MPR=M
      DO 100 J=1,M
      ELOG(J)=0.0
  100 EPR(J)=E(J)
 1000 CONTINUE
```

```
      DO 102 I=1,K
      IF(DEG(I)-TG)102,6,7
    6 DO 103 J=1,K
  103 CUMA(J)=CUMA(J)-CUMA(I)
      GO TO 105
    7 AREF=CUMA(I)+(CUMA(I-1)-CUMA(I))*(DEG(I)-TG)/(DEG(I)-DEG(I-1))
      DO 104 J=1,K
  104 CUMA(J)=CUMA(J)-AREF
      GO TO 105
  102 CONTINUE
      WRITE(6,88)
      GO TO 1001
  105 WRITE(6,96)(CUMA(L),DEG(L),L=1,K)
C     PAIRS OF VALUES OF LOG SHIFT AND TEMP. REL. TO TG
 1001 CONTINUE
   86 FORMAT(20A4)
   87 FORMAT('1',20A4)
   88 FORMAT('0 TG OUT OF RANGE')
   89 FORMAT(20F4.1)
   90 FORMAT(16F5.0)
   91 FORMAT(2I2,2E7.3,F4.1)
   92 FORMAT(I2,E7.3,F4.1)
   93 FORMAT('0RUN',I3,F8.1,' DEG.K',2F10.3)
   95 FORMAT('0',8(F9.3,F7.0))
   96 FORMAT('0',16F8.3)
      STOP
      END
```

Sample Output

```
      100NA-48FA

RUN  1   270.1 DEG.K      0.0        0.0

    0.0      3.   10.528    5.   10.514   10.   10.500   15.      10.575   40.   10.570   50.
10.505     60.   10.498   80.   10.492  100.   10.486  120.      10.530  200.   10.521  250.
10.515    300.   10.507  400.   10.490  500.   10.482  600.      10.462 1200.   10.456 1400.
10.450   1700.   10.444 2000.   10.437 2500.   10.429 3000.      10.399 6000.   10.386 8000.
10.374  10000.

RUN  2   274.3 DEG.K     -0.957     -0.957

    0.0      3.   10.568    5.   10.554   10.   10.543   15.      10.512   40.   10.510   50.
10.503     60.   10.495   80.   10.488  100.   10.483  120.      10.469  200.   10.461  250.
10.457    300.   10.447  400.   10.437  500.   10.432  600.      10.406 1200.   10.401 1400.
10.392   1700.   10.382 2000.   10.372 2500.   10.362 3000.      10.328 6000.   10.313 8000.
10.304  10000.   10.294 12000.

RUN  3   279.4 DEG.K     -0.372     -1.328

   10.561     3.   10.547    5.   10.531   10.   10.519   15.      10.490   40.   10.480   50.
10.481     60.   10.468   80.   10.466  100.   10.461  120.      10.447  200.   10.443  250.
10.438    300.   10.429  400.   10.421  500.   10.414  600.      10.386 1200.   10.378 1400.
10.372   1700.   10.365 2000.   10.355 2500.   10.347 3000.      10.307 6000.   10.291 8000.
10.278  10000.

RUN  9   308.0 DEG.K     -1.477     -5.512

   10.221     3.   10.188    6.   10.166   10.   10.146   15.      10.096   40.   10.083   50.
10.067     60.   10.053   80.   10.041  100.   10.027  120.       9.994  200.    9.977  250.
 9.960    300.    9.937  400.    9.913  500.    9.900  600.       9.832 1200.    9.817 1400.
 9.795   1700.    9.778 2000.    9.754 2500.    9.733 3000.

   0.646 270.300  -0.311 274.300  -0.682 279.400  -1.088 283.600      -3.939 297.900  -4.389 302.200

  -4.866 308.000
```

APPENDIX D

Program for the Conversion of Static Modulus to Dynamic Compliance

The fortran program listed below performs the following operations:

(i) Calculation of reduced modulus versus reduced time. This is done by using the raw stress relaxation data used in the previous program, along with the shift factors and an additional parameter representing the number of points of overlap with the upper envelope for each run, to calculate E_r versus t_r.

(ii) Computation, by simple interpolation, of values of E_r for each run at even logarithmic intervals of t_r (specifically, at intervals of 0.2 log units).

(iii) Computation and sorting of values of E_r on the upper envelope of modulus at even logarithmic intervals of t_r.

(iv) Conversion of the upper envelope of modulus to a lower envelope of compliance by the method of Hopkins and Hamming,[17] which is based on the approximation of convolution integrals. The initial value of D(t) is obtained from Eq. 13. An initial fluctuation in D(t) results from the inaccuracy of the initialization, but the function converges rapidly.

(v) Conversion of the individual curves of modulus to compliance. The values of D(t) from the lower envelope up to the point of deviation in any one run are used to initialize the conversion of the subsequent long-time deviations. In this way, the initial fluctuations in compliance for any one run (except the first) are avoided.

(vi) Calculation of the values of subtracted compliance, as illustrated in Fig. 12, since values on the lower envelope and corresponding values of the deviations are obtained for the same discrete times.

(vii) Conversion of the values of D(t) in any one run to dynamic compliance, D'(ω) and D"(ω), by the method of Schwarzl and Struik.[21] The approximation

$$D(t) = c_0 + c_1 (\ln t) + c_2 (\ln t)^2 + c_3 (\ln t)^3 \qquad (D1)$$

is made. The subroutine CURVFT is used to obtain the best-fitting set of constants to the above relationship. The values of D', D" and tan δ = D"/D' are evaluated at different values of ω according to the following relationships

$$D'(\omega) = D(t) - 0.5772 \frac{dD(t)}{d(\ln t)} - 0.2447 \frac{d^2D(t)}{d(\ln t)^2} - 0.1954 \frac{d^3D(t)}{d(\ln t)^3}$$

$$D''(\omega) = \frac{\pi}{2}\left(\frac{dD(t)}{d(\ln t)^2} - 0.5772 \frac{d^2D(t)}{d(\ln t)^2} + 0.5778 \frac{d^3D(t)}{d(\ln t)^3}\right) \qquad (D2)$$

Program "CONVETOD"

```
C       CONVERSION FROM F TO D
C       DATA CARDS AS IN MASCURVF UNLESS SPECIFIED
        DIMENSION T(150),G(150),Z(150),F(150),Q(150),R(150),TE(150),D(150)
        DIMENSION X(150),Y(150),P(400),S(400),U(50),V(50)
        DIMENSION WORD(20),TIME(60),M(50),MS(50),MJ(50),A(50)
        DIMENSION WT(30),COF(4),XF(1),YF(1),CMPL(30),TLOG(30)
        DIMENSION TJ(8),CMPL1(8),CMPL2(8),TANDFL(8),FREQ(8)
        ENAT=2.302585
        PI=3.14159
        DO 664 J=1,30
  664   WT(J)=1.0
C       WEIGHTING FACTOR IN SUBROUTINE CURVFT
        READ(5,88)NFREQ
C       1 CARD:  NO. OF SETS OF FREQUENCY
```

```
      DO 299 JKLM=1,NFREQ
      READ(5,90)FREQ
C     1 CARD:  SET OF DISCRETE FREQUENCIES
      DO 665 J=1,9
  665 TJ(J)=-ALOG(FREQ(J))
      READ(5,89)NCURV
      DO 299 IJKL=1,NCURV
      READ(5,86)WORD
      WRITE(6,87)WORD
      READ(5,92)L,CORR
      READ(5,90)TIME
      READ(5,91)NN,NSUM,ALPHAG,ALPHAL,TG
      READ(5,93)(A(LL),LL=1,NSUM)
C     1 OR MORE CARDS:  SHIFT FACTORS
      READ(5,88)(MS(LL),LL=1,NSUM)
C     1 CARD OR MORE:  NO. OF POINTS PER RUN ON ENVELOPE
      I=0
      D(1)=A(1)
      DO 101 IJK=1,NN
      READ(5,92)N,CONST
      DO 101 JKL=1,N
      K=0
      L=L+1
      READ(5,92)M(L),DEL,TEMP
      ALPHA=ALPHAG
      IF(TEMP-TG)73,73,74
   74 ALPHA=ALPHAG
   73 C=CONST*TG/TEMP*(1.+3.*ALPHA*(TEMP-TG))
      MM=M(L)
      READ(5,89)(F(LL),LL=1,MM)
      DO 100 J=1,MM
      F(J)=C*F(J)/(DEL-CORR*F(J))
      IF(F(J))71,71,72
   71 M(L)=M(L)-1
      GO TO 100
   72 K=K+1
      X(K)=ALOG10(TIME(J))-A(L)
      Y(K)=ALOG10(F(J))
  100 CONTINUE
      MM=M(L)
      WRITE(6,85)L
      WRITE(6,96)(X(LL),Y(LL),LL=1,MM)
      J=0
      X1=AINT(X(1)*5.)/5.
      MMS=MS(L)
      X2=AINT(X(MMS)*5.)/5.
      MS(L)=(X2-X1)*5.+0.1
      IF(X(1))22,23,23
   22 X1=X1-0.2
      IF(X(MMS))23,23,24
   24 MS(L)=MS(L)+1
   23 IPR=I+1
   50 X1=X1+0.2
   51 J=J+1
      IF(J-MM)54,54,55
   54 IF(X(J)-X1)51,52,53
```

(i)

(ii)

```
 52 I=I+1
    P(I)=X1
    S(I)=Y(J)
    GO TO 50
 53 I=I+1
    P(I)=X1
    S(I)=(Y(J-1)-Y(J))*(X(J)-X1)/(X(J)-X(J-1))+Y(J)
    GO TO 50
 55 M(L)=I-IPR+1
    WRITE(6,84)
    WRITE(6,96)(P(LL),S(LL),LL=IPP,I)
101 CONTINUE
    MS(NSUM)=M(NSUM)
    MSUM=I
    IPR=I
    X(1)=P(1)
    T(1)=10.**X(1)
    NX=5.*(P(MSUM)-P(1))+1.1
    DO 56 I=2,NX
    X(I)=X(I-1)+0.2
 56 T(I)=10.**X(I)
    MJ(1)=1
    KK=MS(1)
    DO 57 J=1,KK
    Y(J)=S(J)
 57 Z(J)=10.**Y(J)
    J1=M(1)+1
    DO 200 L=2,NSUM
    J2=J1+MS(L)-1
    DD=(P(J1)-X(KK))*5.
    IF(DD.LT.-0.1) DD=DD-0.1
    JX=DD+0.05
    IF(MS(L)+JX-1)48,49,49
 48 JX=1-MS(L)
 49 MJ(L)=JX
    JX1=IABS(JX-1)
    IF(JX-1)58,59,60
 58 DO 63 J=1,JX1
    Y(KK-JX1+J)=(Y(KK-JX1+J)+S(J1+J-1))/2.
 63 Z(KK-JX1+J)=10.**Y(KK-JX1+J)
    IF(JX1.EQ.MS(L)) GO TO 200
    J3=J1+JX1
    DO 64 J=J3,J2
    KK=KK+1
    Y(KK)=S(J)
 64 Z(KK)=10.**Y(KK)
    GO TO 200
 60 DO 62 J=1,JX1
    Y(KK+J)=(Y(KK)*(JX-J)+S(J1)*J)/FLOAT(JX)
 62 Z(KK+J)=10.**Y(KK+J)
    KK=KK+JX1
 59 DO 61 J=J1,J2
    KK=KK+1
    Y(KK)=S(J)
 61 Z(KK)=10.**Y(KK)
200 J1=J1+M(L)
```

(iii)

```
      WRITE(6,83)
      WRITE(6,98)(X(LL),Y(LL),LL=1,NX)
      WRITE(6,94)(M(LL),MS(LL),MJ(LL),LL=1,NSUM)
      DO 4 I=1,NX
    4 G(I)=Z(I)/Z(1)
      F(1)=T(1)
      DO 5 I=2,NX
      X(I-1)=X(I-1)+0.1
      DD=(Y(I-1)-Y(I))/0.2
      D(I-1)=SQRT(1./Z(I)/Z(I-1))*SIN(3.14159*DD)/3.14159/DD
    5 F(I)=F(I-1)+(G(I-1)+G(I))*(T(I)-T(I-1))/2.
      C=D(1)
      Q(1)=1.
      U(NSUM)=A(NSJM)
      NSUM1=NSUM+1
      M(NSUM1)=0
      MJ(NSUM1)=1
      DO 58 L1=1,NSUM1
      L=NSUM1-L1+1
      IF(L.EQ.NSUM1) J1=2
      DO 13 I=J1,NX
      I1=I-1
      DO 8 J=1,I1
      TE(J)=T(I)-T(J)
      L0=0
      DO 8 K=2,I
      IF(L0)10,10,8
   10 IF(TE(J)-T(K))9,21,8
    9 L0=1
      GX=G(K-1)+(TE(J)-T(K-1))*(G(K)-G(K-1))/(T(K)-T(K-1))
      TE(J)=F(K-1)+(G(K-1)+GX)*(TE(J)-T(K-1))/2.
      GO TO 8
   21 TE(J)=F(K)
      L0=1
    8 CONTINUE
      IF(I-2)13,13,12
   12 R(I1)=0.
      I2=I-2
      DO 14 J=1,I2
   14 R(I1)=R(I1)+Q(J)*(TE(J)-TE(J+1))
      Q(I1)=(T(I)-R(I1))/TE(I1)
   13 CONTINUE
      NX1=NX-1
      IF(L-NSUM1)67,69,299
   69 DO 70 J=1,NX1
   70 Y(J)=Q(J)*C
      Y(2)=Y(2)/2.
      WRITE(6,82)
      WRITE(6,99)(X(LL),Y(LL),D(LL),LL=1,NX1)
C     LOG TIME; D(T), 2ND AND 1ST APPROX.
      GO TO 65
   67 J1=J1-1
      MSUM=MSUM-M(L)
      KK=0
      IF(L.EQ.1) MSUM=MSUM+1
```

(iv)

```
      DO 65 J=J1,NX1
      MSUM=MSUM+1
      KK=KK+1
      P(MSUM)=X(J)+A(L)
      TIME(KK)=X(J)
      S(MSUM)=Q(J)*C
   66 Y(KK)=S(MSUM)
      IF(L.EQ.1) Y(2)=Y(2)/2.
      WRITE(6,81)L
      WRITE(6,97)(TIME(LL),Y(LL),LL=1,KK)
      DO 127 J=1,KK
  127 TIME(J)=TIME(J)+A(L)
      JJ1=J1-5
      IF(JJ1.LT.3) JJ1=3
      KKK=0
      DO 666 J=JJ1,NX1
      KKK=KKK+1
      CMPL(KKK)=Q(J)*C
  666 TLOG(KKK)=ENAT*(X(J)+A(L))
      CALL CURVFT(TLOG,CMPL,WT,KKK,1,3,COF,NCOF,-1,0,XF,YF)
      WRITE(6,78)NCOF,(COF(J),J=1,NCOF)
      DO 668 J=1,8
      DEL0=COF(1)+COF(2)*TJ(J)+COF(3)*TJ(J)*TJ(J)+COF(4)*TJ(J)*TJ(J)*
     1TJ(J)
      DEL1=COF(2)+2.*COF(3)*TJ(J)+3.*COF(4)*TJ(J)*TJ(J)
      DEL3=6.*COF(4)
      DEL2=DEL3*TJ(J)+2.*COF(3)
      CMPL1(J)=DEL0-.5772*DEL1-.2447*DEL2-.1954*DEL3
      CMPL2(J)=(DEL1-.5772*DEL2+.5778*DEL3)*PI/2.
      CMPL1(J)=ALOG10(CMPL1(J))
      CMPL2(J)=ALOG10(CMPL2(J))
  668 TANDEL(J)=CMPL2(J)-CMPL1(J)
      WRITE(6,80)(FREQ(J),CMPL1(J),CMPL2(J),TANDEL(J),J=1,8)
C     FREQUENCY IN HZ; J',J'',LOSS TANGENT IN LOG UNITS
      IF(L.EQ.1) GO TO 299
   65 J1=NX+2-M(L)-MJ(L)-MS(L-1)
      NX=J1-1+M(L-1)
      MSUM=MSUM-M(L)-M(L-1)
      IF(L.EQ.2) J1=2
      IF(L.EQ.2) MSUM=1
      DO 68 J=J1,NX
      MSUM=MSUM+1
      Z(J)=10.**S(MSUM)
      G(J)=Z(J)/Z(1)
   68 F(J)=F(J-1)+(G(J-1)+G(J))*(T(J)-T(J-1))/2.
  299 CONTINUE
   78 FORMAT('0NCOF =',I2,'  C0 =',E12.5,'  C1 =',E12.5,'  C2 =',E12.5,
     1'C3 =',E12.5)
   80 FORMAT('0',3(E12.3,' HZ',3F8.3))
   81 FORMAT('0 RUN ',I2,'  COMPLIANCE VS TIME')
   82 FORMAT('0  LOWER ENVELOPE OF COMPLIANCE VS TIME')
   83 FORMAT('0  UPPER ENVELOPE OF MODULUS VS TIME')
   84 FORMAT('0                                - INTERPOLATED VALUES')
   85 FORMAT('0 RUN ',I2,'  MODULUS VS TIME - EXPERIMENTAL VALUES')
   86 FORMAT(20A4)
   87 FORMAT('1',20A4)
```

(v)

(vii)

```
88 FORMAT(40I2)
89 FORMAT(20F4.1)
90 FORMAT(16F5.0)
91 FORMAT(2I2,2E7.3,F4.1)
92 FORMAT(I2,E7.3,F4.1)
93 FORMAT(13F6.3)
94 FORMAT('0',11(I5,2I3))
96 FORMAT('0',16(F8.3))
97 FORMAT('0',7(F6.1,E12.4))
98 FORMAT('0',9(F6.1,F8.3))
99 FORMAT('0',4(F6.1,E12.4,E11.3))
   STOP
   END
```

Sample Output

```
[illegible]A-4[illegible]A

RUN  1  MODULUS VS TIME - EXPERIMENTAL VALUES

-[illegible]  11.[illegible]  -4.[illegible]  11.[illegible]  -4.[illegible]  11.01[illegible]  -4.[illegible]  11.[illegible]   -4.[illegible]  11.[illegible]  -[illegible]  1[illegible]
-3.[illegible]  10.[illegible]  -3.[illegible]  10.933  -3.737  10.980  -4.600  10.977   -3.4[illegible]  10.[illegible]  -3.4[illegible]  10.[illegible]
-3.[illegible]  10.[illegible]  -3.[illegible]  10.[illegible]  -3.[illegible]  10.[illegible]  -3.18[illegible]  10.[illegible]   -3.[illegible]  10.[illegible]  -3.[illegible]  10.[illegible]
-2.[illegible]  10.[illegible]  -2.787  10.[illegible]  -2.630  10.925  -2.611  10.919   -2.[illegible]  10.[illegible]  -2.30[illegible]  10.[illegible]

                   - INTERPOLATED VALUES

-5.000  11.[illegible]  -4.800  11.01[illegible]  -4.[illegible]  11.011  -4.400  11.004   -3.900  10.[illegible]1  -2.[illegible]10  10.[illegible]
-3.400  10.[illegible]  -3.[illegible]  10.[illegible]  -3.000  10.940  -2.[illegible]  10.[illegible]

RUN  2  MODULUS VS TIME - EXPERIMENTAL VALUES

-3.931  10.986  -3.755  10.979  -3.533  10.962  -3.387  10.962   -2.931  10.939  -2.834  10.934
-2.755  10.930  -2.648  10.927  -2.630  10.923  -2.533  10.918   -2.329  10.914  -2.273  10.905
-2.23[illegible]  10.902  -2.153  10.897  -2.096  10.895  -2.028  10.892   -1.934  10.879  -1.755  10.876
-1.688  10.872  -1.530  10.959  -1.533  10.864  -1.454  10.857   -1.278  10.868  -1.237  10.844

                   - INTERPOLATED VALUES

-3.800  10.981  -3.600  10.972  -3.400  10.962  -3.200  10.952   -2.600  10.922  -2.400  10.911
-2.200  10.900  -2.000  10.899  -1.800  10.878  -1.600  10.867

RUN 14  MODULUS VS TIME - EXPERIMENTAL VALUES

10.069   9.929  10.245   9.919  10.467   9.897  10.613   9.879   11.069   9.833  11.166   9.820
11.245   9.813  11.312   9.805  11.370   9.799  11.467   9.798   11.671   9.762  11.722   9.755
11.768   9.747  11.847   9.739  11.914   9.726  11.972   9.718   12.166   9.692  12.245   9.693
12.312   9.669  12.370   9.659  12.467   9.639  12.546   9.619   12.722   9.586  12.768   9.574

                   - INTERPOLATED VALUES

10.200   9.921  10.400   9.903  10.600   9.881  10.800   9.858   11.400   9.795  11.600   9.771
11.800   9.744  12.000   9.713  12.200   9.688  12.400   9.653

UPPER ENVELOPE OF MODULUS VS TIME

-5.0  11.026  -4.8  11.019  -4.5  11.011  -4.4  11.004  -4.2  10.997   -3.6  10.973  -3.4  10.963
-3.2  10.952  -3.0  10.942  -2.8  10.932  -2.6  10.922  -2.4  10.911   -1.9  10.878  -1.6  10.866
-1.4  10.855  -1.2  10.843  -1.0  10.832  -0.8  10.821  -0.6  10.808    0.0  10.771   0.2  10.761
 0.4  10.750   0.5  10.739   0.9  10.724   1.0  10.711   1.2  10.699    1.8  10.661   2.0  10.648
 2.2  10.635   2.4  10.623   2.6  10.609   2.8  10.596   3.0  10.582    3.6  10.543   3.8  10.528
 4.0  10.510   4.2  10.492   4.4  10.477   4.6  10.452   4.9  10.447    5.4  10.395   5.6  10.376
 5.9  10.360   6.0  10.342   6.2  10.325   6.4  10.306   6.6  10.286    7.2  10.230   7.4  10.211
 7.6  10.191   7.8  10.169   8.0  10.149   8.2  10.126   8.4  10.101    9.0  10.036   9.2  10.020
 9.4  10.000   9.6   9.990   9.8   9.957  10.0   9.941  10.2   9.920   10.9   9.858  11.0   9.810
11.2   9.917  11.4   9.796  11.6   9.771  11.8   9.744  12.0   9.713   12.6   9.610
```

14 10 1 13 9 -3 13 10 2 13 9 -6 13 9 -5
13 8 -3 14 8 -4 13 13 -1

LOWER ENVELOPE OF COMPLIANCE VS TIME

-4.9	0.9478E-11	0.949E-11	-4.7	0.9871E-11	0.964E-11
-4.1	0.1020E-10	0.101E-10	-3.9	0.1039E-10	0.103E-10
-3.3	0.1105E-10	0.110E-10	-3.1	0.1132E-10	0.112E-10
-2.5	0.1215E-10	0.121E-10	-2.3	0.1245E-10	0.124E-10
-1.7	0.1345E-10	0.134E-10	-1.5	0.1380E-10	0.137E-10
-0.9	0.1493E-10	0.148E-10	-0.7	0.1534E-10	0.152E-10
.	0.1670E-10	0.166E-10	0.1	0.1715E-10	0.171E-10
0.7	0.1857E-10	0.184E-10	0.9	0.1916E-10	0.190E-10
1.5	0.2090E-10	0.208E-10	1.7	0.2152E-10	0.214E-10
2.3	0.2349E-10	0.233E-10	2.5	0.2420E-10	0.240E-10
3.1	0.2654E-10	0.264E-10	3.3	0.2736E-10	0.272E-10
3.9	0.3021E-10	0.299E-10	4.1	0.3144E-10	0.312E-10
4.7	0.3499E-10	0.348E-10	4.9	0.3633E-10	0.360E-10
5.5	0.4091E-10	0.406E-10	5.7	0.4260E-10	0.424E-10
6.3	0.4807E-10	0.476E-10	6.5	0.5022E-10	0.498E-10
7.1	0.5714E-10	0.567E-10	7.3	0.5974E-10	0.593E-10
7.9	0.6864E-10	0.681E-10	8.1	0.7203E-10	0.714E-10
8.7	0.8413E-10	0.835E-10	8.9	0.8853E-10	0.878E-10
9.5	0.1013E-09	0.101E-09	9.7	0.1063E-09	0.105E-09
10.3	0.1219E-09	0.121E-09	10.5	0.1276E-09	0.127E-09
11.1	0.1459E-09	0.145E-09	11.3	0.1544E-09	0.153E-09
11.9	0.1831E-09	0.180E-09	12.1	0.1950E-09	0.194E-09

14 10 -2 13 9 -3 13 9 -4

-4.3	0.1007E-10	0.995E-11
-3.5	0.1081E-10	0.107E-10
-2.7	0.1186E-10	0.118E-10
-1.9	0.1310E-10	0.130E-10
-1.1	0.1456E-10	0.145E-10
-0.3	0.1624E-10	0.161E-10
0.5	0.1804E-10	0.179E-10
1.3	0.2029E-10	0.202E-10
2.1	0.2281E-10	0.227E-10
2.9	0.2576E-10	0.256E-10
3.7	0.2912E-10	0.289E-10
4.5	0.3379E-10	0.336E-10
5.3	0.3919E-10	0.389E-10
6.1	0.4614E-10	0.459E-10
6.9	0.5466E-10	0.542E-10
7.7	0.6542E-10	0.648E-10
8.5	0.8004E-10	0.797E-10
9.3	0.9696E-10	0.962E-10
10.1	0.1163E-09	0.115E-09
10.9	0.1401E-09	0.140E-09
11.7	0.1720E-09	0.169E-09
12.5	0.2254E-09	0.216E-09

RUN 14 COMPLIANCE VS TIME

10.1	0.1163E-09	10.3	0.1214E-09	10.5	0.1278E-09
11.5	0.1625E-09	11.7	0.1720E-09	11.9	0.1831E-09

11.1 0.1460E-09 11.3 0.1544E-09
12.5 0.2254E-09

ORDER = 4 C0 = 0.10945E-09 C1 = 0.10766E-10 C2 = 0.33253E-1303 = 0.13716E-12

0.100E 01 HZ	-9.990	-10.752	-0.772	0.300E 00 HZ	-9.942	-10.758	-0.815
0.300E-01 HZ	-9.947	-10.505	-0.743	0.100E-01 HZ	-9.723	-10.498	-0.635
0.100E-02 HZ	-9.654	-10.260	-0.606	0.300E-03 HZ	-9.571	-10.151	-0.580

RUN 11 COMPLIANCE VS TIME

-0.9	0.9944E-10	0.1	0.9727E-10	0.4	0.9693E-10
10.1	0.1331E-09	10.5	0.1288E-09	10.7	0.1347E-09

9.3 0.1105E-09 10.1 0.1163E-09
11.3 0.1544E-09 11.5 0.1501E-09

ORDER = 4 C0 = 0.93233E-10 C1 = 0.90647E-11 C2 = 0.16234E-1303 = 0.59780E-13

0.100E 01 HZ	-10.113	-10.856	-0.751	0.300E 00 HZ	-10.059	-10.846	-0.798
0.300E-01 HZ	-9.959	-10.671	-0.713	0.100E-01 HZ	-9.711	-10.440	-0.779
0.100E-02 HZ	-9.901	-10.549	-0.705	0.300E-03 HZ	-9.743	-10.473	-0.730

CHAPTER V

SUMMARY: CONTRIBUTIONS TO ORIGINAL KNOWLEDGE AND SUGGESTIONS FOR FURTHER RESEARCH

This thesis is a study of the contributions of ions to the viscoelastic effects observed in polymers. Three types of systems were considered. The first of these was one in which permanent crosslinks were introduced into an ionizable material, so that the inherent effect of ions on rubber elasticity could be observed. From simple considerations of entropy and chain dimensions, equations were developed to predict the modulus of elasticity of a two-component rubber, one component of which is ionizable. Experiments were performed to determine the modulus of such a rubber, namely a crosslinked poly(vinyl alcohol)-poly(acrylic acid) gel, in its acidic and ionic forms. The experimentally determined ratio of the moduli was found to agree semi-quantitatively with the predicted value. Possible reasons for the discrepancy were discussed.

Secondly, the effect of ions on the dilute solution viscoelastic behaviour of linear polymers was studied. Experimental techniques for studying such a system are only now becoming available; therefore, this part of the thesis was an attempt to predict the results of such experiments. The bead-spring model of Rouse for the two simplest cases (two and three beads, respectively) was modified to incorporate charges on the beads.

The variation of dynamic viscosity with frequency was obtained for both the two-bead and three-bead systems, and expressed as a function of the ratio of charge to average end-to-end distance. Calculations from this model indicate moderate increases in both the viscosity and the relaxation times of the ionized material, and also a broadening in the distribution of relaxation times with increasing charge to end-to-end distance. The parameters used in the model were obtained for systems which could well prove to be experimentally possible in the near future.

Finally, the third part of the study was concerned with the effects of ions on the viscoelastic response in concentrated solutions of completely ionizable polymers. In this case, a theoretical approach would have been impossible, but experimental techniques were available for such a study. The polymers chosen were the sodium salts of poly(acrylic acid) with various plasticizers. Pseudo-master curves of modulus versus time and modulus-temperature curves were obtained from stress relaxation data on these materials. The variation in the mechanical properties as a function of the degree of neutralization and of the type and amount of plasticizer was observed.

An X-ray diffraction study was taken in support of the thermomechanical study; the structural implications of the findings were discussed in the light of current theory and of observations by other workers. Using a technique previously applied only to non-phase-separated polymers, the pseudo-master

curves were split into two separate master curves, corresponding to a primary, short-time mechanism and a secondary, long-time mechanism. These two mechanisms were found, by direct and indirect evidence, to be essentially ionic and nonionic in nature. Another supportive study, using a torsion pendulum, was made; the results were correlated with the behaviour of the primary relaxation process. The existence of a third, competing mechanism was suggested.

There are several areas in which further research might prove fruitful. The charged bead-spring model could be modified in two ways. First, a parameter could be included to account for the effect of ionic shielding by a counterion atmosphere (such as a simple Debye radius). This would undoubtedly reduce the magnitude of the viscoelastic effect of ions. Secondly, the three-bead assembly could be generalized to the case of n charged beads. With appropriate consideration of counterion effects, this could be a realistic model for polymers containing multiple charges such as ionizable copolymers. This work would involve considerable iterative approximation since the resulting differential equations would not likely have easily accessible solutions.

Additional studies could be made in the poly(acrylic acid) system. A more complete study of the dynamic compliance should be undertaken to investigate the nature of the sub-T_g process. Knowledge of its variation as a function of the degree of

neutralization and of the type and amount of plasticizer should aid in understanding the viscoelastic effects of ions. Coupled with this study should be a more extensive study of structure, perhaps by a spectroscopic technique as well as X-ray, to more accurately determine the effect of plasticizer on the structure. It would be especially rewarding to study the structure as a function of temperature to see if observations correlate with the thermomechanical investigations.

TABLES OF SUPPORTING DATA FOR FIGURES

Chap. II, Fig. 1, p. 33

Material	E ($\times 10^{-6}$ dyn/cm^2)	V_r
Sample A, acidic	9.58	0.329
	9.12	0.346
	9.40	0.379
	9.79	0.397
	9.86	0.419
	10.14	0.442
	10.53	0.474
Sample B, acidic	8.98	0.304
	9.06	0.332
	9.24	0.357
Sample C, acidic	8.84	0.316
	9.08	0.359
	9.60	0.399
	10.5	0.455
Sample B, ionic	4.5	0.131
	4.6	0.146
	4.45	0.177
	5.5	0.204
	4.77	0.169
	4.33	0.195
	4.74	0.222
	5.43	0.249
	6.38	0.303
Sample C, ionic	4.4	0.135
	4.2	0.142
	4.3	0.157
	4.4	0.168
	5.0	0.205
	5.25	0.229
	5.65	0.230
	6.4	0.251

Chap. III, Fig. 1, p. 71

Case	$[\eta]/[\eta]_o$	λ/λ_o	$-EB^{1/2}$
(i)	1.234	1.106	1.100
(ii)	1.145	1.065	0.635
(iii)	1.395	1.194	2.06
(iv)	0.805	0.915	-0.635

Chap. III, Fig. 2, p. 72

$\omega\lambda$	$[\eta"]/[\eta]$	$([\eta"]/[\eta])_{E=0}$
1/10	0.111	0.099
1/4	0.260	0.235
1/2	0.425	0.400
1	0.493	0.500
2	0.371	0.400
4	0.218	0.235
10	0.095	0.099

Chap. III, Fig. 2, p. 75

Case	$[\eta]/[\eta]_o$	$\lambda_1/3\lambda_2$	$-E(B')_o^{1/2}$
(i)	1.244	1.077	0.78
(ii)	1.145	1.047	0.45
(iii)	1.44	1.13	1.45

Chap. IV, Fig. 2, p. 103

TEMP.	-2.9	1.1	5.2	10.4	19.1	22.0	24.7	29.0	34.8
LOG A	0.65	-0.31	-0.65	-1.07	-2.73	-3.67	-3.95	-4.38	-4.86
TIME	LOG E	LOG E	LOG E	LOG E	LOG E	LOG E	LOG E	LOG E	LOG E
3			10.56	10.54	10.43	10.34	10.32	10.27	10.22
6	10.63	10.57	10.54	10.52	10.40	10.31	10.29	10.24	10.19
10	10.61	10.55	10.53	10.50	10.38	10.29	10.26	10.21	10.17
15	10.60	10.54	10.52	10.49	10.36	10.27	10.24	10.20	10.15
20	10.59	10.53	10.51	10.48	10.35	10.26	10.23	10.19	10.13
30	10.59	10.52	10.50	10.47	10.34	10.24	10.21	10.16	10.11
40	10.58	10.51	10.49	10.46	10.32	10.23	10.20	10.15	10.10
50	10.57	10.51	10.49	10.45	10.32	10.22	10.19	10.14	10.08
60	10.57	10.50	10.48	10.45	10.31	10.21	10.18	10.13	10.07
80	10.56	10.50	10.47	10.44	10.29	10.19	10.16	10.12	10.05
100	10.55	10.49	10.47	10.43	10.29	10.18	10.15	10.10	10.04
120	10.55	10.48	10.46	10.43	10.28	10.17	10.14	10.09	10.03
140	10.54	10.48	10.46	10.42	10.27	10.16	10.13	10.09	10.02
170	10.54	10.47	10.45	10.41	10.26	10.15	10.12	10.08	10.00
200	10.53	10.47	10.45	10.41	10.25	10.14	10.11	10.07	9.99
250	10.52	10.46	10.44	10.40	10.24	10.13	10.10	10.05	9.98
300	10.52	10.46	10.44	10.39	10.23	10.12	10.09	10.04	9.96
400	10.51	10.45	10.43	10.38	10.22	10.10	10.07	10.02	9.94
500	10.50	10.44	10.42	10.37	10.21	10.09	10.05	10.01	9.92
600	10.49	10.43	10.41	10.37	10.20	10.08	10.04	9.99	9.90
800	10.48	10.42	10.40	10.35	10.18	10.06	10.02	9.97	9.87
1000	10.47	10.41	10.39	10.34	10.16	10.04	10.00	9.95	9.85
1200	10.46	10.41	10.39	10.33	10.15	10.02	9.99	9.93	9.83
1400	10.46	10.40	10.38	10.32	10.14	10.01	9.97	9.92	9.82
1700	10.45	10.39	10.37	10.32	10.13	10.00	9.96	9.90	9.79
2000	10.44	10.38	10.36	10.31	10.12	9.98	9.95	9.88	9.78
2500	10.44	10.37	10.35	10.29	10.10	9.96	9.93	9.86	9.75
3000	10.43	10.36	10.35	10.28	10.08	9.94	9.91		9.73
4000	10.41	10.35	10.33	10.27	10.06	9.92	9.88		9.70
5000	10.40	10.33	10.32	10.25	10.04	9.90	9.86		
6000	10.40	10.33	10.31	10.24	10.02	9.88	9.85		
8000	10.39	10.31	10.29	10.22	9.99	9.85	9.82		
10000	10.37	10.30	10.28	10.21	9.97	9.84	9.80		
12000		10.29		10.20					
14000				10.19					

Chap. IV, Fig. 3, p. 104

TEMP.	-40.8	-34.1	-28.8	-23.6	-20.6	-20.3	-15.9	-13.0
LOG A	3.13	1.18	0.18	-1.39	-1.63	-1.86	-3.54	-4.46
TIME	LOG E	LOG E	LOG E	LOG E	LOG E	LOG E	LOG E	LOG E
3	11.00	10.90	10.83	10.64			10.19	9.98
6	10.99	10.88	10.80	10.58	10.52	10.48	10.12	9.90
10	10.98	10.86	10.78	10.53	10.48	10.44	10.07	9.84
15	10.98	10.85	10.75	10.50	10.45	10.40	10.03	9.79
20	10.97	10.84	10.74	10.47	10.42	10.37	10.00	9.76
25	10.97	10.83	10.72	10.45	10.40	10.35	9.97	9.73
30	10.96	10.82	10.71	10.43	10.38	10.34	9.96	9.71
35	10.96	10.82	10.70	10.42	10.37	10.32	9.94	9.69
40	10.96	10.81	10.70	10.41	10.36	10.31	9.92	9.67
50	10.95	10.80	10.68	10.38	10.34	10.29	9.89	9.65
60	10.95	10.79	10.67	10.37	10.32	10.27	9.87	9.63
70	10.94	10.79	10.66	10.35	10.31	10.26	9.86	9.61
80	10.94	10.78	10.65	10.33	10.29	10.24	9.84	9.59
90	10.94	10.78	10.64	10.32	10.28	10.23	9.83	9.58
100	10.93	10.77	10.64	10.31	10.27	10.22	9.82	9.56
120	10.93	10.76	10.62	10.29	10.26	10.20	9.80	9.54
140	10.92	10.76	10.61	10.27	10.24	10.19	9.78	9.52
160	10.92	10.75	10.60	10.26	10.23	10.17	9.76	9.51
180	10.92	10.74	10.59	10.25	10.21	10.16	9.75	9.49
200	10.91	10.74	10.58	10.23	10.20	10.15	9.74	9.48
250	10.91	10.72	10.57	10.21	10.18	10.13	9.71	9.45
300	10.90	10.71	10.55	10.19	10.16	10.12	9.69	9.43
350	10.89	10.70	10.54	10.17	10.14	10.10	9.67	9.41
400	10.89	10.70	10.53	10.16	10.13	10.09	9.65	9.40
500	10.88	10.68	10.51	10.13	10.11	10.06	9.63	9.37
600	10.87	10.67	10.49	10.11	10.09	10.05	9.61	9.34
700	10.87	10.66	10.48	10.10	10.07	10.03	9.59	9.32
800	10.86	10.65	10.46	10.08	10.05	10.02	9.57	9.30
900	10.85	10.64	10.45	10.07	10.04	10.00	9.55	9.28
1000	10.85	10.63	10.44	10.05	10.02	9.99	9.54	9.27
1200	10.84	10.62	10.43	10.03		9.97	9.52	9.24
1400	10.83	10.61	10.41	10.01	10.00	9.96	9.50	9.21
1600	10.82	10.60	10.40	10.00		9.94	9.48	9.19
1800	10.82	10.59	10.38	9.98	9.96	9.93	9.47	9.18
2000	10.81	10.58	10.37	9.97	9.95	9.92	9.46	9.16
2250	10.81	10.56	10.36	9.96		9.91	9.44	9.15
2500	10.80	10.55	10.35	9.94		9.90	9.43	9.13
3000	10.79	10.53	10.32	9.92		9.88	9.41	9.11
3500	10.78	10.52	10.31	9.91		9.86	9.39	9.08
4000	10.77	10.50	10.29	9.89		9.84	9.37	
5000	10.75	10.48	10.27	9.86		9.82		
6000	10.74	10.45	10.24	9.84		9.80		
7000	10.73	10.44	10.22	9.82		9.78		
8000	10.72	10.42	10.21	9.81		9.76		
9000	10.71	10.41	10.19	9.79		9.75		
10000	10.70	10.39	10.17	9.78		9.73		

Chap. IV, Fig. 3 (cont.)

TEMP.	-1.6	3.7	10.5	16.4	24.1	31.3	38.3
LOG A	-5.05	-6.09	-7.17	-8.05	-9.22	-10.2[illegible]	10.93
TIME	LOG E	LOG E	LOG E	LOG E	LOG E	LOG E	LOG E
3			9.23				8.34
6		9.45	9.15	8.92	8.64	8.43	8.29
10		9.38	9.08	8.86	8.59	8.38	8.25
15		9.33	9.04	8.81	8.55	8.35	8.22
20		9.29	9.01	8.78	8.52	8.33	8.20
25	9.57	9.26	8.98	8.76	8.50	8.31	8.19
30	9.54	9.24	8.96	8.74	8.48	8.29	8.18
35	9.52	9.22	8.95	8.72	8.47	8.28	8.17
40	9.51	9.21	8.93	8.71	8.46	8.27	8.16
50	9.48	9.18	8.91	8.69	8.44	8.25	8.15
60	9.45	9.16	8.89	8.67	8.42	8.24	8.14
70	9.43	9.14	8.87	8.65	8.41	8.23	8.13
80	9.42	9.13	8.86	8.64	8.40	8.22	8.12
90	9.40	9.11	8.84	8.63	8.39	8.21	8.11
100	9.39	9.10	8.83	8.62	8.38	8.21	8.11
120	9.37	9.08	8.81	8.60	8.36	8.19	8.10
140	9.35	9.06	8.79	8.59	8.36	8.18	8.09
160	9.33	9.05	8.78	8.57	8.34	8.17	8.08
180	9.32	9.04	8.77	8.56	8.33	8.17	8.08
200	9.30	9.02	8.76	8.55	8.32	8.16	8.06
250	9.28	9.00	8.73	8.53	8.31	8.15	8.05
300	9.25	8.98	8.72	8.52	8.29	8.13	8.05
350	9.23	8.96	8.70	8.50	8.28	8.12	8.03
400	9.22	8.95	8.69	8.49	8.27	8.11	8.02
500	9.19	8.93	8.67	8.47	8.26	8.10	8.01
600	9.17	8.91	8.65	8.46	8.24	8.09	8.00
700	9.15	8.89	8.64	8.44	8.23	8.08	8.00
800	9.13	8.88	8.62	8.43	8.22	8.07	7.99
900	9.12	8.87	8.61	8.42	8.21	8.07	7.98
1000	9.11	8.86	8.60	8.41	8.21	8.06	7.97
1200	9.09	8.84	8.59	8.40	8.19	8.04	7.96
1400	9.07	8.82	8.57	8.38	8.19	8.04	7.95
1600	9.05	8.81	8.56	8.37	8.17	8.03	7.95
1800	9.04	8.80	8.55	8.36	8.17	8.02	7.94
2000	9.03	8.79	8.54	8.35	8.16	8.01	7.93
2250	9.01	8.78	8.53	8.34	8.15	8.00	7.92
2500	9.00	8.77	8.52	8.33	8.14	7.99	7.92
3000	8.98	8.75	8.50	8.32	8.13	7.97	7.90
3500	8.96	8.73	8.49	8.30	8.12	7.96	7.90
4000	8.95	8.72	8.47	8.30	8.11	7.95	7.88
5000	8.92	8.69	8.45	8.28	8.09	7.94	7.86
6000	8.90	8.68	8.43	8.26	8.07		7.85
7000	8.88	8.67	8.42	8.25	8.06		7.84
8000	8.86	8.65	8.40	8.24	8.06		7.83
9000	8.85	8.64		8.23	8.05		7.82
10000	8.84		8.38	8.22	8.04		7.82
12000	8.81	8.62					
14000	8.79						
16000	8.78						
18000	8.76						

Chap. IV, Fig. 4, p. 105

TEMP.	-54.1	-47.5	-37.9	-27.4	-19.6	-12.4	-5.5	-1.6	5.7	11.9	10.3	14.0	24.1	30.6	39.8	50.8
LOG A	3.95	2.26	0.33	-1.83	-3.46	-4.88	-7.13	-7.55	-9.14	-10.11	-10.75	-11.09	-12.22	-12.91	-13.91	-14.61
TIME	LOG E	LOG E	LOG E	LOG E	LOG E	LOG E	LOG E	LOG E	LOG E	LOG E	LOG E	LOG E	LOG E	LOG E	LOG E	LOG E
3	10.83		10.70	10.54		10.06		9.46	9.02				8.17	7.90	7.64	7.48
6	10.82		10.68	10.51	10.29	9.99	9.49	9.35	8.92				8.02	7.81	7.56	7.41
10	10.82	10.78	10.67	10.48	10.25	9.94	9.42	9.30	8.86	8.56	8.49	8.34	7.95	7.75	7.51	7.37
15	10.81	10.77	10.66	10.47	10.21	9.90	9.38	9.25	8.79	8.51	8.42	8.28	7.90	7.70	7.47	7.35
20	10.81	10.77	10.65	10.45	10.18	9.87	9.34	9.22	8.76	8.47	8.36	8.23	7.86	7.67	7.45	7.33
30	10.81	10.76	10.64	10.43	10.15	9.83	9.28	9.17	8.71	8.42	8.29	8.16	7.81	7.63	7.42	7.31
40	10.80	10.75	10.63	10.41	10.12	9.80	9.25	9.13	8.67	8.38	8.24	8.13	7.77	7.60	7.39	7.29
50	10.80	10.75	10.62	10.39	10.10	9.78	9.22	9.11	8.64	8.35	8.20	8.09	7.75	7.58	7.38	7.28
60	10.80	10.74	10.62	10.38	10.09	9.76	9.20	9.08	8.61	8.33	8.17	8.06	7.72	7.56	7.36	7.27
80	10.80	10.74	10.61	10.36	10.06	9.73	9.17	9.05	8.58	8.29	8.12	8.02	7.69	7.54	7.34	7.26
100	10.79	10.73	10.60	10.35	10.04	9.71	9.14	9.02	8.55	8.27	8.08	8.00	7.66	7.51	7.33	7.25
120	10.79	10.73	10.59	10.34	10.03	9.69	9.12	9.00	8.53	8.25	8.05	7.97	7.64	7.49	7.32	7.24
140	10.79	10.72	10.58	10.33	10.01	9.68	9.10	8.98	8.51	8.23	8.03	7.95	7.63	7.48	7.31	7.23
170	10.79	10.71	10.58	10.31	9.99	9.66	9.07	8.96	8.48	8.20	8.00	7.92	7.60	7.46	7.29	7.23
200	10.79	10.71	10.57	10.30	9.97	9.64	9.05	8.94	8.46	8.19	7.97	7.90	7.59	7.45	7.28	7.22
250	10.78	10.70	10.56	10.29	9.95	9.62	9.03	8.91	8.43	8.16	7.93	7.86	7.57	7.43	7.27	7.21
300	10.78	10.70	10.55	10.27	9.93	9.60	9.00	8.89	8.40	8.13	7.90	7.84	7.55	7.41	7.26	7.20
400	10.78	10.69	10.54	10.25	9.90	9.57	8.98	8.86	8.36	8.10	7.86	7.80	7.52	7.39	7.24	7.19
500	10.78	10.68	10.53	10.23	9.88	9.55	8.95	8.84	8.33	8.08	7.82	7.77	7.49	7.37	7.23	7.18
600	10.77	10.67	10.52	10.22	9.86	9.54	8.93	8.80	8.31	8.06	7.79	7.75	7.48	7.36	7.22	7.17
800	10.77	10.66	10.51	10.19	9.83	9.50	8.88	8.76	8.27	8.02	7.74	7.71	7.45	7.33	7.21	7.16
1000	10.77	10.65	10.49	10.17	9.80	9.48	8.87	8.72	8.24	7.98	7.71	7.68	7.42	7.31	7.19	7.15
1200	10.76	10.64	10.48	10.16	9.79	9.46	8.84	8.70	8.21	7.95	7.69	7.66	7.41	7.30	7.18	7.15
1400	10.76	10.64	10.47	10.14	9.77	9.44	8.82	8.67	8.18	7.94	7.66	7.64	7.39	7.28	7.17	7.14
1700	10.76	10.63	10.46	10.13	9.74	9.42	8.78	8.64	8.17	7.93	7.63	7.61	7.37	7.27	7.16	7.14
2000	10.75	10.62	10.45	10.11	9.72	9.40	8.76	8.62	8.15	7.91	7.61	7.59	7.36	7.26	7.15	7.13
2500	10.75	10.61	10.43	10.09	9.70	9.38	8.72	8.58	8.11	7.89	7.58	7.56	7.34	7.24	7.14	7.12
3000	10.74	10.60	10.42	10.07	9.67	9.36	8.68	8.55	8.08	7.85	7.55	7.54	7.32	7.22	7.13	7.10
4000	10.74	10.59	10.39	10.03	9.64	9.32		8.51	8.04	7.82	7.51	7.51	7.29	7.20	7.11	7.09
5000	10.73	10.57	10.37	10.01	9.62	9.30			8.00	7.78	7.48	7.47	7.27	7.17	7.09	7.08
6000	10.73	10.56	10.34	9.99	9.59	9.28			7.98		7.45	7.46	7.25	7.16	7.08	7.07
8000	10.72	10.54	10.33	9.95	9.56	9.24					7.42	7.41	7.24	7.14	7.07	7.05
10000	10.71		10.31	9.93	9.53	9.21					7.41	7.38	7.22	7.11	7.05	7.04
12000				9.90	9.50	9.19					7.39	7.36	7.21	7.10	7.04	7.03
14000				9.89	9.49	9.18						7.34	7.20	7.08	7.03	7.03
17000				9.86	9.47									7.07		7.02
20000				9.84	9.45									7.05		

TEMP.	-31.2	-28.2	-26.4	-24.3	-21.0	-20.2	-17.8	-16.5	-14.3	-11.8	-8.4	-4.9	-3.8	-0.7	1.7	3.8	7.5
LOG A	5.89	5.65	4.98	3.26	1.47	1.39	-0.31	-0.81	-2.29	-2.79	-4.61	-6.92	-8.16	-8.47	-3.90	-9.45	-10.19
TIME	LOG E	LOG E	LOG E	LOG E	LOG E	LOG E	LOG E	LOG E	LOG E	LOG E	LOG E	LOG E	LOG E	LOG E	LOG E	LOG E	LOG E
3	11.15	11.14	11.10	11.00	10.82	10.80	10.58	10.51	10.24	10.15	9.79	9.26			9.75		8.46
6	11.14	11.12	11.08	10.97	10.78	10.77	10.54	10.46	10.19	10.08	9.73	9.18	8.85	8.77	8.67	8.55	8.38
10	11.13	11.11	11.07	10.95	10.75	10.74	10.50	10.42	10.15	10.05	9.68	9.12	8.80	8.71	8.62	8.51	8.33
15	11.12	11.10	11.06	10.94	10.73	10.72	10.48	10.39	10.11	10.01	9.64	9.07	8.75	8.68	8.58	8.47	8.29
20	11.11	11.10	11.05	10.92	10.71	10.70	10.46	10.37	10.08	9.99	9.61	9.03	8.72	8.65	8.56	8.44	8.26
30	11.10	11.09	11.04	10.91	10.69	10.68	10.43	10.34	10.05	9.96	9.57	8.99	8.68	8.61	8.52	8.39	8.22
40	11.09	11.08	11.03	10.90	10.67	10.66	10.41	10.32	10.02	9.93	9.54	8.96	8.65	8.59	8.49	8.37	8.20
50	11.08	11.07	11.03	10.89	10.66	10.65	10.39	10.30	9.99	9.91	9.52	8.93	8.63	8.57	8.47	8.34	8.17
60	11.08	11.07	11.02	10.88	10.65	10.64	10.37	10.29	9.98	9.89	9.50	8.91	8.61	8.55	8.45	8.32	8.16
80	11.07	11.06	11.01	10.86	10.63	10.62	10.35	10.26	9.95	9.87	9.47	8.88	8.58	8.52	8.42	8.29	8.13
100	11.06	11.05	11.00	10.85	10.61	10.60	10.33	10.24	9.92	9.85	9.45	8.85	8.56	8.50	8.40	8.27	8.10
120	11.06	11.05	11.00	10.84	10.60	10.59	10.32	10.22	9.91	9.83	9.43	8.83	8.54	8.48	8.38	8.25	8.08
140	11.05	11.04	10.99	10.83	10.59	10.58	10.30	10.21	9.89	9.83	9.41	8.82	8.53	8.46	8.37	8.24	8.07
170	11.04	11.03	10.99	10.82	10.58	10.57	10.29	10.19	9.87	9.80	9.39	8.80	8.51	8.44	8.35	8.22	8.04
200	11.04	11.03	10.98	10.81	10.57	10.55	10.27	10.18	9.85	9.79	9.37	8.78	8.50	8.42	8.33	8.20	8.03
250	11.03	11.02	10.97	10.80	10.55	10.54	10.25	10.16	9.82	9.77	9.35	8.76	8.48	8.40	8.31	8.18	8.00
300	11.02	11.01	10.96	10.79	10.53	10.52	10.24	10.14	9.81	9.75	9.33	8.75	8.46	8.39	8.29	8.15	7.98
400	11.01	11.00	10.95	10.77	10.51	10.50	10.21	10.12	9.78	9.73	9.30	8.70		8.36			
500	11.00	10.99	10.94	10.75	10.49	10.48	10.18	10.10	9.75	9.70	9.27	8.68		8.34			
600	10.99	10.99	10.93	10.74	10.48	10.47	10.16	10.08	9.73	9.68	9.25	8.65		8.32			
800	10.98	10.97	10.92	10.72	10.45	10.44	10.13	10.04	9.70	9.66	9.22	8.62					
1000	10.96	10.96	10.91	10.70	10.43	10.42	10.10	10.03	9.68	9.63	9.19	8.59					
1200	10.96	10.95	10.90	10.68	10.41	10.40	10.08	10.01	9.66	9.61	9.18	8.56					
1400	10.95	10.94	10.89	10.67	10.39	10.38	10.06	9.99	9.64	9.59	9.16	8.54					
1700	10.94	10.93	10.88	10.65	10.38	10.36	10.03	9.97	9.62	9.57	9.12	8.52					
2000	10.93	10.92	10.87	10.64	10.36	10.35	10.01	9.96	9.60	9.56	9.09	8.49					
2500	10.92	10.90	10.86	10.61	10.34	10.32	9.98	9.94	9.58	9.54	9.06	8.46					
3000	10.91	10.89	10.85	10.59	10.32	10.30	9.95	9.92	9.56	9.52	9.04	8.43					
4000	10.89	10.87	10.83	10.56	10.29	10.27	9.92	9.89	9.53	9.48	9.00	8.39					
5000	10.88	10.85	10.81	10.54	10.26	10.24	9.88	9.87	9.51	9.46	8.97	8.38					
6000	10.87	10.83	10.80	10.52	10.24	10.22	9.86	9.85	9.49	9.44	8.94	8.36					
8000	10.85	10.81	10.78	10.48	10.21	10.19	9.82	9.82	9.46	9.42							
10000	10.83	10.79	10.76	10.45	10.18	10.16	9.78	9.81		9.40							
12000		10.77					9.76										

Chap. IV, Fig. 6, p. 109

100Na-29FA T(°C)	LogE,	67Na-27FA etc.		39Na-25FA		22Na-23FA		10Na-26FA		00Na-23FA	
-28.0	11.07	-22.6	10.97	-40.8	11.02	-40.2	11.02	-59.5	10.80	-51.8	10.57
-20.0	11.05	-10.5	10.95	-33.8	10.98	-35.6	11.00	-49.2	10.78	-45.8	10.55
6.3	11.01	-4.0	10.93	-30.3	10.92	-25.4	10.93	-38.7	10.77	-33.3	10.50
14.5	10.98	3.8	10.90	-20.0	10.86	-14.6	10.86	-26.6	10.69	-20.9	10.42
20.3	10.97	14.9	10.84	-6.8	10.81	-4.6	10.77	-18.8	10.67	-12.9	10.41
33.0	10.92	28.4	10.79	0.4	10.78	7.8	10.65	-8.6	10.59	-3.4	10.36
42.3	10.80	38.1	10.65	13.6	10.68	17.8	10.56	8.2	10.47	8.5	10.27
51.1	10.72	47.7	10.58	23.9	10.65	28.4	10.28	16.8	10.33	17.3	10.00
62.3	10.68	57.8	10.51	34.4	10.55	36.5	9.99	22.6	10.19	22.6	9.49
70.9	10.65	67.7	10.36	45.8	10.33	42.7	9.65	29.4	9.53	34.9	8.15
80.6	10.61	76.5	10.21	53.4	10.16	45.8	9.59	34.9	9.14	43.3	7.70
93.1	10.54	86.2	10.07	56.7	10.05	52.2	9.38	43.5	8.78	58.0	7.24
100.1	10.49	94.5	10.01	64.4	9.89			55.0	8.16	70.8	6.73
111.9	10.42			65.0	9.72			68.2	7.60		
121.4	10.35			77.6	9.28			83.5	7.29		
132.0	10.22							97.1	6.89		
144.2	10.04										
151.8	9.95										

Chap. IV, Fig. 7, p. 111

100Na-22FA		100Na-29FA		100Na-43FA		100Na-52FA		100Na-67FA		100Na-72FA	
-36.6	11.11	-28.0	11.07	-26.8	10.94	-57.2	10.94	-39.0	9.27	-88.0	9.97
-29.4	11.13	-20.0	11.05	-16.0	10.91	-48.2	10.90	-27.8	9.09	-74.4	9.91
-18.0	11.10	6.3	11.01	-5.3	10.81	-33.2	10.76	-11.7	8.83	-71.0	9.82
-7.4	11.11	14.5	10.98	2.0	10.79	-21.2	10.69	0.6	8.53	-67.3	9.72
1.7	11.10	20.3	10.97	9.6	10.74	-10.8	10.52	12.4	8.39	-62.2	9.68
18.3	11.03	33.0	10.92	18.7	10.69	1.2	10.35	22.8	8.28	-52.8	9.44
28.9	11.01	42.3	10.80	27.7	10.62	10.9	10.18	32.2	8.17	-39.3	9.20
39.6	10.99	51.1	10.72	38.4	10.49	22.2	10.00			-31.7	8.81
53.3	10.93	62.3	10.68	47.1	10.38	36.3	9.81			-19.0	8.59
63.6	10.90	70.9	10.65	56.9	10.29					-8.1	8.31
73.8	10.86	80.6	10.61	64.4	10.22					2.5	8.18
83.2	10.77	93.1	10.54	74.5	10.13					10.1	8.09
92.7	10.75	100.1	10.49	82.5	10.07					24.2	7.96
102.7	10.72	111.9	10.42	93.8	9.96						
112.1	10.67	121.4	10.35								
121.3	10.63	132.0	10.22								
132.8	10.56	144.2	10.04								
144.6	10.49	151.8	9.95								
160.4	10.42										

Chap. IV, Fig. 8, p. 112

100Na-54GL		100Na-55GL		100Na-66GL	
-32.2	10.85	-40.8	10.96	-54.1	10.78
-24.0	10.83	-34.1	10.85	-47.5	10.75
-15.8	10.70	-28.8	10.77	-37.9	10.66
-4.6	10.40	-23.6	10.54	-27.4	10.49
5.0	9.98	-20.6	10.49	-19.6	10.27
13.5	9.85	-20.3	10.45	-12.4	9.98
16.5	9.56	-15.9	10.09	-5.5	9.47
19.4	9.38	-13.0	9.87	-1.6	9.35
24.7	9.07	-1.6	0.04	5.7	8.92
33.8	8.73	3.7	9.42	11.9	8.63
38.9	8.61	10.5	9.14	10.3	8.56
46.2	8.49	16.4	8.93	14.0	8.41
54.8	8.40	24.1	8.66	24.1	8.03
66.1	8.35	31.3	8.47	30.6	7.85
74.1	8.29	38.3	8.35	39.8	7.62
85.0	8.23			50.8	7.50

Chap. IV, Fig. 9, p. 113

100Na-50H_2O		100Na-54H_2O		100Na-58H_2O	
-31.2	11.10	-45.3	10.92	-73.0	11.01
-28.2	11.09	-38.5	10.80	-62.2	10.99
-26.4	11.06	-31.3	10.55	-58.5	10.96
-24.3	10.94	-27.2	10.36	-50.2	10.93
-21.0	10.75	-20.8	9.68	-42.7	10.86
-20.2	10.74	-13.4	8.82	-39.6	10.82
-17.8	10.51	-11.3	7.30	-36.9	10.74
-16.5	10.43	-4.0	6.65	-35.8	10.68
-14.3	10.15	3.4	6.26	-30.8	10.42
-11.8	10.05			-25.8	9.88
-8.4	9.69			-22.7	9.15
-4.9	9.14			-21.5	8.89
-3.8	8.82				
-0.7	8.74				
1.7	8.65				
3.8	8.54				
7.5	8.37				

Chap. IV, Fig. 10, p. 115

100Na-54EG	
-43.6	10.66
-38.6	10.64
-31.2	10.52
-22.0	10.37
-9.8	10.11
0.2	9.98
6.6	9.85
14.1	9.73
24.3	9.57
26.1	9.54
40.2	9.45
49.3	9.44
60.7	9.38
66.7	9.25

Chap. IV, Fig. 11, p. 116

100Na-48FA			100Na-55GL			100Na-55H_2O		
T (°C)	G' ($\times 10^{-8}$)	tan δ	T (°C)	G' ($\times 10^{-8}$)	tan δ	T (°C)	G' ($\times 10^{-8}$)	tan δ
-64	252.	.163	-37		.144	-63		.081
-62	224.	.169	-35.5		.135	-61.5	403.	.091
-59.5	212.	.194	-34	151.	.156	-59	403.	.107
-58.5	200.	.199	-32.5		.157	-57	333.	.126
-56	193.	.217	-31.5		.173	-56	319.	.129
-54.5	176.	.236	-30	143.	.183	-54		.144
-53	161.	.246	-28.5		.186	-53		.148
-51	143.	.260	-27	132.	.207	-51		.160
-48	113.	.301	-26	129.	.209	-48.5		.173
-46	108.	.309	-24	126.	.221	-46.5		.192
-44.5	96.	.319	-23	122.	.216	-45		.200
-42	75.	.345	-21.5	117.	.258	-44		.202
-40	71.	.356	-20	113.	.264	-42		.233
-38	63.	.356	-18.5	114.	.291	-40		.249
-35.5	51.	.368	-17	114.	.316	-38		.260
-33.5	43.6	.378	-15.5	109.	.342	-36.5		.277
-31	39.1	.402	-12	94.	.395	-35		.281
-28	32.0	.407	-11	94.	.403	-33.5		.294
-26	27.1	.405	-10	72.	.427	-32		.302
-23.5	23.3	.405	- 8.5	72.	.441	-30	88.6	.313
-22	20.7	.422	- 6	58.	.464	-28.5		.334
-19.5	17.6	.417	- 4.5	54.	.511	-27	71.9	.343
-18	15.9	.414	- 2.5	43.	.522	-25	54.7	.349
-15.5	13.2	.425	+ 1	29.4	.552	-23	44.8	.360
-13.5	10.8	.436	3	23.1	.566	-20.5	38.6	.381
-11.5	8.8	.446	4.5	20.8	.566	-19.5		.396
- 9.5	7.5	.451	5.5	19.3	.591	-18	30.2	.409
- 7	5.6	.486	8.5	13.1		-16.5		.403
- 4.5	4.76	.469	11	9.6	.616	-15.5	23.1	.396
- 2.5	3.85	.465	12.5	8.7	.621	-14	18.5	.421
+ 0.5	2.93	.455	21	1.8		-12	14.1	.444
2.5	2.68	.443	26.5	.66	.769	-11.5	10.6	.480
4.5	2.27	.425	28	.51	.747	- 9.5	9.0	.568
6	1.81	.413	29.5	.40	.775	- 9	6.5	.599
8	1.63	.404	31	.285	.755	- 8	4.8	.726
11.5	1.13	.370	33	.232	.731	0	.204	.953
13	.96	.356	35	.190	.720	1.5	.154	.892
15	.86	.345	36.5	.158	.655	3	.130	.901
17	.75	.327	39	.130	.609	5.5	.055	.626
19	.61	.311	40	.118	.541	7.5	.053	.517
21	.53	.298	42	.096	.483	9.5	.053	.462
23	.483	.285	44	.088	.417	10.5	.045	.438
25.5	.399	.267	46.5	.081	.367	11.5	.045	.426
28	.327	.249	49	.065	.242	12.5	.043	.366
30.5	.276	.228				13.5	.040	.373
33	.253	.228				15.5	.039	.309
34.5	.243	.199						

Chap. IV, Fig. 12, p. 122

T(°C)	-31.2	-28.2	-26.4	-24.3
log t vs. D(t)	-5.4 0.711E-11	-5.0 0.751E-11	-4.4 0.801E-11	-2.6 0.104E-10
	-5.2 0.731E-11	-4.8 0.768E-11	-4.2 0.821E-11	-2.4 0.109E-10
	-5.0 0.750E-11	-4.6 0.785E-11	-4.0 0.841E-11	-2.2 0.113E-10
	-4.8 0.768E-11	-4.4 0.802E-11	-3.8 0.864E-11	-2.0 0.118E-10
	-4.6 0.786E-11	-4.2 0.821E-11	-3.6 0.887E-11	-1.8 0.123E-10
	-4.4 0.806E-11	-4.0 0.844E-11	-3.4 0.913E-11	-1.6 0.128E-10
	-4.2 0.830E-11	-3.8 0.870E-11	-3.2 0.942E-11	-1.4 0.135E-10
	-4.0 0.857E-11	-3.6 0.899E-11	-3.0 0.973E-11	-1.2 0.142E-10
	-3.8 0.888E-11	-3.4 0.929E-11	-2.8 0.101E-10	-1.0 0.150E-10
	-3.6 0.923E-11	-3.2 0.964E-11	-2.6 0.104E-10	-0.8 0.160E-10
	-3.4 0.960E-11	-3.0 0.100E-10	-2.4 0.109E-10	-0.6 0.171E-10
	-3.2 0.100E-10	-2.8 0.105E-10	-2.2 0.113E-10	-0.4 0.184E-10
	-3.0 0.105E-10	-2.6 0.111E-10	-2.0 0.119E-10	-0.2 0.199E-10
	-2.8 0.111E-10	-2.4 0.117E-10	-1.8 0.125E-10	0.0 0.217E-10
	-2.6 0.117E-10	-2.2 0.126E-10	-1.6 0.133E-10	0.2 0.240E-10
	-2.4 0.123E-10	-2.0 0.136E-10	-1.4 0.141E-10	0.4 0.266E-10
	-2.2 0.131E-10	-1.8 0.148E-10	-1.2 0.150E-10	

-21.0	-20.2	-17.8	-16.5
-0.8 0.158E-10	-0.8 0.159E-10	0.8 0.259E-10	1.4 0.314E-10
-0.6 0.167E-10	-0.6 0.169E-10	1.0 0.276E-10	1.6 0.338E-10
-0.4 0.177E-10	-0.4 0.178E-10	1.2 0.294E-10	1.8 0.363E-10
-0.2 0.188E-10	-0.2 0.188E-10	1.4 0.315E-10	2.0 0.391E-10
0.0 0.200E-10	0.0 0.200E-10	1.6 0.337E-10	2.2 0.422E-10
0.2 0.213E-10	0.2 0.212E-10	1.8 0.363E-10	2.4 0.457E-10
0.4 0.227E-10	0.4 0.226E-10	2.0 0.392E-10	2.6 0.496E-10
0.6 0.243E-10	0.6 0.241E-10	2.2 0.425E-10	2.8 0.541E-10
0.8 0.262E-10	0.8 0.259E-10	2.4 0.463E-10	3.0 0.592E-10
1.0 0.282E-10	1.0 0.279E-10	2.6 0.506E-10	3.2 0.649E-10
1.2 0.306E-10	1.2 0.302E-10	2.8 0.555E-10	3.4 0.713E-10
1.4 0.334E-10	1.4 0.329E-10	3.0 0.614E-10	3.6 0.786E-10
1.6 0.367E-10	1.6 0.360E-10	3.2 0.683E-10	3.8 0.870E-10
1.8 0.404E-10	1.8 0.397E-10	3.4 0.767E-10	4.0 0.964E-10
2.0 0.448E-10	2.0 0.440E-10	3.6 0.869E-10	4.2 0.107E-09
2.2 0.499E-10	2.2 0.491E-10	3.8 0.992E-10	4.4 0.118E-09
	2.4 0.552E-10	4.0 0.114E-09	4.6 0.131E-09

Chap. IV, Fig. 12 (cont.)

-14.3		-11.8		-8.4		-4.9	
2.8	0.540E-10	3.4	0.706E-10	5.2	0.159E-09	7.4	0.502E-09
3.0	0.591E-10	3.6	0.775E-10	5.4	0.175E-09	7.6	0.561E-09
3.2	0.645E-10	3.8	0.849E-10	5.6	0.193E-09	7.8	0.630E-09
3.4	0.706E-10	4.0	0.927E-10	5.8	0.212E-09	8.0	0.713E-09
3.6	0.776E-10	4.2	0.101E-09	6.0	0.235E-09	8.2	0.808E-09
3.8	0.855E-10	4.4	0.110E-09	6.2	0.260E-09	8.4	0.915E-09
4.0	0.943E-10	4.6	0.121E-09	6.4	0.289E-09	8.6	0.103E-08
4.2	0.104E-09	4.8	0.133E-09	6.6	0.322E-09	8.8	0.116E-08
4.4	0.116E-09	5.0	0.145E-09	6.8	0.359E-09	9.0	0.131E-08
4.6	0.129E-09	5.2	0.159E-09	7.0	0.402E-09	9.2	0.147E-08
4.8	0.144E-09	5.4	0.175E-09	7.2	0.450E-09	9.4	0.165E-08
5.0	0.161E-09	5.6	0.194E-09	7.4	0.506E-09	9.6	0.185E-08
5.2	0.180E-09	5.8	0.215E-09	7.6	0.569E-09	9.8	0.209E-08
5.4	0.201E-09	6.0	0.240E-09	7.8	0.643E-09	10.0	0.238E-08
5.6	0.225E-09	6.2	0.267E-09	8.0	0.735E-09	10.2	0.274E-08
5.8	0.252E-09	6.4	0.298E-09			10.4	0.315E-08

-3.8		-0.7		1.7	
9.0	0.132E-08	9.4	0.167E-08	9.4	0.167E-08
9.2	0.147E-08	9.6	0.187E-08	9.6	0.187E-08
9.4	0.165E-08	9.8	0.208E-08	9.8	0.209E-08
9.6	0.186E-08	10.0	0.231E-08	10.0	0.232E-08
9.8	0.208E-08	10.2	0.256E-08	10.2	0.257E-08
10.0	0.232E-08	10.4	0.284E-08	10.4	0.285E-08
10.2	0.258E-08	10.6	0.315E-08	10.6	0.315E-08
10.4	0.285E-08	10.8	0.351E-08	10.8	0.349E-08
		11.0	0.390E-08	11.0	0.388E-08

3.8		7.5	
10.4	0.285E-08	10.8	0.350E-08
10.6	0.315E-08	11.0	0.390E-08
10.8	0.350E-08	11.2	0.433E-08
11.0	0.389E-08	11.4	0.482E-08
11.2	0.432E-08	11.6	0.535E-08
11.4	0.481E-08	11.8	0.592E-08
11.6	0.536E-08	12.0	0.657E-08
		12.2	0.733E-08
		12.4	0.819E-08

Chap. IV, Fig. 13, p. 124

T(°C)	-31.2		-28.2		-24.3		-21.0		-20.2		-17.8		-14.3	
log b_T	2.0		1.85		1.4		1.1		1.1		0.7		0.0	
	2.69	0.52	2.46	0.22	2.66	0.37	2.47	0.6	2.59	0.8	2.49	1.5	1.91	0.32
	2.89	0.71	2.66	0.30	2.86	0.65	2.67	1.2	2.79	1.5	2.69	2.3	2.11	0.55
	3.09	0.92	2.86	0.43	3.06	1.09	2.87	2.0	2.99	2.3	2.89	3.8	2.31	0.82
log t	3.29	1.15	3.06	0.61	3.26	1.78	3.07	2.9	3.19	3.4	3.09	6.1	2.51	1.15
vs.	3.49	1.38	3.26	0.87	3.46	2.75	3.27	4.1	3.39	4.9	3.29	9.4	2.71	1.57
D(t)	3.69	1.66	3.46	1.27	3.66	4.02	3.47	5.7	3.59	6.9	3.49	14.3	2.91	2.07
		$\times 10^{-12}$	3.66	1.82		$\times 10^{-12}$	3.67	7.6	3.79	9.4	3.69	21.0	3.11	2.64
			3.86	2.49				$\times 10^{-12}$		$\times 10^{-12}$		$\times 10^{-12}$	3.31	3.28
				$\times 10^{-12}$									3.51	3.97
														$\times 10^{-11}$

Chap. IV, Fig. 15, p. 126

T(°C)	-2.9		1.1		10.4		19.1		22.0		24.7	
log b_T	1.1		1.25		0.95		0.4		0.05		0.0	
	2.95	0.62	3.11	0.31	3.23	0.9	3.17	2.6	2.63	2.0	2.35	1.1
	3.15	0.93	3.31	0.56	3.43	1.6	3.37	4.1	2.83	3.3	2.55	1.8
	3.35	1.34	3.51	0.95	3.63	2.3	3.57	7.1	3.03	4.8	2.75	2.9
log t	3.35	1.79	3.71	1.57	3.83	3.5	3.77	10.7	3.23	6.9	2.95	4.3
vs.	3.75	2.33		$\times 10^{-12}$	4.03	4.8		$\times 10^{12}$	3.43	9.4	3.15	5.8
D(t)		$\times 10^{-12}$				$\times 10^{-12}$			3.63	12.0	3.35	7.1
									3.83	14.4	3.55	8.6
										$\times 10^{-12}$	3.75	9.7
												$\times 10^{-12}$

Chap. IV, Fig. 14, p. 125

T(°C)	-47.5	-37.9	-27.4	-19.6	-5.5
log b_T	4.2	3.9	4.0	3.4	2.3
log t vs. D(t)	3.40 1.07 3.60 1.91 3.80 2.71 4.00 3.94 $\times 10^{-12}$	3.41 0.54 3.61 0.97 3.81 1.46 4.01 2.07 $\times 10^{-12}$	3.65 1.1 3.85 2.3 4.05 4.0 4.25 5.9 $\times 10^{-12}$	3.40 0.30 3.60 0.57 3.80 0.96 4.00 1.43 4.20 2.07 $\times 10^{-11}$	3.27 3.0 3.47 5.3 $\times 10^{-11}$

-1.6	5.7	14.0	24.1	30.6	39.8
2.1	1.3	0.9	0.55	0.4	0.0
3.22 3.4 3.42 7.3 $\times 10^{-11}$	2.78 0.9 2.98 1.7 3.18 2.7 3.38 4.1 3.58 5.8 $\times 10^{-10}$	3.28 0.71 3.48 1.34 3.68 2.32 3.88 3.64 $\times 10^{-9}$	2.98 1.04 3.18 1.56 3.38 2.39 3.58 3.71 3.78 5.38 $\times 10^{-9}$	3.09 1.4 3.29 2.7 3.49 4.5 3.69 7.1 3.89 10.2 4.09 13.9 $\times 10^{-9}$	2.29 0.7 2.49 1.2 2.69 1.7 2.89 2.5 3.09 3.6 3.29 4.9 3.49 6.6 3.69 8.7 3.89 11.2 $\times 10^{-9}$

Chap. IV, Fig. 20, p. 139

	0.1 hz		0.01 hz		0.001 hz	
T(°C)	-log D'(ω)	-log tan δ	-log D'(ω)	-log tan δ	-log D'(ω)	-log tan δ
-26.8	11.009	1.458	10.977	1.204	10.931	1.105
-18.0	10.966	1.143	10.915	1.076	10.860	1.058
- 5.3	10.859	1.060	10.799	.939	10.716	.808
2.0	10.828	1.049	10.771	1.009	10.705	.950
9.6	10.769	1.043	10.710	.971	10.635	.858
18.7	10.697	1.008	10.634	.988	10.567	.958
27.7	10.619	.998	10.554	.948	10.478	.882
38.4	10.480	.913	10.400	.845	10.303	.774
47.1	10.365	.871	10.276	.799	10.168	.727
56.9	10.270	.839	10.173	.736	10.046	.642
64.4	10.194	.789	10.084	.706	9.952	.643
74.5	10.086	.786	9.979	.725	9.853	.662
82.5	10.016	.800	9.916	.779	9.808	.744
93.8	9.905	.802	9.799	.695	9.660	.605

Chap. IV, Fig. 21, p. 149

TEMP.	-51.8	-45.8	-33.3	-20.9	-12.9	-3.4	8.5	17.3	22.6	34.9	43.3	58.0	70.8
LOG A	7.05	6.45	4.75	2.49	1.94	0.65	-1.20	-3.35	-5.07	-7.69	-8.76	-10.60	-12.30
TIME	LOG E	LOG E	LOG E	LOG E	LOG E	LOG E	LOG E	LOG E	LOG E	LOG E	LOG E	LOG E	LOG E
2	10.68	10.66	10.59	10.49	10.46	10.40	10.31	10.09	9.73	8.45	7.93	0.0	6.85
3	10.68	10.65	10.58	10.48	10.46	10.40	10.30	10.07	9.66	8.37	7.85	0.0	6.79
5	10.67	10.64	10.57	10.47	10.44	10.39	10.28	10.02	9.58	8.26	7.75	7.25	6.72
7	10.66	10.64	10.56	10.46	10.44	10.38	10.27	10.00	9.52	8.18	7.70	7.21	6.68
10	10.66	10.63	10.55	10.45	10.43	10.37	10.26	9.98	9.46	8.10	7.64	7.17	6.64
15	10.65	10.62	10.55	10.45	10.42	10.36	10.25	9.94	9.38	8.01	7.59	7.11	6.59
20	10.64	10.62	10.54	10.44	10.42	10.36	10.24	9.92	9.33	7.95	7.54	7.08	6.54
25	10.64	10.61	10.54	10.44	10.41	10.35	10.23	9.89	9.29	7.91	7.51	7.04	6.52
30	10.64	10.61	10.53	10.43	10.41	10.35	10.22	9.88	9.25	7.87	7.49	7.01	6.49
35	10.63	10.61	10.53	10.43	10.41	10.35	10.22	9.86	9.22	7.84	7.47	6.99	6.47
40	10.63	10.60	10.53	10.43	10.40	10.34	10.21	9.84	9.19	7.82	7.45	6.98	6.44
50	10.63	10.60	10.53	10.42	10.40	10.34	10.20	9.81	9.15	7.78	7.43	6.94	6.42
60	10.62	10.60	10.52	10.42	10.40	10.34	10.20	9.79	9.11	7.75	7.40	6.91	6.39
70	10.62	10.59	10.52	10.42	10.39	10.33	10.19	9.78	9.07	7.73	7.38	6.89	6.37
80	10.62	10.59	10.52	10.41	10.39	10.33	10.18	9.76	9.04	7.70	7.37	6.86	6.36
90	10.61	10.59	10.51	10.41	10.39	10.33	10.18	9.75	9.01	7.68	7.35	6.84	6.34
100	10.61	10.59	10.51	10.41	10.39	10.32	10.17	9.74	8.99	7.67	7.34	6.83	6.33
120	10.61	10.58	10.51	10.41	10.38	10.32	10.16	9.71	8.95	7.64	7.32	6.79	6.30
140	10.61	10.58	10.51	10.40	10.38	10.32	10.16	9.69	8.91	7.61	7.31	6.77	6.27
160	10.60	10.58	10.50	10.40	10.38	10.31	10.15	9.67	8.88	7.59	7.29	6.74	6.25
180	10.60	10.58	10.50	10.40	10.37	10.31	10.14	9.64	8.85	7.57	7.28	6.72	6.22
200	10.60	10.57	10.50	10.39	10.37	10.30	10.13	9.63	8.83	7.56	7.27	6.69	6.21
250	10.59	10.57	10.50	10.39	10.36	10.30	10.12	9.59	8.77	7.53	7.25	6.66	
300	10.59	10.56	10.49	10.38	10.36	10.29	10.10	9.56	8.72	7.50	7.23	6.62	
350	10.58	10.56	10.49	10.37	10.35	10.29	10.09	9.53	8.67	7.48	7.21	6.59	
400	10.58	10.56	10.49	10.37	10.35	10.28	10.08	9.50	8.64	7.46	7.20	6.56	
500	10.58	10.55	10.48	10.37	10.34	10.27	10.06	9.46	8.58	7.44	7.18	6.50	
600	10.57	10.55	10.48	10.36	10.34	10.26	10.05	9.41	8.54	7.41	7.17		
700	10.57		10.47	10.36	10.33	10.26	10.03		8.50	7.40	7.15		
800	10.56		10.47		10.33	10.25	10.02		8.46	7.39	7.14		
900	10.56		10.47		10.33	10.25	10.01		8.44	7.37	7.13		
1000	10.56		10.46		10.32	10.24	10.00		8.42	7.37			

TEMP.	-59.5	-49.2	-38.7	-26.6	-18.8	-8.6	8.2	16.8	22.6	29.4	34.9	43.5	55.0	68.2	83.5	97.1
LOG A	8.69	6.87	5.62	3.34	2.75	1.23	-0.76	-2.13	-3.02	-5.19	-6.18	-7.24	-9.07	-10.79	-11.85	-13.30
TIME	LOG E	LOG E	LOG E	LOG E	LOG E	LOG E	LOG E	LOG E	LOG E	LOG E	LOG E	LOG E	LOG E	LOG E	LOG E	LOG E
2	10.92	10.89	10.86	10.76	10.74	10.64	10.52	10.39	10.29	9.75	9.39				7.39	6.96
3	10.92	10.88	10.85	10.75	10.73	10.64	10.50	10.37	10.26	9.69	9.34			7.67	7.33	6.91
5	10.91	10.88	10.84	10.75	10.72	10.62	10.49	10.34	10.22	9.60	9.22			7.60	7.26	6.85
7	10.91	10.88	10.84	10.74	10.71	10.62	10.47	10.33	10.19	9.55	9.16	8.78		7.54	7.22	6.81
10	10.91	10.87	10.84	10.73	10.70	10.61	10.46	10.31	10.16	9.49	9.10	8.72	8.09	7.51	7.18	6.77
15	10.91	10.87	10.83	10.73	10.69	10.59	10.44	10.29	10.12	9.42	9.03	8.65	8.01	7.43	7.13	6.73
20	10.90	10.87	10.83	10.72	10.69	10.59	10.43	10.27	10.10	9.37	8.98	8.61	7.97	7.40	7.10	6.71
25	10.90	10.86	10.82	10.71	10.68	10.58	10.42	10.25	10.07	9.33	8.94	8.57	7.93	7.37	7.08	6.68
30	10.90	10.86	10.82	10.71	10.68	10.57	10.41	10.24	10.05	9.30	8.91	8.53	7.90	7.35	7.06	6.65
35	0.0	10.86	10.82	10.71	10.67	10.57	10.40	10.23	10.03	9.26	8.89	8.50	7.88	7.33	7.04	6.63
40	10.90	10.86	10.81	10.70	10.67	10.57	10.40	10.22	10.01	9.23	8.87	8.48	7.86	7.31	7.03	6.61
50	10.90	10.85	10.81	10.70	10.66	10.56	10.39	10.20	9.98	9.20	8.85	8.45	7.83	7.28	7.00	6.58
60	10.90	10.85	10.81	10.69	10.66	10.55	10.39	10.18	9.96	9.18	8.83	8.42	7.80	7.26	6.97	6.55
70	10.90	10.85	10.80	10.69	10.66	10.55	10.38	10.17	9.94	9.16	8.81	8.40	7.78	7.24	6.94	6.52
80	10.89	10.85	10.80	10.68	10.65	10.54	10.37	10.15	9.92	9.14	8.78	8.37	7.76	7.23	6.93	6.49
90	10.89	10.85	10.80	10.68	10.65	10.54	10.37	10.14	9.90	9.12	8.76	8.35	7.74	7.21	6.91	6.47
100	10.89	10.85	10.80	10.68	10.64	10.54	10.36	10.13	9.89	9.10	8.74	8.34	7.72	7.20	6.90	6.44
120	10.89	10.84	10.80	10.68	10.64	10.53	10.35	10.12	9.87	9.07	8.72	8.31	7.70	7.18	6.88	6.37
140	10.89	10.84	10.79	10.67	10.64	10.53	10.34	10.10	9.85	9.04	8.69	8.29	7.68	7.16	6.85	
160	10.89	10.84	10.79	10.67	10.63	10.53	10.33	10.09	9.83	9.00	8.65	8.27	7.66	7.15	6.83	
180	10.89	10.84	10.78	10.67	10.63	10.52	10.32	10.08	9.82	8.99	8.64	8.25	7.64	7.14	6.81	
200	10.88	10.83	10.78	10.66	10.62	10.52	10.32	10.06	9.80	8.96	8.60	8.24	7.63	7.13	6.80	
250	10.88	10.83	10.77	10.66	10.62	10.52	10.32	10.03	9.78			8.21	7.60		6.76	
300	10.88	10.83	10.77	10.65	10.62	10.51	10.30	10.00	9.75			8.18	7.58		6.72	
350	10.88	10.83	10.76	10.65	10.61	10.50	10.29	9.98				8.16	7.57			
400	10.88	10.82	10.75	10.64	10.61	10.50	10.28	9.96	9.70			8.15	7.55			
500			10.75	10.64	10.60	10.50	10.28	9.93				8.12				
600			10.74	10.63	10.59	10.48	10.25	9.90				8.10				
700			10.73	10.62	10.59		10.24					8.08				
800			10.73	10.62	10.58							8.07				
900			10.72		10.58							8.05				
1000			10.72									8.04				
			10.71													

TEMP.	-40.2	-35.6	-25.4	-14.6	-4.6	7.8	17.8	28.4	36.5	42.7	45.8	52.2
LOG A	5.49	4.76	3.26	1.98	0.53	-1.41	-2.48	-4.56	-6.30	-7.84	-8.09	-9.13
TIME	LOG E	LOG E	LOG E	LOG E	LOG E	LOG E	LOG E	LOG E	LOG E	LOG E	LOG E	LOG E
2	11.12	11.08	11.01	10.92	10.83	10.68	10.60	10.36	10.08	9.76	9.70	9.46
3	11.11	11.08	11.00	10.91	10.81	10.66	10.58	10.32	10.04	9.71	9.66	9.41
5	11.10	11.07	10.98	10.90	10.80	10.65	10.56	10.29	10.00	9.67	9.60	9.36
7	11.09	11.06	10.98	10.89	10.79	10.64	10.55	10.26	9.97	9.63	9.58	9.33
10	11.09	11.05	10.97	10.88	10.78	10.63	10.53	10.24	9.94	9.59	9.53	9.31
15	11.08	11.05	10.96	10.87	10.77	10.62	10.51	10.21	9.90	9.55	9.50	9.27
20	11.07	11.04	10.95	10.86	10.76	10.61	10.50	10.19	9.88	9.53	9.46	9.24
25	11.07	11.03	10.94	10.86	10.75	10.60	10.49	10.18	9.86	9.51	9.44	9.23
30	11.07	11.03	10.94	10.85	10.74	10.59	10.48	10.16	9.84	9.49	9.42	9.21
35	11.06	11.03	10.94	10.84	10.74	10.59	10.47	10.15	9.83	9.47	9.41	9.20
40	11.06	11.02	10.93	10.84	10.74	10.58	10.46	10.14	9.82	9.45	9.41	9.19
50	11.06	11.02	10.92	10.83	10.73	10.57	10.44	10.13	9.80	9.43	9.40	9.18
60	11.05	11.01	10.92	10.83	10.72	10.56	10.43	10.12	9.78	9.41	9.38	9.17
70	11.05	11.01	10.92	10.82	10.72	10.56	10.42	10.10	9.76	9.39	9.35	9.15
80	11.05	11.01	10.91	10.82	10.71	10.55	10.41	10.09	9.75	9.38	9.34	9.14
90	11.04	11.00	10.91	10.81	10.71	10.54	10.41	10.08	9.73	9.37	9.32	9.12
100	11.04	11.00	10.90	10.81	10.71	10.54	10.40	10.07	9.71	9.36	9.31	9.11
120	11.04	10.99	10.90	10.81	10.70	10.53	10.39	10.06	9.70	9.34	9.29	9.10
140	11.04	10.99	10.89	10.80	10.69	10.52	10.38	10.05	9.68		9.28	9.09
160	11.03	10.99	10.89	10.80	10.69	10.51	10.37	10.04	9.66		9.27	9.08
180	11.03	10.98	10.88	10.79	10.68	10.51	10.37	10.03	9.64		9.25	9.07
200	11.03	10.98	10.88	10.79	10.68	10.50	10.36	10.02	9.63		9.24	9.06
250		10.97	10.87	10.78	10.67	10.49	10.35	10.01	9.60		9.22	
300		10.97	10.86	10.78	10.66	10.47	10.33	9.99	9.58		9.20	
350		10.96	10.86	10.77	10.65	10.46	10.32	9.98	9.55		9.19	
400		10.96	10.85	10.76	10.65	10.45	10.32	9.97	9.54		9.18	
500		10.95	10.84	10.76	10.64	10.43	10.30	9.95	9.52		9.16	
600		10.95	10.83	10.75	10.63	10.41	10.29	9.93	9.49		9.14	
700		10.94		10.74	10.62		10.27	9.92	9.47			
800		10.94		10.74	10.61		10.27	9.90	9.46			
900		10.94			10.60		10.26	9.90	9.44			
1000		10.93			10.60		10.24	9.89				

Chap. IV, Fig. 24, p. 150

TEMP.	-40.8	-33.8	-30.3	-20.0	-6.8	0.4	13.6	23.9	34.4	45.8	53.4	56.7	64.4	65.0	77.6
LOG A	10.33	8.32	6.31	4.62	3.25	2.61	0.80	-0.10	-1.62	-3.59	-4.71	-5.23	-6.15	-6.88	-8.53
TIME	LOG E	LOG E	LOG E	LOG E	LOG E	LOG E	LOG E	LOG E	LOG E	LOG E	LOG E	LOG E	LOG E	LOG E	LOG E
2	11.13	11.10	11.03	10.95	10.89	10.85	10.74	10.69	10.60	10.39	10.24	10.14	9.97		
3	11.13	11.09	11.03	10.94	10.88	10.84	10.73	10.68	10.58	10.38	10.22	10.10	9.93		
5	11.12	11.08	11.02	10.94	10.86	10.83	10.72	10.67	10.57	10.35	10.18	10.07	9.89		9.31
7	11.12	11.08	11.02	10.93	10.86	10.82	10.71	10.66	10.56	10.32	10.15	10.04	9.87		9.26
10	11.12	11.07	11.01	10.92	10.85	10.82	10.70	10.65	10.54	10.30	10.12	10.01	9.84	9.67	9.21
15	11.12	11.07	11.00	10.91	10.84	10.80	10.69	10.64	10.52	10.28	10.09	9.98	9.80	9.62	9.16
20	11.11	11.07	10.99	10.91	10.83	10.79	10.68	10.63	10.51	10.26	10.06	9.96	9.78	9.59	9.13
25	11.11	11.07	10.99	10.90	10.83	10.79	10.68	10.63	10.50	10.24	10.04	9.94	9.76	9.56	9.10
30	11.11	11.06	10.98	10.90	10.82	10.78	10.67	10.62	10.50	10.23	10.02	9.93	9.74	9.54	9.07
35	11.11	11.06	10.98	10.89	10.82	10.78	10.67	10.62	10.49	10.22	10.01	9.91	9.73	9.52	9.05
40	11.11	11.06	10.98	10.89	10.81	10.78	10.67	10.61	10.49	10.21	10.00	9.90	9.71	9.50	9.04
50	11.11	11.06	10.97	10.89	10.81	10.77	10.66	10.61	10.48	10.19	9.97	9.88	9.68	9.48	9.01
60	11.11	11.06	10.97	10.88	10.81	10.76	10.65	10.60	10.47	10.18	9.95	9.86	9.65	9.45	8.98
70	11.11	11.06	10.96	10.88	10.80	10.76	10.65	10.60	10.46	10.17	9.94	9.85	9.63	9.43	8.96
80	11.10	11.05		10.88	10.80	10.76	10.65	10.59	10.45	10.16	9.92	9.84	0.0	9.42	8.95
90	11.10	11.05		10.88	10.80	10.75	10.64	10.59	10.44	10.15	9.91	9.83	9.62	9.41	8.93
100	11.10	11.05		10.87	10.79	10.75	10.64	10.59	10.44	10.14	9.89	9.82	9.58	9.39	8.92
120	11.10	11.05		10.87	10.79	10.75	10.64	10.58	10.43	10.13	9.88	9.80	9.57	9.36	8.90
140	11.10	11.04		10.86	10.78	10.74	10.64	10.58	10.42	10.12		9.79	9.55	9.35	8.88
160	11.10	11.04		10.86	10.78	10.74	10.63	10.57	10.42	10.11		9.78	9.53	9.33	8.87
180	11.10	11.04		10.86	10.77	10.73	10.63	10.57	10.41	10.10		9.76	0.0	9.32	8.86
200	11.09	11.04		10.85	10.77	10.73	10.63	10.56	10.40	10.08		9.74	9.49	9.31	8.84
250	11.09	11.04		10.85	10.76	10.73	10.62	10.56	10.38	10.07		9.72	9.47	9.28	8.82
300	11.09	11.03		10.84	10.75	10.72	10.62	10.55	10.37	10.04		9.69		9.26	8.80
350	11.09	11.03		10.84	10.75	10.71	10.61	10.54	10.36	10.02		9.68		9.25	8.78
400	11.09	11.03		10.84		10.71	10.61	10.54	10.35	10.01		9.66		9.23	8.76
500	11.08	11.02		10.83		10.70	10.61	10.52	10.34	9.99		9.63		9.21	8.73
600	11.08	11.02		10.82		10.70	10.60	10.51	10.33	9.96		9.62		9.18	8.70
700	11.08	11.02		10.81		10.69	10.60	10.50	10.32	9.96		9.60		9.17	8.67
800	11.08	11.01		10.81		10.69	10.59	10.50	10.31	9.94		9.60		9.15	8.65
900		11.01		10.81		10.69	10.59	10.49	10.30	9.92		9.58		9.14	8.64
1000		11.01		10.81		10.69	10.59	10.48	10.29	9.90		9.58		9.13	8.61

TEMP°	-22.6	-10.5	-4.0	3.8	14.9	28.4	38.1	47.7	57.8	67.7	76.5	86.2	94.5
LOG A	8.12	6.45	5.93	4.95	3.71	2.55	0.34	-0.88	-1.97	-3.58	-5.05	-6.38	-7.00
TIME	LOG E	LOG E	LOG E	LOG E	LOG E	LOG E	LOG E	LOG E	LOG E	LOG E	LOG E	LOG E	LOG E
2	11.08	11.04	11.02	10.98	10.92	10.85	10.70	10.63	10.54	10.40	10.25	10.10	10.03
3	11.08	11.04	11.02	10.98	10.91	10.84	10.69	10.61	10.52	10.38	10.23	10.08	10.01
5	11.07	11.03	11.01	10.97	10.89	10.82	10.68	10.59	10.51	10.36	10.21	10.06	9.98
7	11.07	11.03	11.00	10.96	10.89	10.81	10.67	10.58	10.50	10.35	10.19	10.04	9.97
10	11.07	11.02	11.00	10.95	10.88	10.80	10.66	10.57	10.49	10.33	10.17	10.02	9.95
15	11.06	11.01	10.99	10.94	10.87	10.79	10.64	10.56	10.47	10.31	10.15	9.99	9.93
20	11.06	11.01	10.99	10.93	10.86	10.79	10.64	10.55	10.46	10.30	10.14	9.98	9.91
25	11.06	11.00	10.98	10.93	10.86	10.78	10.63	10.54	10.45	10.29	10.12	9.97	9.90
30	11.06	11.00	10.98	10.93	10.85	10.78	10.62	10.53	10.45	10.28	10.12	9.96	9.89
35	11.06	11.00	10.97	10.92	10.85	10.77	10.62	10.53	10.44	10.27	10.11	9.95	9.88
40	11.06	10.99	10.97	10.92	10.84	10.77	10.61	10.52	10.43	10.27	10.10	9.94	9.88
50	11.05	10.99	10.97	10.91	10.84	10.76	10.61	10.51	10.43	10.25	10.09	9.93	9.86
60	11.05	10.99	10.96	10.91	10.83	10.76	10.60	10.50	10.42	10.24	10.08	9.92	9.85
70	11.05	10.98	10.96	10.90	10.83	10.75	10.60	10.50	10.41	10.23	10.07	9.91	9.85
80	11.05	10.97	10.95	10.90	10.82	10.75	10.59	10.50	10.40	10.23	10.06	9.90	9.84
90	11.05	10.97	10.95	10.90	10.82	10.74	10.59	10.49	10.40	10.22	10.05	9.90	9.83
100	11.04	10.97	10.95	10.90	10.82	10.74	10.59	10.48	10.39	10.21	10.05	9.89	9.83
120	11.04	10.96	10.94	10.89	10.81	10.74	10.59	10.47	10.39	10.20	10.03	9.87	9.81
140	11.04	10.95	10.94	10.89	10.81	10.73	10.58	10.47	10.38	10.19	10.02	9.87	9.81
160	11.04	10.95	10.94	10.88	10.80	10.73	10.58	10.46	10.37	10.18	10.01	9.86	9.80
180	11.03	10.94	10.94	10.88	10.80	10.73	10.57	10.45	10.37	10.18	10.00	9.85	9.79
200	11.03	10.94	10.93	10.88	10.79	10.72	10.57	10.45	10.36	10.17	10.00	9.84	9.78
250	11.03	10.94	10.93	10.87	10.79	10.71	10.56	10.44	10.35	10.16	9.98	9.83	9.78
300	11.03		10.92	10.86	10.78	10.71	10.55	10.44	10.34	10.14	9.97	9.81	9.77
350	11.03		10.92	10.86	10.77	10.70	10.55	10.43	10.34	10.13	9.96	9.80	9.76
400	11.02		10.91	10.85	10.77	10.70	10.55	10.43	10.33	10.12	9.95	9.78	9.75
500	11.02		10.90	10.84	10.76	10.69	10.54	10.42	10.31	10.10	9.94		9.74
600	11.02		10.90	10.83	10.75	10.68	10.54	10.40	10.29	10.08	9.92		9.72
700	11.01		10.89	10.83	10.75	10.68	10.53	10.39	10.28	10.07			9.71
800	11.01		10.88	10.82	10.74	10.68	10.52	10.38	10.27	10.06			9.71
900	11.00		10.88	10.82	10.74	10.67	10.51	10.37	10.26	10.05			9.70
1000	11.00		10.88	10.81	10.73	10.67	10.51	10.37	10.25	10.05			9.69

Chap IV, Fig. 26, p. 151

TEMP.	-36.6	-29.4	-18.0	-7.4	1.7	18.3	28.9	39.6	53.3	63.6
LOG A	17.20	17.20	15.14	14.33	13.05	10.05	8.92	7.93	6.00	4.78
TIME	LOG E	LOG E	LOG E	LOG E	LOG E	LOG E	LOG E	LOG E	LOG E	LOG E
2	11.31	11.31	11.27	11.26	11.23	11.15	11.12	11.09	11.01	10.96
3	11.30	11.31	11.27	11.26	11.23	11.15	11.11	11.08	11.00	10.96
5	11.30	11.31	11.26	11.25	11.23	11.14	11.10	11.07	11.00	10.95
7	11.30	11.30	11.26	11.25	11.22	11.14	11.10	11.06	10.99	10.94
10	11.30	11.30	11.26	11.25	11.22	11.13	11.10	11.06	10.98	10.93
15	11.30	11.30	11.26	11.25	11.22	11.13	11.09	11.05	10.98	10.93
20	11.30	11.30	11.26	11.24	11.21	11.12	11.09	11.05	10.97	10.92
25	11.30	11.30	11.26	11.24	11.21	11.12	11.08	11.04	10.97	10.92
30	11.30	11.30	11.25	11.24	11.21	11.12	11.08	11.04	10.97	10.92
35	11.29	11.30	11.25	11.24	11.21	11.12	11.08	11.04	10.96	10.91
40	11.29	11.30	11.25	11.24	11.21	11.11	11.07	11.04	10.96	10.91
50	11.29	11.29	11.25	11.24	11.20	11.11	11.07	11.03	10.96	10.91
60	11.29	11.29	11.25	11.23	11.20	11.11	11.07	11.03	10.95	10.91
70	11.29	11.29	11.25	11.23	11.20	11.11	11.06	11.03	10.95	10.90
80	11.29	11.29	11.25	11.23	11.20	11.10	11.06	11.03	10.95	10.90
90	11.29	11.29	11.25	11.23	11.20	11.10	11.06	11.02	10.95	10.90
100	11.29	11.29	11.25	11.23	11.20	11.10	11.06	11.02	10.94	10.90
120	11.29	11.28	11.24	11.23	11.19	11.10	11.06	11.02	10.94	10.89
140	11.28	11.28	11.24	11.22	11.19	11.09	11.05	11.02	10.94	10.89
160	11.28	11.28	11.24	11.22	11.19	11.09	11.05	11.01	10.94	10.89
180	11.28	11.28	11.24	11.22	11.19	11.09	11.05	11.01	10.93	10.89
200	11.28	11.27	11.24	11.22	11.19	11.09	11.05	11.01	10.93	10.89
250	11.28	11.27	11.24	11.22	11.18	11.08	11.04	11.00	10.93	10.88
300		11.27	11.23	11.21	11.18	11.08	11.04	11.00	10.92	10.88
350			11.23	11.21	11.18	11.08	11.03	11.00	10.92	10.87
400			11.23	11.21	11.17	11.08	11.03	11.00	10.92	10.87
500			11.22	11.21	11.17	11.07	11.02	10.99	10.91	10.87
600			11.22		11.17	11.07	11.02	10.99	10.91	10.86
700			11.22			11.06	11.02	10.99	10.90	10.86
800			11.22		11.16	11.06	11.01	10.98	10.90	10.86
900			11.22			11.06	11.01	10.98	10.90	10.86
1000			11.21		11.16	11.06	11.01	10.98	10.89	10.85

Chap. IV, Fig. 26 (cont.)

TEMP.	73.8	83.2	92.7	102.7	112.1	121.3	132.8	144.6	160.4
LOG A	3.62	1.20	0.46	-0.67	-2.02	-3.13	-4.90	-6.37	-8.20
TIME	LOG E	LOG E	LOG E	LOG E	LOG E	LOG E	LOG E	LOG E	LOG E
2	10.92	10.82	10.79	10.74	10.68	10.63	10.55	10.48	10.39
3	10.91	10.81	10.78	10.73	10.67	10.62	10.54	10.47	10.38
5	10.90	10.80	10.77	10.72	10.67	10.61	10.53	10.46	10.37
7	10.90	10.79	10.76	10.72	10.66	10.61	10.53	10.45	10.36
10	10.89	10.79	10.76	10.71	10.65	10.60	10.52	10.45	10.36
15	10.88	10.78	10.75	10.71	10.64	10.59	10.51	10.44	10.35
20	10.88	10.78	10.75	10.70	10.64	10.59	10.51	10.44	10.35
25	10.87	10.77	10.74	10.70	10.64	10.58	10.50	10.43	10.34
30	10.87	10.77	10.74	10.69	10.63	10.58	10.50	10.43	10.34
35	10.87	10.77	10.74	10.69	10.63	10.58	10.50	10.43	10.33
40	10.87	10.76	10.74	10.69	10.63	10.57	10.49	10.42	10.33
50	10.86	10.76	10.73	10.68	10.62	10.57	10.49	10.42	10.32
60	10.86	10.76	10.73	10.68	10.62	10.57	10.49	10.42	10.32
70	10.86	10.75	10.73	10.67	10.62	10.57	10.48	10.41	10.32
80	10.86	10.75	10.72	10.67	10.61	10.56	10.48	10.41	10.31
90	10.86	10.75	10.72	10.67	10.61	10.56	10.48	10.41	10.31
100	10.85	10.75	10.72	10.67	10.61	10.56	10.47	10.40	10.31
120	10.85	10.74	10.72	10.66	10.60	10.56	10.47	10.40	10.30
140	10.85	10.74	10.71	10.66	10.60	10.55	10.47	10.40	10.30
160	10.84	10.74	10.71	10.66	10.60	10.55	10.46	10.39	10.30
180	10.84	10.74	10.71	10.66	10.59	10.55	10.46	10.39	10.29
200	10.84	10.74	10.71	10.65	10.59	10.54	10.46	10.39	10.29
250	10.83	10.73	10.70	10.65	10.58	10.54	10.45	10.38	10.28
300	10.83	10.73	10.70	10.65	10.58	10.54	10.45	10.38	10.27
350	10.83	10.72	10.69	10.64	10.58	10.53	10.44	10.37	10.27
400	10.82	10.72	10.69	10.64	10.57	10.53	10.44	10.37	10.26
500	10.82	10.72	10.69	10.63	10.56	10.52	10.44	10.36	10.25
600	10.81	10.72	10.68	10.63	10.56	10.52	10.43	10.35	10.24
700		10.71	10.68	10.63	10.55	10.51	10.43	10.34	10.23
800		10.71	10.68	10.62	10.55	10.51	10.42	10.33	10.23
900		10.71	10.67	10.62	10.54	10.51	10.42	10.33	10.22
1000		10.71	10.67	10.62	10.54	10.50	10.42	10.33	10.21

Chap. IV, Fig. 27, p. 152

TEMP.	-28.0	-20.0	6.3	14.5	20.3	33.0	42.3	51.1	62.3	70.9
LOG A	12.75	11.05	7.85	6.84	6.38	5.11	3.23	1.78	0.85	-0.01
TIME	LOG E	LOG E	LOG E	LOG E	LOG E	LOG E	LOG E	LOG E	LOG E	LOG E
2	11.22	11.19	11.13	11.09	11.07	11.01	10.89	10.79	10.73	10.69
3	11.22	11.19	11.12	11.08	11.06	11.00	10.87	10.78	10.72	10.68
5	11.22	11.19	11.11	11.07	11.05	10.98	10.86	10.77	10.71	10.67
7	11.22	11.19	11.11	11.06	11.04	10.97	10.85	10.75	10.70	10.66
10	11.21	11.18	11.10	11.06	11.03	10.96	10.84	10.75	10.69	10.65
15	11.21	11.18	11.09	11.05	11.03	10.95	10.83	10.74	10.69	10.64
20		11.18	11.09	11.04	11.02	10.95	10.82	10.73	10.68	10.64
25	11.21	11.18	11.08	11.04	11.02	10.94	10.81	10.72	10.68	10.63
30		11.18	11.08	11.03	11.01	10.94	10.81	10.72	10.67	10.63
35	11.21	11.17	11.08	11.03	11.01	10.94	10.80	10.72	10.67	10.62
40			11.07	11.03	11.00	10.93	10.80	10.71	10.67	10.62
50	11.21	11.17	11.07	11.02	11.00	10.93	10.80	10.71	10.66	10.61
60			11.07	11.02	10.99	10.92	10.79	10.70	10.66	10.61
70	11.20	11.17	11.06	11.01	10.99	10.92	10.79	10.70	10.65	10.61
80			11.06	11.01	10.99	10.91	10.78	10.69	10.65	10.61
90		11.17	11.06	11.01	10.98	10.91	10.78	10.69	10.65	10.61
100	11.20		11.06	11.00	10.98	10.90	10.78	10.69	10.64	10.60
120		11.16	11.06	11.00	10.97	10.90	10.77	10.68	10.64	10.60
140			11.05	11.00	10.97	10.89	10.77	10.68	10.64	10.59
160	11.20	11.16	11.05	11.00	10.97	10.89	10.77	10.68	10.64	10.59
180	11.20	0.0	11.04	10.99	10.97	10.88	10.76	10.67	10.63	10.58
200	11.20	11.16	11.04	10.99	10.96	10.88	10.76	10.67	10.63	10.58
250	11.20	11.16	11.03	10.98	10.96	10.87	10.75	10.66	10.63	10.58
300	11.19	11.15	11.03	10.98	10.95	10.87	10.75	10.66	10.62	10.57
350	11.19		11.02	10.97	10.95	10.86	10.74	10.65	10.61	10.57
400	11.18	11.15	11.02	10.97	10.95	10.86	10.73	10.64	10.61	10.56
500	11.18		11.01	10.96	10.94	10.85	10.73	10.64	10.60	10.55
600	11.17	11.15	11.01	10.96	10.93	10.85	10.72	10.63	10.59	10.55
700	11.17		11.00	10.95	10.93	10.84	10.71	10.62	10.58	10.54
800	11.16		11.00	10.95	10.92	10.84	10.71	10.62	10.57	10.54
900	11.16	11.14	10.99	10.94	10.92	10.83	10.70	10.62	10.57	10.53
1000	11.16		10.99	10.94	10.92	10.83	10.70	10.61	10.56	10.53

Chap. IV, Fig. 27 (cont.)

TEMP.	80.6	93.1	100.1	111.9	121.4	132.0	144.2	151.8
LOG A	-1.11	-2.35	-3.50	-4.85	-6.17	-7.91	-9.52	-10.15
TIME	LOG E	LOG E	LOG E	LOG E	LOG E	LOG E	LOG E	LOG E
2	10.63	10.56	10.49	10.42	10.34	10.22	10.07	9.97
3	10.62	10.55	10.48	10.41	10.33	10.20	10.04	9.95
5	10.61	10.53	10.47	10.40	10.32	10.18	10.01	9.91
7	10.60	10.53	10.47	10.39	10.31	10.17	9.99	9.89
10	10.60	10.52	10.46	10.38	10.30	10.16	9.96	9.86
15	10.58	10.51	10.45	10.37	10.29	10.14	9.91	9.83
20	10.57	10.51	10.44	10.36	10.28	10.13	9.89	9.80
25	10.57	10.50	10.43	10.36	10.27	10.12	9.88	9.78
30	10.57	10.50	10.43	10.36	10.27	10.11	9.87	9.76
35	10.56	10.49	10.43	10.35	10.26	10.11	9.82	9.76
40	10.56	10.49	10.42	10.35	10.25	10.10	9.82	9.75
50	10.56	10.48	10.42	10.34	10.25	10.09	9.80	9.73
60	10.55	10.48	10.42	10.34	10.24	10.08	9.80	9.71
70	10.55	10.48	10.41	10.33	10.24	10.06	9.79	9.67
80	10.54	10.47	10.41	10.33	10.23	10.06	9.74	9.65
90	10.54	10.47	10.41	10.32	10.23	10.05	9.72	9.64
100	10.54	10.47	10.40	10.32	10.23	10.04	9.71	9.62
120	10.53	10.46	10.40	10.31	10.22	10.03	9.69	9.59
140	10.52	10.46	10.39	10.31	10.22	10.02	9.67	9.57
160	10.52	10.46	10.39	10.31	10.21	10.02	9.64	9.55
180	10.51	10.45	10.39	10.30	10.20	10.01	9.62	9.54
200	10.51	10.45	10.38	10.30	10.20	10.00	9.59	9.51
250	10.51	10.44	10.38	10.29	10.19	10.00	9.56	9.48
300	10.50	10.44	10.37	10.29	10.18	9.98	9.51	
350	10.50	10.43	10.36	10.28	10.17	9.97	9.47	
400	10.49	10.43	10.36	10.28	10.17	9.96		
500	10.48	10.43	10.36	10.27	10.16	9.95		
600	10.48	10.42	10.35	10.26	10.15	9.93		
700	10.47	10.42	10.35	10.25	10.15	9.92		
800	10.46	10.41	10.34	10.25	10.14	9.90		
900	10.46	10.41	10.34	10.25	10.13	9.89		
1000	10.45	10.40	10.34	10.25	10.13	9.88		

TEMP.	-24.0	-20.2	-11.8	2.2	11.8	23.7	34.2	46.1	53.7	61.8	74.1	85.2	102.1	104.6	120.5
LOG A	7.95	7.56	6.85	5.45	4.54	3.10	0.98	-0.12	-1.24	-1.96	-3.87	-5.24	-7.14	-8.55	-9.63
TIME	LOG E	LOG E	LOG E	LOG E	LOG E	LOG E	LOG E	LOG E	LOG E	LOG E	LOG E	LOG E	LOG E	LOG E	LOG E
2	11.13	11.12	11.12	11.08	11.05	10.97	10.87	10.81	10.76	10.72	10.61	10.53	10.39	10.29	
3	11.13	11.12	11.11	11.07	11.04	10.97	10.86	10.80	10.75	10.71	10.60	10.51	10.38	10.27	10.17
5	11.13	11.12	11.11	11.07	11.03	10.95	10.85	10.79	10.73	10.70	10.58	10.50	10.36	10.25	10.14
7	11.12	11.12	11.11	11.06	11.03	10.95	10.84	10.78	10.73	10.69	10.58	10.49	10.35	10.24	10.13
10	11.12	11.12	11.10	11.06	11.02	10.94	10.83	10.78	10.72	10.68	10.57	10.48	10.34	10.22	10.12
15	11.12	11.11	11.10	11.05	11.01	10.93	10.82	10.77	10.71	10.67	10.56	10.47	10.33	10.21	10.10
20	11.12	11.11	11.10	11.05	11.01	10.92	10.82	10.76	10.70	10.66	10.55	10.46	10.32	10.20	10.09
25	11.12	11.11	11.10	11.05	11.00	10.92	10.81	10.75	10.70	10.66	10.54	10.46	10.31	10.19	10.08
30	11.12	11.11	11.09	11.04	11.00	10.92	10.81	10.75	10.69	10.66	10.54	10.45	10.30	10.18	10.08
35	11.11	11.11	11.09	11.04	11.00	10.91	10.81	10.75	10.69	10.65	10.53	10.45	10.30	10.17	10.07
40	11.11	11.11	11.09	11.04	10.99	10.91	10.80	10.74	10.68	10.65	10.53	10.44	10.30	10.16	10.06
50	11.11	11.11	11.09	11.03	10.99	10.91	10.80	10.74	10.68	10.64	10.53	10.43	10.29	10.16	10.06
60	11.11	11.10	11.08	11.03	10.99	10.90	10.79	10.73	10.68	10.64	10.52	10.43	10.28	10.15	10.05
70	11.11	11.10	11.08	11.03	10.98	10.90	10.79	10.73	10.67	10.64	10.52	10.42	10.27	10.14	10.04
80	11.11	11.10	11.08	11.02	10.98	10.90	10.79	10.73	10.67	10.63	10.51	10.42	10.27	10.13	10.04
90	11.11	11.10	11.08	11.02	10.98	10.89	10.78	10.73	10.67	10.63	10.51	10.42	10.26	10.13	10.03
100	11.11	11.10	11.07	11.02	10.97	10.89	10.78	10.72	10.67	10.63	10.50	10.41	10.26	10.12	10.03
120	11.11	11.10	11.07	11.01	10.97	10.89	10.78	10.72	10.66	10.62	10.50	10.41	10.25	10.11	10.02
140	11.11	11.10	11.07	11.01	10.96	10.88	10.77	10.72	10.66	10.62	10.50	10.40	10.25	10.11	10.02
160	11.10	11.10	11.07	11.01	10.96	10.88	10.77	10.72	10.65	10.62	10.49	10.40	10.24	10.10	10.01
180	11.10	11.09	11.06	11.00	10.96	10.88	10.77	10.71	10.65	10.61	10.49	10.39	10.24	10.09	10.01
200	11.10	11.09	11.06	11.00	10.95	10.87	10.76	10.71	10.65	10.61	10.48	10.39	10.23	10.08	10.00
250	11.10	11.09	11.05	10.99	10.94	10.87	10.76	10.70	10.64	10.61	10.47	10.38	10.23	10.07	9.99
300	11.10	11.09	11.05	10.99	10.94	10.86	10.75	10.70	10.64	10.60	10.47	10.38	10.22	10.06	9.98
350	11.10	11.09	11.04	10.98	10.93	10.86	10.75		10.63	10.59	10.46	10.37	10.21	10.05	9.98
400	11.10	11.08	11.04	10.98	10.92	10.86	10.75		10.63	10.59	10.46	10.36	10.21	10.04	9.97
500	11.09	11.08	11.03	10.97	10.92	10.85	10.74		10.62	10.58	10.45	10.35	10.19	10.03	9.96
600	11.09	11.08	11.02	10.96	10.91	10.85	10.74		10.62	10.57	10.44	10.35	10.18	10.02	9.95
700	11.09	11.08		10.96	10.91	10.85	10.74			10.57	10.43	10.34	10.18	10.01	9.94
800	11.09	11.08		10.95	10.90	10.84	10.73			10.56	10.43	10.34	10.17	10.00	9.94
900	11.09	11.08		10.95	10.90	10.84	10.73			10.56	10.43	10.33	10.17	10.00	9.93
1000	11.09			10.95	10.89	10.84	10.73			10.55	10.42	10.32	10.16	9.99	9.93

Chap. IV, Fig. 29, p. 153

TEMP.	-26.8	-16.0	-5.3	2.0	9.6	18.7	27.7	38.4	47.1	56.9	64.4	74.5	82.5	93.8
LOG A	5.39	4.23	2.17	1.67	0.66	-0.49	-1.73	-3.70	-5.08	-6.15	-6.94	-7.96	-8.60	-9.77
TIME	LOG E	LOG E	LOG E	LOG E	LOG E	LOG E	LOG E	LOG E	LOG E	LOG E	LOG E	LOG E	LOG E	LOG E
2	11.03	10.99	10.88	10.85	10.79	10.72	10.65	10.51	10.40	10.30	10.23	10.12	10.05	9.94
3	11.02	10.98	10.87	10.84	10.78	10.71	10.64	10.50	10.38	10.29	10.21	10.10	10.03	9.92
5	11.01	10.97	10.86	10.83	10.77	10.70	10.62	10.48	10.36	10.27	10.19	10.08	10.02	9.90
7	11.01	10.96	10.85	10.82	10.76	10.69	10.61	10.47	10.35	10.25	10.17	10.07	10.00	9.89
10	11.00	10.95	10.84	10.81	10.75	10.68	10.60	10.46	10.34	10.24	10.16	10.05	9.99	9.87
15	11.00	10.95	10.83	10.80	10.74	10.67	10.59	10.44	10.32	10.22	10.14	10.03	9.97	9.85
20	10.99	10.94	10.83	10.79	10.74	10.66	10.58	10.43	10.31	10.21	10.13	10.02	9.96	9.84
25	10.99	10.93	10.82	10.79	10.73	10.66	10.58	10.42	10.30	10.20	10.11	10.01	9.95	9.83
30	10.99	10.93	10.82	10.79	10.72	10.65	10.57	10.42	10.29	10.19	10.11	10.00	9.94	9.82
35	10.98	10.93	10.81	10.78	10.72	10.65	10.57	10.41	10.29	10.19	10.10	9.99	9.93	9.81
40	10.98	10.92	10.81	10.78	10.72	10.64	10.56	10.41	10.28	10.18	10.09	9.99	9.92	9.81
50	10.98	10.92	10.80	10.77	10.71	10.64	10.55	10.40	10.28	10.17	10.08	9.98	9.91	9.79
60	10.97	10.91	10.79	10.77	10.71	10.63	10.55	10.39	10.27	10.16	10.07	9.97	9.90	9.78
70	10.97	10.91	10.79	10.76	10.70	10.63	10.55	10.39	10.26	10.15	10.06	9.96	9.90	9.78
80	10.97	10.91	10.79	10.76	10.70	10.62	10.54	10.38	10.25	10.15	10.06	9.95	9.89	9.77
90	10.97	10.90	10.78	10.76	10.70	10.62	10.54	10.38	10.25	10.14	10.05	9.95	9.89	9.76
100	10.96	10.90	10.78	10.75	10.69	10.62	10.53	10.37	10.25	10.13	10.04	9.94	9.88	9.75
120	10.96	10.90	10.77	10.75	10.68	10.61	10.53	10.37	10.24	10.13	10.03	9.93	9.87	9.74
140	10.96	10.89	10.77	10.75	10.68	10.61	10.52	10.36	10.23	10.12	10.02	9.92	9.86	9.73
160	10.95	10.89	10.76	10.74	10.68	10.60	10.52	10.35	10.22	10.11	10.02	9.91	9.86	9.72
180	10.95	10.89	10.76	10.74	10.67	10.60	10.52	10.35	10.22	10.10	10.01	9.91	9.85	9.72
200	10.94	10.88	10.75	10.73	10.67	10.60	10.51	10.34	10.21	10.10	10.00	9.90	9.85	9.71
250	10.94	10.88	10.74	10.73	10.66	10.59	10.50	10.33	10.20	10.08	9.99	9.89	9.84	9.70
300	10.94	10.88	10.73	10.72	10.65	10.58	10.50	10.33	10.19	10.07	9.98	9.88	9.83	9.69
350	10.93	10.87	10.73	10.72	10.65	10.58	10.49	10.32	10.18	10.06	9.97	9.87	9.82	9.67
400	10.93	10.87	10.72	10.71	10.64	10.58	10.49	10.31	10.18	10.05	9.96	9.86	9.82	9.67
500	10.92	10.86	10.71	10.71	10.63	10.57	10.48	10.30	10.16	10.03	9.94	9.84	9.81	9.65
600	10.92	10.86	10.70	10.70	10.63	10.56	10.47	10.29	10.15	10.02	9.93	9.83	9.80	9.62
700	10.91	10.85	10.69	10.69	10.62	10.56	10.46	10.28	10.14	10.01	9.92	9.82	9.79	9.61
800	10.91	10.85	10.69	10.69	10.61	10.56	10.46	10.27	10.13	10.00	9.91	9.81	9.78	9.60
900	10.91	10.85			10.61	10.55	10.45	10.26	10.12	9.99	9.90	9.80	9.77	9.59
1000	10.90	10.84			10.60	10.55	10.45	10.26	10.11	9.98	9.90	9.79	9.77	9.58

Chap. IV, Fig. 30, p. 153

TEMP.	-57.2	-48.2	-33.2	-21.2	-10.8	1.2	10.9	22.2	36.3
LOG A	5.86	4.70	2.26	1.08	-0.96	-2.98	-4.49	-6.00	-7.30
TIME	LOG E	LOG E	LOG E	LOG E	LOG E	LOG E	LOG E	LOG E	LOG E
2	11.05	10.99	10.84	10.76	10.58	10.39	10.22	10.04	9.86
3	11.04	10.99	10.83	10.74	10.56	10.37	10.20	10.02	9.83
5	11.03	10.98	10.82	10.72	10.54	10.35	10.18	9.99	9.79
7	11.02	10.97	10.81	10.71	10.53	10.34	10.16	9.97	9.76
10	11.01	10.96	10.79	10.70	10.52	10.32	10.15	9.94	9.74
15	11.01	10.95	10.78	10.68	10.50	10.30	10.13	9.92	9.71
20	11.00	10.94	10.77	10.67	10.49	10.29	10.11	9.90	9.69
25	10.99	10.94	10.77	10.67	10.48	10.28	10.10	9.88	9.67
30	10.99	10.93	10.76	10.66	10.47	10.27	10.09	9.87	9.65
35	10.99	10.93	10.76	10.65	10.47	10.26	10.08	9.86	9.64
40	10.98	10.93	10.75	10.65	10.46	10.26	10.07	9.85	9.63
50	10.98	10.92	10.74	10.64	10.45	10.24	10.06	9.84	9.61
60	10.97	10.91	10.73	10.63	10.45	10.24	10.05	9.83	9.59
70	10.97	10.91	10.73	10.63	10.44	10.23	10.04	9.81	9.58
80	10.97	10.91	10.72	10.62	10.43	10.22	10.04	9.80	9.56
90	10.97	10.90	10.71	10.61	10.43	10.21	10.03	9.79	9.55
100	10.96	10.90	10.71	10.61	10.43	10.21	10.02	9.78	9.54
120	10.96	10.89	10.70	10.60	10.42	10.20	10.01	9.77	9.52
140	10.96	10.89	10.69	10.60	10.41	10.19	10.00	9.76	9.50
160	10.96	10.89	10.68	10.59	10.41	10.18	9.99	9.74	9.48
180	10.95	10.88	10.68	10.58	10.40	10.17	9.99	9.73	9.46
200	10.95	10.88	10.67	10.58	10.40	10.17	9.98	9.72	9.45
250	10.95	10.87	10.66	10.57	10.39	10.15	9.96	9.69	9.41
300	10.95	10.86	10.65	10.56	10.38	10.14	9.95	9.67	9.38
350	10.95	10.86	10.64	10.55	10.37	10.13	9.94	9.64	9.34
400	10.95	10.85	10.63	10.54	10.36	10.13	9.93	9.63	9.31
500	10.94	10.85	10.61	10.53	10.34	10.11	9.91	9.59	
600	10.94	10.84	10.61	10.52	10.33	10.10	9.90	9.55	
700	10.93		10.60	10.51	10.32			9.54	
800				10.50	10.31			9.52	
900				10.49	10.30			9.50	
1000				10.49	10.29			9.47	

Chap. IV, Fig. 31, p. 154

TEMP.	-39.0	-27.8	-11.7	0.6	12.4	22.8	32.2
LOG A	0.0	-1.11	-2.16	-3.35	-4.03	-4.63	-5.30
TIME	LOG E	LOG E	LOG E	LOG E	LOG E	LOG E	LOG E
2	9.28	9.14	8.87	8.54	8.39	8.23	8.11
3	9.25	9.10	8.83	8.50	8.34	8.20	8.07
5	9.22	9.04	8.77	8.44	8.28	8.15	8.02
7	9.19	9.01	8.73	8.40	8.24	8.12	7.99
10	9.17	8.98	8.69	8.37	8.21	8.09	7.96
15	9.15	8.94	8.64	8.32	8.18	8.06	7.93
20	9.14	8.91	8.61	8.30	8.15	8.03	7.91
25	9.13	8.88	8.58	8.27	8.13	8.01	7.89
30	9.11	8.86	8.56	8.25	8.11	8.00	7.88
35	9.10	8.85	8.54	8.24	8.10	7.99	7.87
40	9.10	8.83	8.53	8.23	8.09	7.98	7.86
50	9.09	8.79	8.50	8.20	8.07	7.96	7.85
60	9.08	8.76	8.48	8.19	8.06	7.94	7.84
70	9.07	8.74	8.46	8.17	8.05	7.93	
80	9.06	8.72	8.44	8.16	8.03	7.92	
90	9.06	8.70	8.43	8.15	8.02	7.91	
100	9.05	0.0	8.42	8.14	8.02	7.90	
120			8.40	8.12	8.00	7.89	
140			8.38	8.10	7.99	7.88	
160			8.36	8.09	7.98	7.87	
180			8.34	8.07	7.97	7.86	
200			8.33	8.05	7.96	7.85	
250				8.04	7.94	7.83	
300				8.02	7.93	7.82	
350				8.00	7.91	7.81	
400				7.99	7.90	7.80	
500						7.78	
600						7.76	
700						7.75	
800						7.74	
900						7.74	
1000						7.73	

TEMP.	-88.0	-74.4	-71.0	-67.3	-62.2	-52.8	-39.3	-31.7	-19.0	-8.1	2.5	10.1	24.2
-OG A	0.0	-1.94	-3.20	-4.60	-5.33	-8.10	-10.59	-13.37	-14.85	-16.19	-16.88	-17.34	-18.04
TIME	LOG E	LOG E	LOG E	LOG E	LOG E	LOG E	LOG E	LOG E	LOG E	LOG E	LOG E	LOG E	LOG E
2	9.96	9.89	9.80	9.71	9.65	9.41	9.16	8.78		8.30	8.17	8.06	7.92
3	9.95	9.88	9.78	9.69	9.64	9.39	9.14	8.75	8.54	8.26	8.12	8.01	7.87
5	9.95	9.87	9.77	9.67	9.62	9.37	9.11	8.72	8.50	8.21	8.07	7.96	7.82
7	9.95	9.86	9.76	9.66	9.61	9.36	9.10	8.70	8.47	8.18	8.03	7.93	7.79
10	9.94	9.85	9.75	9.65	9.59	9.34	9.08	8.68	8.44	8.14	8.00	7.90	7.75
15	9.93	9.83	9.74	9.64	9.58	9.33	9.06	8.65	8.40	8.11	7.96	7.86	7.72
20	9.93	9.82	9.73	9.63	9.57	9.31	9.04	8.64	8.38	8.08	7.93	7.83	7.70
25	9.93	9.82	9.72	9.62	9.56	9.31	9.03	8.62	8.36	8.06	7.91	7.82	7.68
30	9.93	9.81	9.72	9.62	9.56	9.30	9.02	8.61	8.34	8.04	7.89	7.80	7.66
35	9.92	9.81	9.72	9.61	9.55	9.29	9.01	8.60	8.32	8.03	7.87	7.79	7.65
40	9.92	9.80	9.71	9.61	9.55	9.29	9.01	8.59	8.31	8.02	7.86	7.78	7.64
50	9.91	9.79	9.71	9.60	9.54	9.28	8.99	8.58	8.29	8.00	7.84	7.76	7.63
60	9.91	9.79	9.70	9.59	9.53	9.27	8.98	8.57	8.27	7.98	7.82	7.74	7.61
70	9.91	9.78	9.69	9.59	9.53	9.26	8.97	8.56	8.26	7.96	7.81	7.73	7.60
80	9.91	9.78	9.69	9.58	9.52	9.26	8.97	8.55	8.24	7.95	7.80	7.71	7.59
90	9.90	9.77	9.69	9.58	9.52	9.25	8.96	8.54	8.23	7.94	7.79	7.70	7.58
100	9.90	9.77	9.68	9.57	9.52	9.25	8.95	8.53	8.22	7.93	7.77	7.69	7.58
120	9.90	9.76	9.68	9.57	9.51	9.24	8.94	8.52	8.20	7.90	7.75	7.68	7.56
140	9.89	9.76	9.67	9.56	9.50	9.24	8.93	8.50	8.18	7.89	7.74	7.66	7.55
160	9.89	9.75	9.67	9.56	9.50	9.23	8.92	8.49	8.16	7.87	7.73	7.65	7.54
180	9.88	9.75	9.66	9.55	9.49	9.22	8.91	8.48	8.14	7.86	7.71	7.64	7.53
200	9.88	9.74	9.66	9.55	9.49	9.22	8.90	8.47	8.13	7.85	7.70	7.63	7.52
250	9.88	9.73	9.65	9.55	9.48	9.21	8.89	8.46	8.11	7.83	7.68	7.61	7.50
300	9.87	9.73	9.64	9.54	9.47	9.20	8.87	8.44	8.09	7.81	7.66	7.59	7.49
350	9.87	9.72	9.64	9.53	9.47	9.19	8.86	8.42	8.06	7.79	7.64	7.57	7.48
400	9.86	9.71	9.63	9.53	9.46	9.19	8.85	8.41		7.78	7.63	7.56	7.47
500	9.86	9.70	9.62	9.52	9.45	9.17	8.83	8.39		7.75	7.61	7.53	7.45
600	9.85	9.69	9.61	9.52	9.44	9.16	8.81	8.38		7.73	7.59	7.51	7.43
700	9.85		9.61	9.51	9.44	9.16	8.79	8.37		7.72	7.57	7.49	7.42
800			9.60	9.51	9.43	9.15	8.78	8.35		7.70	7.55	7.47	7.41
900			9.59	9.51	9.43	9.14	8.76	8.34		7.68	7.54	7.45	7.40
1000			9.59	9.50	9.42	9.14	8.75	8.33		7.67	7.52	7.43	7.39

Chap. IV, Fig. 33, p. 155

TEMP.	-43.6	-38.6	-31.2	-22.0	-9.8	0.2	6.6	14.1	24.3	26.1	40.2	49.3	60.7	66.7
LOG A	3.91	3.51	1.99	0.19	-2.65	-3.94	-5.15	-6.17	-7.46	-7.75	-8.51	-8.69	-9.30	-10.16
TIME	LOG E	LOG E	LOG E	LOG E	LOG E	LOG E	LOG E	LOG E	LOG E	LOG E	LOG E	LOG E	LOG E	LOG E
2	10.76		10.59	10.43	10.16	10.03	9.89	9.77	9.60	9.57	9.46	9.44	9.36	9.23
3	10.74		10.58	10.42	10.14	10.01	9.87	9.74	9.58	9.54	9.44	9.41	9.34	9.21
5	10.72	10.69	10.56	10.40	10.12	9.98	9.84	9.71	9.55	9.51	9.41	9.39	9.31	9.18
7	10.71	10.68	10.55	10.38	10.10	9.96	9.82	9.70	9.53	9.49	9.39	9.37	9.29	9.16
10	10.70	10.67	10.53	10.37	10.09	9.94	9.80	9.68	9.51	9.47	9.37	9.35	9.27	9.13
15	10.68	10.66	10.52	10.36	10.07	9.93	9.79	9.66	9.49	9.45	9.35	9.33	9.24	9.10
20	10.67	10.65	10.51	10.35	10.06	9.91	9.77	9.64	9.47	9.43	9.33	9.31	9.23	9.08
25	10.67	10.64	10.50	10.34	10.05	9.90	9.76	9.63	9.46	9.42	9.32	9.30	9.21	9.07
30	10.66	10.64	10.50	10.33	10.04	9.89	9.75	9.62	9.45	9.41	9.31	9.29	9.20	9.06
35	10.66	10.63	10.49	10.32	10.03	9.89	9.74	9.61	9.44	9.40	9.30	9.28	9.19	9.04
40	10.66	10.63	10.49	10.32	10.03	9.88	9.73	9.60	9.43	9.39	9.29	9.27	9.18	9.03
50	10.65	10.62	10.48	10.31	10.02	9.87	9.72	9.59	9.42	9.38	9.28	9.26	9.16	9.02
60	10.64	10.61	10.47	10.30	10.01	9.86	9.71	9.58	9.41	9.37	9.27	9.25	9.15	9.00
70	10.64	10.61	10.46	10.29	10.00	9.85	9.70	9.57	9.40	9.36	9.26	9.24	9.13	8.99
80	10.64	10.60	10.46	10.29	9.99	9.84	9.70	9.56	9.39	9.35	9.25	9.23	9.12	8.98
90	10.63	10.59	10.46	10.28	9.99	9.84	9.69	9.55	9.38	9.34	9.24	9.22	9.12	8.97
100	10.63	10.59	10.45	10.28	9.98	9.83	9.68	9.55	9.37	9.34	9.24	9.21	9.11	8.96
120	10.63	10.58	10.44	10.27	9.97	9.82	9.67	9.54	9.36	9.33	9.22	9.20	9.09	8.94
140	10.63	10.58	10.44	10.26	9.96	9.82	9.66	9.53	9.35	9.32	9.21	9.19	9.08	8.93
160	10.62	10.57	10.43	10.26	9.96	9.81	9.65	9.52	9.34	9.31	9.20	9.18	9.07	8.92
180		10.57	10.42	10.25	9.95	9.80	9.64	9.51	9.34	9.31	9.19	9.17	9.06	8.90
200		10.56	10.42	10.24	9.94	9.80	9.64	9.51	9.33	9.30	9.19	9.16	9.05	8.89
250		10.55	10.41	10.23	9.93	9.78		9.49	9.31	9.29	9.17	9.14	9.02	8.87
300		10.54	10.40	10.23	9.92	9.77		9.48	9.30	9.27	9.16	9.13	9.00	8.85
350		10.53	10.40	10.22	9.91	9.76		9.48	9.29	9.27	9.14	9.12	8.98	8.83
400		10.53	10.39	10.21	9.91	9.75		9.47	9.28	9.26	9.13	9.10	8.97	8.82
500		10.51	10.38	10.20	9.90	9.73			9.26		9.12	9.08	8.94	8.79
600		10.50	10.37	10.19	9.89	9.72			9.25		9.10	9.07	8.91	8.77
700		10.49		10.19		9.71			9.24		9.09	9.05	8.89	8.75
800				10.18		9.70			9.23		9.07	9.04	8.87	8.74
900				0.0		9.70			9.22		9.06	9.02	8.86	8.73
1000				10.17		9.69			9.21		9.05	9.01		8.71
1200				10.16								9.00		

TEMP.	-32.2	-24.0	-15.8	-4.6	5.0	13.5	16.5	19.4	24.7	33.8	38.9	46.2	54.8	66.1	74.1	85.0
LOG A	3.06	2.55	1.23	-0.86	-3.03	-3.72	-5.03	-5.83	-7.21	-8.87	-9.42	-9.99	-10.48	-10.87	-11.31	-11.82
TIME	LOG E	LOG E	LOG E	LOG E	LOG E	LOG E	LOG E	LOG E	LOG E	LOG E	LOG E	LOG E	LOG E	LOG E	LOG E	LOG E
2	10.94	10.91	10.80	10.52	10.11	9.97	9.71	9.52				8.58	8.46	8.36	8.29	8.21
3	10.92	10.90	10.78	10.48	10.08	9.93	9.66	9.46				8.53	8.42	8.33	8.26	8.18
5	10.90	10.88	10.75	10.44	10.02	9.88	9.60	9.41		8.75		8.48	8.37	8.30	8.23	8.15
7	10.90	10.87	10.73	10.42	9.99	9.85	9.56	9.37		8.71		8.45	8.34	8.27	8.20	8.13
10	10.89	10.86	10.71	10.39	9.96	9.82	9.52	9.33	9.02	8.67	8.54	8.42	8.31	8.25	8.18	8.11
15	10.88	10.84	10.69	10.36	9.93	9.78	9.48	9.29	8.98	8.63	8.50	8.38	8.28	8.22	8.16	8.08
20	10.87	10.83	10.68	10.34	9.90	9.76	9.44	9.26	8.95	8.60	8.47	8.36	8.26	8.20	8.14	8.07
25	10.86	10.82	10.67	10.33	9.88	9.73	9.42	9.24	8.93	8.58	8.45	8.34	8.25	8.19	8.13	8.06
30	10.86	10.81	10.66	10.31	9.86	9.71	9.41	9.22	8.92	8.56	8.44	8.32	8.23	8.18	8.11	8.04
35	10.85	10.81	10.65	10.30	9.84	9.69	9.39	9.20	8.90	8.54	8.42	8.31	8.22	8.17	8.10	8.03
40	10.85	10.80	10.64	10.29	9.83	9.68	9.38	9.19	8.89	8.53	8.41	8.29	8.21	8.16	8.09	8.03
50	10.84	10.79	10.63	10.28	9.81	9.66	9.36	9.17	8.87	8.51	8.39	8.27	8.20	8.14	8.08	8.01
60	10.84	10.78	10.61	10.26	9.79	9.65	9.33	9.16	8.86	8.49	8.37	8.26	8.19	8.13	8.07	8.00
70	10.83	10.77	10.60	10.25	9.78	9.63	9.32	9.14	8.84	8.47	8.36	8.24	8.18	8.12	8.06	7.99
80	10.83	10.77	10.60	10.24	9.77	9.63	9.31	9.12	8.83	8.46	8.35	8.23	8.17	8.12	8.05	7.98
90	10.82	10.76	10.59	10.22	9.77	9.61	9.30	9.11	8.82	8.45	8.34	8.22	8.16	8.11	8.04	7.98
100	10.81	10.76	10.58	10.22	9.76	9.60	9.29	9.10	8.81	8.44	8.33	8.21	8.15	8.10	8.04	7.97
120	10.81	10.75	10.57	10.20	9.75	9.59	9.27	9.09	8.80	8.43	8.32	8.20	8.14	8.09	8.03	7.96
140	10.80	10.74	10.56	10.18	9.74	9.57	9.26	9.08	8.78	8.42	8.30	8.19	8.13	8.08	8.02	7.95
160	10.79	10.74	10.55	10.17	9.73	9.55	9.25	9.06	8.77	8.41	8.29	8.19	8.12	8.07	8.01	7.94
180		10.73	10.53	10.16	9.72	9.54	9.23	9.05	8.76	8.40	8.28	8.18	8.11	8.06	8.00	7.93
200		10.73	10.53	10.15	9.70	9.52	9.22	9.04	8.75	8.40	8.27	8.17	8.11	8.06	7.99	7.93
250		10.70	10.52	10.13	9.68	9.50	9.20	9.02	8.73	8.39	8.26	8.16	8.09	8.04	7.98	7.91
300		10.69	10.50	10.12	9.67	9.48	9.18	9.00	8.71	8.37	8.24	8.15	8.08	8.03	7.97	7.90
350		10.67	10.49	10.10	9.65	9.45	9.17		8.70	8.36	8.23	8.14	8.07	8.02	7.96	7.89
400		10.66	10.48	10.09	9.62	9.43	9.16		8.68	8.34	8.21	8.13	8.06	8.02	7.95	7.88
500		10.65	10.46	10.07		9.39	9.14		8.67	8.30	8.18	8.12	8.05	8.00	7.94	7.87
600		10.64	10.45	10.05		9.36	9.13		8.65	8.27	8.16	8.11	8.04	7.99	7.92	7.85
700		10.63	10.43	10.03		9.34	9.11		8.64	8.25		8.10	8.03	7.98	7.91	7.84
800		10.62	10.42			9.31	9.10		8.63	8.24		8.09	8.02	7.98	7.91	7.84
900		10.62				9.29	9.08		8.62			8.09	8.01	7.97	7.90	7.83
1000						9.27	9.07		8.61			8.08	8.00	7.96	7.89	7.82
1200														7.95		

Chap. IV, Table VI, p. 148

TEMP.	-45.3	-38.5	-31.3	-27.2	-20.8	-13.4	-11.3	-4.0	3.4
LOG A	9.50	5.50	2.40	1.00	-1.80	-4.50	-8.00	-10.00	-12.00
TIME	LOG E	LOG E	LOG E	LOG E	LOG E	LOG E	LOG E	LOG E	LOG E
2		10.84	10.55	10.48		9.09	7.65	6.84	6.37
3	10.97	10.84	10.63	10.45	9.84	8.99	7.55	6.77	6.33
5	10.96	10.83	10.60	10.42	9.78	8.91	7.43	6.69	6.28
7	10.96	10.83	10.58	10.39	9.73	8.86	7.36	6.66	6.25
10	10.96	10.82	10.56	10.36	9.67	8.80	7.28	6.62	6.22
15	10.95	10.81	10.53	10.34	9.61	8.74	7.20	6.58	6.18
20	10.95	10.81	10.51	10.31	9.57	8.70	7.15	6.56	6.16
25	10.95	10.81	10.50	10.30	9.53	8.67	7.11	6.54	6.14
30	10.94	10.80	10.48	10.28	9.51	8.64	7.08	6.52	6.13
35	10.94	10.80	10.47	10.27	9.48	8.62	7.05	6.52	6.11
40	10.94	10.80	10.46	10.26	9.46	8.60	7.03	6.50	6.10
50	10.93	10.79	10.44	10.24	9.43	8.57	6.99	6.49	6.08
60	10.93	10.79	10.43	10.22	9.40	8.55	6.97	6.47	6.06
70	10.93	10.78	10.42	10.20	9.37	8.53	6.95	6.46	6.04
80	10.92	10.78	10.41	10.19	9.35	8.51	6.93	6.45	6.03
90	10.92	10.78	10.40	10.17	9.33	8.50	6.91	6.44	6.01
100	10.92	10.77	10.39	10.16	9.31	8.48	6.89	6.43	6.01
120	10.92	10.77	10.37	10.14	9.29	8.46	6.87	6.41	5.99
140	10.91	10.76	10.36	10.12	9.26	8.44	6.84	6.40	5.97
160	10.91	10.76	10.35	10.11	9.24	8.42	6.82	6.38	5.96
180	10.91	10.75	10.34	10.09	9.22	8.40	6.81	6.37	5.94
200	10.90	10.75	10.33	10.08	9.20	8.38	6.80	6.36	5.92
250	10.90	10.74	10.31	10.05	9.17	8.35	6.77	6.34	5.90
300	10.89	10.74	10.29	10.02	9.14	8.32	6.75	6.32	5.88
350	10.89	10.73	10.28	9.99	9.11	8.30	6.72	6.31	5.86
400	10.88	10.72	10.26	9.97	9.09	8.28	6.71	6.30	5.85
500	10.87	10.71	10.24	9.93	9.06	8.21	6.69		5.82
600	10.86	10.70	10.22	9.89	9.03	8.16	6.67		5.79
700	10.86	10.69	10.21	9.85	9.00		6.66		5.77
800	10.85	10.68	10.19	9.82	8.99		6.64		5.75
900	10.85	10.68	10.18	9.79	8.97				5.74
1000	10.84	10.67	10.17	9.76	8.96				5.71

Chap. IV, Table VI, p. 148

TEMP.	-73.0	-62.2	-58.5	-50.2	-42.7	-39.6	-36.9	-35.8	-30.8	-25.8	-22.7
LOG A	15.27	13.04	11.85	10.15	8.60	7.40	5.50	4.70	1.60	-1.55	-3.60
TIME	LOG E	LOG E	LOG E	LOG E	LOG E	LOG E	LOG E	LOG E	LOG E	LOG E	LOG E
2										10.05	9.48
3			11.03		10.91	10.87	10.78	10.73	10.49	10.00	9.39
5	11.09	11.06	11.02		10.90	10.86	10.77	10.72	10.47	9.95	9.29
7	11.09	11.06	11.02		10.90	10.85	10.76	10.71	10.45	9.91	9.21
10	11.09	11.06	11.02	10.97	10.89	10.84	10.75	10.70	10.43	9.87	9.14
15	11.09	11.05	11.01	10.96	10.88	10.83	10.74	10.68	10.40	9.83	9.05
20	11.09	11.05	11.01	10.96	10.88	10.83	10.73	10.67	10.38	9.80	9.00
25	11.09	11.05	11.01	10.95	10.87	10.82	10.72	10.66	10.37	9.77	8.95
30	11.08	11.04	11.00	10.95	10.87	10.82	10.72	10.66	10.36	9.75	8.91
35	11.08	11.04	11.00	10.95	10.86	10.81	10.71	10.65	10.35	9.73	8.88
40	11.08	11.04	11.00	10.94	10.86	10.81	10.71	10.65	10.33	9.71	8.85
50	11.08	11.03	11.00	10.94	10.86	10.80	10.70	10.64	10.32	9.68	8.79
60	11.08	11.03	11.00	10.94	10.85	10.80	10.69	10.63	10.30	9.66	8.75
70	11.08	11.03	11.00	10.93	10.85	10.80	10.68	10.62	10.29	9.63	8.71
80	11.08	11.03	10.99	10.93	10.85	10.79	10.68	10.62	10.28	9.62	8.68
90	11.08	11.03	10.99	10.93	10.85	10.79	10.67	10.61	10.27	9.60	8.65
100	11.07	11.02	10.99	10.92	10.84	10.79	10.67	10.61	10.26	9.58	8.63
120	11.07	11.02	10.99	10.92	10.84	10.78	10.66	10.60	10.25	9.56	8.59
140	11.07	11.02	10.99	10.92	10.83	10.78	10.65	10.59	10.23	9.53	
160	11.07	11.02	10.99	10.91	10.83	10.77	10.64	10.58	10.22	9.51	
180	11.07	11.01	10.98	10.91	10.83	10.76	10.64	10.58	10.21	9.49	
200	11.07	11.01	10.98	10.90	10.83	10.76	10.63	10.57	10.20	9.48	
250	11.07	11.01	10.98	10.90	10.82	10.75	10.62	10.56	10.18	9.44	
300	11.07	11.00	10.97	10.89	10.81	10.75	10.61	10.55	10.16	9.40	
350	11.07	11.00	10.97	10.89	10.81	10.74	10.60	10.54	10.14	9.37	
400	11.07	11.00	10.97	10.89	10.80	10.74	10.59	10.54	10.13	9.35	
500	11.06	11.00	10.97	10.88	10.80	10.73	10.58	10.52	10.10	9.30	
600	11.06	11.00	10.97	10.87		10.72	10.57	10.51	10.08	9.25	
700	11.06	10.99	10.96	10.87		10.71	10.56	10.50	10.05	9.22	
800	11.06	10.99	10.96	10.86		10.71	10.55	10.49	10.03	9.18	
900	11.06	10.99	10.96	10.86		10.70	10.53	10.48	10.01	9.15	
1000	11.06	10.98	10.96	10.86		10.70	10.53	10.48	9.99	9.12	
1200	11.06	10.98	10.96			10.68	10.51	10.46	9.95	9.06	
1400	11.06	10.98	10.95			10.67	10.50	10.45	9.92	9.01	
1600	11.06	10.98	10.95			10.67	10.48	10.44	9.89		
1800	11.06					10.66	10.46	10.43	9.87		
2000						10.65		10.42	9.84		
2300						10.64			9.80		
2600						10.63			9.78		